INSIGHTS INTO A HETEROMERIC PROTEIN ARGININE *N*-METHYLTRANSFERASE COMPLEX

by

Laam Pak

B.Sc., The University of British Columbia, 2006

A THESIS SUBMITTED IN PARTIAL FULFILLMENT OF THE REQUIREMENTS FOR THE DEGREE OF

DOCTOR OF PHILOSOPHY

in

THE FACULTY OF GRADUATE STUDIES
(Pharmaceutical Sciences)

THE UNIVERSITY OF BRITISH COLUMBIA
(Vancouver)

April 2012

Abstract

Protein arginine *N*-methyltransferases (PRMTs) act in signaling pathways and gene expression by methylating arginine residues within target proteins. PRMT1 is responsible for most cellular arginine methylation activity and can work independently or in collaboration with other PRMTs. In this Ph.D. thesis I demonstrated an interaction between PRMT1 and -2 using co-immunoprecipitation and bimolecular fluorescence complementation (BiFC). As a result of this interaction, PRMT2 stimulated PRMT1 methyltransferase activity, affecting its apparent V_{max} and K_m values *in vitro*, and increasing the production of methylarginines in cells. Active site mutations and regional deletions on PRMT1 and -2 were also investigated, which demonstrated that complex formation required full-length, active PRMT1. However, the interaction between PRMT1 and -2 proved insensitive to methylation inhibition in the absence of the PRMT2 Src homology 3 (SH3) domain, which suggests that the PRMT2 SH3 domain may mediate this interaction between PRMT1 and -2 in a methylation-dependent fashion.

The role of the PRMT2 SH3 domain was investigated through screening for its associated proteins using GST-pull down assays followed by LC-MS/MS proteomic analysis. The result of this study revealed associations of the PRMT2 SH3 domain with at least 29 splicing-related proteins, suggesting a potential role of PRMT2 in regulating pre-mRNA processing and splicing. The interaction between PRMT2 and the Src substrate associated in mitosis of 68 kDa (Sam68) possibly through the PRMT2 SH3 domain was demonstrated using co-immunoprecipitation. Additionally, immunofluorescence results present herein imply that the PRMT2 SH3 domain could affect Sam68 sub-cellular localization in hypomethylated HeLa cells.

The biological functions of PRMT2 and the PRMT1/2 heteromeric complex were explored by pursuing the identity of associated proteins common to both PRMT1 and -2 using mass spectrometry proteomics. Approximately 50% of the identified protein hits have reported roles in controlling gene expression, while other hits are involved in diverse cellular processes such as protein folding, degradation, and metabolism. Importantly, three novel PRMT2 binders, p53, promyelocytic leukemia protein (PML), and extra eleven nineteen (EEN) were uncovered, suggesting that PRMT2 could participate in regulation of transcription and apoptosis through PRMT2-protein interactions.

Preface

This dissertation is based on work conducted in Dr. Adam Frankel's Laboratory by multiple researchers, including Dr. Ted M. Lakowski, Dylan Thomas, Mynol Islam Vhuiyan, Kristina Hüsecken, and myself. I performed all tissue culture and confocal microscopy studies, and prepared samples for the analyses of methylation in cells. I also subcloned most of the DNA constructs, designed and conducted all of the *in vivo* bimolecular fluorescence complementation (BiFC) experiments as well as all *in vitro* and *in vivo* co-immunoprecipitation (co-IP) experiments presented in Chapter 2. With the exception of LC-MS/MS analyses presented in Chapters 3 and 4, I conducted all other experiments mentioned in these chapters.

Dylan Thomas designed the BiFC constructs. Dr. Ted M. Lakowski and Dylan Thomas subcloned, expressed and purified GST-PRMT2, GST-E220Q(PRMT2), 6xHis-PRMT1, and 6xHis-E153Q(PRMT1). Dr. Lakowski and Mr. Thomas also performed all *in vitro* methylation assays and were responsible for the enzyme kinetics studies present in Chapter 2. Mynol Islam Vhuiyan helped with the expression and purification of GST-E220Q(PRMT2) and some of the *in vitro* methylation assays. Kristina Hüsecken expressed and purified GST-SH3(Abl). A summer student, Jenny J. Kim expressed and purified GST-SH3(PRMT2). Another summer student, Daisy Ji helped with the DNA construct design, expression and purification of GST.

DNA constructs for pET28b-PRMT1 splice variants used for studies in Chapter 2 were gifts generously donated by Dr. Jocelyn Côté at the University of Ottawa. The DNA constructs GST-SH3(Abl) and GST-SH3(PRMT2) used for the GST-pull down study in Chapter 3 were gifts from Dr. Mark Bedford at the University of Texas M.D. Anderson Cancer Center, Science Park-Research Division. The baculovirus lysates for 6×His-PML-I and 6×His-PML-IV used for the GST-pull down study in Chapter 4 were kindly provided by Dr. Graham Dellaire at Dalhousie University.

The LC-MS/MS proteomic studies in Chapter 3 and 4 were preformed in the Proteomics Core Facility at UBC. The Core Facility manager, Suzanne C. Perry digested the protein samples and conducted all proteomic studies including LC-MS/MS analysis and MASCOT database searches.

I wrote the majority of the manuscript. However, the two sections entitled "PRMT2 and Its Inactive Mutant Potentiate the Methylation Activity of PRMT1 in Vitro" and "Ectopic Expression of PRMT1 and -2 Synergistically Increases Protein Arginine Methylation in Cells" were originally drafted by Dr. Lakowski.

Please see footnotes in the first pages of these chapters for similar information.

Table of Contents

List of Tables

List of Figures

List of Abbreviations

82-FIP	nuclear fragile X mental retardation-interacting protein 2
aDMA	ω-N^G,N^G-dimethylarginine
AdoHcy	*S*-adenosyl-L-homocysteine
AdoMet	*S*-adenosylmethionine
AdOx	adenosine dialdehyde
AF4P12	protein furry homolog-like
ALL	acute lymphoid leukemia
AML	acute myeloid leukemia
APL	acute promyelotic leukemia
AR	androgen receptor
AS	alternative splicing
ASF/SF2	alternative splicing factor/splicing factor 2
BAD	Bcl-2 antagonist of cell death
BAF53	actin-like protein 6A
BAX	Bcl-2-associated X protein
Bcl-2	B-cell lymphoma 2
β-MHC	beta-myosin heavy chain
BPS	branchpoint sequence
CARM1	coactivator-associated arginine methyltransferase 1
Cdk	cyclin-dependent kinase
CDYL	chromodomain Y-like protein
CMS	CD2-associated protein
CPSF	cleavage and polyadenylation specificity factor
CRLs	cullin-RING E3 ubiquitin-protein ligase complexes
Csf-1	macrophage colony-stimulating factor 1
CUL4B	Cullin-4B
DBD	DNA-binding domain
DRG1	developmentally-regulated GTP-binding protein 1
DSB	DNA double-strand break
DUBs	deubiquitinating enzymes
ECM29	proteasome-associated protein ECM29 homolog
EEN	extra eleven nineteen
eIF3I	initiation factor 3 subunit I
eIF4E2	initiation factor 4E type 2
EMT	epithelial-to mesenchymal transition
ERα	estrogen receptor α
ERKs	extracellular signal-regulated kinases
ESE	exonic splicing enhancer
ESS	exon splicing silencer
EWS	Ewing sarcoma

FBXO30	F-box only protein 30
FHL2	four and a half LIM domains protein 2
FMRP	fragile X mental retardation protein
FNBP3	pre-mRNA-processing factor 40 homolog A
FOXO1	forkhead transcription factors of Class O1
FXR	farnesoid X receptor
GAN1	gigaxonin
GCF2	leucine-rich repeat flightless-interacting protein 1
GR	glucocorticoid receptor
hCAF1	human CCR4-associated factor 1
HDAC	histone deacetylase
HMGA1	high mobility group protein HMG-I/HMG-Y
HNF4	hepatocyte nuclear factor 4
hnRNP A1	heterogeneous ribonucleoprotein A1
hRod	protein kinetochore-associated protein 1
HSC70	heat shock cognate 71 kDa protein
HSP70-1/HSP70-2	heat shock 70 kDa protein 1A/1B
HSPB1	heat shock protein beta-1
HTPS	high throughput screen
IκBs	inhibitors of κB
IKK	IκB kinase
ILF3	interleukin enhancer-binding factor 3
Imp7	importin-7
ISE	intron splicing enhancer
ISS	intron splicing silencer
JCV(E)	JC virus early promoter-enhancer
JMJD6	Jumonji domain-containing 6 protein
KH domain	hnRNP K homology domain
LBD	ligand-binding domain
LPS	lipopolysaccharide
LRH-1	liver receptor homologue-1
Luc7L3	Luc7-like protein 3
LysRS	lysyl-tRNA synthetase
MBP	myelin basic protein
MCM7	DNA replication licensing factor
MCM-BP	mini-chromosome maintenance complex-binding protein
MDM2	mouse double-minute 2 protein
MLL	mixed lineage leukemia
MMA	ω-N^G-monomethylarginine
$MRCK_\beta$	serine/threonine-protein kinase MRCK beta
mRNP	mRNA binding protein
NCAPD3	Condensin-2 complex subunit D3

NEMO/IKKγ	NF-κB essential modulator
NES	nuclear export signal
NOH61	probable ATP-dependent RNA helicase DDX56
NUP43	nucleoporin NUP43
OASL/TRIP14	59 kDa 2'-5'-oligoadenylate synthase-like protein
$p54^{nrb}$	Non-POU domain-containing octamer-binding protein
PAD4	peptidylarginine deiminase 4
PCNA	proliferating cell nuclear antigen
PDCD7 /U11-59K	programmed cell death protein 7
PGC-1α	proliferators-activated receptor gamma co-activator 1
PML	promyelocytic leukemia protein
PML-NB	PML nuclear body
pol δ	DNA polymerase δ
PP1	protein phosphatase 1
PP2A	serine/threonine-protein phosphatase 2A
PPARγ	peroxisome proliferators-activated receptor gamma
Ppp1CC	catalytic subunit of the protein phosphatase 1
Ppp4c	catalytic subunit of protein phosphatase 4
PR	progesterone receptor
pRb	retinoblastoma tumor suppressor protein
PRMT1	protein arginine *N*-methyltransferase 1
PRMT2	protein arginine *N*-methyltransferase 2
PSF	proline- and glutamine-rich splicing factor
PSMA4	proteasome subunit alpha type-4
PSMB1	proteasome subunit beta type-1
PSMD11	26S proteasome non-ATPase regulatory subunit 11
PSPC1	paraspeckle component 1
PTM	post-translational protein modification
PUF60	poly(U)-binding-splicing factor PUF60
PXR	pregnane X receptor
RA	retinoic acid
RB	retinoblastoma gene product
RBM25	RNA-binding protein 25
RBM39	RNA-binding protein 39
RF-C	replication factor C
RIP140	receptor interacting protein 140
RNAPII	RNA polymerase II
rpS2	ribosomal protein S2
RPS27L	40S ribosomal protein S27-like
RRE	Rev-response element
RRM	RNA recognition motif
Rrp41	exosome complex component RRP41

RXR	retinoid X receptor
S100A4	protein S100-A4
Sam68	Src substrate associated in mitosis of 68 kDa
sDMA	ω-N^{G},N'^{G}-dimethylarginine
SF1	splicing factor 1
SF3A	splicing factor 3A
SF3B	splicing factor 3B
SH3	Src homology 3
SMA	spinal muscular atrophy
Smac	second mitochondria-derived activator of caspase
SmB/B´	small nuclear ribonucleoprotein-associated proteins B and B´
SMN	survival of motor neurons
snRNA	small nuclear RNA
snRNPs	small nuclear ribonucleoproteins
SPF30	splicing factor 30 kDa
SR proteins	serine/arginine-rich protein
SRSF2/ SC35	serine/arginine-rich splicing factor 2
STAR	signal transducers and activator of RNA
STAT1	signal transducers and activators of transcription 1
STAT3	signal transducers and activators of transcription 3
TAF15	TATA-binding protein-associated factor 2N
TDRD3	tudor domain-containg 3
TFB5	general transcription factor IIH subunit 5
TGF-β	transforming growth factor-β
TR	thyroid hormone (T3) receptor
TRIP12	probable E3 ubiquitin-protein ligase TRIP12
TRIP6	thyroid receptor-interacting protein 6
U1-70K	U1 small nuclear ribonucleoprotein 70 kDa
U2AF	U2 auxiliary factor
U2B"	U2 small nuclear ribonucleoprotein B"
UAP56	RNA helicase DDX39B
USP10	ubiquitin carboxyl-terminal hydrolase 10
USP24	ubiquitin carboxyl-terminal hydrolase 24
USP9X	probable ubiquitin carboxyl-terminal hydrolase FAF-X
WBP-11	WW domain-binding protein 11
WDR68	DDB1- and CUL4-associated factor 7
WRNIP1	ATPase WRNIP1
YY1	Yin Yang 1

Acknowledgements

First and foremost, I would like to express my heartfelt thanks to my supervisor Dr. Adam Frankel for providing me the opportunity to work on this thesis in his laboratory, and also for his continuous support, guidance, and encouragement. It has been a privilege to be his first Ph.D. student. His optimism and enthusiasm for science has always impressed and motivated me.

I would like to extend my deepest gratitude to my committee members: Dr. David Grierson; Dr. Eric Jan; Dr. Marc Levine; and Dr. Larry Lynd for their advice during my research. I would never forget the many helps on tissue culture and Western blotting I got from Dr. Ujendra Kumar, Dr. Kathleen Macleod, Dr. Brian Rodrigues, Dr. Judy Wong and the researchers from their labs.

I owe a lot to my colleagues over the years, particularly to Dr. Ted Lakowski, Mr. Dylan Thomas, Mr. Mynol Islam Vhuiyan, and Ms. Kristina Hüsecken. My colleagues not only offered me specific advice that helped me to solve technical problems, but also shared my joys and frustrations during my research.

I am very much grateful to Dr. Bin Wang and Dr. Ming Zhong for their suggestions on the co-immunoprecipitation and proteomic studies. I also benefited by the outstanding scientists and equipment at the Faculty of Pharmaceutical Sciences, the BioImaging Facility, and the Proteomics Core Facility at the University of British Columbia. I would like to especially thank Dr. Kevin Hodgson and Dr. Eiko Kawamura for providing training on the FV10i microscope. This work would not have been done without the technical support on LC-MS/MS that I received from Ms. Suzanne C. Perry.

I sincerely acknowledge the funding sources that made my Ph.D. work possible. This work was supported by the Canadian Institutes of Health Research Grant (MOP 79271), the Canada Research Chairs program, and the BC Proteomics Network Small Project Health Research Grant.

Last but not least, I would like to thank my family and friends for their love and understanding. Very special thanks go to my parents, Ms. Sui Fong Hui and Mr. Chi Yin Pak, who raised me to think critically and believe in myself. I am greatly indebted to my husband Dr. Dehong Zhang for his endless patience, sacrifice, and care throughout the years, especially during the rough days.

1 Introduction

1.1 Protein Arginine *N*-Methyltransferases

A cell responds to changes in its external and internal environments partially through triggering a vast array of post-translational protein modifications (PTMs) such as phosphorylation, acetylation, ubiquitylation, and sumoylation, thereby alternating molecular interactions and regulating gene expression as well as dynamic cell growth [reviewed in (*1*)]. Protein arginine *N*-methyltransferases (PRMTs) are a group of PTM enzymes that catalyze the transfer of one or two methyl groups from the methyl donor *S*-adenosylmethionine (AdoMet) to the terminal guanidine nitrogens of arginine residues, yielding methylated arginine residues and *S*-adenosyl-L-homocysteine (AdoHcy) as reaction products [Figure 1.1, reviewed in (*2*)]. This enzyme family contributes to signals that controls chromatin organization and cell growth.

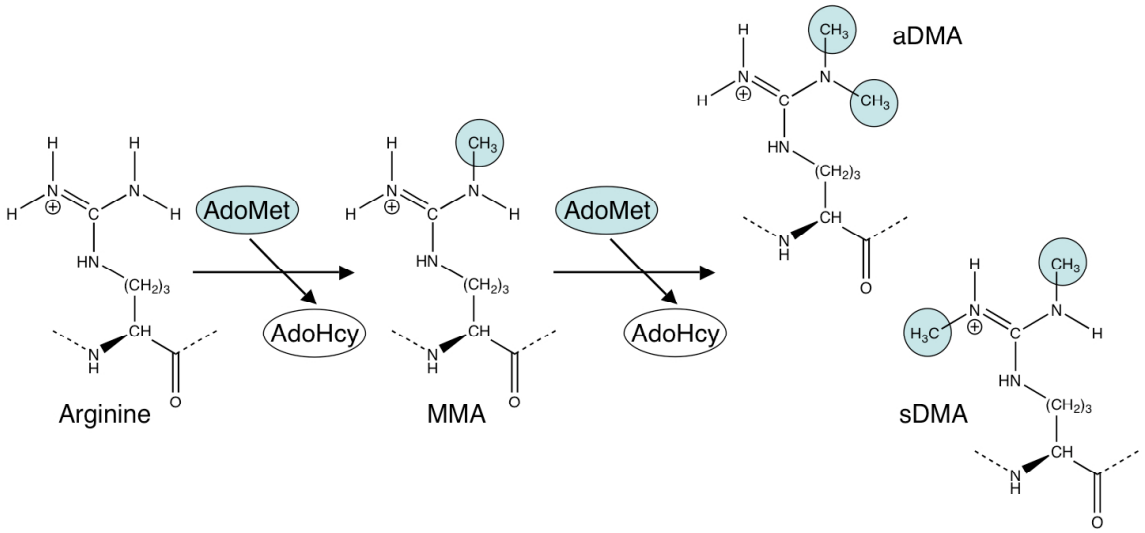

Figure 1.1. PRMT reactions. Methyl groups (highlighted in *blue*) are transferred from AdoMet to terminal guanidino nitrogens on arginine residues.

The discovery of PRMTs. Protein arginine methylation was first discovered in the late 1960s (*3, 4*). Dr. Sangduk Kim's group isolated a mixture of proteins that demonstrated arginine methylation activity from calf thymus later named as "protein methylase I". In the early days, researchers believed that the predominant endogenous substrates for the "protein methylase I" were various histones. By the end of the 1980s, the same group who first purified "protein methylase I" uncovered two methylation activities in "protein methylase I": one preferentially mono- and symmetrically dimethylated arginine residues on myelin basic protein (MBP), whereas the other preferred histones as substrates (*5*). A few years later, they identified the heterogeneous ribonucleoprotein A1 (hnRNP A1) as another *in vivo* substrate for the "histone-specific protein methylase I" (*6*). In 1996, the research groups of Drs. Harvey Herschman and Steven Clarke identified a protein that interacted with the mammalian immediate-early TIS21 protein and leukemia-associated BTG1 protein by a two-hybrid analysis (*7*). This protein was able to mono- and asymmetrically dimethylated arginine residues on hnRNP A1 and histones but showed no methyltransferase activity towards MBP. These researchers then termed the gene they identified from their cDNA library encoding this methyltransferase *PRMT1*, for *protein arginine N-methyltransferase 1* (*7*). Since then, scientists have discovered that "protein methylase I" is comprised of multiple protein arginine methyltransferases. Indeed, nine members of the PRMT family have been reported to date. Except for PRMT9(4q31) where activity has yet to be reported (*8*), PRMT1 (*7*), PRMT2 (*9*), PRMT3 (*10*), coactivator-associated arginine methyltransferase 1 (CARM1/PRMT4) (*11, 12*), PRMT6 (*13*), and PRMT8 (*14*) all form ω-N^G-monomethylarginine (MMA or NMMA) and asymmetric ω-N^G,N^G-dimethylarginine (aDMA), and are known as Type I enzymes. Considered Type II enzymes, PRMT5 forms MMA

and symmetric ω-N^G,N'^G-dimethylarginine (sDMA) (*15*). On the other hand, PRMT7 only forms MMA, therefore is categorized as a Type III enzyme (*16*).

Structures and domains of PRMTs. It has been suggested that PRMTs existed since the beginning of the eukaryote lineage because no prokaryotic or archaebacterial homolog of *PRMT* has been found (*17*). Homologs of *PRMT1* and *PRMT5* have been found in almost all eukaryotes, and homologs of *PRMT3* can be found in all eukaryotes except nematodes, saccharomycotine fungi and basal eukaryotes. Interestingly, *PRMT8* has been suggested as a vertebrate-specific duplicate of *PRMT1*. Homologs of *CARM1* and *PRMT6* have been observed in all chordates and plants, while homologs of *CARM1* are also found in arthropods. Homologs of *PRMT7* exist in animals and plants, and homologs of *PRMT9* can only be found in animals [reviewed in (*17*)].

PRMTs are highly conserved in their core catalytic and AdoMet binding domain of ~310 amino acids (*18*). Within their catalytic core, all PRMT family members share signature "double E" and "THW" sequence motifs (*19*), and a β-sheet structure, commonly known as a Rossmann fold, which contains four highly conserved motifs denoted I, post-I, II, and III (*5*) (Figure 1.2). Pair-wise amino acid sequence comparisons of PRMT catalytic cores reveal that PRMT1, 3, and 8 share the most sequence identity (50-80%) with each other, and PRMT5, 7, and 9 share the least sequence identity (17-35%) with other family members. However, certain PRMTs do harbor unique domains outside the conserved catalytic core (Figure 1.2), which may be important for localization and/or substrate specificity of the enzyme. It has been reported that a truncated mutant of PRMT3 devoid of its N-terminal zinc finger domain demonstrated reduced activity towards certain substrates (*10*). CARM1 contains a unique N-terminal region and a C-terminal autonomous activation domain that have been shown to be required for CARM1

transcriptional coactivator function (*20*). Interestingly, PRMT8 is N-terminally myristoylated and this modification makes it reside in the plasma membrane (*14*), while the sub-cellular localizations of other PRMTs is specific to cell type and/or PRMT splice variant. With the exception of PRMT6 localizes exclusively to the nucleus and PRMT3 localizes to the cytoplasm, all other PRMTs can be found in both cellular compartments (*21*). Moreover, all PRMTs are ubiquitously expressed throughout the body, except for PRMT8, which can only be found in brain tissue (*14*).

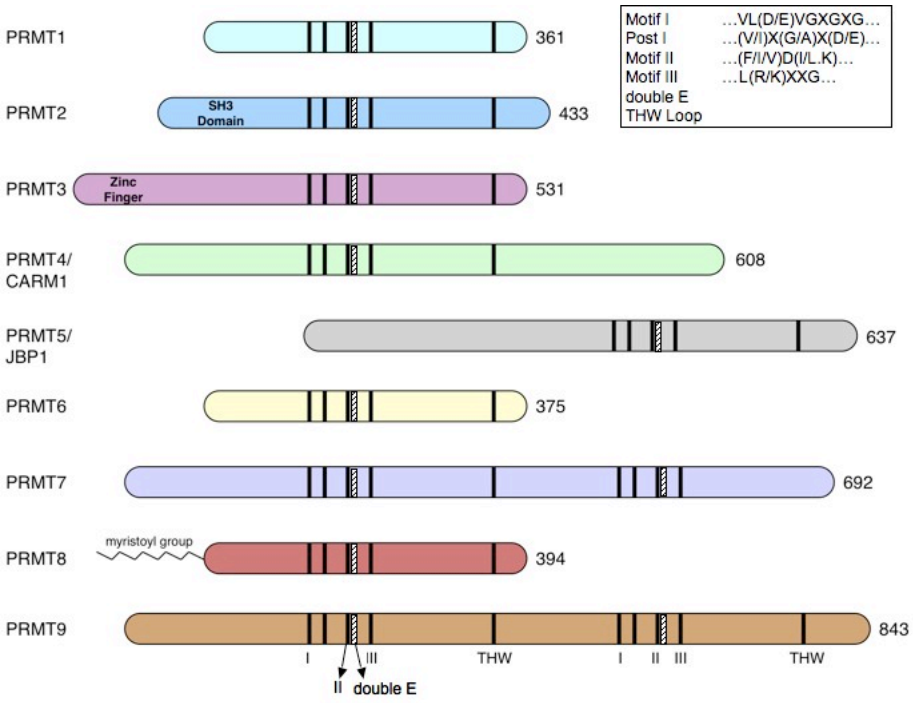

Figure 1.2. **Human PRMT family**. Human PRMTs are shown with the relative positions of signature arginine methyltransferase motifs (*boxed*). This figure is adapted from (*2*).

The crystal structures for Type I PRMTs such as rat PRMT1 (*22*), mouse CARM1 (*23, 24*), the catalytic domain of mouse PRMT3 (*18*) as well as the yeast homologue of PRMT1, Rmt1p/Hmt1p (*25*) have been solved. These structures show virtually identical PRMT protein folds in the catalytic core, such that the overall monomeric structures are composed of an N-terminal AdoMet binding domain, a middle β-barrel domain, and a C-terminal helix-turn-helix dimerization arm (Figure 1.3).

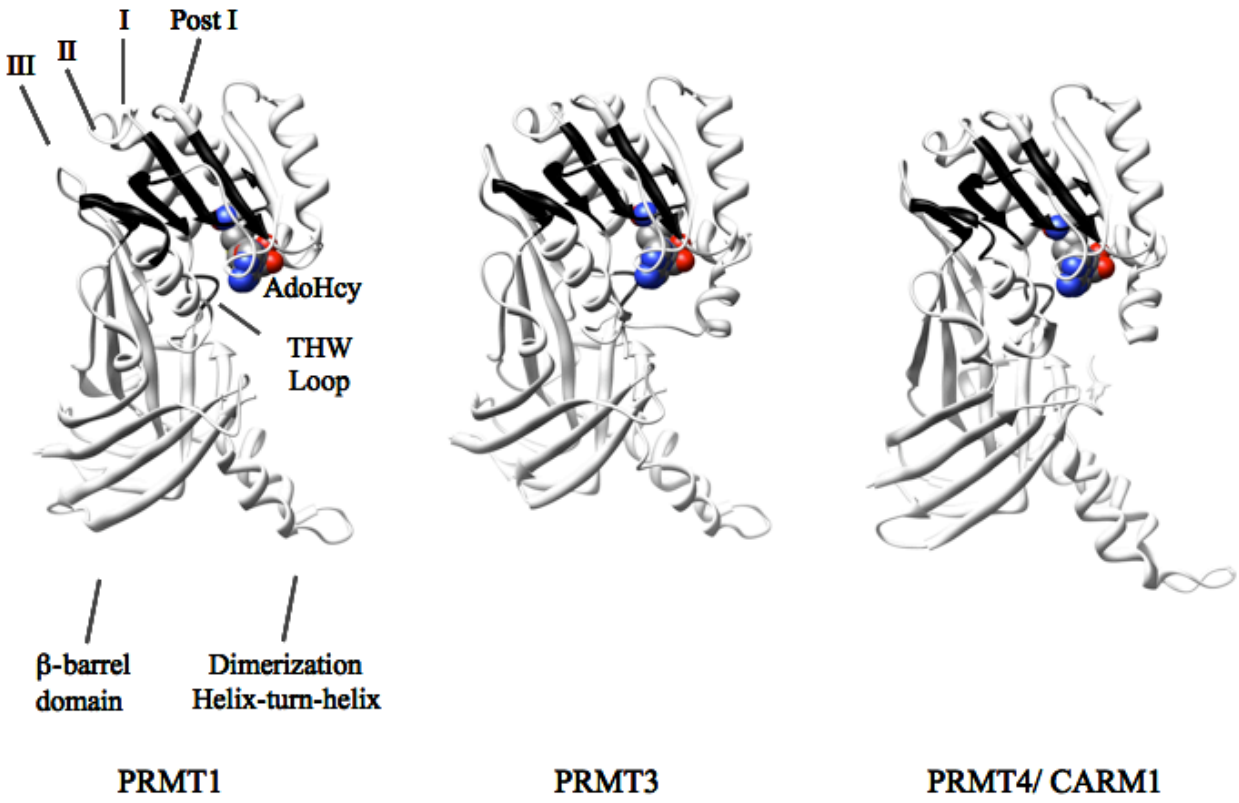

Figure 1.3. Structural conservation of the Type I PRMT catalytic core. PRMT1, PRMT3, and PRMT4 crystal structures are shown side-by-side to illustrate how they share the same folding pattern for cofactor binding, signature arginine methyltransferase motifs, and dimerization arm. PRMT1 (PDB 1OR8), PRMT3 (PDB 1F3L), and PRMT4 (PDB 2V74) structures were created in Chimera (UCSF).

PRMTs form homodimers where a dimerization arm (helix-turn-helix motif) from one subunit makes reciprocal contact with the other subunit in the AdoMet-binding domain to form a ring structure with 2-fold symmetry. However, the central cavity of CARM1 dimer is larger than those of PRMT1 and PRMT3. It has been proposed that CARM1 adaptes a wider central cavity in order to accommodate its unique C-terminal extension (*23*). Additionally, CARM1 crystal structure reveals an unexpected PH domain, which is a scaffold important for regulating protein-protein interactions (*24*). As evidence for PRMT homodimerization, endogenous PRMTs have been co-immunoprecipitated by their ectopically expressed and tagged PRMT counterparts in cells (*14, 26*).

Recently the crystal structure for *C. elegans* PRMT5, which is a Type II PRMT, has been reported by Sun *et al.* (*27*). These researchers demonstrated that similar to other PRMT structures that PRMT5 exists as a homodimer in the crystal structure and in solution; and PRMT5 catalytic core also consists of clearly defined Rossmann-fold, β-barrel, and dimerization arm domains. However, the PRMT5 crystal structure reveals a unique TIM-barrel domain at its N-terminus. The PRMT5 homodimeric interaction not only occurs through the dimerization arm but also via the TIM-barrel and β-barrel domains. The authors suggested that the TIM-barrel domain is important but not necessary for PRMT5 dimerization, whereas it may be essential for PRMT5-protein interactions and regulate PRMT5 substrate selectivities. Astonishingly, mutation of the conserved phenylalanine residue 379 in the PRMT5 active site into a methionine increased PRMT5 enzymatic activity, and also introduced Type I PRMT activity to PRMT5.

Phenotypes of PRMT knockout mice. The phenotypes of *PRMT* gene knockouts in mice vary. The *PRMT1* knockout mouse resulted in embryonic lethality (*28, 29*), and *CARM1* knockout mice appeared smaller than their littermates and died soon after birth (*30*). *PRMT2*

knockout mice were hypophagic, lean, and have significantly reduced serum leptin levels (*31*). The *PRMT2* knockout mice embryo fibroblasts also had an increased activity of NF-κB and were more resistant to apoptosis comparing to wild type cells (*32*). The embryos for *PRMT3* knockout mice were smaller, within which a known PRMT3 substrate ribosomal protein S2 (rpS2) was hypomethylated. However, the adult *PRMT3* knockout mice were similar to their wild type littermates (*33*). The distinct phenotypes displayed in mice with different *PRMTs* knocked out suggest the functional non-redundancy of PRMTs.

Substrate specificities of PRMTs. The non-redundant functions of PRMTs *in vivo* have also been elaborated by the fact that PRMTs exhibit different substrate specificities (*21*). The first identified Type I enzyme, PRMT1 has very broad substrate specificities, including histone H4, RNA binding proteins, nuclear hormone receptors, and transcription factors [reviewed in (*34*)]. PRMT1 has been shown to be the predominant arginine methyltransferase in human cells responsible for at least 85% of all arginine methylation activity (*35*). In contrast, two other major Type I PRMT enzymes, PRMT4 and PRMT6 demonstrate more defined substrate specificities. PRMT4 was first named as coactivator-associated arginine methyltransferase 1 (CARM1) due to its interaction with members of the p160 family of transcription coactivators. In fact, CARM1 itself can also act as a transcription coactivator and methylate histone H3 on Arg 17 position, which is generally considered as an activating signal for transcription (*11*). PRMT6 is a nuclear protein and exhibits specificity towards select nuclear substrates like DNA polymerase β (*36*) and histone H3 on Arg 2 (*37*).

PRMT3 is a minor Type I enzyme that predominantly expresses in the cytosol and is mainly responsible for the methylation of protein S2 of the small ribosomal subunit. Upon methylation by PRMT3, S2 has been found to be less prone to ubiquitin-mediated proteolysis

(*38, 39*). The only reported substrate for another minor Type I enzyme, PRMT8, is the oncoprotein Ewing sarcoma (EWS) (*40*), which is also a known substrate for PRMT1 and -3 (*41*). The N-terminal domain may regulate PRMT8 activity in additional to regulating its sub-cellular localization. Removal of the N-terminal domain of PRMT8 has been shown to enhance its methyltransferase activity (*42*).

On the other hand, PRMT2 has not been well characterized yet. The only three reported *in vitro* and *in vivo* substrates for PRMT2 so far are histone H4, which is also a substrate for PRMT1 (*9*), the RNA-binding protein E1B-AP5 (*43*), and the DNA-binding protein STAT3 (*44*). In addition, histone H3 has also been proposed as a potential *in vivo* substrate of PRMT2 (*45*).

PRMT5 is the only well-characterized Type II enzyme so far. Unlike the two Type I enzymes PRMT1 and -2, PRMT5 mono- and symmetrically dimethylates histone H4 on Arg 3, thereby acting as a transcriptional corepressor. PRMT5 is also able to methylate the tumor suppressor p53 and has been shown to mediate p53-dependent cell cycle arrest (*46, 47*). PRMT7 only catalyzes the formation of MMA (*16*), and its methylation activity has been shown to be required for biogenesis of Sm-class ribonucleoproteins (*48*). The *PRMT94q31* gene was identified in 2005 together with *PRMT8* based on sequence identity with other PRMTs, but the biological activity and substrate specificity of PRMT9 still needs to be characterized (*14*).

Collaborations among PRMTs. In addition to distinct substrate specificities and sub-cellular localizations of PRMTs, studies have demonstrated that they may collaborate with each other in specific cellular pathways. For example, PRMT1 and CARM1 have been shown to activate gene transcription synergistically (*49-52*). Additionally, PRMT1 and 6 have been shown to work together in the base excision repair pathway by methylating DNA polymerase β *in vivo* in response to DNA damage (*36, 53*). PRMT5 and -7 have been demonstrated to exist within the

same protein complex, and both enzymes are required for snRNP biogenesis by functioning nonredundantly in Sm protein methylation (*48*). However, whether these collaborations among PRMTs require direct PRMT-PRMT interactions remains unclear.

Impacts of arginine methylation. Although many substrates and interacting protein partners for PRMTs have been identified, the downstream "readers" of the methylation signal remains to be explored. Very little information is available on the impact of arginine methylation on protein-protein interactions. Protein-protein interactions usually occur through highly conserved domains. Arginine methylation has been shown to affect two types of protein-protein interactions. One of which is the interaction between a SH3 domain-containing protein and a proline-rich domain containing protein. It has been reported that arginine methylation within proline-rich peptides resulted in preventing interactions with certain SH3 domains while not affecting interactions with WW domains, which are binding modules similar to SH3 domains (*54*). This example will be discussed in more detail later in section 1.3. In contrast, another binding module called a tudor domain first identified in the *D. melanogaster* TUD protein and later found in many RNA-binding proteins in other eukaryotic organisms has been shown to recognize methylated amino acid residues [reviewed in (*55*)]. The tudor domains of the spinal muscular atrophy gene product SMN, the splicing factor 30 kDa (SPF30), as well as the tudor domain-containg 3 (TDRD3) proteins all selectively bind symmetrically dimethylated arginines (*56*).

PTM on PRMTs. While PRMTs can post-translationally modify their substrates, they can also undergo post-translational modifications. PRMTs can automethylate themselves *in vitro* and *in vivo* (*42*), though the role of this modification remains unclear. Moreover, phosphorylation of Ser-229 within the dimerization region of CARM1 prevents its

homodimerization, resulting in compromised enzyme activity (*57*). Contrastingly, phosphorylation at Ser-217 does not affect CARM1 homodimerization but disrupts AdoMet binding and abolishes its methyltransferase activity (*58*).

Protein arginine demethylases. As more PRMTs and their substrates were being uncovered within the past decade, researchers started to look for protein arginine demethylases that can "erase" the arginine methylation signal. However, none of these efforts turned out to be fruitful. In 2007, the Jumonji domain-containing 6 protein (JMJD6) was proposed to be a histone arginine demethylase (*59*). Unfortunately, JMJD6 was later shown to be a lysine hydroxylase of the splicing factor U2 small nuclear ribonucleoprotein auxiliary factor 65-kilodalton subunit (U2AF65) (*60*). Although the attempt to find demethylases was not successful, researchers were able to identify an enzyme named peptidylarginine deiminase 4 (PAD4) that can deiminate unmethylated and monomethylated but not dimethylated arginine residues, and convert them into citrulline residues (*61*). PAD4 may not play a physiological demethylation role since it converts unmethylated arginine residues to citrulline at a much faster rate than the methylated ones (*62*). It is generally believed that the only way to reverse the effects of protein arginine methylation is through protein degradation.

Inhibitors of PRMTs. As metioned above, PRMTs can methylate an array of proteins and participate in multiple physiological pathways. Therefore, the deregulation of PRMTs could potentially result in the pathogenesis of diseases. Mounting evidence has been observed linking PRMTs to diseases such as cancer, cardiovascular disease, viral pathogenesis, and spinal muscular atrophy (SMA) [reviewed in (*2*)]. Therefore, developing potent and selective PRMT inhibitors as therapeutic agents could be beneficial. One of the widely used non-selective methyltransferase inhibitors is adenosine dialdehyde (AdOx), which acts by inhibiting AdoHcy

hydrolase to raise intracellular levels of AdoHcy that globally inhibit AdoMet-dependent methylation reactions (*63*) (Figure 1.2). A compound named AMI-1 was identified from a high throughput screen (HTPS) and appeared selective for PRMT inhibition over other AdoMet-dependent methyltransferases (*64*). Another strategy used to develop PRMT inhibitors has been the rational design of bi-substrate compounds that contain both AdoMet and arginine moieties. Through this approach, compounds that selectively inhibit PRMT1 over CARM1 were designed and tested (*65, 66*). My colleagues Lakowski *et al.* were able to generate peptides containing an arginine residue substituted at the guanidine nitrogen (N^{η}) with an ethyl group bearing zero to three fluorine atoms that turned out to be potent inhibitors of PRMT1 and PRMT6, but not of CARM1 (*67*).

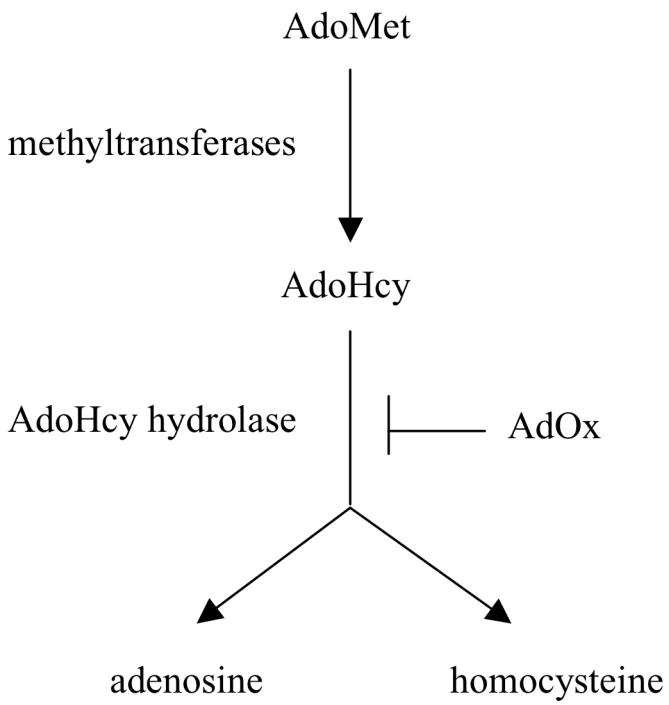

Figure 1.4. Adenosine dialdehyde inhibits AdoHcy hydrolase. Adenosine dialdehyde inhibits AdoHcy hydrolase, thus raises intracellular levels of AdoHcy (*63*).

In this dissertation, I will focus on two members of the PRMT family, the well-characterized PRMT1, and the less studied PRMT2. I will present evidence for an interaction between PRMT1 and -2, then discuss the relationship between these two PRMTs. What are the potential consequences of the PRMT1/2 interaction on the activity of either enzyme? PRMT2 has been considered to be an inactive member of the PRMT family since its discovery more then a decade ago until a weak in vitro activity has been demonstrated in our lab recently (9). What are the possible interacting partners and physiological roles of PRMT2? Last but not least, what are the common binding partners of both PRMT1 and -2? Are there proteins that specifically recognize the PRMT1/2 complex? By answering these questions, we will gain a better understanding of the physiological roles and the regulatory mechanisms of these PRMTs and their activities.

1.2 Protein Arginine *N*-Methyltransferase 1 (PRMT1)

Early characterization of PRMT1. PRMT1, which is the first isolated human PRMT and probably the most intensively investigated Type I PRMT to date, was first identified as a binding partner for the mammalian immediate-early TIS21 protein and leukemia-associated BTG1 protein in a yeast two-hybrid screen (*7*). As mentioned in section 1.1, PRMT1 is known as the predominant arginine methyltransferase in human cells responsible for at least 85% of all arginine methylation activity (*35*). The first group that cloned *PRMT1* tested the gene product for its activity against three previously reported proteins that undergo arginine methylation: histones, hnRNP A1, and MBP (*5, 6*). These authors found that a recombinant PRMT1, purified from *E. coli* demonstrated Type I activities (mono- and asymmetrical arginine dimethylation) toward histones and hnRNP A1. More importantly, the enzymatic activity of the recombinant PRMT1 appeared to be modulated by its binding partners, namely TIS21 and BTG1 proteins. The immediate-early/primary response gene *TIS21* is remarkably similar to *BTG1* (*68*); the gene product of the latter had been known for its antiproliferative role (*69*). The authors thereby hypothesized TIS21 and BTG1 are involved in ligand-induced signal transduction mediated through PRMT1. Since one of the PRMT1 substrates, hnRNP A1 had been known as a key factor in regulating alternative mRNA splicing (*70, 71*), the authors then proposed that modulation of splicing could be a potential target for PRMT1-mediated signal transduction.

Human *PRMT1* and splice variants. The human *PRMT1* gene, which is composed of 15 exons and 14 introns, spans 11.2 kb of genomic sequence on chromosome 19q13.3 (*72, 73*). In the first human PRMT1 expression analysis, *PRMT1* mRNA was found in total RNA isolated from a panel of 26 human tissues with variable levels of expression. Cerebellum, mammary

gland, prostate, brain, and thyroid tissues showed the highest levels of *PRMT1* expression (*72*). In another more detailed study on *PRMT1* genomic structure, seven *PRMT1* mRNA splice variants were detected that resulted in unique PRMT1 isoform variants with different N-terminal lengths and sequences (*73*). The authors also reported differential protein expression levels of PRMT1 variants in different human tissues with the exception of PRMT1v6, which was not detected in any of the tissue samples tested. PRMT1v1 was mostly expressed in the kidney, liver, lung, skeletal muscle, and spleen; PRMT1v2 was mainly found in kidney, liver, and pancreas whereas the expression level of PRMT1v3 was low in all tested tissues; PRMT1v4 was solely expressed in the heart; PRMT1v5 was expressed predominantly in the pancreas; and PRMT1v7 presented in the heart and skeletal muscle. Interesting, PRMT1v2 showed a unique cytoplasmic localization pattern, which is likely due to the leucine-rich nuclear export signal (NES) harbored in PRMT1v2, while all other PRMT1 splice variants distributed in both cytoplasm and nucleus. In the same study, the authors also tested the *in vitro* enzymatic activities for all seven PRMT1 isoforms and revealed that these isoforms demonstrated various substrate specificities toward a panel of known PRMT1 substrates. These authors also pointed out that PRMT1v7 appeared to be enzymatically inactive under their experimental conditions.

The regulation of PRMT1. In addition to TIS21 and BTG1, more factors involving in the regulation of PRMT1 activity were identified in the past decade. Robin-Lespinasse and co-workers demonstrated that PRMT1 co-localized with a BTG1 binding partner, hCAF1 (human CCR4-associated factor 1) in a dynamic sub-structure of the nucleus involved in splicing called a nuclear speckle. They showed that BTG1 and hCAF1 exert different regulatory effects on PRMT1 catalyzed arginine methylation in a substrate dependent manner (*74*). Results from another study also suggest that PRMT1 is recruited to the glucocorticoid receptor (GR) gene

promoter in a BTG1-dependent manner (*75*). Moreover, Passeri and co-authors revealed that PRMT1 worked in concert with BTG2, which is highly similar to BTG1 and indeed a human homologue of rodent TIS21 (*76*), as well as the histone deacetylase Sin3A, thus promoting histone methylation and deacetylation within the same protein complex (*77*). More studies still need to be done before the regulation of PRMT1 can be fully understood.

Histone H4 as a PRMT1 substrate. To investigate the biological functions of PRMT1, scientists started by searching for substrates of this enzyme. Since PRMT1 was shown to methylate histones, people then asked which histone molecule(s) could serve as the PRMT1 substrate(s). In 2001, two groups independently identified that PRMT1 specifically methylates histone H4 at the arginine 3 position *in vitro* and *in vivo* (*78, 79*). Intriguingly, methylation of H4R3 facilitates subsequent acetylation of H4 tails by p300, a histone acetylase.

RNA binding proteins as PRMT1 substrates. Back in the late 1970s, Boffa *et al.* reported that hnRNPs contain about 65% of total ω-N^G,N^G-dimethylarginine (aDMA) found in cell nucleus, and approximately 12% of the arginine residues in total hnRNPs appear to be methylated (*80*). It has also been shown that arginine is in fact the only known methylated residue in hnRNPs (*81, 82*). The long list of hnRNPs that undergo *in vivo* methylation includes hnRNP A, B, D, E, G, H, J, K, P, Q, R, and U (*83*), out of which hnRNP A1 (*7*), hnRNP A2 (*84*), hnRNP K (*85*), hnRNP Q (*86*), and hnRNP U (*87*) have been found as substrates for PRMT1.

The methylated arginines have been frequently observed in the Arg-Gly-Gly (RGG) repeats also known as glycine- and arginine-rich (GAR) motifs, which then become a postulated recognition motif for protein arginine *N*-methyltransferases (*88*). For example, all identified methylated arginine residues of hnRNP A1 fall into the RGG repeats regions within hnRNP A1 (*89*). RGG repeats are present in many hnRNPs and other RNA-binding proteins; it has been

shown to demonstrate RNA-binding ability (*90*). Furthermore, the arginines in RGG repeats were considered to be crucial for RNA-binding (*91*), and arginine methylation may abolish the proposed H-bonding interactions between the arginine side chain and the RNA (*91*). One study showed that unmethylated hnRNP A1 binds nucleic acid more tightly than methylated hnRNP A1 (*92*).

Many hnRNPs shuttle between the nucleus and the cytoplasm and take part in mRNA metabolism, and evidence suggests that methylation is involved in their nucleocytoplasmic shuttling. Treatment with AdOx appeares to cause the cytoplasmic accumulation of hnRNP A2 (*84*) and hnRNP Q (*86*). However, arginine methylation on hnRNPs does not always result in changes in hnRNP localization nor alter interactions between hnRNPs and RNA. PRMT1 is the only known enzyme that methylates hnRNP K *in vitro* and *in vivo*, yet methylation of hnRNP K did not influence its RNA-binding activity and its cellular localization. Instead, arginine methylation of hnRNP K reduces its interaction with the tyrosine kinase c-Src and suppresses c-Src activity, which led to hypophosphorylation of hnRNP K (*93, 94*).

In addition to hnRNPs, many other RNA-binding proteins have been identified as PRMT1 substrates. Src-associated in mitosis 68 kDa (Sam68), a member of the signal transducers and activator of RNA (STAR) family of RNA-binding proteins, is a PRMT1 substrate (*95*). A possible role of the methylation modification may be to regulate the interactions between Sam68 and its interacting partners as aforementioned (*54*), which will be further discussed in section 1.3. The fragile X mental retardation protein (FMRP), which binds to a subset of mRNA and regulates their translation, is also methylated by PRMT1 on its RGG repeats. Arginine methylation of FMRP reduces its RNA binding ability (*96*). Taken together,

the fact that PRMT1 methylates various RNA-binding proteins suggests a potential role that PRMT1 plays in mRNA metabolism.

PRMT1 and transcriptional regulation. Evidence that PRMT1 acts as a transcriptional coactivator began shortly after CARM1 was shown to perform a similar function (*11*). It has been proposed that the transcriptional co-regulating function of PRMT1 is a consequence of methylating histone H4R3 after being recruited to the promoter regions of targeted genes (*50, 78, 79*). PRMT1 also methylates transcription factors in order to regulate gene expression. PRMT1 methylates the TATA-binding protein-associated factor 2N (TAF15) at its RGG repeats, and this modification is required for the cytoplasmic localization of TAF15 and promotes the expression of TAF15-target genes (*97*). Yin Yang 1 (YY1), a sequence-specific DNA-binding transcription factor and PRMT1 substrate, recruits PRMT1 to an YY1-activated promoter (*98*). PRMT1 mediated methylation of the signal transducers and activators of transcription 1 (STAT1) protein is essential for STAT1 DNA-binding ability and STAT1-mediated IFNα/β-induced transcription (*99*). The pregnane X receptor (PXR) is a ligand-dependent transcription factor that plays an important role in regulating gene expression of enzymes and transporters involved in xenobiotic/drug metabolism. It has been shown that PXR can recruit PRMT1 to the promoters of its target genes so that it can methylate H4R3 for activated transcription (*100*).

PRMT1 can also act as a transcriptional regulator by methylating nuclear receptors or transcriptional co-activators. It can methylate the hepatocyte nuclear factor 4 (HNF4) at its DNA-binding domain and thereby enhance the affinity of HNF4 for its DNA binding site (*101*). PRMT1 can be subsequently recruited to the HNF4 ligand-binding domain and methylate H4R3 (*101*). These methylation activities of PRMT1 together with the recruitment of the histone acetyltransferase p300 eventually lead to transcriptional activation (*101*). PRMT1 also

methylates the estrogen receptor α (ERα) within the DNA-binding domain, thereby triggering estrogen-induced interactions of ERα with kinases PI3K and Src, which in turn results in Akt activation important for cell proliferation and survival (*102*). Although it is unclear whether PRMT1 methylates the androgen receptor (AR), it has been reported that PRMT1 activity is required for it to act as a co-activator of AR-dependent transcriptional activation (*79*). The activity of the peroxisome proliferators-activated receptor gamma co-activator 1 (PGC-1α), a tissue-specific and inducible transcription co-activator for serval nuclear receptors, is potentiated by PRMT1 mediated methylation (*103*). PRMT1 can also promote transcription by methylating and suppressing the function of the receptor interacting protein 140 (RIP140), a ligand-dependent co-repressor for nuclear factors (*104*).

PRMT1 also exerts its transcriptional co-regulator function without methylating the nuclear receptors but merely through protein-protein interactions. Ligands of farnesoid X receptor (FXR) and retinoid X receptor (RXR) were able to enhance the formation of FXR/RXR/PRMT1 complex, induce H4R3 methylation and thus promote FXR-responsive genes expression (*105*). PRMT1, PGC-1α, and interleukin enhancer-binding factor 3 (ILF3) have been reported to act synergistically as the liver receptor homologue-1 (LRH-1) co-activator (*106*). PRMT1 can also function as a co-activator in thyroid hormone (T3) receptor (TR)-mediated transcription by enhancing TR DNA-binding (*107*). Lastly, PRMT1 can interact directly with NF-κB subunit p65 and activate NF-κB-dependent transcription in concert with CARM1, and p300/CBP (*52*).

Crosstalk between PRMT1 and other PTM enzymes. Histones (H1, H2A, H2B, H3, and H4) are a group of proteins that organize chromatin structure by packaging DNA into nucleosomes to form higher-order chromatin fibers. The nucleosomes are dynamic structures;

histones can either "tightly" wind DNA into heterochromatin where transcription is suppressed, or "loosely" pack DNA in euchromatin where transcription is activated. According to the "histone code" hypothesis proposed by Strahl and Allis in 2000, post-translational modifications on the tail regions of histones can act sequentially or in combination, causing changes in the degrees of condensation of the chromatin fibers that affects the accessibility of genes for transcription (*108*).

PRMT1 is one of the many "histone code writers", and has been shown to work in concert with the other "writers" to modulate transcription. As mentioned above, the first group that showed histone H4 as a PRMT1 substrate also reported that methylation of H4R3 by PRMT1 facilitates subsequent acetylation of H4 tails by p300, a histone acetylase, while acetylation of H4 inhibits its methylation by PRMT1 (*79*). In 2004, An *et al.* proposed an ordered cooperative mechanism through which PRMT1 together with p300 and CARM1 activate p53-dependent transcription (*50*). The authors presented results suggesting that PRMT1, p300, and CARM1 are recruited to the p53 targeted promoter regions by interacting with p53. Methylation of H4R3 by PRMT1 stimulates histone H4 acetylation by p300, which then induces histone H3R17 methylation by CARM1 that led to chromatin decondensation and transcriptional activation. Additional evidence suggesting crosstalk between PRMT1 and other PTM enzymes have been observed including the necessity of H4R3 methylation by PRMT1 for the subsequent histone acetylation in 6C2 erythroleukemia cells (*109*).

PRMT1 also regulates transcription by affecting the sub-cellular localization and stability of certain transcription factors in concert with other PTM enzymes. Methylation of the forkhead transcription factor of Class O1 (FOXO1) catalyzed by PRMT1 directly blocks Akt-mediated phosphorylation of FOXO1 (*110*). Akt-mediated phosphorylation of FOXO1 is known to cause

subsequent effects such as nuclear exclusion, polyubiquitination, and proteasomal degradation of this transcription factor in order to suppress transcription of its target genes, whereas PRMT1-mediated methylation of FOXO1 has been shown to stabilize it in the nucleus and promote its transcriptional activity.

Recently, another group of researchers reported that the PRMT1-catalyzed methylation of Bcl-2 antagonist of cell death (BAD) also inhibits Akt-mediated phosphorylation of BAD and promoted apoptosis (*111*). However, a different study revealed that PRMT1 could negatively regulate apoptosis by methylating the apoptosis signal-regulating kinase (ASK1) to suppress its signaling (*112*). These findings suggest that PRMT1 can either positively or negatively regulate apoptosis by methylating different substrates involved in various signal transduction pathways.

PRMT1 and DNA damage repair. PRMT1 also takes part in DNA double-strand breaks (DSBs) repair. Proteins involved in DSBs repair such as MRE11 and 53BP1 have been confirmed to be PRMT1 substrates (*113, 114*). Arginine methylation of MRE11 is required for its localization to DNA damage foci and proper regulation of its exonuclease activity (*113, 115*). In the case of 53BP1, arginine methylation is essential for its DNA-binding ability (*114*).

1.3 Protein Arginine *N*-Methyltransferase 2 (PRMT2)

Human *PRMT2* and isoforms. Two different groups mapped out the human *PRMT2* gene independently in the late 1990s (*116, 117*). Both groups reported the *PRMT2* gene to contain 11 exons and 10 introns located on chromosome 21q22.3. Neither group observed any splice variant of PRMT2, although the Fisher group proposed alternative splicing might occur for *PRMT2*. Both groups showed that the *PRMT2* gene expressed ubiquitously with higher expression levels in brain and plancenta and reduced levels in liver and lung. The Henry group tested more tissues and revealed elevated *PRMT2* expression level in adult ovary and heart, as well as in fetal brain, lung, and kidney. Recently, three PRMT2 alternative splicing variants with distinct C-termini, referred to as PRMT2α, PRMT2β, and PRMT2γ, have been isolated from breast cancer cells (*118*). Although these PRMT2 splice variants showed a slightly different sub-cellular localization where PRMT2α and PRMT2γ are predominantly nuclear but not in nucleoli and PRMT2γ localization included nucleoli, all three PRMT2 splice variants can bind to ERα and promote ERα-mediated transcriptional activation (*118*). This same group also recently identified a novel transcript of human *PRMT2* that is generated from alternative polyadenylation at intron 7, resulting in a gene product named PRMT2L2 that lacks a portion of the PRMT2 C-terminus (*119*). In contrast to PRMT2 localization predominantly in the nucleoplasm of T47D cells, PRMT2L2 mainly expresses in the cytoplasm with higher perinuclear levels. This result suggests that the C-terminal region is important for the sub-cellular localization of PRMT2.

The SH3 domain of PRMT2. PRMT2 is the only member of PRMT family that bears an N-terminal Src homology 3 (SH3) domain. Interestingly, unlike the PRMT1 isoforms showing differences in the N-terminal sequences, all reported PRMT2 variants share the same N-

terminal sequence containing the AdoMet-binding domain and the SH3 domain [(*119*) and UniProt database].

The SH3 domain is a small non-catalytic sequence of 50 to 60 amino acids found in many intracellular signaling proteins, especially in the non-receptor tyrosine kinases such as Src and Abl (*120*). The SH3 domain is found in all eukaryotic organisms but not in prokaryotes (*121*). It is considered to be an important binding module involved in protein-protein interactions. Since it is present in many membrane and cytoskeletal proteins, the SH3 domain may help to mediate the cellular localization of proteins (*122*). It can also modulate enzymatic activities. For instance, it has been demonstrated that the activity of Abl tyrosine kinase is negatively regulated by its SH3 domain (*122*). Moreover, the SH3 domain plays roles in recruiting specific substrates to enzymes and mediates interactions with viral proteins [reviewed in (*121*)]. Crystal structures of SH3 domains from different kinases reveal a well conserved overall topology that consists of two perpendicular β sheets formed by five antiparallel β strands (*121*). It has been reported that the SH3 domain prefers to bind to ligands that adopt a left-handed type II polyproline (PPII) helix with three residues per turn. The common feature in SH3 domain ligands is the PxxP motif (where x is any amino acid) (*123*). Further elaboration of these ligands revealed that they bind to the SH3 domain in one of two opposite orientations, thus allowing for two ligand classes: Class I ligands contain the consensus sequence RxxPxxP, and Class II ligands contain the consensus sequence xPxxPxR (*124*).

It is interesting that the SH3 domain, which is generally considered to be a signature domain conserved among signal transduction proteins, is found in PRMT2. The only study that may give us a clue about the potential function of the PRMT2 SH3 domain was a large-scale screen using a protein-domain microarray to identify protein-protein interactions (*125*). One of

the twenty-four SH3 domains immobilized to the protein-domain microarray used in this study was the PRMT2 SH3 domain, while all other SH3 domains were from signal transducers including various kinases. The PRMT2 SH3 domain interacts with peptide sequences from Sam68, as did some other kinases. In an earlier study, Bedford and coworkers reported that arginine methylation on Sam68 peptides near proline-rich regions prevents binding to several SH3 domains, whereas WW domains that also recognizes proline-rich sequences are not affected in their binding to the same methylated peptides (*54*). Consistent with this result, the protein-domain microarray also reveals that the PRMT2 SH3 domain lost its affinity for the methylated Sam68 peptides (*125*). Taken together, the results from these two studies suggest that PRMT2 could be a potential "reader" of arginine methylation signals, and it may participate in the crosstalk between arginine methylation and signal transduction pathways.

PRMT2 substrates and activity. Relative to PRMT1, less is known about PRMT2 activity and its substrates. Only four PRMT2 substrates have been reported so far. The first identified PRMT2 substrate is E1B-AP5 (hnRNP U-like 1), which belongs to the hnRNP family. Similar to other hnRNP family members that generally contain methylation modifications in their RGG repeats, E1B-AP5 is also methylated in its RGG repeats in a PRMT2-dependent manner (*43*). E1B-AP5 contains proline-rich regions, which can serve as potential recognization motifs for the PRMT2 SH3 domain. The authors of the study presented data to suggest that the SH3 domain of PRMT2 is essential for the PRMT2/E1B-AP5 interaction *in vivo* (*43*). Another known PRMT2 substrate is histone H4, which is also a substrate of PRMT1. Our group has demonstrated that PRMT2 could selectively methylate the N-terminal tail of histone H4 *in vitro*, however the catalytic turnover number of PRMT2 (k_{cat}) is about 800-fold less than the k_{cat} of PRMT1 (*9*). The third reported potential substrate for PRMT2 is histone H3, which was

previously known as a substrate for CARM1, PRMT5, and PRMT6 [reviewed in (*2*)]. Using siRNA targeted against PRMT2, Blythe *et al.* demonstrated abolishment of H3R8 methylation, leading them to suggest that H3R8 could serve as an *in vivo* substrate for PRMT2 (*45*). It has been proposed that a transcription factor named β-catenin could recruit PRMT2 to target promoters where PRMT2 then establishes H3R8 methylation resulting in transcriptional activation (*45*). Recently, the signal transducers and activators of transcription 3 (STAT3), a transcription factor from the same family as the PRMT1 substrate STAT1 (*99*) has been proposed as a PRMT2 substrate (*31*). STAT3 appears to play an opposite role in tumorigenesis compared to STAT1 (*44*) and is a key component in the leptin-induced pathway that regulates energy intake and expenditure (*31*). PRMT1 has been reported to methylate STAT1 on the conserved Arg31 site (*99*). Similarly, the methylation of STAT3 at the same Arg31 position and the subsequent modulation of STAT3-dependent leptin signaling required PRMT2 (*31*).

PRMT2 and transcriptional regulation. Similar to PRMT1, PRMT2 has also been shown to act as a co-activator of transcription in response to ligand-dependent activation of nuclear receptors such as AR, ERα and ERβ, progesterone receptor (PR), peroxisome proliferator-activated receptor gamma (PPARγ), RARα, and TRβ (*126, 127*). Although none of these nuclear receptors have been reported to be PRMT2 substrates, a functional PRMT2 was required for its co-activator activity with these receptors. As discussed in the previous section, the co-regulator function of PRMT1 has been attributed to its methylation of H4R3, nuclear receptors, and other co-regulators (see references in section 1.2). Our recent demonstration that PRMT2 can selectively methylate the N-terminal tail of histone H4, albeit several orders of magnitude less *in vitro* than PRMT1, suggests that its co-activator function may be a direct result of this activity (*9*).

On the other hand, PRMT2 can also act as a transcriptional co-repressor. Out of the PRMT family members that have been tested, PRMT2 is the only one that showes affinity for the retinoblastoma gene product (RB) (*128*). A study showed that PRMT2 can form a ternary complex with RB and the transcriptional activator E2F1, resulting in direct repression of E2F1 transcriptional activity (*128*). Additionally, NF-κB-dependent transcription can be promoted by PRMT1 and CARM1, but inhibited by PRMT2 (*32, 52*). Studies have indicated that both PRMT1 and PRMT2 can bind to NF-κB subunit p65, yet PRMT2 also interactes with another NF-κB subunit p50 as well as the NF-κB inhibitor IκB-α (*32*). PRMT2 carries out its repressor function by blocking nuclear export of IκB-α. The resulting increase in nuclear IκB-α decreased NF-κB DNA-binding. These studies have also provided some evidence that the SH3 domain may be mediating the PRMT2 interaction with p50 and p65, but not with IκB-α.

PRMT2 and inflammation. As aforementioned, PRMT2 modulates the activity of NF-κB, suggesting that PRMT2 may play a role in regulating inflammation and immune response. It has been reported that lung PRMT2 transcript and protein levels in adult mice exposed to chronic hypoxia are significantly up-regulated while other PRMT levels remains unchanged, which correlates with an increase in free amino acid aDMA levels in lung tissues (*129, 130*). Indeed, aDMA and MMA both act as potent competitive inhibitors of all three isoforms of nitric oxide synthase (NOS), including the inflammatory inducible iNOS (*131*). NOS produces the inflammatory mediator nitric oxide from L-arginine. In particular, expression of the iNOS isoform can be induced by multiple inflammatory cytokines and lipopolysaccharide (LPS) through NF-κB-mediated transcription (*132*). Nitric oxide deficiency caused by aDMA in lung eqithelial tissue has been found to potentiate lung inflammation in a mouse model of allergic asthma (*133*). Recently, PRMT2 has been proposed to serve as a new member of the NF-κB

pathway that regulates LPS-induced inflammatory response in lung in a dosage-sensitive manner (*134*). Taken together, PRMT2 may control the inflammatory response through aDMA production as well as repression of NF-κB activity.

1.4 Hypotheses and Research Objectives

PRMT1 and -2 share overlapping substrate specificities *in vitro*, and they are likely to be involved in the same pathways such as nuclear receptors- and NF-κB-dependent transcriptional regulation. More importantly, a sequence alignment of PRMT1 and PRMT2 fragments at their homodimer interfaces illustrates a 62.3% similarity within these regions (Figure 1.5). Thus, I hypothesize that PRMT1 works together with PRMT2 by forming a heteromeric complex. My first research objective was to determine the formation mechanism and enzymatic activity of the PRMT1/2 heteromeric complex. Since PRMT2 contains a unique SH3 domain that may facilitate PRMT2-protein interactions, my second research objective was to uncover the binding partners of the PRMT2 SH3 domain and determine a plausible role of the PRMT2 SH3 domain in regulating the formation of PRMT2-containing protein complexes including the PRMT1/2 heteromeric complex. Further, studies present herein aimed to explore the biological functions of PRMT2 and the PRMT1/2 complex by screening for PRMT1 and/or -2 binding partners. My third research objective was to identify proteins that associate with the PRMT1/2 complex in an effort to explore possible biological functions of the heteromeric interaction.

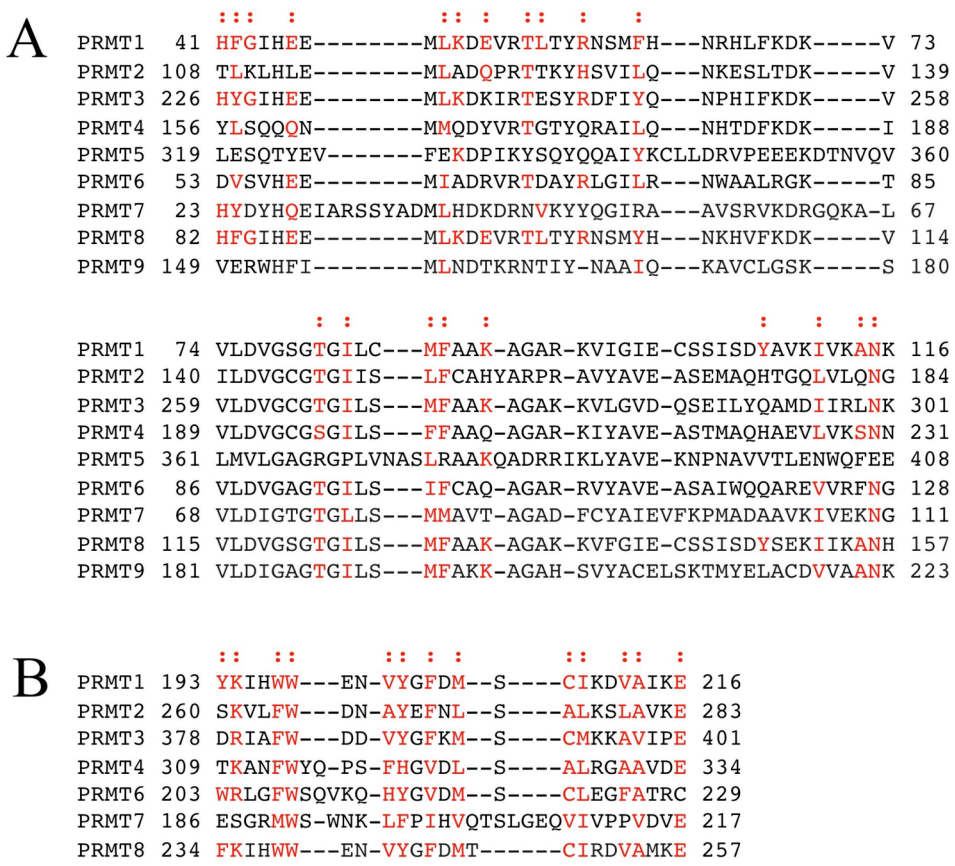

Figure 1.5. **Sequence alignment of residues at the PRMT dimer interface.** Sequences for human PRMTs that may be involved in dimer contacts were aligned using protein-protein BLAST (NCBI). In some instances sequences could not be aligned due to insufficient similarity and are not included. Residues reported in PRMT crystal structures to make direct contacts at the dimer interface between sequences in (A) and (B) are indicated with a *colon* and dimer residues (*18, 22-25*) similar to PRMT1 sequence highlighted in *red*.

2 A PRMT1 and -2 Heteromeric Interaction Increases PRMT1 Enzymatic Activity[1,2]

2.1 Introduction

In this study, the relationship between PRMT1 and -2 was investigated. Since both enzymes share overlapping substrate specificity *in vitro*, my colleagues and I initiated a series of experiments to see whether PRMT2 would affect PRMT1 activity towards histone H4 or *vice versa*, and we observed a synergistic (*i.e.*, non-additive) increase in substrate methylation. Assaying combinations of wild type and catalytically inactive PRMTs indicated that both PRMT1 and -2 mutants increased PRMT1 activity. The interaction between PRMT1 and -2 was confirmed *in vitro* and in HeLa cells by co-immunoprecipitation, as well as by bimolecular fluorescence complementation (BiFC). The BiFC technique can demonstrate a direct interaction in cells between two proteins that, when bound, mediate the reassembly of a fluorescent protein from its N- and C-terminal fragments attached to each binding partner (40, 41). I analyzed combinations of wild type and mutant PRMT1 and -2 to further investigate their interaction in cells, and determined that binding required the dimerization arm and catalytic activity of PRMT1. In the presence of adenosine dialdehyde (AdOx), which globally inhibits methylation, the interaction between PRMT1 and -2 was compromised, yet deletion of the PRMT2 SH3

[1] A version of chapter 2 has been published. Pak, M.L., Lakowski, T.M., Thomas, D., Vhuiyan, M.I., Hüsecken, K. and Frankel, A. (2011) A Protein Arginine *N*-methyltransferase 1 (PRMT1) and 2 Heteromeric Interaction Increases PRMT1 Enzymatic Activity. Biochemistry. 50(38):8226-40. I designed and conducted all of the *in vivo* bimolecular fluorescence complementation (BiFC) experiments as well as all *in vitro* and *in vivo* co-immunoprecipitation (co-IP) experiments.

I preformed all tissue culture and confocal microscopy studies. I prepared samples for the methylation in cells study. Dr. Ted M. Lakowski and Dylan Thomas expressed and purified GST-PRMT2, GST-E220Q(PRMT2), 6xHis-PRMT1, and 6xHis-E153Q(PRMT1), and preformed all *in vitro* methylation assays and were responsible for the enzyme kinetics studies. Mynol Islam Vhuiyan helped with the expression and purification of GST-E220Q(PRMT2) and some of the *in vitro* methylation assays. Kristina Hüsecken contributed to helpful discussion.

[2] DNA constructs for pET28b-PRMT1 splice variants were gifts from Dr. Jocelyn Côté.

domain restored the interaction in AdOx-treated cells or when PRMT1 was inactive. These results reveal that the SH3 domain regulates the interaction between PRMT1 and -2 in a methylation-dependent manner. Moreover, this work represents the first evidence for a direct interaction between two PRMTs that culminates in a change in activity for one of the enzymes.

2.2 Methods

DNA constructs. All DNA primers used in this study are listed in Table A.1. Humanized rat *PRMT1* gene coding for PRMT1v1 (isoform 1) (*135*) was sub-cloned into pcDNA3.1(+)/Neo (Invitrogen) using *BamHI* and *XhoI* restriction sites. The human *PRMT2* gene previously sub-cloned in pGEX-2T (*9*) was PCR-amplified with primers as described in Table A.1, digested with *BamHI* and *XhoI*, and sub-cloned into pcDNA3.1(+)/Neo. Mutually annealing primers generated DNA sequences flanked by *NheI* sites coding for the hemagglutinin (HA) (YPYDVPDYA) and the c-Myc (EQKLISEEDL) tags. *NheI*-digested DNA fragments coding for the c-Myc tag were sub-cloned into the pcDNA3.1(+)/Neo-PRMT1 to generate pcDNA3.1(+)/Neo-c-myc-PRMT1 that codes for an N-terminal c-Myc-tagged PRMT1 protein. *NheI*-digested DNA fragments coding for the HA tag were sub-cloned into pcDNA3.1(+)/Neo-PRMT2 to generate pcDNA3.1(+)/Neo-HA-PRMT2 that codes for an N-terminal HA-tagged PRMT2 protein. The gene for histone H4 in pET3 was a generous gift from Dr. Karolin Luger at Colorado State University.

BiFC constructs coding for either mCitrineN (amino acid residues 1-173 of mCitrine) fused to the N-terminus of a PRMT, or mCitrineC (amino acid residues 174-239 of mCitrine) fused to the C-terminus of a PRMT each contained a short and flexible amino acid linker (GGGGS) separating the fluorescent protein fragment from the enzyme that was successfully used in another study (*136*). In order to make BiFC constructs, PRMT genes were first cloned into the pET28a vector at *NdeI* and *XhoI* sites for mCitrineN constructs, and at *BamHI* and *XhoI* sites for mCitrineC constructs. The mCitrineN-PRMTs were then PCR-amplified with primers containing *HindIII* and *XhoI* sites, and the mCitrineC-PRMTs were amplified with primers containing *BamHI* and *EcoRI* sites. The amplicons were sub-cloned into pcDNA3.1(+)/Hygro

and pcDNA3.1(+)/Neo, respectively. Control constructs pcDNA3.1(+)/Hygro-mCitrineN-Only and pcDNA3.1(+)/Neo-mCitrineC-Only were made by PCR with primers containing *HindIII* and *BamHI* sites for mCitrineN, and *XhoI* site for mCitrineC. The amplicons were sub-cloned into pcDNA3.1(+)/Hygro for mCitrineN-Only and pcDNA3.1(+)/Neo for mCitrineC-Only.

Primers used for mutagenesis are listed in Table A.2. Site-directed mutagenesis reactions were done using the QuikChange method (Agilent Technologies).

Protein expression and purification. GST-PRMT2, GST-E220Q (PRMT2), 6xHis-PRMT1, and 6xHis-E153Q (PRMT1) were expressed and purified using previously described methods (*9, 135*). Histone H4 and its R3K mutant were overexpressed in BL21 DE3 pLysS *E. coli* cells (Agilent Technologies) according to previously described methods (*137*). Histone H4 and its R3K mutant were purified from inclusion bodies by denaturation in 20 mM Tris (pH 8.0), 8.0 M guanidinium hydrochloride, 4.0 mM DTT, followed by rapid dilution in 100 mM Tris (pH 8.0), 400 mM arginine, 2 mM EDTA, 1 mM PMSF, and 0.5 mM oxidized glutathione and 5.0 mM reduced glutathione (total dilution ~1/50). Histone H4 and its R3K mutant were further purified using a Zorbax 9 × 250 mm C8 semi-preparative reverse phase HPLC column using 0.1% TFA in water and 0.1% TFA in acetonitrile (5 to 95% gradient developed over 20 min). Enzyme concentrations were determined using a previously described method (*9*). The concentrations of histone H4 and its R3K mutant were determined using UV spectroscopy (e_{280} = 5120 M^{-1} cm^{-1}).

Tissue culture. HeLa cells were cultured in Dulbecco's Modified Eagle's Medium (DMEM) (Sigma) supplemented with 5% fetal bovine serum (FBS) (Gibco) and 100 μg/mL Primocin (InvivoGen) at 37 °C in 5% CO_2. Approximately 0.1 × 10^6 HeLa cells were seeded in each well of a 24-well plate containing a 12-mm microscope cover glass (Fisher) coated with

poly-D-lysine (Sigma), and grown in standard growth medium 24-h prior to transfection. Immediately before transfection the growth medium was replaced with Opti-MEM medium (Invitrogen). HeLa cells were transiently co-transfected with the desired BiFC constructs (0.4 μg DNA each) using Lipofectamine 2000 (Invitrogen) per the manufacturer's instructions. The medium was replaced with DMEM supplemented with 5% FBS, but without antibiotic 7 h post-transfection. The transfected cells were cultured for an additional 18 h before they were fixed. To inhibit cellular methylation, HeLa cells were transfected in a growth medium supplemented with 20 μM of periodate-oxidized adenosine (AdOx) (Sigma).

Confocal microscopy. The cells were allowed to grow for 25 h after co-transfection with BiFC constructs and before fixation with a 4% paraformaldehyde solution in phosphate-buffered saline (PBS) (Gibco, cat. # 10010). The cells were then stained with Alexa Fluor 594 phalloidin (Invitrogen) and 2-(4-carbamimidoylphenyl)-1H-indole-6-carboximidamide (DAPI) (Invitrogen). Representative cell images of BiFC combinations were examined using a FluoView FV10i confocal microscope (Olympus), which provided an initial scan at 10x magnification to aid in identifying fluorescence signal in all cells. High-resolution cell images were then captured with an oil lens at 60x magnification and they were subsequently processed with ImageJ software (NIH image). Due to the high background signal caused by the PRMT1E153Q-mCitrineC construct (Figure A.1), the laser input used for generating images of cells co-transfected with PRMT1E153Q-mCitrineC construct was reduced by half to 7.2%. Otherwise, all images for BiFC were obtained with the same aperture (1x), sensitivity (49.6%), and laser input (14.1%) settings, and were processed without brightness and contrast adjustment.

Immunoprecipitation and Western blotting. For immunoprecipitation of proteins from cells, 8×10^6 HeLa cells cultivated in a 100-mm dish for 24 h were transfected with 24 μg DNA

using Lipofectamine 2000 (Invitrogen) according to the manufacturer's protocol. To inhibit cellular methylation, HeLa cells were transfected in a growth medium supplemented with 20 μM AdOx.

After transfection, cells were harvested and lysed in 250 μl of hypotonic lysis buffer [20 mM HEPES-KOH pH 7.4, 2 mM $MgCl_2$, 0.2 mM EGTA, 10% glycerol, 1x protease inhibitor cocktail (Roche #04693132001)] by repeated freezing and thawing. The NaCl concentration was then adjusted to 400 mM. The lysed cells were incubated on ice for 5 min and centrifuged at 14,000 rpm at 4 °C for 15 min in an Eppendorf centrifuge (5417 R). Cell lysate (500 μg protein) was aliquoted and the buffer was adjusted to 50 mM HEPES-KOH, 150 mM NaCl. Aliquoted cell lysate was then supplemented with 2.0 μg of monoclonal anti-HA antibody (HA-7, Sigma), monoclonal anti-c-Myc antibody (9E10, Sigma), or mouse IgG (15381, Sigma), and the volume was adjusted to 500 μL with co-IP buffer [50 mM HEPES-KOH, pH 7.4, 150 mM NaCl, 1x protease inhibitor cocktail (Roche #04693132001)]. The protein/antibody mixtures were incubated at 4 °C for 4 h with rotation. The cell lysate/antibody mixture was added to 50 μL pre-washed protein G-sepharose (Invitrogen) and was rotated at 4 °C for 16 h. Subsequently, the resin was washed thoroughly with 0.05% (v/v) Tween 20 in PBS five times before the bound proteins were eluted in SDS-PAGE sample buffer.

For *in vitro* immunoprecipitation, purified recombinant enzymes were pre-incubated at 37 ˚C for 1 h in 10 μL methylation buffer (see below) without DTT, followed by the addition of 2.0 μg anti-PRMT2 antibody (PRMT2-340, Abcam) or 2.0 μg mouse IgG (15381, Sigma), and the volume was adjusted to 500 μL with co-IP buffer [50 mM HEPES-KOH, pH 7.4, 150 mM NaCl, 1× protease inhibitor cocktail]. The protein/antibody mixtures were incubated at 4 ˚C for 4 h with rotation before combining with 50 μL pre-washed protein G-sepharose (Invitrogen) and

incubating with rotation overnight at 4 ˚C. The resin was washed with PBS six times before the bound proteins were eluted in SDS-PAGE sample buffer.

For Western blots, proteins were separated on 10% SDS-PAGE gels and transferred to nitrocellulose membranes. The membranes were blocked with 5% (w/v) milk in TBS buffer (50 mM Tris-HCl, pH7.6, 150 mM NaCl) at 37°C for 2 h and blotted with monoclonal anti-c-Myc antibody (9E10, Sigma), monoclonal anti-HA antibody (HA-7, Sigma), monoclonal anti-PRMT1 antibody (PRMT1-171, Sigma), or monoclonal anti-PRMT2 antibody (PRMT2-340, Abcam) in 3% (w/v) milk in TBST buffer [50 mM Tris-HCl, pH7.6, 150 mM NaCl, 0.1% Tween 20 (v/v)] at 4 °C for 16 h. Goat anti-mouse light chain horseradish peroxidase-conjugated secondary antibody (Millipore) or goat anti-mouse IgG-HRP (sc-2005, Santa Cruz) and ECL Western blotting detection reagents (GE Healthcare) were used for protein visualization. All co-IPs and Western blots present in this dissertation have been repeated at least twice with minor modifications to procedures. Experimental conditions listed herein as well as in section 3.2 and section 4.2 are the optimized conditions.

Methylation assays. Purified PRMTs and mutants were pre-incubated at 37 ˚C for 1 h in methylation buffer (50 mM HEPES-KOH, pH 8.0, 10 mM NaCl, 1 mM DTT) as previously described to equilibrate heteromeric complexes (*9, 135*) before initiating the methylation reaction with final concentrations of 10 μM histone H4 and 100 μM *S*-adenosyl-L-[*methyl*-^{14}C]methionine (Perkin Elmer; 1.8056 Gbq mmol^{-1}; concentrated as described in (*135*)). Either wild type or mutant PRMT concentrations were fixed and the other increased to molar ratios of 0, 2, 4, 7, 11, 19, 30, and 50 with one noted exception (Figure 2.1C). The final concentration of glycerol was less than 2.5% so that enzyme activities were not affected (*9, 135*). Methylation proceeded at 37 ˚C for 1 h where PRMT1 was held constant and 16 h where PRMT2 was held

constant, and stopped by a 10-min incubation at 90 ˚C. Proteins from reactions were separated on 15% tricine gels and exposed to storage phosphor screens for 18 h before imaging on a Typhoon 9400 (GE Healthcare).

Enzyme kinetics. Apparent enzymatic kinetic parameters were determined at a 25:750 nM (1:30) ratio for PRMT1 with its E153Q mutant, and PRMT1 with the PRMT2 E220Q mutant. Reactions were preformed similar to the gel assays described above in methylation buffer with a 1-h pre-incubation of the enzymes at 37 ˚C in the absence of substrates to equilibrate heteromeric complexes. The 1:30 ratio was chosen because it is the minimum ratio that produces the maximum increase in PRMT1 activity observed in Figure 2.1, and the PRMT1 concentration falls within the linear range of the enzyme since a linear increase in the formation of methylated arginines with increasing enzyme from 6.25 to 100 nM was observed (Figure A.2). For both groups of enzymes, reactions to determine the apparent kinetic parameters with histone H4 were performed with a constant 100 μM AdoMet and varied histone H4 concentrations of 0, 0.25, 0.5, 1.0, 2.0, 5.0, 10, 20, 30, and 40 μM. Reactions to determine the apparent kinetic parameters for AdoMet were performed with a constant 40 μM histone H4 and varied AdoMet concentrations of 0, 0.25, 0.5, 1.0, 2.0, 5.0, 10, 20, 50, and 100 μM. Reactions were stopped by a 10-min incubation at 90 ˚C and the dried samples were hydrolyzed with 6.0 M HCl at 110 ˚C for 24 h under vacuum. All titration experiments have been repeated at least twice.

An Agilent 1290 Infinity LC system was connected to a Waters UPLC BEH C18 column (2.1 x 100 mm) at a 0.15 mL/min flow rate at 45 ˚C. The mobile phases 0.1% aqueous formic acid and 0.05% TFA (A) and 0.1% formic acid, 0.05% TFA, and 30% methanol (B) were used in a linear gradient of 0 to 20% B over 2.3-min. Samples were analyzed on an AB SCIEX 5500 QTRAP tandem mass spectrometer using positive ion multiple reaction monitoring in separate

channels for MMA and aDMA. Parent and fragment ions, respectively, used for quantitation corresponded to amino acids as follows: MMA, 189 m/z and 74 m/z; aDMA, 203 m/z and 46 m/z. The cone voltage was 30 V and the collision energy was 20 eV for aDMA and 17 eV for MMA. Apparent enzymatic kinetic parameters were determined by fitting the data to the Michaelis–Menten equation using SigmaPlot 8 (SYSTAT). The k_{cat} values were calculated based on the molecular weight of the active monomer.

Methylation in cells. Approximately 8×10^6 HeLa cells cultivated in a 100-mm dish were transfected with mammalian expression vectors (24 μg total DNA; 12 μg each construct for co-transfections) using Lipofectamine 2000 (Invitrogen) following the manufacturer's protocol. After transfection, cells were harvested and resuspended in 1.0 mL 50 mM sodium phosphate, pH 7.5. Cells were lysed by four 10-s sonicator pulses (50% duty; setting "2") on ice, and centrifuged at 18,000 × *g* for 30 min at 4 ˚C. Total protein concentrations were determined using Bradford protein assay (Biorad).

For simultaneous quantification of MMA, aDMA, and sDMA using mass spectrometry, 100 μL aliquots (approximately 200 μg protein) of cell lysates from transfected HeLa cells described above were mixed with an equal volume of acetone and dried in a vacuum centrifuge. Dried samples were hydrolyzed as described above and reconstituted in 300 μL of 10 mM NaH_2PO_4, pH 5.0 and basic amino acids were purified using Oasis MCX solid phase extraction cartridges (Waters) according to previously described methods (45). Dried purified samples were reconstituted in 100 μL 0.1% aqueous formic acid and 0.05% TFA. Simultaneous quantification of MMA, aDMA, sDMA, and histidine was achieved with a Waters Acquity chromatographic system using the column, mobile phases, and conditions as described in the *Enzyme kinetics* section. A Quatro Premier XE electrospray tandem mass spectrometer

(Micromass MS Technologies) was operated in positive ion mode multiple reaction monitoring in separate channels for MMA, aDMA, sDMA, and histidine. Parent and fragment ions, respectively, used for quantitation corresponded to amino acids as follows: MMA, 189 m/z, and 74 and 144 m/z; aDMA, 203 m/z and 46 m/z; sDMA, 203 m/z and 172 m/z; histidine 156 m/z and 110 m/z. In all cases the cone voltage was 30 V and the collision energy was 20 eV except for MMA where it was 17 eV.

Using the above conditions we were able to unambiguously differentiate aDMA and sDMA despite having similar retention times and the same parent ion mass. Even at concentrations used for standards, 5.0 μM or higher aDMA was not spuriously detected as sDMA and *vice versa* (Figure A.3). Standards of MMA, aDMA, and sDMA (Sigma) were used to prepare standard curves for quantification. All derived concentrations for MMA, aDMA, and sDMA were normalized by the relative peak area for histidine to control for differences in total protein (values typically varied less than 10%). Histidine was used for this purpose because it is a basic amino acid that is retained on SPE cartridges along with arginine derivatives (data not shown). All samples were prepared in quadruplet and total MMA, aDMA, and sDMA derived from vector-only controls (average values are 0.73 ± 0.05, 8.2 ± 0.4, and 1.1 ± 0.05 μM, respectively) were subtracted from experimental values. HeLa cells untransfected and transfected with the vector-only controls differed less than 10% in methylarginine content.

2.3 Results

PRMT2 and its inactive mutant potentiate the methylation activity of PRMT1 *in vitro*. In our previous work, the comparatively high activity of PRMT1 towards histone H4 contrasted to the approximately 600-fold lower activity of PRMT2 towards the same substrate (*9*). My collegues and I wanted to then test if these two enzymes could interact and thereby change their respective activities. In the present study when we mixed both enzymes with substrates at stoichiometric concentrations no change in histone H4 methylation occurred (data not shown). When 2- to 50-fold excess PRMT2 was pre-incubated for 1 h with PRMT1 prior to the addition of AdoMet and histone H4, up to a 6.7-fold increase in methylation activity was found at the highest enzyme ratio as measured by densitometry (Figure 2.1A). Importantly, to elicit the synergistic increase in methylation activity, PRMT1 and -2 were pre-incubated for 1 h without substrates in accordance with our previous studies on PRMT interactions (*135*). These facts suggest that the effect was caused by a direct interaction between PRMT1 and -2.

We wanted to then determine who was activating whom by first creating catalytically inactive PRMT1 mutation E153Q (*22*) and the corresponding E220Q mutation in PRMT2 (Figure A.5A). As shown in Figure 2.1B and Figure 2.1C, increasing E153Q or E220Q with a constant concentration of wild type PRMT1 demonstrated a maximum 15-fold and 8-fold increase in histone H4 methylation, respectively. To show that the results from Figure 2.1A-C were not the result of non-specific protein binding, the same amounts of bovine serum albumin (BSA) were pre-incubated with PRMT1, which showed in Figure 2.1D a comparatively modest increase (1.8-fold) in PRMT1 activity at the highest BSA concentration. These results imply that the increase in PRMT1 activity observed with PRMT2 (Figure 2.1A), as well as with the mutants of PRMT1 (Figure 2.1B) and PRMT2 (Figure 2.1C) were the result of specific protein-protein

interactions. In contrast, increasing wild type PRMT2 with a constant concentration of E153Q did not result in any above-background methylation of histone H4 (Figure 2.1E). These results indicate that PRMT2, independent of its own activity, increased the activity of PRMT1. Moreover, the synergistic effect of E153Q on PRMT1 activity suggests that a higher order oligomeric complex may be required for maximum PRMT1 activity.

In order to test for any change in PRMT2 activity in response to other PRMT subunits, a constant concentration of PRMT2 was incubated with increasing concentrations of E153Q (Figure 2.1F) and E220Q (Figure 2.1G). Increasing E153Q and E220Q resulted in 1.4-fold and 2.1-fold increases in PRMT2 activity up to molar ratios of 11 and 19, respectively, before dropping off to background levels. Similar titrations were performed with constant PRMT2 and increasing BSA, which exhibited no increase in PRMT2 activity (Figure 2.1H).

Since PRMT1 methylation of histone H4 at the Arg-3 position has already been well established (*78, 79*), and we have demonstrated PRMT2 activity towards histone H4 *in vitro* (*9*) (Figure A.5), we wanted to determine if PRMT2 affected where PRMT1 methylates histone H4. Wild type histone H4 and its R3K mutant were used as substrates for pre-incubated PRMT1, PRMT2, and a mixture of both enzymes. In all cases where the histone H4 R3K mutant was employed the level of methylation was similar to the level of automethylation for the respective enzyme, whereas when wild type histone H4 was used the level of methylation was higher than the no-substrate control and histone H4 R3K substrate reactions (Figure A.6). The pre-incubated combination of PRMT1 and -2 produced the highest amount of arginine methylation formed on wild type histone H4. These results confirmed that the major site of methylation on histone H4 *in vitro* is R3 for PRMT1 and -2 individually and together.

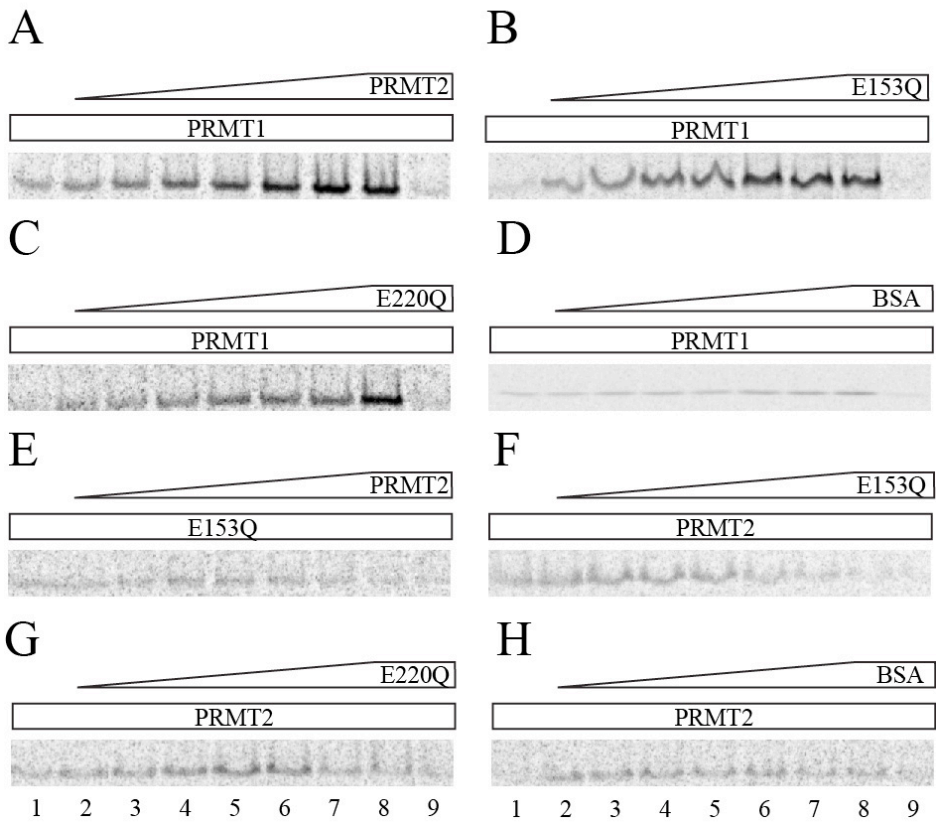

Figure 2.1. Synergistic methylation of histone H4 by PRMT1 and -2. Pre-incubations of enzymes without substrates were performed at 37 ˚C for 1 h in methylation buffer prior to initiating 1-h methylation reactions. (A) Reactions included 100 nM PRMT1 alone (*lane 1*), 100 nM PRMT1 with 210 to 5000 nM PRMT2 (*lanes 2-8*), and 5000 nM PRMT2 alone (*lane 9*). Similar reactions were prepared with PRMT1 and (B) PRMT1 E153Q, (C) 100 to 2500 nM PRMT2 E220Q, and (D) BSA. (E) Samples were prepared as in (A) except 100 nM PRMT1 E153Q was used in place of PRMT1. (F) Pre-incubations were performed as in (A) with 400 nM PRMT2 alone (*lane 1*), 400 nM PRMT2 with 800 to 20000 nM PRMT1 E153Q (*lanes 1-8*), and 20000 nM PRMT1 E153Q alone (*lane 9*) prior to initiating 16-h methylation reactions. Similar reactions were prepared with PRMT2 and (G) PRMT2 E220Q, and (H) BSA. Coomassie-stained gels and full-size storage phosphor images are shown in Figure A.4.

The effect of the interactions between PRMT1 and the inactive mutants of PRMT1 and PRMT2 on enzyme kinetics of PRMT1 were determined by estimation of apparent enzyme kinetic parameters. We intentionally avoided estimations where both enzymes were active since this scenario would be too complex to model and difficult to interpret. We note, however, that the potential for catalytically inactive enzyme to bind substrate could be a possible confounding variable in the estimation of apparent K_M.

The initial rate of PRMT1 in the presence of E153Q or E220Q with a fixed concentration of AdoMet and variable histone H4 are plotted in Figure 2.2A and the apparent kinetic parameters are displayed in Table 2.1. Both enzyme combinations demonstrated enhanced activities comparing to PRMT1. When combined with E153Q the histone H4 V_{max} for PRMT1 was more than 4-fold greater than PRMT1 alone and the k_{cat} was more than 2.5-fold higher. Smaller increases in V_{max} and k_{cat} were also observed for PRMT1 with E220Q. This difference appears to be driven primarily by a doubling in the rate of formation of aDMA in the PRMT1/E153Q groups versus the PRMT1/E220Q groups (Figure A.7). PRMT1 with E153Q or E220 resulted in a 2- or 4-fold reduction in K_M for histone H4, respectively when compared to PRMT1 alone. The changes to PRMT1 activity were also reflected in a 6- to 5-fold increase in the histone H4 specificity constant (k_{cat}/K_M) for PRMT1 with E153Q or E220Q, respectively.

The initial rate of PRMT1 in the presence of E153Q or E220Q with a fixed concentration of histone H4 and variable AdoMet is plotted in Figure 2.2B and the apparent kinetic parameters are displayed in Table 2.1. As with histone H4 the AdoMet V_{max} and k_{cat} for PRMT1 with either mutant were increased with respect to PRMT1 alone. However, the AdoMet K_M for PRMT1 with E153Q resulted in a 3.5-fold increase compared to PRMT1 alone; a change not observed for PRMT1 with E220Q. The addition of mutants to PRMT1 resulted in an AdoMet k_{cat}/K_M for

PRMT1 with E153Q that was 0.33-fold less than PRMT1 alone while an AdoMet k_{cat}/K_M for PRMT1 with E220Q was 1.25-fold higher. Altogether, the results of these kinetic experiments suggest that various oligomeric combinations of PRMT1 with mutants of PRMT1 and PRMT2 exhibit different enzymatic activities and substrate specificities.

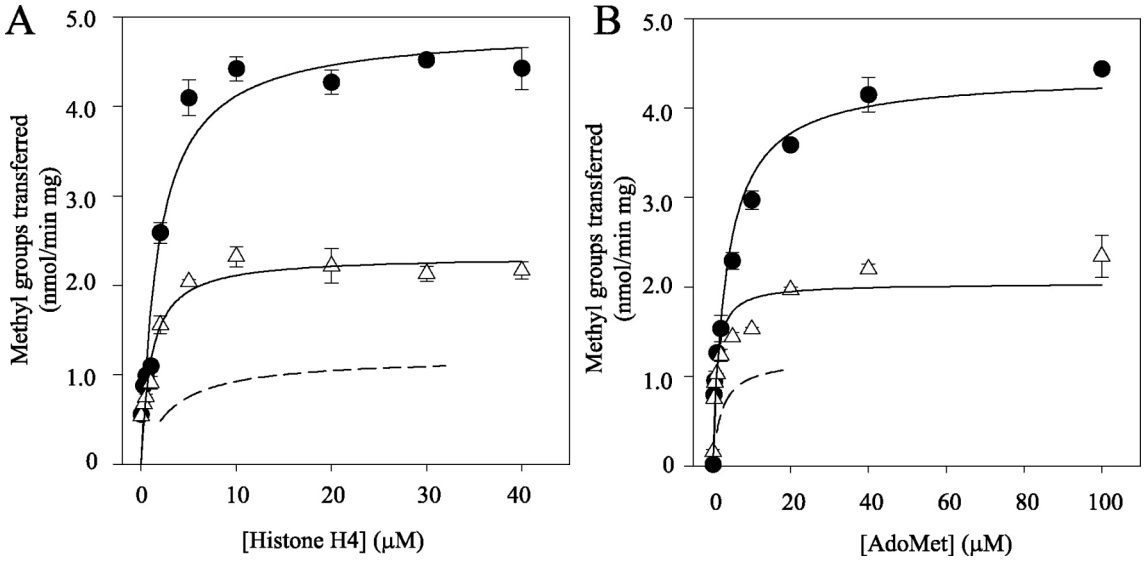

Figure 2.2. Synergistic methylation of histone H4 by PRMT1 with inactive PRMT1 and -2 mutants. The initial rate of enzymatic activity of PRMT1 with its E153Q mutant at a 25:750 nM ratio (*black circles*), and PRMT1 with the E220Q mutant of PRMT2 at a 25:750 nM ratio (*open triangles*). (A) The concentration of AdoMet was held constant at 100 μM and histone H4 was varied. (B) The concentration of histone H4 was held constant at 40 μM and AdoMet was varied. Shown are means and standard deviations of two samples determined using UPLC MS/MS. Total methylation was summed using the equation (2aDMA+MMA). For comparison, the initial rate of enzymatic activity of PRMT1 in the absence of other PRMTs (*dashed line*) using data replotted from reference (4) is shown. In this case the concentration of AdoMet was constant at 20 μM while histone H4 was varied (A), and the concentration of histone H4 was constant at 32 μM while AdoMet was varied (B).

Table 2.1. Apparent kinetic parameters for PRMT1 with E153Q or E220Q. The apparent kinetic parameters were determined by measuring initial rate of enzymatic activity of PRMT1 with its E153Q mutant at a 25:750 nM ratio, and PRMT1 with the E220Q mutant of PRMT2 at a 25:750 nM ratio, and were derived from the amount of total methylation. The values are listed as mean (S.D.) of two measurements.

Enzyme	Substrate	K_M (μM)	V_{max} (nmol/min mg)	k_{cat} (x10^{-3} s^{-1})	k_{cat}/K_M (M^{-1} s^{-1})
PRMT1/E153Q	AdoMet	3.5 (0.4)	4.4 (0.02)	3.2 (0.02)	910 (100)
PRMT1/E153Q	Histone H4	1.8 (0.1)	4.9 (0.1)	3.6 (0.1)	2000 (40)
PRMT1/E220Q	AdoMet	0.9 (0.04)	2.0 (0.07)	1.5 (0.05)	1700 (10)
PRMT1/E220Q	Histone H4	1.0 (0.01)	2.3 (0.1)	1.7 (0.08)	1700 (70)
PRMT1[a]	AdoMet	1.0 (0.1)	1.2 (0.2)	1.3 (0.2)	1400 (20)
PRMT1[a]	Histone H4	4.2 (0.2)	1.2 (0.2)	1.4 (0.2)	320 (40)

[a]Values derived from reference (4).

Ectopic expression of PRMT1 and -2 increases methylarginines in cells. To test whether PRMT2 and its inactive mutant can also potentiate the methylation activity of PRMT1 in a cellular environment, we transiently transfected HeLa cells with wild type and mutant PRMT1 and -2 individually and in combination. Cell lysates were hydrolyzed and analyzed for their MMA, aDMA, and sDMA content via tandem mass spectrometry. As shown in Figure 2.3, the concentrations of methylarginines are displayed after background subtraction from vector-only controls. The ectopic expression of PRMT1 or -2 alone resulted in small increases in MMA and aDMA as a likely consequence of increased PRMT levels. Interestingly, the levels of sDMA also increased, which neither PRMT1 nor PRMT2 are expected to make. HeLa cells transfected with E153Q or E220Q produced similar amounts of methylarginines to vector-only controls. On the other hand, HeLa cells co-transfected with PRMT1 and PRMT2 or its E220Q mutant produced a synergistic increase in aDMA and to a lesser extent MMA; results consistent with the observed increases in methylation *in vitro* (Figure 2.1). Surprisingly, a similar synergistic increase in the formation of sDMA was also observed with PRMT1 and -2 co-transfected cells, but not with PRMT1 and E220Q or E153Q and PRMT2, implying that the combination of enzymes can increase the formation of sDMA when PRMT1 is active. These dramatic increases in methylarginines detected by tandem mass spectrometry was not shown by Western blotting for aDMA in proteins (Figure A.8), so we were unable to pinpoint which substrates other than histone H4 were methylated higher in response to ectopically-expressed PRMT1 and -2 as compared to controls.

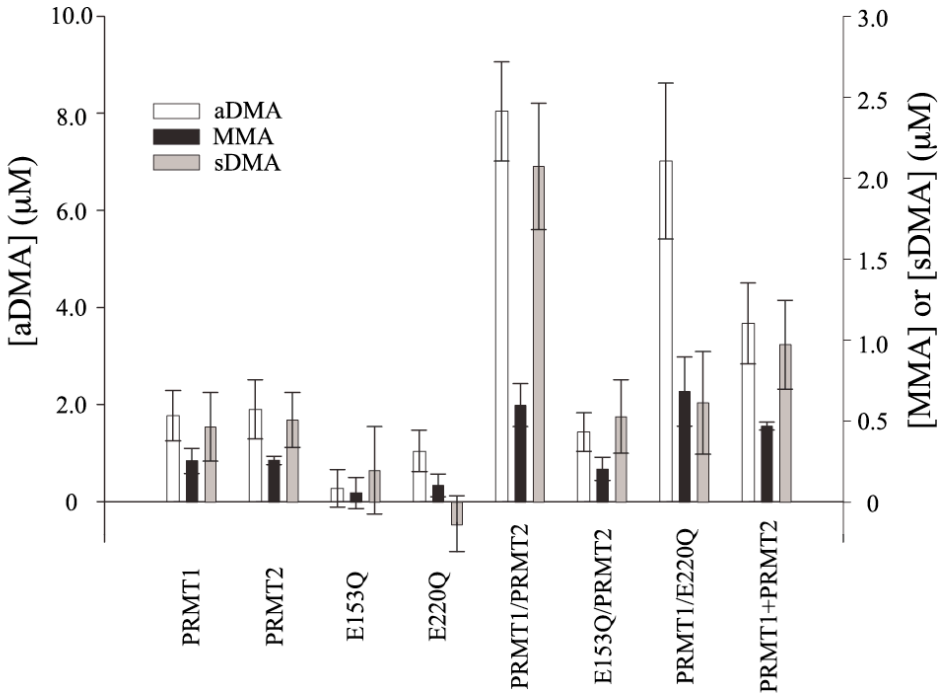

Figure 2.3. PRMT1- and PRMT2-dependent increases in cellular methylarginines. Cell lysates from transfected HeLa cells were prepared for tandem mass spectrometry to quantify protein-associated MMA, aDMA and sDMA. Concentrations are reported after background subtraction from the vector-only control. The set of bars on the *far right* shows the sum of PRMT1 and -2 groups to reveal the synergistic methylation with PRMT1/2 and PRMT1/E220Q groups. Values represent the mean and standard deviation (n = 4). Due to large differences in analyte concentrations, the *right* y-axis is scaled for MMA and sDMA, and the *left* y-axis is scaled for aDMA.

PRMT1 and -2 interact *in vitro* and in cells. To confirm a direct interaction between PRMT1 and -2 implied by *in vitro* experiments described above, I performed *in vitro* co-immunoprecipitation experiments between wild type and inactive mutants of PRMT1 and PRMT2. Regardless of whether the enzymes were wild type or mutant, the immunoprecipitated proteins were enriched above the level of the IgG controls (Figure 2.4A). These results demonstrated that PRMT1 and PRMT2 can interact directly in the absence of both AdoMet and protein substrates. Moreover, the *in vitro* interaction between these enzymes was not dependent upon their enzymatic activities based on binding results with E153Q and E220Q mutants.

I then tested if PRMT1 and -2 interact in cells. I expressed HA-tagged PRMT1, E153Q, PRMT2, and E220Q in HeLa cells, immunoprecipitated the HA-tagged proteins, and performed Western blots for endogenous PRMTs. Consistent with the *in vitro* co-immunoprecipitation results, endogenous PRMT2 was co-immunoprecipitated with HA-tagged PRMT1 or E153Q (Figure 2.4B). Similarly, endogenous PRMT1 was co-immunoprecipitated with HA-tagged PRMT2 or E220Q (Figure 2.4C). These results suggest that PRMT1 and -2 interact in cells as well. I also noticed that endogenous PRMT2 was also co-immunoprecipitated with HA-tagged PRMT2 or E220Q (Figure A.9A).

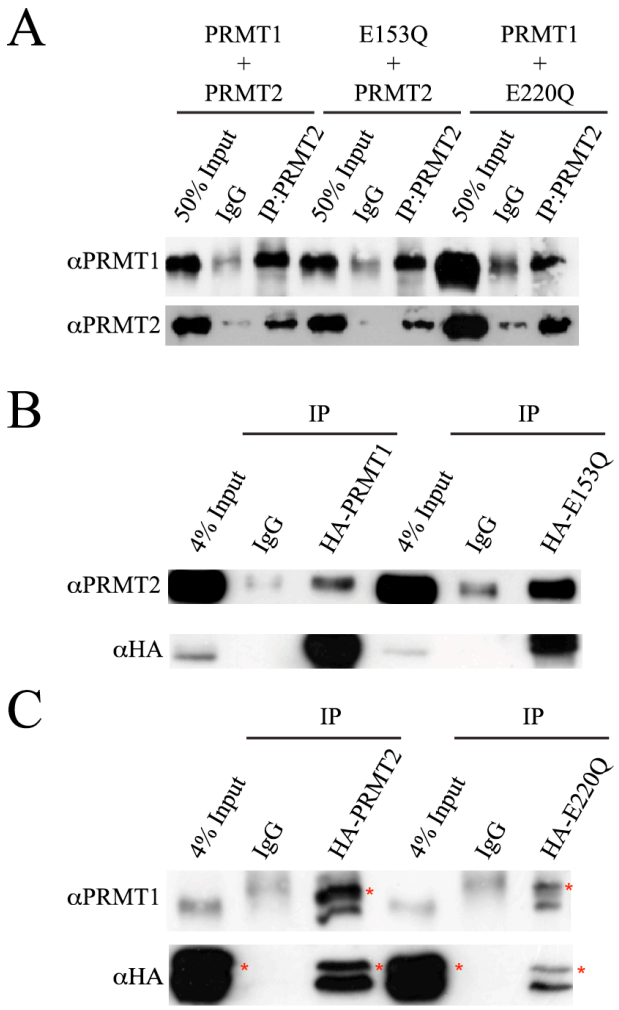

Figure 2.4. PRMT1 and -2 co-immunoprecipitate *in vitro* and in cells. (A) Indicated combinations of PRMTs (0.5 μg each) were pre-incubated at 37 ˚C for 1 h in methylation buffer and subsequently immunoprecipitated with anti-PRMT2 antibody, or with mouse IgG (negative control). Immunoprecipitates were immunoblotted with either anti-PRMT1 (*top)* or anti-PRMT2 (*bottom)* antibodies. (B) HA-PRMT1 and HA-E153Q were expressed in HeLa cells and cell lysate was immunoprecipitated with anti-HA antibody, or with mouse IgG (negative control). Immunoprecipitates were immunoblotted with anti-PRMT2 (*top)* or anti-HA (*bottom)* antibodies. (C) HA-PRMT2 or HA-E220Q was expressed in HeLa cells, and cell lysate was immunoprecipitated with anti-HA antibody, or with mouse IgG (negative control). Immunoprecipitates were immunoblotted with anti-PRMT1 (*top)* or anti-HA (*bottom)* antibodies. Non-specific bands are labeled with *red asterisks*.

Visualization of PRMT interactions in cells. In order to capture potential interactions between PRMTs in cells, I employed a technique that was initially pioneered by Regan and coworkers, who showed that the stable reconstitution of green fluorescent protein (GFP) from its N- and C-terminal fragments (*i.e.*, separate polypeptides) is only mediated by interacting proteins attached to each fragment of GFP (*138, 139*). Kerppola and coworkers adapted this concept to fluorescence microscopy in mammalian cells, which is referred to as bimolecular fluorescence complementation (BiFC) (*140*). BiFC has since emerged as a powerful tool for capturing images of specific and even transient protein-protein interactions in cells (*141-144*). An important feature of this technique is that requisite post-translational modifications, sub-cellular localization, and association with other proteins that may facilitate specific protein binding can occur within the native environment provided by the mammalian host cell. Expression vectors that produce N- and C-terminal fragments of the fluorescent protein mCitrine (*145*) fused to wild type and mutant PRMTs were designed to test for reconstituted fluorescence as evidence of PRMT-PRMT interactions in cells. Negative control vectors were devoid of PRMT genes.

Using BiFC in HeLa cells that were transiently co-transfected with mCitrineN-PRMT1 and PRMT1-mCitrineC (Figure 2.5A), I observed robust fluorescence signal via confocal microscopy that provides direct evidence that PRMT1 has the capacity to self-associate in the nucleus of cells (Figure 2.5Bi). When PRMT2 was tested in different BiFC combinations, only co-expression of mCitrineN-PRMT2 and PRMT1-mCitrineC resulted in a fluorescence signal (Figure 2.5Biv), revealing a potential orientation-specific interaction between PRMT1 and -2. Although detected in co-immunoprecipitation experiments (Figure A.9A), PRMT2 homodimerization with BiFC was not observed (Figure 2.5Bv). This result may be a function of the inability of PRMT2-mCitrineC to form any BiFC interactions despite its successful

expression in cells (data not shown). Additionally, the mCitrineN-PRMT1/ PRMT2-mCitrineC pair did not produce any above-background signal as well (Figure 2.5Bii), which may have been caused by insufficient expression of mCitrineN-PRMT1 (Figure A.10): this scenario is unlikely because the fusion protein was capable of participating in other BiFC complexes. In order to demonstrate that BiFC was selective for PRMT-PRMT interactions, HeLa cells were co-transfected with mCitrineN-Only or mCitrineC-Only in combination with mCitrine fragments attached to PRMTs, and these cells exhibited low-level background fluorescence (Figure 2.5Biii, Figure 2.5Bvi- Figure 2.5Bix). Therefore, fluorescence signals generated from PRMT1 and PRMT1/2 complexes represent specific protein-protein interactions in HeLa cells.

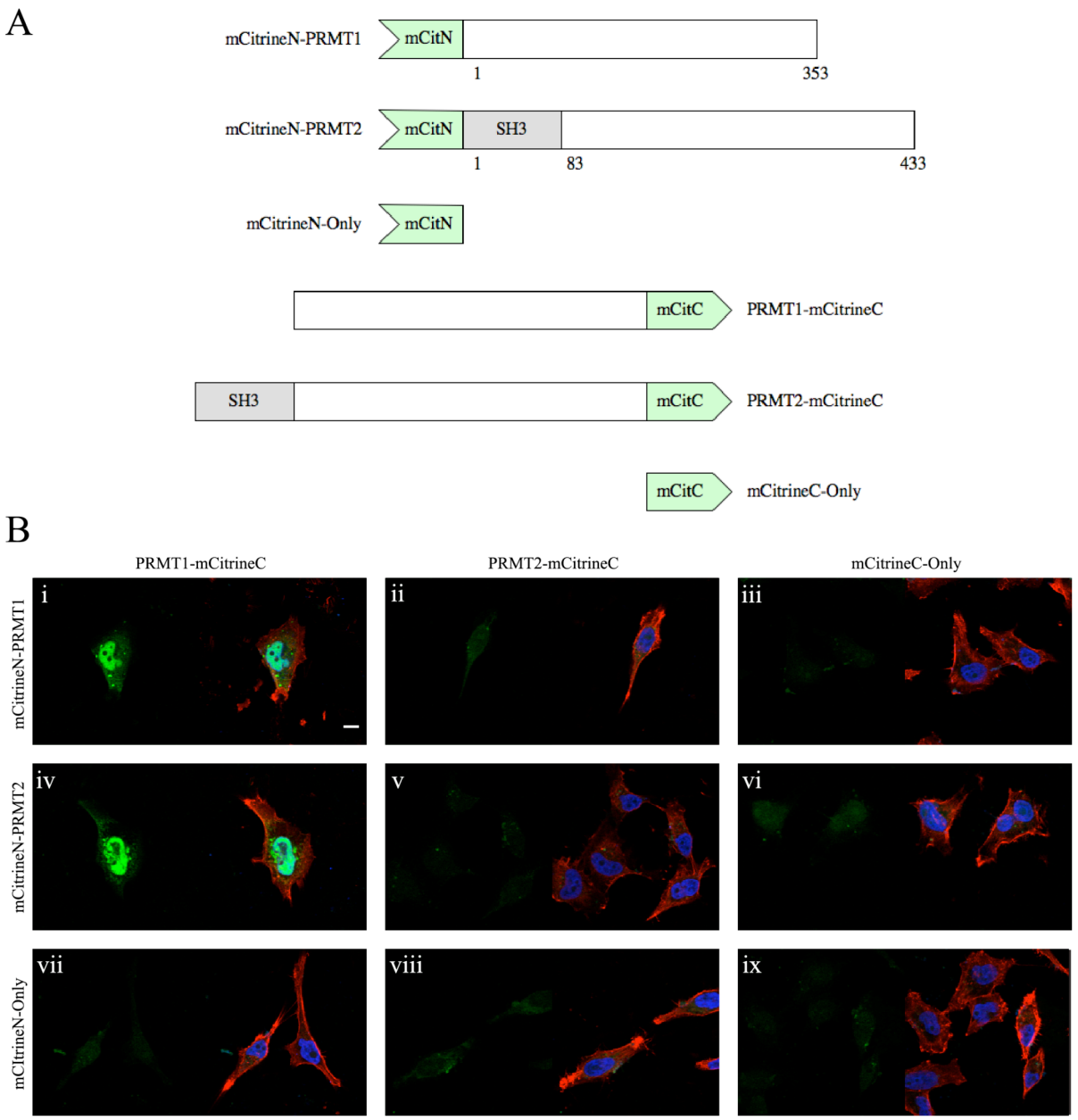

Figure 2.5. Visualization of PRMT1 and -2 interactions via BiFC. (A) An illustration of BiFC fusion proteins used in these experiments. (B) HeLa cells were co-transfected with the two constructs indicated in columns and rows (representative images are shown). The left image of each panel shows the formation of a BiFC complex. The right image of each panel shows an overlay of BiFC *(green),* DAPI (*blue*), and fluorescence-labeled phalloidin (*red*). The scale bar indicates 10 μm.

PRMT domains required for BiFC complex formation in cells. Having established an interaction between human PRMT1 and -2, I sought to determine the structural features important for their binding. Although no structure of the PRMT2 catalytic core has been solved, its 64% sequence similarity to PRMT1 within the arm region (PRMT1: residues 188-222; PRMT2: residues 256-294) evokes the possibility that PRMT2 may exhibit a similar binding modality (Figure 1.5). In order to test this hypothesis, BiFC constructs of PRMT1 and -2 lacking their respective dimerization arms were co-transfected in combination with wild type enzymes (Figure 2.6A). Consistent with results from a previous study that showed the requirement of the dimerization arm for PRMT1 oligomerization (*22*), the PRMT1Δ188-222 mutant did not yield any fluorescence indicative of a PRMT1 complex (Figure 2.6Bi and Figure 2.6Bii) or PRMT1/2 complex (Figure 2.6Bv). These negative BiFC results were not due to unsuccessful co-transfection of HeLa cells since these proteins were detected by Western blot analysis (Figure A.10). Some fluorescence signal in cells expressing the mCitrineN-PRMT2Δ256-294/ PRMT1-mCitrineC pair were detected; however, co-immunoprecipitation results between HA-PRMT2Δ256-294 and endogenous PRMT1 did not show any interaction **(**Figure A.9B), making our results pertaining to the dimerization arm of PRMT2 inconclusive.

I explored the possibility that the SH3 domain of PRMT2 may mediate complex formation. Clarke, Bedford and coworkers had previously shown that the PRMT2 SH3 domain could interact with the N-terminus of PRMT8, which contains two stretches of proline-rich amino acid sequences (*42*). Even though PRMT1 does not contain any polyproline sequences, perhaps the SH3 domain of PRMT2 could potentially mediate an interaction with PRMT1. Therefore, the BiFC construct in which the PRMT2 SH3 domain was deleted (ΔSH3PRMT2) was co-transfected with PRMT1-mCitrineC to explore this possibility. As shown in Figure 2.6Bvii,

even without its SH3 domain PRMT2 was still able to form the BiFC complex with PRMT1. This result indicates that the SH3 domain was not directly responsible for the interaction between PRMT1 and -2.

PRMT activity requirements for BiFC complex formation in cells. To further explore conditions that affect PRMT-PRMT interactions in HeLa cells, BiFC constructs of E153Q and E220Q mutants were employed (Figure 2.7A). Cells expressing combinations of wild type and mutant PRMT1 showed BiFC signals (Figure 2.7Bi, Figure A.11i, and Figure A.11ii), indicating that enzyme activity from one or both subunits was not a requirement for self-association. When E153Q was tested with PRMT2, no above-background fluorescence was observed (Figure 2.7Bii), thus directly implicating PRMT1 activity as a requirement for the formation of the BiFC complex between PRMT1 and -2 in cells. This result contrasts with the co-immunoprecipitation results for E153Q and PRMT2 for which an interaction was detected (Figure 2.4), revealing that PRMT1 inactivity from the E153Q mutation prevented reassembly of fluorescent protein fragments. Interestingly, when the combination of E153Q and ΔSH3PRMT2 was tested for BiFC, a predominantly nuclear fluorescence signal was observed (Figure 2.7Biii). The results of these pairings imply that the BiFC complex between PRMT1 and -2 requires PRMT1 activity, but not when the SH3 domain of PRMT2 is removed.

The E220Q mutation behaved similarly to wild type PRMT2 in the BiFC assay with wild type PRMT1 (Figure A.11iii) and E153Q (Figure 2.7Biv). These results indicate that PRMT2 activity is not required for its interaction with PRMT1 and does not contribute to formation of the PRMT1/2 complex.

Since the PRMT1 E153Q mutation prevented its interaction with full length PRMT2, I wanted to see if small-molecule inhibition of methyltransferase activity could also affect the

interaction between PRMT1 and -2. Thus, I tested these BiFC combinations in the presence of 20 μM AdOx, which raises the intracellular levels of *S*-adenosyl-L-homocysteine to globally inhibit the methylation of arginine residues and other AdoMet-dependent enzyme substrates (*35, 63*). HeLa cells grown in AdOx did not appear to affect BiFC complex formation for PRMT1 constructs (Figure 2.7Bv), thus providing further evidence that PRMT1 activity is not essential for its self-association. When PRMT1 was tested for BiFC with PRMT2 in AdOx-treated cells, however, little if any fluorescence was observed (Figure 2.7Bvi and Figure 2.7Bviii). This result is similar to what occurred between both wild type and mutant versions of PRMT2 and E153Q (Figure 2.7Bii and Figure 2.7Biv), and it is also consistent with the result for the PRMT1/2 co-immunoprecipitation performed in AdOx-treated cells for which no enrichment over background was observed (Figure 2.8A). In contrast, deletion of the PRMT2 SH3 domain did not affect its interaction with PRMT1 in the presence of AdOx as determined by BiFC (Figure 2.7Bvii) and by co-immunoprecipitation (Figure 2.8B), providing additional evidence that the interaction between PRMT1 and -2 exhibits an SH3-dependent sensitivity to the state of methylation within the cell.

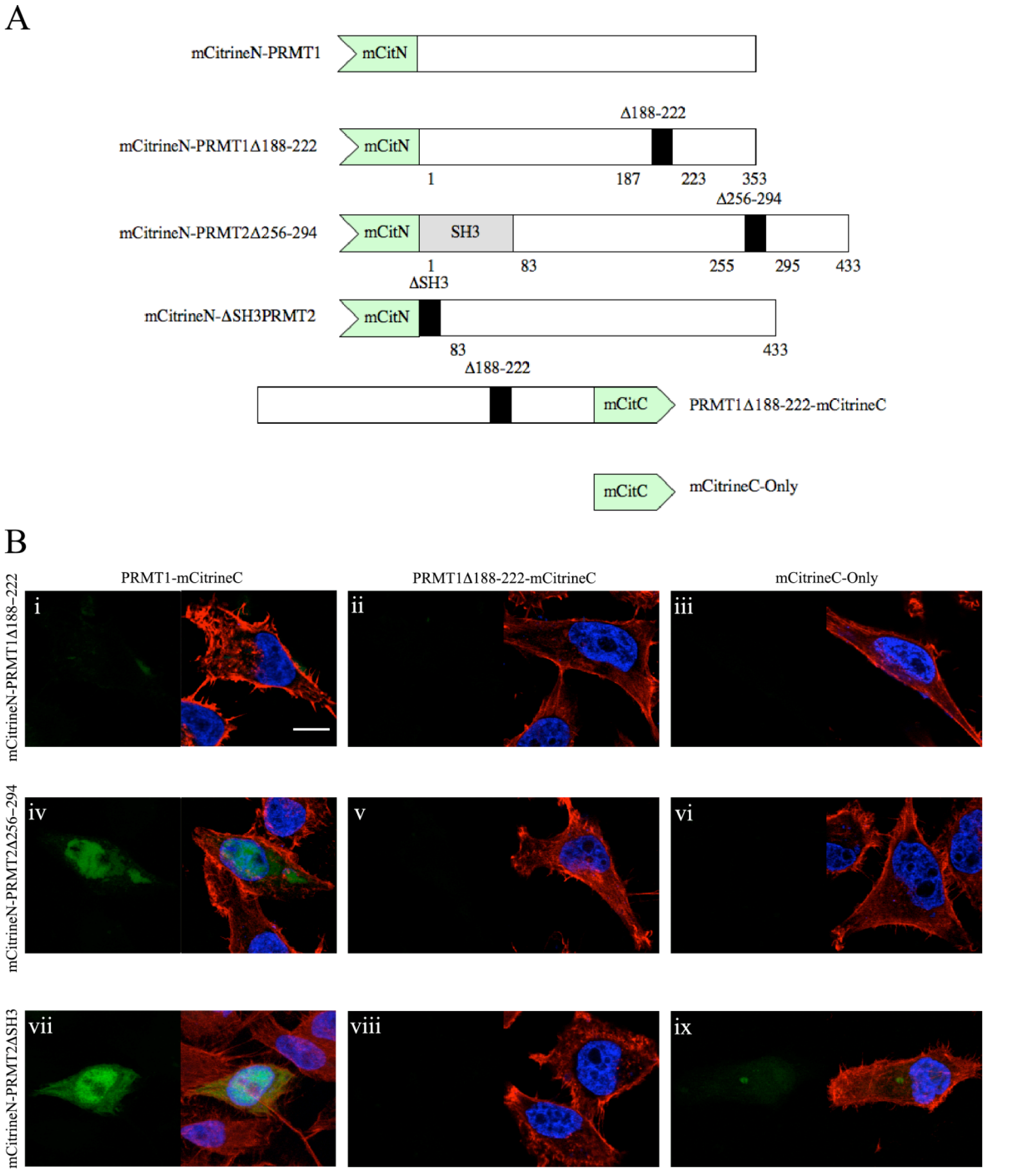

Figure 2.6. Effects of domain deletions in PRMT1 and -2 on BiFC complex formation. (A) An illustration of BiFC fusion proteins used in these experiments. (B) HeLa cells were co-transfected with the two constructs indicated in the columns and rows (representative images are shown). The left image of each panel shows the formation of a BiFC complex. The right image of each panel shows an overlay of BiFC (*green*), DAPI (*blue*), and fluorescence-labeled phalloidin (*red*). The scale bar indicates 10 μm.

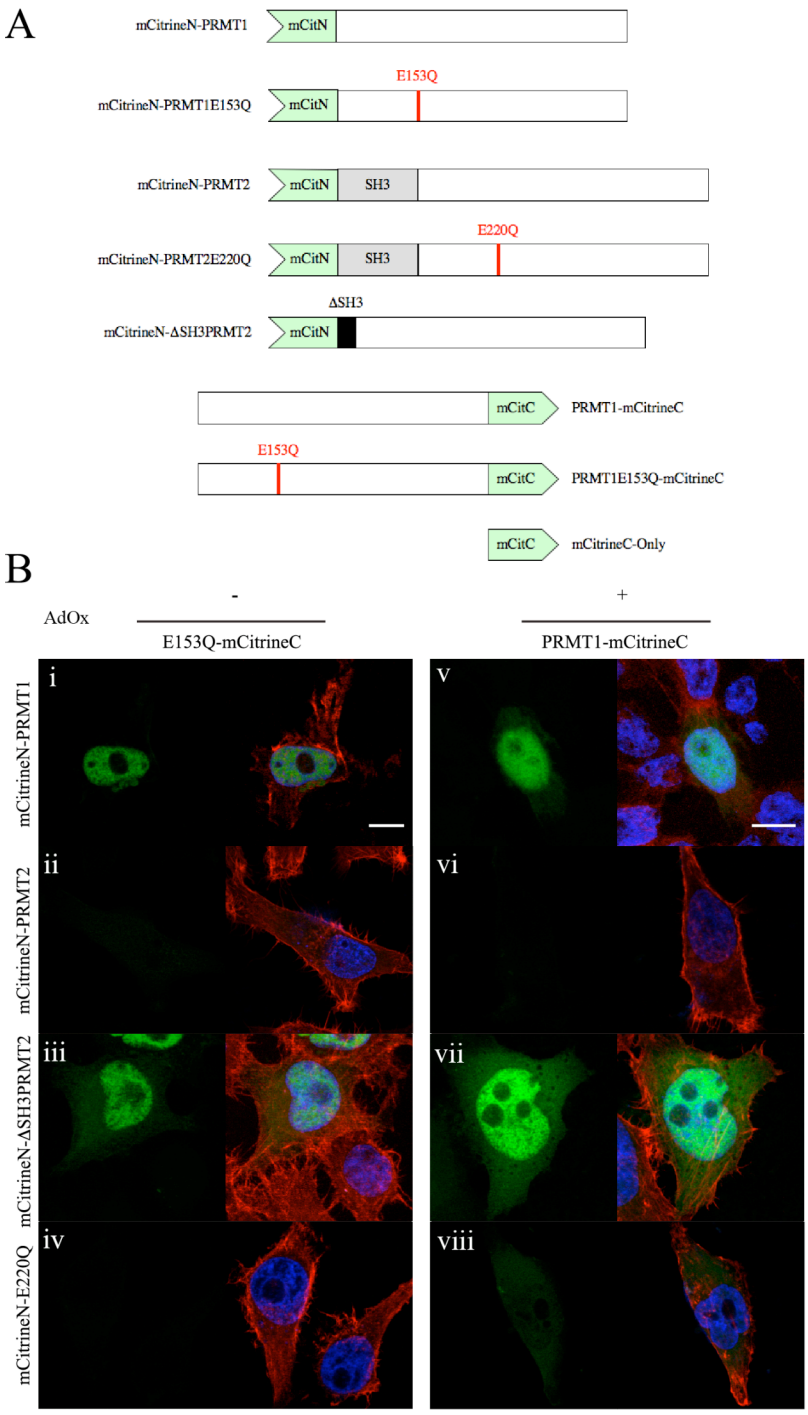

Figure 2.7. Effects of catalytically inactive PRMT1 and -2 on BiFC complex formation. (A) An illustration of BiFC fusion proteins used in these experiments. (B) HeLa cells treated with or without 20 μM AdOx were co-transfected with the two constructs indicated in the columns and rows (representative images are shown). The left image of each panel shows the formation of a BiFC complex. The right image of each panel shows an overlay of BiFC *(green),* DAPI (*blue*), and fluorescence-labeled phalloidin (*red*). The scale bar indicates 10 μm.

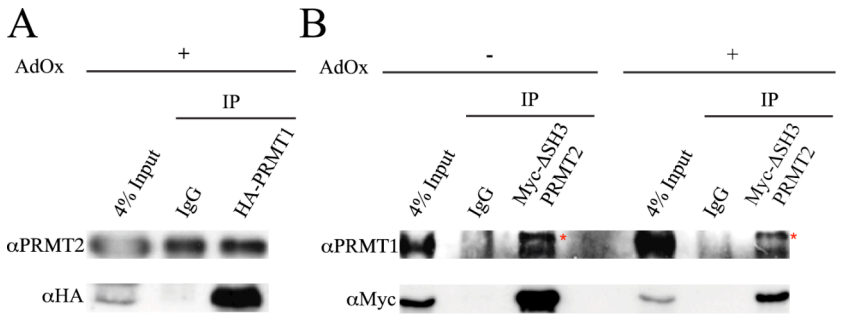

Figure 2.8. Co-immunoprecipitations of PRMT1 and PRMT2 in hypomethylated cells. (A) HA-PRMT1 was expressed in HeLa cells treated with 20 μM AdOx, and cell lysate was immunoprecipitated with anti-HA antibody, or with mouse IgG (negative control). Immunoprecipitates were immunoblotted with anti-PRMT2 (*top)* or anti-HA (*bottom)* antibodies. (B) c-Myc-ΔSH3PRMT2 was expressed in HeLa cells treated with or without 20 μM AdOx, and cell lysate was immunoprecipitated with anti-Myc antibody, or with mouse IgG (negative control). Immunoprecipitates were immunoblotted with anti-PRMT1 (*top)* or anti-Myc (*bottom)* antibodies. Non-specific bands are labeled with *red asterisks*.

2.4 Discussion

Activated PRMT1 via PRMT2 association. The observation that PRMT1 is responsible for the bulk of total arginine methylation activity in cells (*29, 35*) suggests two possibilities: (i) PRMT1 is the enzyme solely responsible for most of this activity, or (ii) most of the activity is dependent on PRMT1, but not to the exclusion of other PRMTs. In this study a novel interaction between PRMT1 and -2 has been identified, providing evidence for the latter possibility in which PRMT1 shoulders most of the burden of transferring methyl groups as an activated complex with PRMT2.

Some studies have indicated that PRMT2 function in cells may be independent of any enzymatic activity, as in the cases where PRMT2 in complex with the retinoblastoma gene product RB is shown to repress the transcriptional activity of E2F1 (*128*), or where it is demonstrated to promote apoptosis by retaining IκB-α in the nucleus and prevent NF-κB-dependent transcription (*32*). The transcriptional co-activator functions of PRMT2, however, have been shown to require a functional enzyme (*45, 126, 127*). The ability of wild type and catalytically inactive PRMT2 to potentiate PRMT1 activity *in vitro* supports an interaction between the two enzymes in which PRMT2 plays a scaffolding role for PRMT1. This role is further supported by the observed increase in methylarginine levels when PRMT2 as wild type or inactive mutant was overexpressed in HeLa cells (Figure 2.3). The fact that sDMA also increased along with aDMA and MMA implies that PRMT5 activity or expression may have been affected by the PRMT2-dependent activation of PRMT1.

The role that PRMT2 played in activating PRMT1 in cells appeared to result from its ability to serve as a subunit of a heteromeric complex as demonstrated in our *in vitro* studies. The apparent kinetic parameters for both combinations of PRMT1 with either E153Q or E220Q

mutants showed augmented V_{max} and k_{cat} values compared to PRMT1 alone (Table 2.1), and differences in K_M values for PRMT1 towards histone H4 and AdoMet. Similar changes in enzymatic activity and substrate specificity have been observed with PRMTs based on interactions with other proteins. For example, immediate-early/primary response gene products have been shown to modulate PRMT1 activity (*7*). In addition, the substrate preference of PRMT5 can change depending on its interaction with either co-factor protein pICln or MEP50 (*146*). It follows then that other heteromeric complexes involving PRMT1 may form and exhibit altered activity and/or substrate specificity. In this study we can only speculate that the increases in PRMT1 activity with excess PRMT1 or PRMT2 subunits (Figure 2.2 and Figure 2.3) can be attributed to the formation of higher order oligomeric structures, perhaps resembling complexes observed for crystal structures of PRMT1 and its yeast homologue (*22, 25*).

PRMT1 and -2 associations in cells. The association between endogenous PRMT1 or 2 and HA-tagged PRMT1 or 2 from HeLa cells was demonstrated by Western blot analysis after co-immunoprecipitation (Figure 2.4B and Figure 2.4C). This interaction can barely be seen in a Western blot from another study where GFP-PRMT1 was co-immunoprecipitated from cells with GFP-PRMT2 using anti-PRMT2 antibodies (*21*), indicating that the interaction between PRMT1 and -2 may be transient with weaker binding affinity than what has been observed for PRMT1 and -6 homodimers (*135*). The use of BiFC in this instance has provided for an alternative means to capture direct partnering between PRMT1 subunits, as well as between PRMT1 and -2 subunits. Since deletion of the SH3 domain on PRMT2 did not eliminate complex formation, I was able to rule it out as a possible binding module directly responsible for the PRMT1/2 interaction Figure 2.6Bvii). Despite the fact that two PRMT2 subunits did not form a BiFC complex (Figure 2.5Bv), I was able to co-immunoprecipitate endogenous PRMT2

with HA-tagged PRMT2 (Figure A.9A). Indeed, Fackelmayer and coworkers as well as our own group have previously reported evidence for PRMT2 dimerization (*9, 21*).

In this study I used only one of the seven PRMT1 splice variants, PRMT1v1 (*73*). Both PRMT1v1 and PRMT2 do not contain nuclear localization signals within their sequences, but it is possible that the observed complexes may initially associate in either cytoplasmic or nuclear compartments and become trapped in the nucleus (Figure 2.5Bi and Figure 2.5Biv). I am aware that differences in the efficiency of fixation for organelles from experiment to experiment have been reported as a source of potential artifacts in the localization of soluble proteins (*147*). PRMT1, 2, and ΔSH3PRMT2 expressed individually in HeLa cells as fusions with full-length mCitrine were localized in both cellular compartments consistent with previous results (*13*), and this pattern was not altered when cells co-expressed mCitrine-PRMT1 and mCitrine-PRMT2 (Figure A.12). Fackelmayer and co-workers have demonstrated that PRMT sub-cellular localization can be different depending on the cell type (*21*). Thus, it is unclear if the mostly nuclear localization of BiFC complexes for PRMT1 and -2 observed in HeLa cells is representative of where they may reside in other cells. Additionally, PRMT1 isoforms characterized by Côté and coworkers that exhibited distinct sub-cellular localizations, particularly the PRMT1v2 isoform bearing a nuclear export signal that localizes it to the cytoplasm (*73*), may impact where PRMT1 interactions present as BiFC complexes in cells.

I have initiated experiments to see if PRMT2 can interact with any of the seven PRMT1 isoforms. My preliminary result indicates that a BiFC complex between PRMT2 and PRMT1v2 forms in both the cytoplasm and the nucleus (Figure A.13A, panel b), indicating that PRMT1v2 can be retained in the nucleus by interacting with PRMT2. Additionally, PRMT2 interacts with PRMT1v5 predominantly in the nucleus similar to what was observed with PRMT1v1 (Figure

A.13A, panel a, and Figure A.13A, panel d). The BiFC signal for PRMT2 and PRMT1v7 appears to concentrate in some type of nuclear granule structures (Figure A.13A, panel f). Lastly, only weak fluorescence signals at a comparable level to background fluorescence (Figure A.13A, panel g) was captured when mCitrineN-PRMT2 and PRMT1v4-mCitrineC or PRMT1v6-mCitrineC were co-expressed in HeLa cells (Figure A.13A, panel c, and Figure A.13A, panel e).

BiFC complexes formed from combinations of PRMT1 isoforms showed a range of different distributions within HeLa cells (Figure A.13A, panels h to y), including the nucleus (Figure A.13A, panel h, Figure A.13A, panel n, Figure A.13A, panel f), the cytoplasm (Figure A.13A, panel o, Figure A.13A, panel u, and Figure A.13A, panel v), large perinuclear cytoplasmic aggregates (Figure A.13A, panels h-m, p-s, and w-y), and nuclear granules (Figure A.13A, panel m, Figure A.13A, panel s, and Figure A.13A, panel y). To test whether PRMT7v7-mCitrineC interacts with mCitrineN-PRMT2 or the other mCitrineN tagged PRMT1 isoforms in the nucleolus, HeLa cells co-expressing mCitrineN-PRMT1v7 and PRMT1v7-mCitrineC were immunostained with the nucleolar marker Nop1 (Figure A.13B), which showed that these BiFC complexes do not localized to the nucleolus. Since all PRMT1v7-mCitrineC-containing BiFC complexes appeared to accumulate in large cytoplasmic and nuclear aggregates, it is possible that these aggregates are artifacts resulting from the expression of PRMT1v7-mCitrineC.

Methylation-dependent mediation of PRMT1/2 complex formation. The inactive PRMT1 E153Q mutant has been previously shown to exhibit similar oligomeric structure and AdoMet binding ability to that of the wild type enzyme (*22*). Using this mutation in our BiFC assay confirmed that PRMT1 self-association is independent of its catalytic activity (Figure

2.7Bi, Figure A.7i, and Figure A.7ii). AdOx treatment to reduce the methylation potential of the cell also did not impact PRMT1 pairing (Figure 2.7Bv), which is consistent with the finding from Fackelmayer and coworkers that a PRMT1-GFP fusion protein maintains a presence in a high molecular mass complex with or without AdOx treatment (*21*). In contrast, the interaction between PRMT1 and -2 was solely dependent upon PRMT1 activity as determined either by inactive mutant E153Q (Figure 2.7Bii, Figure 2.7Biv, and Figure A.7iii), as well as by AdOx treatment (Figure 2.7Bvi, Figure 2.7Bviii, and Figure 2.8A). Unlike PRMT1, AdOx treatment was shown to significantly reduce the mobility of PRMT2-GFP in cells, indicating, as the authors point out, that PRMTs respond differently to the accumulation of unmethylated substrates (*21*). In this study I have found that the interaction between PRMT1 and -2 appeared sensitive to the methylation state of one or more unknown substrates, which were presumably modified by PRMT1 based on evidence presented above.

A deletion of the SH3 domain in PRMT2 had restored PRMT1/2 complex formation regardless of PRMT1 inactivity or AdOx treatment. These results imply that the recognition of SH3 domain ligands, possibly as methylated substrates, impacts PRMT1/2 complex assembly. I propose that the SH3 domain or another mediator bearing a proline-rich sequence to which the SH3 domain can bind controls the formation of the complete complex.

A handful of PRMT2 SH3 domain ligands that are also methyl acceptors have already been identified. The first ligand shown to bind to PRMT2 through its SH3 domain is the arginine methyltransferase substrate hnRNP E1B-AP5, an interaction that is initially found via a yeast two-hybrid screen and demonstrated using co-immunoprecipitation and *in situ* immunofluorescence (*43*). In a protein domain microarray an immobilized GST-SH3 (PRMT2) was able to tightly bind to the core small nuclear ribonucleoprotein SmB′ and Sam68 (*125*), both

of which contain poly-proline stretches that are known recognition sequences for SH3 domain binding (*123*). Indeed, the proline-rich N-terminus of PRMT8 has also been shown to bind to the PRMT2 SH3 domain (*42*). Recently, a yeast two-hybrid screen identified an interaction between the PRMT2 SH3 domain and mammalian cleavage factor I (CF I_m59), which is an hnRNP and PRMT substrate that contains poly-proline sequences (*146*). Given the importance of the SH3 domain in mediating interactions for PRMT2, it is conceivable that the methylation state of specific substrates affects the interaction between PRMT1 and -2. The association of PRMT1 with its substrates such as hnRNP U (*87*) and Sam68 (*95*) suggests that these RNA-binding proteins are ideal candidates to serve an additional scaffolding role in mediating the interaction between PRMT1 and -2. Sam68 has been shown to bridge the interaction between PRMT1 and the *Mixed Lineage Leukemia* oncogenic complex (MLL-EEN) as a required scaffold for hematopoietic cell transformation, and mediating this interaction is the SH3 domain from MLL-EEN binding to poly-proline sequences in Sam68 (*148*). Since the SH3 domain is a unique feature of PRMT2 within its enzyme family, the identification of its endogenous ligands will aid in our understanding of its role in PRMT2 interactions.

3 Identification of Potential Binding Partners of the PRMT2 SH3 Domain[3]

3.1 Introduction

In the previous Chapter, I illustrated an example for a heteromeric PRMT complex, in which PRMT1 and -2 interact and result in an increased PRMT1 enzymatic activity. Evidence presented in Chapter 2 suggested that the PRMT2 SH3 domain, though was not required for the PRMT1/-2 interaction, may regulate this heteromeric PRMT complex formation by directing the associations among the PRMT2 subunit of the PRMT1/-2 complex and other PRMT2-associated proteins in a methylation-dependent fashion. In order to gain a better understanding of the formation mechanism of the PRMT1/-2 complex, I attempted to identify proteins interacting with PRMT2 through the PRMT2 SH3 domain. The PRMT2 SH3 domain-associated proteins, especially the ones that sense the methylation state in cells, are likely to be plausible regulators of the PRMT1/-2 complex. Additionally, recognizing the interacting partners of PRMT2 will help us to explore the functions of the less studied PRMT2 as well as the newly discovered heteromeric PRMT1/-2 complex.

In this Chapter, I will present a list of PRMT2 SH3 domain-associated proteins I have identified using GST-pull down assays. The fact that the majority of these identified PRMT2

[3] The DNA constructs GST-SH3(Abl) and GST-SH3(PRMT2) used for the GST-pull down study were gifts from Dr. Mark Bedford. A summer student, Jenny J. Kim expressed and purified GST-SH3(PRMT2). Kristina Hüsecken expressed and purified GST-SH3(Abl). Another summer student, Daisy Ji helped with the DNA construct design, expression and purification of the GST protein.

The PRMT1 knockdown HeLa cells were gifts from Dr. Jocelyn Côté. The mouse embryonic fibroblasts (MEFs) and the PRMT2 knockout MEFs were gifts from Dr. Maria Hatzoglou.

The LC-MS/MS proteomic study was preformed in the Proteomics Core Facility at UBC. The Core Facility manager, Suzanne C. Perry digested the protein samples and ran them on a LC-MS/MS followed by a MASCOT database search.

SH3 domain-associated proteins are splicing-related factors suggests that PRMT2 could play a potential role in pre-mRNA processing. A previously reported PRMT2 SH3 domain binder (*125*), Sam68 has also been identified in my GST-pull down assays. Moreover, the results presented in this Chapter reveal that Sam68, a known PRMT1 substrate (*95*), interacts with PRMT2 possibly through the PRMT2 SH3 domain in cells; and this interaction appears to affect the subcellular localization of Sam68 in HeLa cells treated with or without AdOx.

3.2 Methods

DNA constructs. A DNA construct coding for the glutathione-*S*-transferase (GST) protein from *Schistosoma japonicum* was generated by inserting a stop codon at the 3' end of the *GST* coding sequence in the pET41a(+) plasmid (Novagen) using the QuickChange site-directed mutagenesis method (Agilent Technologies) (see Table A.2 for primer sequences). pGEX-GST-SH3(Abl) and pGEX-GST-SH3(PRMT2) were gifts from Dr. Mark Bedford.

Protein expression and purification. Recombinant proteins GST, GST-SH3(Abl), and GST-SH3(PRMT2) were expressed in *E. coli* and purified using previously described methods (*9, 135*).

GST-pull down. Cells were harvested and lysed as described in section 2.2. Sample lysates containing 10 mg total protein from HeLa cells, or 2 mg total protein from wild type mouse embryonic fibroblast (MEFs), *PRMT2*$^{-/-}$ MEFs, and induced or non-induced *PRMT1* knock-down HeLa cells were incubated with 100 μg of GST, GST-SH3(Abl), or GST-SH3(PRMT2) in co-IP buffer [50 mM HEPES (pH 7.4), 150 mM NaCl, 1x proteases inhibitor cocktail (Roche)] at 4 °C for 2 hours with rotation. A volume of 50 μL of pre-washed glutathione (GSH)-sepharose (Genescript) was then added to each mixture. The GST pull down experiments were carried out at 4 °C for 2 hours with rotation in co-IP buffer with 0.1% NP-40 (Sigma). The resin was then washed five times with 1 mL of PBS (Gibco) with 0.01% NP-40. The bound proteins were eluted with 50 μL of 50 mM Tris-HCl (pH 8.0) and 10 mM reduced GSH (Sigma). For the negative control, cell lysate added to GST protein (100 μg) in co-IP buffer with 0.1% NP-40 was also incubated with 50 μL of pre-washed GSH-sepharose, and the samples were processed in the same way as for the experimental groups. Eluents from GST-pull downs were loaded onto two 10% SDS-PAGE gels. Proteins were visualized by Colloidal

Coomassie Blue stain on one gel. Six unique bands in GST-SH3(PRMT2) pull down were excised and submitted for identification by LC-MS/MS. Resolved proteins on the other 10% SDS-PAGE gel were transferred to a piece of PVDF membrane and blotted for aDMA using a polyclonal anti-aDMA antibody (Active Motif). Goat anti-rabbit IgG-HRP (Santa Cruz) antibody and ECL Western blotting detection reagents (GE Healthcare) were used for protein visualization.

For micrococcal nuclease (MNase) treatment of lysates to disassemble protein complexes dependent on RNA or DNA, 4 mg total protein from HeLa or HEK 293 cell lysates were supplemented with 5 mM $CaCl_2$ and then treated with 10,000 gel units of micrococcal nuclease (M0247S, New England BioLabs) at 37°C for 30 minutes. GST-pull down assays were performed with the MNase-treated cell lysates as described above. Cell lysates without MNase treatment were used as additional controls.

Proteomic study. The six isolated gel slices as well as a slice of gel cut from an empty lane on the same 10% SDS-PAGE gel were submitted to the Proteomics Core Facility within the Centre for High-Throughput Biology at UBC for *de novo* sequencing of unique PRMT2 SH3 domain-associated proteins using LC-MS/MS. The samples were digested with trypsin and desalted using ZipTip (Millipore) C-18 cartridges. Tryptic fragments were analyzed by an API QSTAR PULSARI Hybrid LC-MS/MS and identified by a human database search using the MASCOT (Matrix Science) search engine. Identified peptide sequences considered insignificant ($p \geq 0.05$) based on MASCOT scoring or found in the negative control were eliminated from the list of hits.

Far Western blotting. Cell lysates containing approximately 30 μg total protein from HeLa, HEK 293, MEF, *PRMT2*$^{-/-}$ MEF, and induced or non-induced *PRMT1* knockdown

HeLa cells were loaded onto a 10% SDS-PAGE gel and proteins were resolved by gel electrophoresis. Proteins were then transferred onto a piece of nitrocellulose membrane, and were denatured and re-natured on the membrane as previously described (*149*). The membrane was blocked with 5% TBS-milk solution at 37°C for 1 h, and was subsequently incubated with purified GST-SH3(PRMT2) (0.5 μg) in 5 ml PBS buffer at 4°C overnight. Unbound bait GST-SH3(PRMT2) was washed off by rinsing the membrane three times (10-min wash each time) with TBST buffer. The blot was then incubated with an anti-GST antibody (sc-33613, Santa Cruz) at a 1:500 dilution at room temperature for 1 h, washed with TBST three times (10-min wash each time). Goat anti-rabbit IgG-HRP (Santa Cruz) and ECL Western blotting detection reagents (GE Healthcare) were used for protein visualization.

Immunoprecipitation and Western blotting. HA-PRMT2 and HA-ΔSH3PRMT2 were overexpressed in HeLa cells as previously described (*150*). HeLa cells were harvested 72 h after transfection using hypotonic lysis buffer, and the cell lysates were fractionated into cytoplasmic and nuclear fractions as described in (*151*). Cell lysate (700 μg protein for the cytoplasmic lysate and 250 μg protein for the nuclear lystate) was aliquoted and the buffer was adjusted to 50 mM HEPES-KOH, 150 mM NaCl. Aliquoted cell lysate was then supplemented with 2.0 µg of monoclonal anti-HA antibody (HA-7, Sigma) or mouse IgG (15381, Sigma), and the volume was adjusted to 0.6 mL with co-IP buffer [50 mM HEPES-KOH, pH 7.4, 150 mM NaCl, 1x protease inhibitor cocktail (Roche #04693132001)]. The protein/antibody mixtures were incubated at 4 °C for 16 h with rotation. The cell lysate/ antibody mixture was added to 50 μL pre-washed protein G-sepharose (Invitrogen) and was rotated at 4 °C for 2 h. Subsequently, the resin was washed thoroughly with 0.05% (v/v) Tween 20 in PBS five times before the bound proteins were eluted in SDS-PAGE sample buffer.

For Western blots, proteins were separated on 10% SDS-PAGE gels, transferred to PVDF membranes, and then blotted with a polyclonal anti-Sam68 antibody (Santa Cruz). Goat anti-rabbit IgG-HRP (Santa Cruz) and ECL Western blotting detection reagents (GE Healthcare) were used for protein visualization.

Immunofluorescence and confocal microscopy. Approximately 1.0×10^7 HeLa cells were transiently transfected with pcDNA3.1(+)/Neo-mCitrine-PRMT2 or pcDNA3.1(+)/Neo-mCitrine-ΔSH3PRMT2 (24 μg) using Lipofectamine 2000 (Invitrogen) per the manufacturer's instructions. The Opti-MEM medium was replaced with standard growth medium (DMEM supplemented with 5% FBS, 50 units/mL penicillin, and 50 μg/mL streptomycin) 8 h post-transfection. The transfected cells were split 24-h post-transfection and re-seeded onto a 12-mm microscope cover glass (Fisher) coated with poly-D-lysine (Sigma) in a 24-well plate in standard growth medium. To inhibit cellular methylation, cells were treated with 20 μM AdOx at this point. The cells were then allowed to grow to 80% confluency for an additional 24 h before fixation with a 4% paraformaldehyde solution in PBS.

The cell membrane was permeabilized by incubating the cells in 0.1% Triton X-100 in PBS at room temperature for 5 min, followed by three 5-min washes with PBS. To block non-specific binding of the antibody, the cells were incubated in 1% BSA (w/v) in PBS at room temperature for 30 min. The cells were first blotted with an anti-Sam68 antibody (Santa Cruz) at 1:50 dilution, then with an Alexa Fluor 546-conjugated goat anti-rabbit secondary antibody (Invitrogen) at a 1:1000 dilution, both in 1% BSA (w/v) in PBS with 0.1% Tween-20 (v/v) (PBST) at room temperature for 1 h, with three 5-min washes in between each step. Subsequently, the cells were stained with 50 nM DAPI at room temperature for 10-min before they were washed and mounted on microscope slides (Fisher). Cell images were captured using

a FluoView FV10i confocal microscope (Olympus) with an oil lens at 60x magnification, and were processed with ImageJ software (NIH image).

3.3 Results

PRMT2 SH3 domain-associated proteins. To identify potential PRMT2-protein interactions mediated through the PRMT2 SH3 domain, I performed a GST-pull down assay using the purified GST tagged SH3 domain region of PRMT2 [GST-SH3(PRMT2)]. The GST-SH3(PRMT2) was allowed to bind with proteins in HeLa cell lysate for 2 hours, then the protein complex was immobilized, washed, eluted, and visualized on a 10% SDS-PAGE gel. GST-pull down assays using the purified GST tagged SH3 domain region of a tyrosine kinase, Abl [GST-SH3(Abl)], or the purified GST tag itself as baits were also performed in the same way as positive and negative controls, respectively. As shown in Figure 3.1A, the GST-SH3(PRMT2) and GST-SH3(Abl) pull downs showed similar protein banding patterns, which implies that the two SH3 domains may recognize a similar array of ligands. However, at least six bands (indicated as red asterisks in the Figure 3.1A) were enriched in the GST-SH3(PRMT2) pull down in comparison to the two controls, suggesting that the SH3 domain of PRMT2 may display a unique binding selectivity towards some ligands. These six bands were isolated and proteins within each band were identified by LC-MS/MS analysis. The PRMT2 SH3 domain-associated proteins are listed in Table 3.1. A discussion of these proteins that interact with PRMT2 SH3 can be found later in this chapter.

Since PRMT2 has Type I methylation activity and interacts with the predominant arginine methyltransferase PRMT1, I then tested the PRMT2 SH3 domain-associated proteins for aDMA modifications by blotting them with an anti-aDMA antibody. Despite the similarity in protein banding pattern between GST pull downs for the SH3 domains of PRMT2 and Abl, the aDMA level in the PRMT2 SH3 domain pull down sample was higher (Figure 3.1B). The fact that the banding pattern in the PRMT2 SH3 domain pull down by Colloidal Coomassie Blue

staining reflected in the anti-aDMA blot implies that the majority of PRMT2 SH3 domain-associated proteins contain aDMA. These results indicate that PRMT2 may associate with Type I PRMT substrates through SH3 domain-mediated interactions.

To further explore whether these PRMT2 SH3 domain-associated proteins directly interact with the PRMT2 SH3 domain, a Far Western blotting experiment was conducted using the purified GST-SH3(PRMT2) to probe protein from different cell lysates (Figure 3.1C). This Far Western blot exhibited a similar banding pattern as that for GST-SH3(PRMT2) pull down visualized by Colloidal Coomassie Blue stain (Figure 3.1A), suggesting that the PRMT2 SH3 domain directly interacts with most of its identified interacting partners.

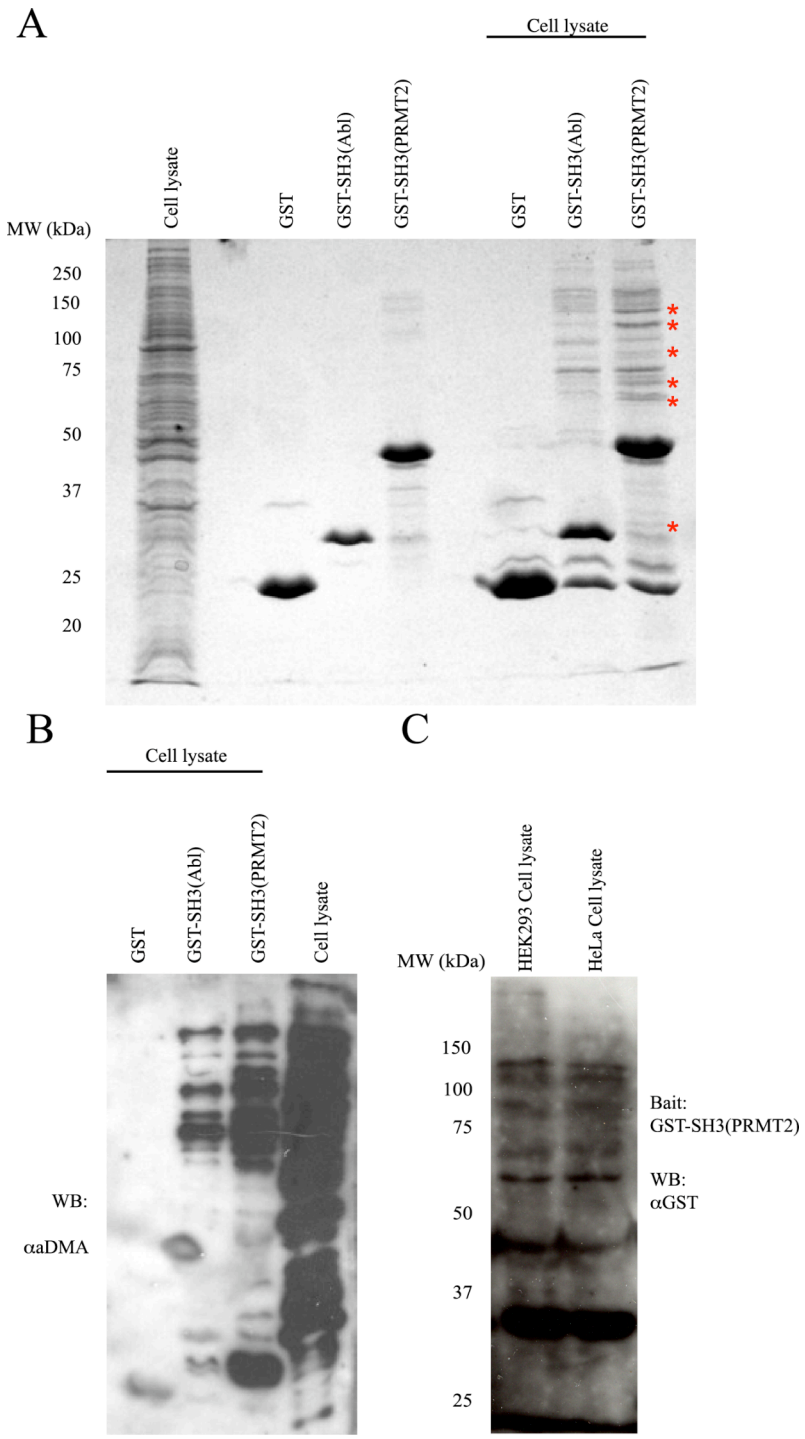

Figure 3.1. PRMT2 SH3 domain-associated proteins contain aDMA. (A) Eluents of indicated GST-pull down experiments were visualized by Colloidal Coomassie Blue stain of resolved proteins on a 10% SDS-PAGE gel. *Red asterisks* indicate protein bands that were isolated for proteomic analysis. (B) aDMA content in pulled down proteins was assessed by Western blot. (C) Total proteins in HEK293 and HeLa cell lysates were resolved on a 10% SDS-PAGE gel, then transferred to a piece of nitrocellulose membrane and were subsequently denatured and refolded on the membrane. GST-SH3(PRMT2) was allowed to incubate with proteins on the membrane for over night at 4°C. Direct interactions in between PRMT2 SH3 domain and proteins on the membrane were detected by blotting with an anti-GST antibody.

Table 3.1. Summary of identified PRMT2 SH3 domain binders. The PRMT2 SH3 domain binders identified in our proteomic study have been listed. The known and identified arginine methylation states of these proteins are indicated in the far right column. Proteins that are annotated as arginine methylated in both the Uniprot database and in our proteomic study are indicated as (∗∗). Proteins that are annotated as arginine methylated in the Uniprot database but not identified as arginine methylated in our proteomic study are indicated as (∗). Proteins that are not annotated as arginine methylated in the Uniprot database but identified as arginine methylated in our proteomic study are indicated as (Δ). Proteins that are neither annotated as arginine methylated in the Uniprot database nor in our proteomic study are indicated as (-).

Gene Name	Protein Name	Note	Arginine Methylation	Score
Sm/LsmCore snRNP protein		**Major and minor spliceosomes**		
SNRPB	Small nuclear ribonucleoprotein-associated proteins B and B´	PxxP motif	**	225
U1 snRNP-specific protein		**Major spliceosome, spliceosomal E complex**		
SNRNP70	U1 small nuclear ribonucleoprotein 70 kDa	RGG motif, clustered Arg-Ser dipeptides; PxxP motif	-	367
U2 snRNP-specific proteins		**Major spliceosome, spliceosomal A complex**		
SNRPB2	U2 small nuclear ribonucleoprotein B"	PxxP motif	-	67
SF3A1	Splicing factor 3A subunit 1	Pro-rich domain	-	1142
SF3A2	Splicing factor 3A subunit 2	Pro-rich domain	-	541
SF3A3	Splicing factor 3A subunit 3	PxxP motif	Δ	130
SF3B3	Splicing factor 3B subunit 3	Also is a component of U11/U12 di-snRNP;PxxP motif	-	528
DDX42	ATP-dependent RNA helicase DDX42	Also known as SF3B125; Also is a component of U11/U12 di-snRNP;PxxP motif	-	122
U4/U6.U5 snRNP-specific proteins		**Major spliceosome, spliceosomal B complex**		
USP39	U4/U6.U5 tri-snRNP-associated protein 2	Arg-rich domain;PxxP motif	-	67
U11/U12 snRNP-specific proteins		**Minor spliceosome**		
PDCD7	Programmed cell death protein 7	Pro-rich domain	-	74
Known H complex components				
FUS	RNA-binding protein FUS	PxxP motif; Arg/Gly-rich domain	**	515
HNRNPK	Heterogeneous nuclear ribonucleoprotein K	A known PRMT1 substrate; Pro-rich domain; KH domain	*	64
HNRNPL	Heterogeneous nuclear ribonucleoprotein L	Pro-rich domain	Δ	89
HNRNPR	Heterogeneous nuclear ribonucleoprotein R	PxxP motif; RGG motif	*	158
HNRNPU	Heterogeneous nuclear ribonucleoprotein U	PxxP motif; RGG motif	*	118
HSPA1A	Heat shock 70 kDa protein 1A/1B	PxxP motif	-	484
HSPA8	Heat shock cognate 71 kDa protein	Forms a mRNA granule complex with hnRNP L, -R,-U, and HSPA1A; PxxP motif	-	362
Other splicing-related proteins				
NONO	Non-POU domain-containing octamer-binding protein	Pro-rich domain	-	1933
*RBM39**	RNA-binding protein 39	Arg/Ser-rich (RS) domain	-	283
SF1	Splicing factor 1	Pro-rich domain, KH domain	-	203
SFPQ	Splicing factor, proline- and glutamine-rich	Pro-rich domain	**	829
WBP11	WW domain-binding protein 11	Pro-rich domain	-	388
RBM25	RNA-binding protein 25	PxxP motif; PWI domain; Arg-rich domain	-	396
*LUC7L3**	Luc7-like protein 3	Arg/Ser-rich (RS) domain	-	152
KHDRBS1	Src-associated in mitosis 68 kDa protein	A known PRMT1 substrate; interacts with PRMT1 and -2; KH domain; Pro-rich domain	*	74
PUF60	Poly(U)-binding-splicing factor PUF60	PxxP motif	-	143
PSPC1	Paraspeckle component 1	Interacts with SFPQ and p54nrb; PxxP motif	Δ	106
HSPB1	Heat shock protein beta-1	Displays temperature-dependent chaperone activity	-	65
Proteins with roles in pre-mRNA metabolism processes linked to splicing				
NUDT21	Cleavage and polyadenylation specificity factor subunit 5	PxxP motif	Δ	426
CPSF6	Cleavage and polyadenylation specificity factor subunit 6	Pro-rich domain	-	609
CPSF7	Cleavage and polyadenylation specificity factor subunit 7	Pro-rich domain	-	363
HNRNPUL1	Heterogeneous nuclear ribonucleoprotein U-like protein 1	A known PRMT2 substrate; Pro-rich domain	*	57
Possible splicing-related proteins				
CCT3	T-complex protein 1 subunit gamma	Molecular chaperone involved in folding of actin and tublin ; complexes with CCT4 and CC7	-	86
CCT4	T-complex protein 1 subunit delta	Molecular chaperone involved in folding of actin and tublin; complexes with CCT3 and CC7	-	182
CCT7	T-complex protein 1 subunit eta	Molecular chaperone involved in folding of actin and tublin; complexes with CCT3 and CC4	-	99
Proteins without demonstrated role in splicing				
WASL	Neural Wiskott-Aldrich syndrome protein	Regulates actin polymerization; Pro-rich domain	-	168
WIPF1	WAS/WASL-interacting protein family member 1	Induces actin polymerization and redistribution; participate in WASL regulation;Pro-rich domain	Δ	249

* Proteins do not contain any PxxP motif or Pro-rich domain

To test whether the detected PRMT2 SH3 domain-mediated interactions require the presence of endogenous PRMT1 or -2, the GST-SH3(PRMT2) pull downs were performed using PRMT1 knockdown HeLa cell (PRMT1 k./d.) lysate or PRMT2 knockout mouse embryonic fibroblast (PRMT2 k./o. MEF) lysate. The patterns of PRMT2 SH3 domain-associated proteins in the absence of endogenous PRMT1 or PRMT2 were almost identical. One band pulled down with GST-SH3(PRMT2) in wild type HeLa cell lysate that migrated below the 75 kDa molecular weight marker (annotated with an red asterisk) was not detected in the PRMT1 k./d. pull down sample, while another band that migrated at a slightly lower molecular weight (annotated with an red asterisk) was enriched in the PRMT1 k./d. pull down sample (Figure 3.2). It is reasonable to speculate that a certain subset of the PRMT2 SH3 domain-mediated interactions is regulated by endogenous PRMT1, possibly through the PRMT1/2 interaction. In the absence of endogenous PRMT1, PRMT2 may exhibit altered affinities for certain binders.

Likewise, GST-SH3(PRMT2) pull downs performed with the wild type MEF or PRMT2 k./o. MEF lysates also demonstrated similar protein banding patterns with the exception that three weakly-stained bands in the wild type MEF pull down (annotated with red asterisks) were reduced in intensity or disappeared in the PRMT2 k./o. pull down (Figure 3.2). One possible explanation for this observation is that the presence of endogenous PRMT2 can affect specific interactions between the PRMT2 SH3 domain and its interacting partners.

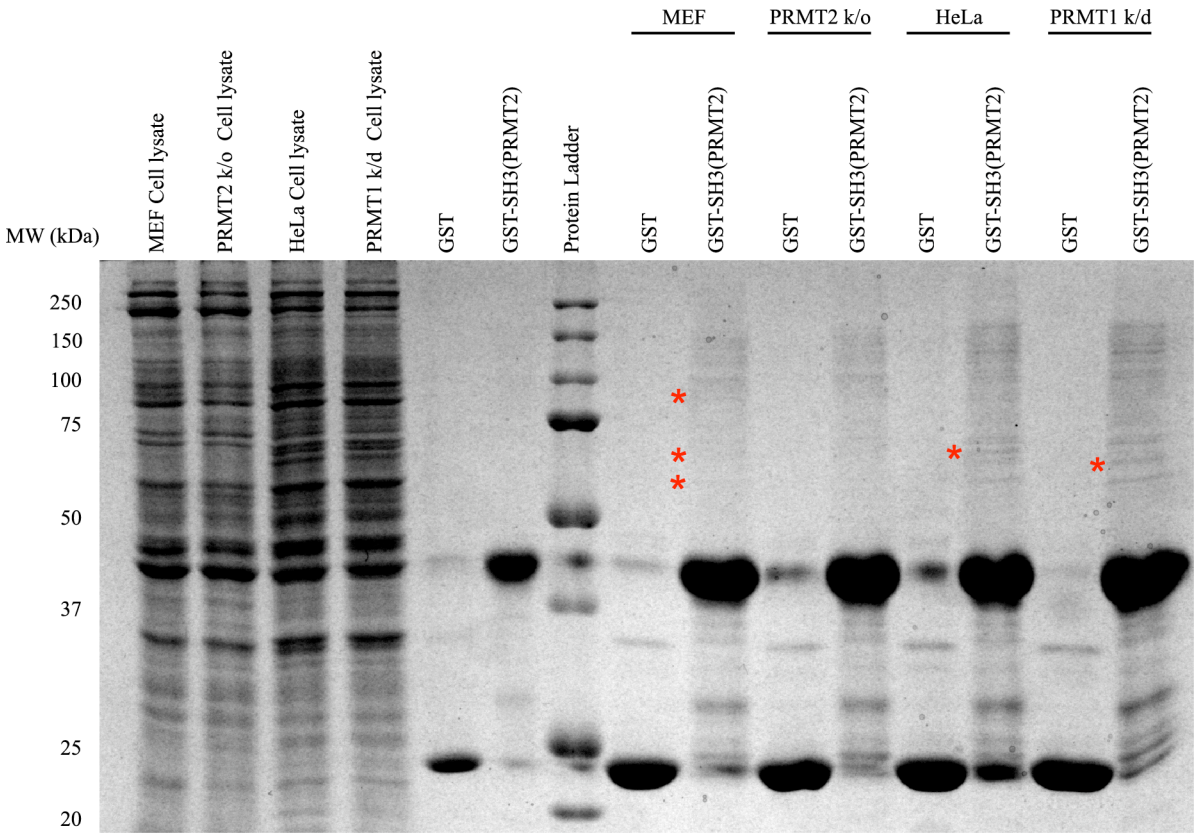

Figure 3.2. PRMT2 SH3 domain-mediated interactions in the absence of endogenous PRMT1 or -2. Eluents of indicated GST-pull down experiments using wild type cell lysates, or cell lysates containing no endogenous PRMT1 or -2 as prey were visualized by Colloidal Coomassie Blue stain of resolved proteins on a 10% SDS-PAGE gel. *Red asterisks* indicate unique protein bands detected only in the presence or absence of endogenous PRMT1 or -2.

SH3 domain mediates PRMT2 interactions with splicing-related proteins. Since many proteins in a total cell lysate can have similar apparent molecular weights, more than one protein can be identified from an excised protein band. As shown in Table 3.1, thirty-seven proteins have been identified from the six isolated protein bands that appeared enriched from the GST-SH3(PRMT2) pull down (bands annotated with red asterisks in Figure 3.1A) by LC-MS/MS analysis, however, the specific protein(s) responsible for the enrichment in protein band intensities has yet to be determined. Interestingly, twenty-nine of these proteins were splicing-related proteins, including components of both major and minor spliceosomes, spliceosome-

associated factors, RNA-binding proteins with demonstrated roles in splicing, and proteins involved in pre-mRNA metabolism processes linked to splicing (annotation of biological functions from UniProt database at www.uniprot.org, as well as from references herein). In addition, six of the identified proteins could possibly take part in splicing based on the current understanding on their functions and interacting partners. This result suggests that PRMT2 may play a role in mRNA splicing and/or pre-mRNA processing.

Nucleic acids stabilize PRMT2 SH3 domain-mediated protein complexs. Since most of the splicing-related proteins identified as PRMT2 SH3 domain-associated proteins are DNA- and/or RNA-binding proteins (see references within the previous sections), I then tested whether the presence of nucleic acids are required for the detected PRMT2 SH3 domain-mediated interactions.

Micrococcal nuclease (MNase) is a relatively non-specific endonuclease that digests both double- and single-stranded nucleic acids (*152*). Thus HeLa and HEK293 cell lysates were subjected to MNase treatment in order to degrade the nucleic acids within these samples. The GST-SH3(PRMT2) pull down assays were performed in a similar fashion as the one presented above, but using the HeLa and HEK293 cell lysates treated with MNase as sources of total protein. The proteins that bound to the PRMT2 SH3 domain in the absence of nucleic acids were resolved and visualized on a 10% SDS-PAGE gel in parallel with the GST-SH3(PRMT2) pull down samples obtained using cell lysates without MNase treatment. As shown in Figure 3.3, the intensities of the pulled down bands decreased in both experiments performed with MNase-treated HeLa and HEK293 cell lysates when compared to those experiments done with non-treated cell lysates, whereas the patterns of bands in all samples appeared unchanged. The fact that these PRMT2 SH3 domain-mediated interactions were sensitive to MNase treatment

suggests the identified protein-protein interactions may be tethered by nucleic acids. Since the banding patterns were not affected by the MNase treatment, it is possible that the presence of nucleic acids is not a prerequisite for the SH3 domain-facilitated interactions. Instead, nucleic acids may stabilize the PRMT2-associated splicing-related protein complexes.

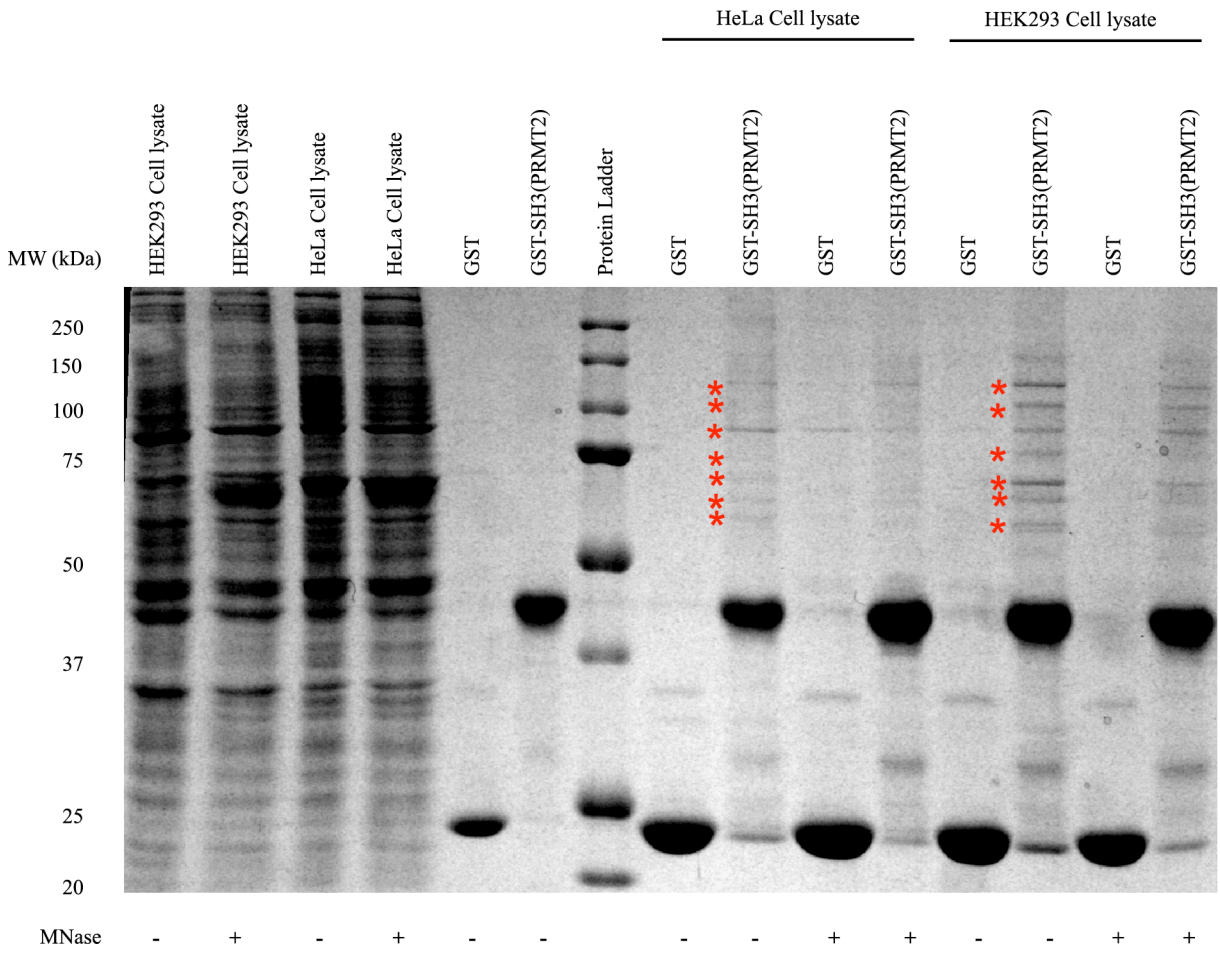

Figure 3.3. Micrococcal nuclease treatments affect PRMT2 SH3 domain-mediated interactions. HeLa or HEK293 cell lysate was treated with micrococcal nuclease to digest nucleic acids. GST-pull down experiments were performed using the corresponding cell lysates as labeled. Eluents of were visualized by Colloidal Coomassie Blue stain of resolved proteins on a 10% SDS-PAGE gel. *Red asterisks* indicate protein bands enriched in the presence of nucleic acids.

Sam68 associates with the PRMT2 SH3 domain. One protein identified from the GST-SH3(PRMT2) pull down that caught my attention was Sam68. Sam68 has been identified as a binder for the SH3 domain of PRMT2 in a large-scale screen using a protein-domain microarray (*125*). Importantly, arginine methylation of Sam68 appeares to interrupt its binding with the SH3 domain (*125*). Sam68 is a protein that is phosphorylated on its tyrosine residues and functions as a substrate for Src family tyrosine kinases during mitosis. It has five proline-rich domains and has been shown to associate with several SH3 domain-containing proteins (*153*). Sam68 is also a substrate for PRMT1, and arginine methylation is essential for its nuclear localization (*95*). Interestingly, it has been shown that Sam68 can interact with hnRNP A1 and regulate alternative splicing (*154, 155*).

The association of Sam68 with the PRMT2 SH3 domain was confirmed by blotting the GST-SH3(PRMT2) and GST-SH3(Abl) pulled-down proteins with an anti-Sam68 antibody. Sam68 was detected in both GST-SH3 domain pull down samples, but not in the GST-alone pull down control. Additionally, the level of Sam68 pulled down by the PRMT2 SH3 domain appeared higher than by the Abl SH3 domain (Figure 3.4), suggesting that the PRMT2 SH3 domain may be selective for this ligand.

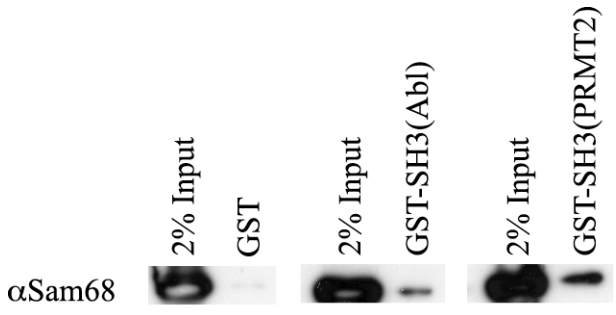

Figure 3.4. GST-SH3(PRMT2) associates with Sam68. Eluents of indicated GST-pull down experiments were resolved on a 10% SDS-PAGE gel and blotted with an anti-Sam68 antibody.

Sam68, a newly confirmed PRMT2 binder. Since Sam68 associated with the SH3 domain of PRMT2, I then asked the question if the full length PRMT2 could also interact with Sam68. If so, is the SH3 domain essential for such an interaction? To answer these questions, I expressed either the HA tagged full-length PRMT2 or ΔSH3PRMT2 in HeLa cells. Since Sam68 bears a nuclear localization sequence (NLS) and may have distinct functions in the cytoplasm versus in the nucleus (*156*), the HeLa cell lysates expressing the ectopic HA tagged full-length or truncated PRMT2 were separated into nuclear and cytoplasmic fractions. Then the PRMT2 protein complexes in each sub-cellular fraction were immunoprecipitated using an anti-HA antibody, and endogenous Sam68 was detected with an anti-Sam68 antibody. The co-IP results indicate that only the full-length PRMT2 but not the PRMT2 lacking its SH3 domain was able to pull down endogenous Sam68 in the nuclear fraction, and none of the epitope-tagged wild type and mutant PRMT2 could co-immunoprecipitate Sam68 in the cytoplasmic fraction (Figure 3.5). However, we have noticed that HA-ΔSH3PRMT2 did not express in the nuclear fraction to the same level as the full-length PRMT2 did, which may be part of the reason for why the SH3 deletion on PRMT2 did not associate with Sam68. In contrast, HA-ΔSH3PRMT2 expressed at a comparable level as the HA-PRMT2 in the cytoplasmic fraction (Figure 3.5), which suggested that the low expression level of HA-ΔSH3PRMT2 in the nucleus was unlikely to be caused by an unsuccessful transfection but possibly due to the change in relative expression level in different sub-cellular compartments when the SH3 domain of PRMT2 was removed. Nevertheless, the GST-SH3(PRMT2) pull down and co-IP results suggest that the PRMT2 SH3 domain is important for the PRMT2/Sam68 interaction, although the detailed mechanism for this interaction requires further investigation.

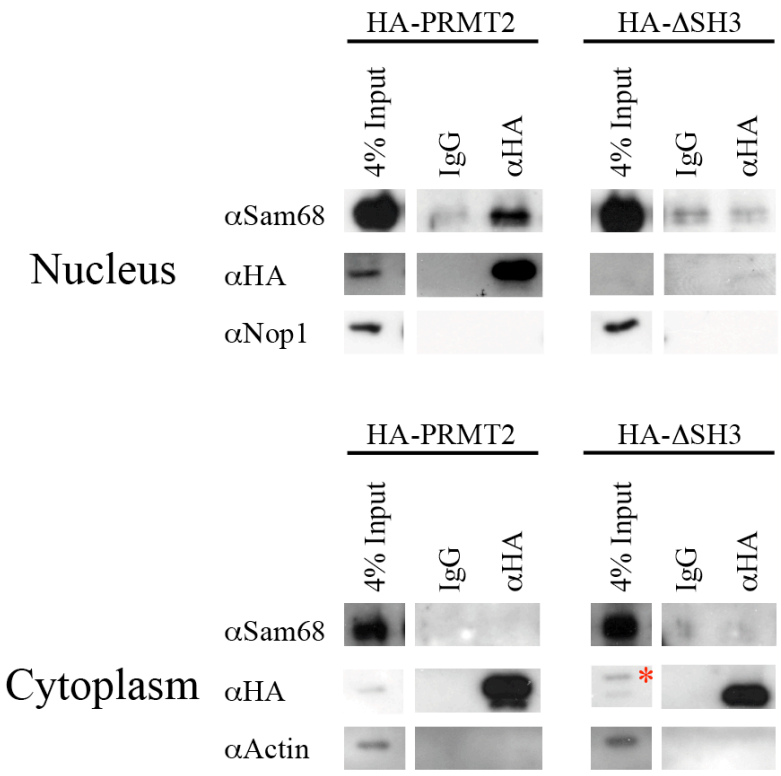

Figure 3.5. PRMT2 and Sam68 co-immunoprecipitate in cells. HA-PRMT2 or HA-ΔSH3PRMT2 was expressed in HeLa cells and cell lysate was fractionated into nucleus (*top)* and cytoplasm (*bottom)* fractions. Both cell lysate fractions were immunoprecipitated with anti-HA antibody, or with mouse IgG (negative control). Immunoprecipitates were immunoblotted with anti-Sam68 or anti-HA antibodies as indicated. Immunoblots blotted with anti-Nop1 or anti-Actin antibodies were also preformed as negative controls for nuclear or cytoplasmic proteins, respectively. The non-specific band is labeled with a *red asterisk.*

PRMT2 affects Sam68 sub-cellular localization in hypomethylated HeLa cells. It has been shown that arginine methylation of Sam68 by PRMT1 was required for its nuclear localization in HeLa cells, and Sam68 accumulated in the cytoplasm in the presence of the methylase inhibitor AdOx (*95*). I tested if PRMT2 plays a role in the sub-cellular localization of Sam68. HeLa cells were transfected with mCitrine-PRMT1, mCitrine-PRMT2, or mCitrine-ΔSH3PRMT2 to enable visualization of the fluorescence protein fusions *in situ*. These cells were allowed to grow either in standard growth medium or in the presence of 20 μM AdOx. The sub-cellular localization of Sam68 in the transfected HeLa cells as well as in wild type HeLa cells was then visualized by immunoblotting with an anti-Sam68 antibody followed by a secondary antibody conjugated to Alexa Fluor 546. Figure 3.6A illustrates that Sam68 resides predominantly in the nucleus in wild type HeLa cells as previously reported by Côté *et al.* (*95*). However, these authors have also noticed an increase in cytoplasmic Sam68 in the presence of 1.0 mM AdOx dissolved in DMSO. In contrast, I did not observe any obvious change in Sam68 localization when the wild type HeLa cells were treated with 20 μM AdOx dissolved in PBS (Figure 3.6A). Strikingly, only HeLa cells overexpressing mCitrine-PRMT2 (Figure 3.6C), but neither those expressing mCitrine-PRMT1 (Figure 3.6B) or mCitrine-ΔSH3PRMT2 (Figure 3.6D) demonstrated a methylation-dependent Sam68 sub-cellular localization such that Sam68 accumulated in the cytoplasm of the HeLa cells in the presence of 20 μM AdOx. On the other hand, mCitrine-PRMT1, mCitrine-PRMT2 and mCitrine-ΔSH3PRMT2 all predominantly localized in the nucleus in the absence of AdOx. Only mCitrine-PRMT2 accumulated in the cytoplasm in the presence of AdOx (Figure 3.6). Moreover, Sam68 appeared to co-localize with the mCitrine tagged PRMTs in HeLa cells treated with or without AdOx (Figure 3.6). Altogether, these results imply that the PRMT2 SH3 domain may affect the sub-cellular

localization of PRMT2 and certain PRMT2 binders under conditions of hypomethylation, and only the full-length PRMT2 co-localizes with Sam68 in the cytoplasm in hypomethylated HeLa cells that overexpress PRMT2. I am aware that some phase contrast images presented in the Figure 3.6 reveal debris-like dots, which may due to the transfection reagent or cell culture contamination.

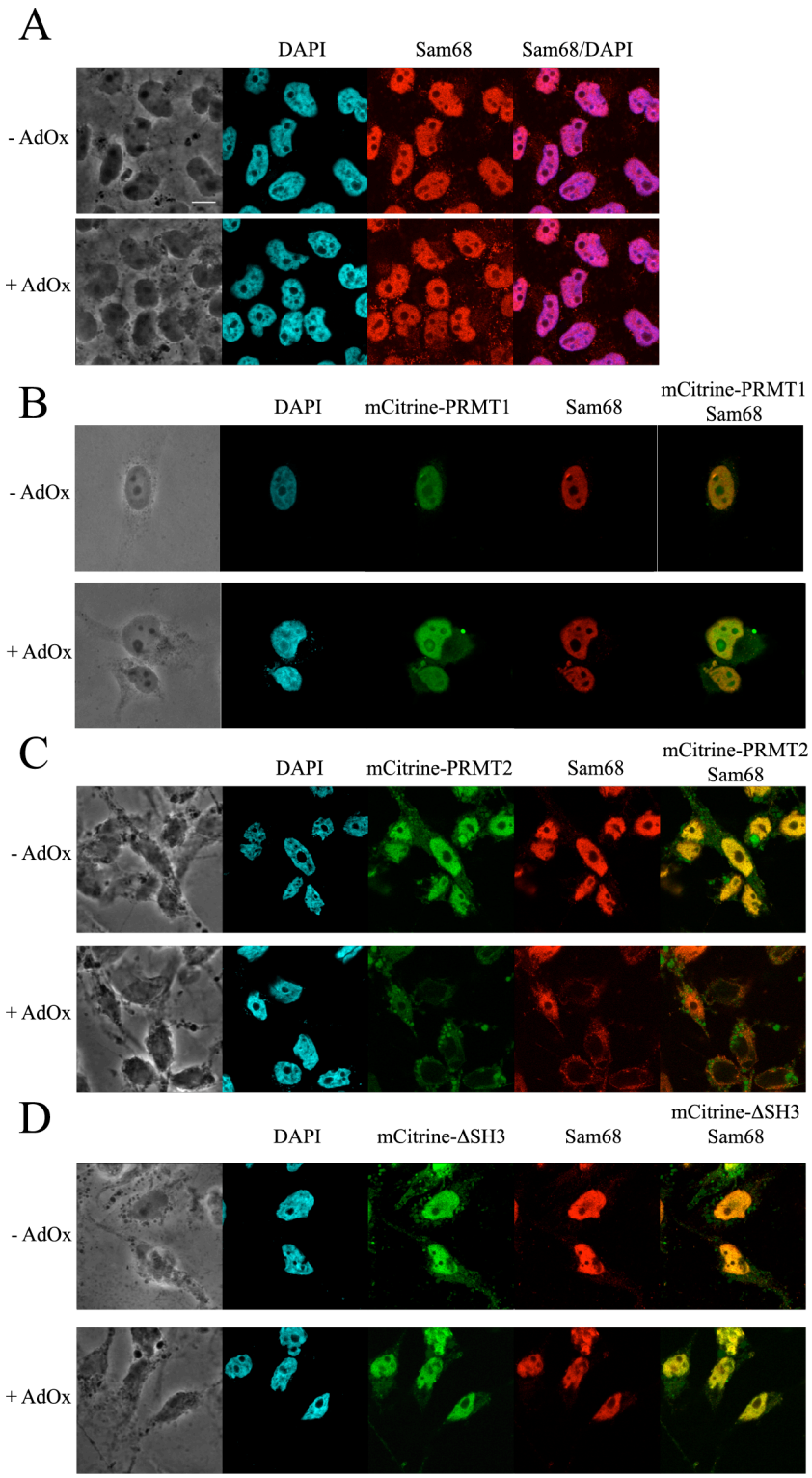

Figure 3.6. The change of Sam68 sub-cellular localization in hypomethylated HeLa cells overexpressing PRMT1, PRMT2, or ΔSH3PRMT2. Wild type HeLa cells (A) and HeLa cells transfected with mCitrine-PRMT1 (B, *green*), mCitrine-PRMT2 (C, *green*) or mCitrine-ΔSH3 (D, *green*) were treated with or without 20 μM AdOx as indicated. The cells were fixed and immunostained with an anti-Sam68 antibody followed by a secondary antibody conjugated to Alexa Fluor 546 (*red*). Nuclei were visualized by the DAPI stain (*cyan*). The phase contrasted images (*left*) and the merged images (*right*) are also shown. The scale bar indicates 10 μm.

The localization of PRMT1, PRMT2, and Sam68 in HeLa cells co-expressing mCitrine tagged full-length or truncated PRMT2 and HA-tagged wild type or inactive PRMT1 was also investigated in cells treated with or without 20 μM AdOx. Surprisingly, overexpressed HA-PRMT1 co-localized with mCitrine-PRMT2 in the nucleus in hypomethylated HeLa cells (Figure A.15A). However, HA-PRMT1 co-localized with mCitrine-ΔSH3PRMT2 in the cytoplasm in AdOx treated HeLa cells (Figure A.15B), though neither PRMT1 nor ΔSH3PRMT2 localized to the cytoplasm upon AdOx treatment when individually expressed (Figure 3.6A and Figure 3.6D). It has been shown in Chapter 2 that the inactive HA-PRMT1E153Q only interacted with ΔSH3PRMT2 but not the full-length PRMT2 (Figure 2.7). However, HA-PRMT1E153Q, mCitrine-PRMT2, and mCitrine-ΔSH3PRMT2 all demonstrated nuclear localizations regardless of AdOx treatment (Figure A.15C and Figure A.15D). On the other hand, Sam68 co-localized with the two overexpressed PRMTs in the presence or absence of AdOx (Figure A.15). The inconsistency of data makes the interpretation of these results difficult. The current experimental design does not control for the relative expression level of the two ectopically tagged PRMTs. And the present immunofluorescence studies were conducted in wild type HeLa cells in the presence of all endogenous PRMTs, some of which are able to interact with the overexpressed PRMTs, thereby potentially influencing the sub-cellular localization of the ectopically tagged PRMTs and overall arginine methylation activity in cells. These drawbacks may contribute to the inconsistency of immunofluorescence results. Nevertheless, it is clear that PRMT2 affects the sub-cellular localization of Sam68 likely through the SH3 domain. However, the detailed mechanism of PRMT2 and Sam68 interaction in cells with different methylation states still needs to be further investigated.

3.4 Discussion

Splicing. Eukaryotic mRNA transports genetic information encoded by DNA out of the nucleus and serves as a template for protein synthesis. Nascent mRNA transcripts or pre-mRNA contain not only expressed sequences (exons) but also non-coding intervening sequences (introns), and they need to be further processed into a mature form through 5' capping, 3' cleaving and polyadenylating, and splicing prior to ribosomal translation (*157*). One key pre-mRNA processing event that contributes to gene regulation and increased proteome diversity is alternative splicing (AS), during which multiple mRNA splice variants can be made from a single piece of pre-mRNA through intramolecularly joining different exons by the spliceosome (*158*). Alternative splicing allows for more than one transcript to be generated from a single gene in order to diversify RNA species, produce different protein splice variants, and increase biological complexity.

The initial draft of human genome announced in 2001 indicates that the human genome contains somewhere between 30,000 and 35,000 protein-coding genes (*159*). Three years later, the completed human genome provides an even lower estimate of only 20,000 to 25,000 genes (*160*). Surprisingly, the number of human genes is only slightly higher than the gene numbers of *Drosophila melanogaster* (~13,500) by less than 2-fold. Scientists then propose that the increased physiological complexity of vertebrates might result from regulatory events such as post-translational modifications and alternative splicing (*161*). Consistent with this hypothesis, independent research groups have estimated that alternative splicing may occur in up to 80% of human genes (*162*). Therefore, researchers have shown an increased interest in exploring the regulatory mechanism of the splicing pathway.

The spliceosome is a dynamic complex made up of small nuclear RNAs (snRNAs) and proteins (*163*). Two types of spliceosomes exist: the major or U2 type and the minor or U12 type (*163*). The major spliceosome is highly expressed in eukaryotes; it is a 60S complex composed of five major small nuclear ribonucleoproteins (snRNPs) referred to as U1, U2, U4, U5, and U6 snRNPs. Each of these snRNPs contains their own snRNA and makes additional interactions with more than a hundred distinct non-snRNP proteins (*164*). After the formation of the E complex in which the U1 snRNP is recruited to the 5' splice site (*165*), the U2 snRNP subsequently binds to the branchpoint sequence (BPS) located upstream of the 3' splice site of an intron thereby yields the A complex (*166*). The pre-assembled U4/U6.U5 tri-snRNP is then associated with the intron to give rise to an activated spliceosome called the B complex [reviewed in (*165*)]. On the other hand, the minor spliceosome also contains a U5 snRNP but four other snRNPs: U11, U12, U4atac, and U6atac (*163*).

At least two groups of elements are involved in regulating alternative splicing. The first group is the *cis*-acting regulatory sites located within the pre-mRNA transcript itself; assembly of spliceosome on the pre-mRNA is guided by splice-site consensus sequences located at the ends of introns, as well as by auxiliary consensus sequences such as exon splicing enhancers and silencers (ESEs and ESSs) and intron splicing enhancers and silencers (ISEs and ISSs) [reviewed in (*162*)]. The second group is the *trans*-acting proteins able to recognize the consensus sequences. For example, the U1, U5, and U6 snRNAs all interact with the 5' splice site by base pairing with the consensus sequence (*167*). The splicing factor SF1 directly binds the BPS through its hnRNP K homology (KH)-domain (*168*), which is an evolutionarily conserved domain demonstrating affinity for RNA (*169*). On the other hand, the U2 auxiliary factor 2 (U2AF2) and U2 auxiliary factor 1 (U2AF1) cooperatively recognize the polypyrimidine tract,

which locates downstream of BPS, and the 3' splice site consensus sequence, respectively (*170*). Additionally, the serine/arginine-rich (SR) proteins bind ESEs utilizing their N-terminal RRM; meanwhile, SR proteins also facilitate protein-protein interactions via their C-terminal RS domains (*171*). For example, U1 small nuclear ribonucleoprotein 70 kDa (U1-70K) binds to U1 snRNA at the 5' splice site while interacting with the RS domain of the SR protein alternative splicing factor/splicing factor 2 (ASF/SF2), thereby strengthening the association between the spliceosomal complex and the 5' splice site (*172, 173*). In contrast, hnRNPs have been observed to interact with ESSs and ISSs through their KH domains or RRMs, and are generally considered to be splicing silencers [reviewed in (*162*)]. As an example, hnRNP A1 can antagonize the splicing activation function of ASF/SF2, and the relative concentrations of hnRNP A1 and ASF/SF2 can control the 5' splice site selection by the U1 snRNP (*174*). Many spliceosome components were identified as PRMT2 SH3 domain-associated proteins in this study, which include an Sm core snRNP protein and splicing regulators.

PRMT2 SH3 domain associates with an Sm core snRNP protein. Two of the identified PRMT2 SH3 domain-associated proteins are the small nuclear ribonucleoprotein-associated proteins B and B′ (SmB/B′), which are essential for the biogenesis of most of the snRNPs except U6 and U6atac (*175*). SmB and SmB′ are two nearly identical splicing variants encoded by the gene *SNRPB*, except that SmB′ has an additional repeat of a proline-rich motif at its C-terminus (*176*). Together with five other Sm proteins, SmB/B′ constitutes the core domain of the snRNPs that is required for snRNP relocation to the nucleus by forming a heptameric ring around a conserved sequence motif on the snRNA termed the "Sm-site" [reviewed in (*175*)]. Both SmB and SmB′ contain multiple proline-rich motifs on their C-termini (*176*), which can be theoretically recognized by the SH3 domain. Espejo *et al.* has detected the interaction between

the PRMT2 SH3 domain and a peptide containing the last 24 amino acid residues at the C-terminus of SmB′ using a protein-domain microarray (*125*). My observation that SmB/B′ associated with PRMT2 SH3 domain suggests that PRMT2 may be involved in the core domain formation of snRNPs, yet whether PRMT2 directly interacts with the C-terminal proline-rich motifs of SmB and SmB′ through the SH3 domain *in vivo* still needs to be further explored.

PRMT2 SH3 domain associates with spliceosome components. Besides the two Sm core proteins, a handful of spliceosome components were pulled down from HeLa cell lysate with GST-SH3(PRMT2). One of them is the aforementioned U1-70K, which is a U1 snRNP-specific protein that bridges between stem-loop I of the U1 snRNA (*177*) and splicing factors such as the serine/arginine-rich splicing factor 2 (SRSF2/ SC35) and ASF/SF2 (*172, 173*), thus facilitating the 5' splice site recognition by the U1 snRNP. Additionally, several of the U2 snRNP-specific proteins were found to interact with the PRMT2 SH3 domain based on the results of my study, including the U2 small nuclear ribonucleoprotein B" (U2B"/SNRPB2) that binds with the stem-loop IV of the U2 snRNA (*178*), all three splicing factor 3A (SF3A) subunits, and two out of the eight splicing factor 3B (SF3B) subunits (*179, 180*). It has been reported that the multi-subunit complexes SF3A and SF3B help to stabilize the binding of U2 snRNP to the BPS (*181*). Moreover, a U4/U6.U5 snRNP-specific protein that is essential for the recruitment of the tri-snRNP to the pre-splicing complex A (*180, 182*) called U4/U6.U5 tri-snRNP-associated protein 2 (65K) has been identified as a PRMT2 SH3 domain-associated protein in this study.

A component of the minor U11 snRNP, the programmed cell death protein 7 (PDCD7 /U11-59K) showed up in the list of PRMT2 SH3 domain interacting partners. During the formation of a minor U12-type pre-spliceosome, the U11 and U12 snRNP, which are functional

analogs of the U1 and U2 snRNP, cooperatively binds to the 5' splice site and BPS of an U12-type intron, respectively (*183*). The U11-59K bridges the U11 and U12 snRNPs and promotes the formation of the U11/U12 di-snRNP, which is known as the U12-type pre-spliceosome (*184*). Taken together, these results indicate that PRMT2 can potentially take part in splicing regulation by associating with the components of both major and minor spliceosome through its SH3 domain.

PRMT2 SH3 domain associates with the H complex components. Members of the hnRNP and SR (serine/arginine-rich) protein families are two major groups of splicing regulators that can modulate interactions among non-snRNP proteins, snRNPs, and pre-mRNA to control alternative pre-mRNA splicing (*185*). Although no SR proteins have been identified as PRMT2 SH3 domain-associated proteins in this study, six hnRNPs were pulled down with the SH3 domain of PRMT2.

hnRNPs have been previously found in a complex named the H complex, which contains proteins bound to RNA in the absence of splicing [summarized in (*164*)], and they have been frequently observed as binders of splicing silencers that inhibit the use of splice sites (*186, 187*). Therefore, hnRNPs were first considered as splicing inhibitors. Two identified PRMT2 SH3 domain-associated hnRNPs, hnRNP R and hnRNP U, have been reported as components of the repressive H complex (*164*). The PRMT2 SH3 domain was able to pull down the RNA-binding protein FUS also known as hnRNP P2, which has been reported as a negative regulator of intron splicing by associating with hnRNP A1 and SC35 to recognize an intronic silencer sequence (*188*). However, hnRNPs could also promote splicing at certain splice sites [reviewed in (*189*)]. One of the identified PRMT2 SH3 domain interacting partners hnRNP K has been shown to enhance splicing of the alternative exon 6A from chicken β-tropomyosin pre-mRNA (*190*).

Another PRMT2 SH3 domain-associated protein hnRNP L can act as repressor and stimulator of splicing (*191, 192*). Interestingly, an hnRNP that is highly similar to hnRNP U called hnRNP U-like protein 1 (hnRNP UL1) that is not known as a component of the H complex (*193*) was identified as a PRMT2 SH3 domain associated-protein in this study.

Lastly, a non-hnRNP member of the H complex (*164*), the heat shock 70 kDa protein 1A/1B (HSP70-1/HSP70-2) was pulled down by the SH3 domain of PRMT2. Additionally, the heat shock cognate 71 kDa protein (HSC70) that is involved in the same mRNA binding protein (mRNP) granule complex together with HSC70-1/HSC70-2, hnRNP L, -R, and -U (Uniprot Database) was identified in this pull down assay.

PRMT2 SH3 domain associates with other splicing-related proteins. This GST-SH3(PRMT2) pull down study revealed the association of the PRMT2 SH3 domain to a number of other splicing-related proteins that have not been found in the H complex but displayed roles in splicing regulation. Among these PRMT2 SH3 domain-associated proteins, the non-POU domain-containing octamer-binding protein ($p54^{nrb}$) and the proline- and glutamine-rich splicing factor (PSF), sharing a 71% sequence identity within their RNA recognition motif (RRM) (*194*), interact with each other and bind to the U5 snRNA and the U4/U6.U5 tri-snRNP (*195*). Another two identified PRMT2 SH3 domain-associated splicing regulators that are known to work cooperatively in directing alternative splicing are RNA-binding protein 25 (RBM25) and Luc7-like protein 3 (Luc7L3). It has been shown that RBM25 can associate with Luc7L3 and promote the formation of the pro-apoptotic Bcl-x_s versus the anti-apoptotic Bcl-x_L through alternative splicing (*196*). Moreover, both Luc7L3 and another newly discovered PRMT2 SH3 domain-associated protein RNA-binding protein 39 (RBM39) contain the arginine/serine-rich (RS) domain that is a signature structure conserved for splicing enhancers such as the SR proteins able

to recognize the exonic splicing enhancer (ESE) sequence (*197*). Both Luc7L3 and RBM39 have been reported as binders of a SR-like protein termed SRrp53 (*198*). Indeed, RBM39 is highly homologous to the U2AF2 that binds to the polyprimidine tract at the 3' splice site and forms the pre-splicing complex E in concert with U1 snRNP and SR proteins (*199*).

The U2AF is also necessary for the binding of U2 snRNP to the BPS, resulting in the formation of the pre-splicing complex A (*200*). Although U2AF was not identified as a PRMT2 SH3 interacting partner in this assay, most of essential elements for the formation of pre-splicing complex A have been found in the PRMT2 SH3 domain-associated protein complex, which include U2B" and the SF3A and SF3B subunits mentioned above, as well as the splicing factor 1 (SF1) (*168*).

This GST-SH3(PRMT2) pull down study also identified the WW domain-binding protein 11 (WBP-11) as a PRMT2 SH3 domain-associated protein. The poly(G)-binding pre-mRNA splicing factor WBP-11, which co-localizes with two other pre-mRNA splicing factors SC35 and U2B" (U2B" was pulled down in this study as mentioned above) within the nucleus, was first isolated as a binder that selectively interacted with the SH3 domain of $p47^{phox}$, p85α, and c-Src (*201, 202*). Whether WBP-11 directly interacts with U2B" or these two proteins co-localize through one or more common SH3 domain-containing proteins still needs to be further explored.

Moreover, the poly(U)-binding-splicing factor PUF60 was pulled down by the GST-SH3(PRMT2). It has been shown that PUF60 binds to the polyprimidine tract at the 3' splice site together with U2AF2 and one other identified PRMT2 SH3 domain interacting partner PSF. The activities of all three factors are required for pre-slicing E complex formation (*203*).

In addition, the paraspeckle component 1 (PSPC1) identified in this pull down assay may potentially act in splicing. Paraspeckles are dynamic sub-nuclear compartments found in the

interchromatin space of mammalian cells (*204, 205*), and comprised of long nonprotein-coding RNAs and at least the three core proteins PSPC1, p54^{nrb}, and PSF. Interestingly, all three core-members of the paraspeckle have been identified in this study. In addition, another PRMT SH3 domain-associated protein, the cleavage and polyadenylation specificity factor 6 (CPSF6) has also been considered as a possible factor of the paraspeckle (*206*). Although the function of the paraspeckle has yet to be determined, evidence suggests that the paraspeckle contributes to pre-mRNA splicing through its adjacent localization to splicing speckles enriched in pre-mRNA splicing machinery (*207*) where it can provide an ordered localization of its component proteins (*204, 208*). It has also been proposed that paraspeckles could play a role in transcriptional regulation and nuclear retention of RNA (*209-211*).

Lastly, the heat shock protein beta-1 (HSPB1) also showed up in the list of proteins that interact with the PRMT2 SH3 domain. HSPB1 co-localizes with the splicing factor SC35 upon stress-induced phosphorylation in nuclear speckles (*212*). It has been suggested that HSPB1 may couple signaling transduction and pre-mRNA splicing in order to response for the actin cytoskeleton reorganization under heat stress activation (*212, 213*).

PRMT2 SH3 domain associates with the pre-mRNA 3' processing factors. In additional to spliceosome components and their associated proteins, results of this GST-pull down study included the cleavage and polyadenylation specificity factors as interacting partners of the PRMT2 SH3 domain. In order to prepare the mature 3'-end of a eukaryotic mRNA, the pre-mRNA must undergo an endonucleolytic cleavage followed by the addition of a poly(A) tail to the upstream cleavage product [reviewed in (*214*)]. A heteromeric complex of cleavage and polyadenylation specificity factors (CPSFs) comprised of three major polypeptides of 25, 59, and 68 kDa and one minor polypeptide of 72 kDa recognizes the highly conserved AAUAAA

sequence element downstream of the poly(A) site and catalyzes the endonucleolytic cleavage reaction (*215*). Surprisingly, all three of the major polypeptides, also known as NUDT21/CPSF5 (25 kDa), CPSF6 (68 kDa), CPSF7 (59 kDa) have been found as PRMT2 SH3 domain-associated proteins. In fact, the 3' end processing of pre-mRNA is not an isolated event but happens during the orchestration of other pre-mRNA processing steps, including splicing [reviewed in (*216*)]. CPSF6 has an RRM and a RS-like domain containing repeats of arginine-serine dipeptides that interact with members of the SR family of splicing factors (*206*). A previous study has shown that both the CPSF6 and NUDT21/CPSF5 associates to U1 snRNP and may coordinate the coupling of pre-mRNA splicing and 3'-end maturation, while NUDT21/CPSF5 specifically interactes with U1-70K (*206, 217*) that was also identified in this study. Therefore, the PRMT2 SH3 domain interacting partners NUDT21/CPSF5, CPSF6, CPSF7 were categorized as splicing-related proteins despite their own 3'-end processing functions. These results suggest that PRMT2 may regulate splicing through the coordination of pre-mRNA 3'-end processing and splicing.

PRMT2 SH3 domain associates with three possible splicing-related proteins. In addition to the splicing-related proteins discussed above, three possible splicing-related proteins were found to associate with the SH3 domain of PRMT2, namely, the T-complex protein 1 subunit gamma (CCT3), -delta (CCT4), and -eta (CCT7). These proteins are components of the eukaryotic chaperonin CCT complex that is essential for the folding of a subset of cytosolic proteins including the pre-mRNA splicing factor Prp46 [a yeast homologue of the human splicing factor PLRG1 (*218*)] (*219, 220*).

Non-splicing-related PRMT2 SH3 domain-associated proteins. While the majority of the identified PRMT2 SH3 domain-associated proteins are known or possible splicing-related

proteins, two of these pulled-down hits, the WAS/WASL-interacting protein family member 1 (WIPF1) and the neural Wiskott-Aldrich syndrome protein (WASL) have no previously reported roles in splicing. However, they may interact with each other, and are responsible for the formation and function of the WIPF1/WASL complex that connects signaling cascades to actin polymerization (*221, 222*).

Plausible roles of PRMT2 in alternative splicing and RNA export. The vast majority of identified PRMT2 SH3 domain-associated proteins with only two exceptions contain proline-rich domains or PxxP motifs that could be generally recognized by SH3 domains (**Error! Reference source not found.**Table 3.1, Uniprot Database). Consistent with this observation, the Far Western blot also revealed a comparable banding pattern as the one shown in the GST-SH3(PRMT2) pull down SDS-PAGE (Figure 3.1), suggesting that PRMT2 SH3 domain may physically interact with most of its identified interacting partners. Moreover, the association of the PRMT2 SH3 domain with its interacting partners was not hugely affected by MNase treatment; once again implying that a direct protein-protein interaction between the PRMT2 SH3 domain and associated splicing-related proteins may occur. However, MNase treatment resulted in an overall reduction in the amount of isolated proteins (Figure 3.3), suggesting that the presence of RNA species may help to stabilize the PRMT2 SH3 domain-associated splicing complex. Indeed, RNA-RNA as well as protein-RNA interactions have been reported to be essential for pre-mRNA splicing. For instance, U1 snRNA is required for the formation of the U1 snRNP complex (*223*), and protein-RNA interactions also stabilize the U1 snRNP on the pre-mRNA (*224*).

On the other hand, eight of the identified PRMT2 SH3 domain-associated splicing related proteins have been reported to bear arginine methylation modifications (Uniprot Database).

Although not designed for capturing arginine-methylated protein complexes exclusively, the present proteomic approach was still able to detect methylated arginine-containing tryptic peptides, three of which were previously reported (Table 3.1). Five of the methylarginine-containing PRMT2 SH3 domain-associated proteins, however, were novel (Table 3.1).

One of the methylated PRMT2 SH3 domain-associated proteins is PSF, which contains three RGG repeats that can be recognized and methylated by Type I PRMTs [reviewed in (*225*)]. It has been reported that the three arginines located within the RGG repeats of PSF are asymmetrically dimethylated consistent with the present proteomic result (*81*), yet the PRMT responsible for this methylation activity has not been established. These arginine methylation modifications have been proposed to decrease the RNA-binding ability of PSF (*226*).

In contrast, one of the identified PRMT2 SH3 domain-associated proteins denoted E1B-AP5 (also known as hnRNP UL1) has been suggested to be a PRMT2 substrate (*43*). Kzhyshkowska *et al.* pointed out that although PRMT1 can methylate E1B-AP5 *in vitro*, PRMT2 was the Type I methyltransferase responsible for the arginine methylation of the RGG-box domain of E1B-AP5 in cells. These authors have also stated that the SH3 domain of PRMT2 is essential for its interaction with E1B-AP5 in cells (*43*). The present result further suggests that the PRMT2 SH3 domain is sufficient for the interaction between PRMT2 and E1B-AP5 *in vitro*. However, since this proteomic study was not designed to capture and enrich for methylarginine-containing tryptic peptides, the methylation state of pulled-down E1B-AP5 was not observed.

Multiple RNA-binding proteins have been identified as PRMT2 SH3 domain-associated proteins in the present study. Besides acting as splicing-regulators, hnRNPs are critical for RNA export out of the cell nucleus (*227*). Intriguingly, hnRNPs contain about 65% of Type I methylated arginine in the cell nucleus (*80*). Further, arginine methylation of hnRNPs is

important for RNA nuclear export (*228*). Additionally, Sam68 is also responsible for the nucleocytoplasmic transport of HIV RNAs (*229*), and arginine methylation is essential for Sam68 RNA export function (*95*). Therefore, PRMT2 may also be involved in controlling nuclear export of mature RNAs.

Plausible roles of PRMT2 in transcriptional regulation. PRMT2 is able to act as a coactivator for several nuclear receptors (*126, 127*). A yeast two-hybrid screen revealed an interaction between the C-terminal fragment of PRMT2 and the C-terminal DNA-binding domain (DBD) and the ligand-dependent transcriptional activation domain (AF-2) of AR (*126*). Despite the association between AR and the C-terminal domain of PRMT2, the N-terminal fragment of PRMT2 was required for androgen-dependent coactivation of transcription (*126*). It has also been found that the PRMT2 C-terminal domain is able to bind to the N-terminal activation function 1 (AF-1) domain, DBD, and the C-terminal AF-2 domain of ERα, which resulte in an enhanced ERα transcriptional activity in a cell type- and ligand-dependent manner, suggesting the involvement of other differentially expressed coregulators (*126, 127*). Unlike PRMT1 whose coactivator function depends on its methylation activity towards AR and ERα (*79, 102*), PRMT2 does not methylate AR and ERα (*126, 127*). However, the detailed mechanism of how PRMT2 acts as a coactivator of nuclear receptor-dependent transcriptional activation has not been well understood. Coincidentally, several of the newly identified PRMT2 SH3 domain-associated proteins have been known to act as transcriptional coregulators, which provide more clues in solving the role PRMT2 may play in regulating gene expression.

FUS. Du *et al.* have shown that PRMT1 methylates FUS within its GAR domain and activates transcription at the survivin promoter synergistically with FUS (*230*). These authors also found that the enzymatic activity of PRMT1 was required for this synergistic transcriptional

activation. Consistent with this previous observation, data presented here also revealed arginine methylation within the GAR domain of FUS co-purified with the PRMT2 SH3 domain. Arginine methylation of FUS may also positively influence its nuclear import and affect its nucleocytoplasmic shuttling (*231*). Interestingly, FUS can also act as a transcriptional coactivator of AR in prostate cancer cells similar to PRMT2 (*232*).

PRMT1 may not necessarily be the only enzyme responsible for FUS methylation. In the previous chapter, I have shown that PRMT1 and -2 synergistically methylated their common substrate by forming a heteromeric PRMT1/2 complex. Amino acid sequence of FUS reveals two PXXP motifs located at its N- and C-termini, while the methylated GAR sequences sit in the middle (Uniprot Database), providing binding sites for both PRMT1 and PRMT2. Further studies are required to determine if the SH3 domain of PRMT2 can directly interact with FUS, and influence FUS methylation and transcription activity.

Additionally, it has been observed that FUS interactes with the p65 subunit of NF-κB and enhances NF-κB-dependent transcriptional activation induced by physiological stimuli (*233*). Similarly, PRMT1 also interacts with p65 and coactivates the NF-κB pathway (*52*). On the other hand, PRMT2 inhibits NF-κB-dependent transcription by interacting with its p50 and p65 subunits via the PRMT2 SH3 domain, and by binding to the NF-κB inhibitor IκB-α through other regions of PRMT2 at the same time (*32*). These observations imply PRMT1, PRMT2, and FUS may play different roles in the NF-κB pathway depending on different cellular backgrounds and stimuli. It is interesting that these three proteins are able to interact with the same subunit of NF-κB, although these interactions do lead to different outcomes. Perhaps PRMT1, PRMT2, and FUS can synergistically activate NF-κB-mediated transcription, while PRMT2 could also negatively regulate the same pathway through a feedback mechanism.

PSF and p54^{nrb}. Two other proteins identified in the PRMT2 SH3 domain pull down involved in transcriptional regulation can exist in the same complex with FUS. Like FUS, PSF also binds to the DBD of thyroid hormone receptor (TR) and retinoid X receptor (RXR) mediated by its C-terminus, while p54^{nrb} associates with these receptors through an interaction with PSF (*234*). PSF then recruits the transcriptional repressor Sin3A, which mediates gene silencing by interacting with histone deacetylases (HDACs) to prime for histone deacetylation (*234*). In contrast to ER and AR that bind DNA and activate transcription in a ligand-dependent fashion, TR and RXR associate with their cognate DNA sequences and recruit repressors in the absence of ligands, and activators in the presence of ligands (*235*). It has been observed that suppression of TR- and RXR-dependent transcription is mediated by a protein complex consisting of FUS, PSF, p54^{nrb}, Sin3A, and HDACs (*234*).

Surprisingly, PRMT1 has been found in the same complex with Sin3A that down-regulated RARα/RXR-dependent transcription by facilitating histone H4 methylation and deacetylation, whereas retinoic acid treatment resulted in detachment of this repressive complex (*77*). Another study has uncovered that PRMT1, Sam68, PSF, and p54^{nrb} are involved in the same protein complex using a GST-pull down assay (*148*). Additionally, it has been documented that SF1, which was also identified in the PRMT2 SH3 domain pull down, binds to the *CYP17* gene promoter and regulates *CYP17* transcription in concert with PSF, p54^{nrb}, Sin3A, and HDACs (*236*).

Sam68. The data herein demonstrates an interaction between the splicing-related protein Sam68 and PRMT2, which appeared to be likely mediated by the PRMT2 SH3 domain. Since Sam68 has six proline-rich motifs, it can interact with SH3 domain-containing proteins such as multiple members of the Src tyrosine kinase family, p85 phos-hatidylinositol 3-kinase (PI3K),

phospholipase C gamma-1 (PLC-γ-1), Ras-GAP-binding protein 1 (G3BP1), and several signal transduction adaptor proteins such as the growth factor receptor-bound protein 2 (Grb2), Grb2-related adapter protein (Grap), and noncatalytic region of tyrosine kinase (Nck) adapter protein family members (*237, 238*). In addition, Sam68 has also been found to bind to the WW domains of the formin-binding proteins FBP21 and FBP30 through its proline-rich motifs (*54*). Therefore, Sam68 is best known as an adaptor protein capable of playing a role in signal transduction pathways by mediating interactions with numerous signaling proteins.

Additionally, Sam68 has been shown to be involved in regulating transcription and gene expression. Sam68 binds to CBP and represses CBP-dependent transcription activation, though Sam68 may also exert repressor function independent of its CBP-binding ability (*239*). Intriguingly, the transcriptional repression activity of Sam68 is independent of its RNA-binding ability, suggesting that RNA-processing and transcriptional regulation are two separate functions of Sam68 (*239*). Sam68 also interacts with hnRNP K (*240*), which has also been identified from the pull down assay in the present study. It has been reported that Sam68 enhances HIV-1 Rev-response element (RRE)-mediated gene expression and virus replication (*229*), and hnRNP K-activates transcription of the human *c-myc* gene (*241*). Strikingly, association of Sam68 and hnRNP K suppresses the transcriptional activation activities of both proteins (*240*). Additionally, elevated Sam68 expression levels have been found in prostate tumours, and Sam68 has also been shown to enhance AR-mediated transactivation (*242*). Mice with Sam68 haploinsufficiency display a delayed onset of mammary tumorigenesis driven by the mammary-targeted polyoma middle T-antigen (*MMTV-PyMT*) oncogene, which is under transcriptional control of the ER-dependent MMTV promoter (*243*). Sam68 has then been proposed as a co-activator of ER-dependent transcription in mammary tumorigenesis and metastasis (*244*).

Collectively, Sam68 and PRMTs share common interacting partners such as CBP and hnRNP K, and are involved in the same transcriptional regulation pathways. Moreover, Sam68, CBP, and hnRNP K have been reported as substrates for Type I PRMTs (*93, 95, 245*). Most of the previous studies of PRMT-mediated transcriptional regulation have been focused on PRMTs activities towards histones and CBP. It will be interesting to test if PRMT-mediated arginine methylation of signaling proteins such as Sam68 and hnRNP K can also take part in controlling gene expression through a complex model coupling signal transduction with transcriptional regulation.

Plausible roles of PRMT2 in Sam68-mediated signal transduction and alternative splicing. Figure 3.1 illustrates a similar set of interacting partners for the SH3 domains of Abl and PRMT2. Although different SH3 domains have been observed to display various binding selectivities, the SH3 domain of PRMT2 and other signal proteins share some common binding partners (*123, 125, 246*). For example, the SH3 domain of PRMT2, PI3K, and PLC-γ-1 all bind to Sam68 and SmB′ [(*125*) and Table 3.1], while Nck has been documented to associate with five of the newly determined PRMT2 SH3 domain-associated proteins, namely hnRNP K, WASL, WIPF1, PSF, and $p54^{nrb}$ (*247*). Collectively, PRMT2 may play a role in Sam68-mediated signal transduction by associating with Sam68 along with other signaling proteins. Furthermore, the methylation of Sam68 by PRMT1 in close proximity to its proline-rich motifs can attenuate its interactions with certain SH3 domains while not affecting its interactions with WW domains (*54, 95*). Regardless of whether PRMT2 increases PRMT1 activity towards Sam68, which still needs to be tested, it is clear that Type I arginine methylation can interfere with Sam68-protein interactions, and thus may potentially modulate the function of Sam68 in signaling pathways.

Other than acting as an adaptor protein in signal transduction pathways, Sam68 can also bind to RNA through its KH domain (*248*). It has been shown that the RNA binding capacity of Sam68 is able to regulate alternative splicing, playing crucial roles in apoptosis, oncogenesis, tumor metastasis, spermatogenesis, and neurogenesis (*154, 249-254*). The RT-PCR technique allowed researchers to identify a panel of target exons regulated by Sam68 (*253*). Interestingly, knockdown of Sam68 causes either increases in exon inclusion or skipping (*253*), implying that Sam68 imposes variable regulatory mechanisms to control alternative splicing.

It has been demonstrated that Sam68 can interact with hnRNP A1, and these two proteins cooperatively promote alternative splicing of the small pro-apoptotic isoform of *Bcl-x* termed *Bcl-*x_S over the large anti-apoptotic *Bcl-*x_L (*154*). Recently, Paronetto *et al*. have reported that Sam68 interacted with the proximal region of *CCND1* gene intron 4 and prevented the recruitment of U1-70K from binding to the 5' splice site, thus resulting in the inclusion of intron 4 and the expression of the *CCND1* gene to code for the cyclin D1b isoform, which demonstrated higher oncogenic potential than the cyclin D1a isoform devoid of the intron 4 (*249*). As another example, CD44 antigen is a transmembrane glycoprotein that renders cells response to extracellular stimuli (*250*). The *CD44* gene contains 10 constitutively spliced exons and 10 variable exons; expression of the variable 5 exon (v5) has been correlated with enhanced tumor malignancy and invasiveness (*250*). Importantly, Sam68 binds to the splice-regulatory sequences within *CD44* exon v5 and enhances exon v5 inclusion in conjunction with the splicing coactivator SRm160 (*250, 251*). Another role of Sam68 in tumor metastasis is its function in promoting retention of the 3' UTR-intron of *SF2/ASF*, which generates the proto-oncoprotein SF2/ASF that triggers the epithelial-to mesenchymal transition (EMT), leading to cell invasion (*252*).

Null mutations of survival of motor neurons 1 (*SMN1*) gene have been observed in patients with a neurodegenerative disease named spinal muscular atrophy (SMA). Strikingly, a highly homologous *SMN2* gene is unable to compensate for *SMN1* deficiency in SMA patients due to *SMN2* exon 7 skipping caused by the splicing repressor hnRNP A1 recruited to this exon by Sam68 (*155*). Increased Sam68 expression has been noticed during neuronal differentiation of P19 cells, correlating with changes in expression and splicing of many Sam68-targeted transcripts (*253*). Notably, alternative splicing of an exon of the *Hnrpa1* gene encoding mouse hnRNP A1 is also negatively controlled by Sam68 during neuogenesis (*253*). Sam68 not only represses inclusion of exon 8 of the epsilon sarcoglycan (*Sgce*) gene in order to promote neuogenesis (*253*), but also recruits phosphorylated RNAPII for transcriptional termination (*255*) at the intron 7/exon 8 boundary while preventing U2AF from binding to the 3' splice site of exon 8, thereby enhancing exon 8 skipping during mammalian spermatogenesis (*254*).

Post-translational modifications can affect Sam68 functions. For example, Src family kinase $p59^{fyn}$-mediated Sam68 phosphorylation inhibits Sam68 homo-oligomerization and prevents Sam68 from associating with RNA (*256*). In contrast, lysine acetylation of Sam68 has been shown to enhance Sam68 RNA binding ability (*257*). Arginine methylation catalyzed by PRMT1 is critical for the nuclear localization of Sam68 and is required for Sam68-dependent RNA export (*95*), and negatively regulates the interactions between Sam68 and SH3 domain-containing proteins (*54*). It has been speculated that Sam68 may have distinct functions in the nucleus versus in the cytoplasm, and arginine methylation of Sam68 may switch Sam68 cytoplasmic functions to predominantly nuclear functions by preventing Sam68 from interacting with cytoplasmic SH3 domain-containing proteins (*156*). PRMT2 expresses in both nuclear and cytoplasmic compartments, though the relative concentration of PRMT2 in these two sub-

cellular compartments can be different depending on cell types and the presence of nuclear receptor ligands (*21, 126*). The immunofluorescence images presented in this study show that PRMT2 co-localizes with Sam68 predominantly in the nucleus of HeLa cells, as well as in the cytoplasm upon AdOx treatment. On the other hand, ΔSH3PRMT2 may act as a dominant-negative of PRMT2 and impair nucleocytoplasmic shuttling of Sam68 in hypomethylated HeLa cells (Figure 3.6). Therefore, PRMT2 may serve as a plausible regulator of the nucleocytoplasmic switch of Sam68.

It has been determined that nuclear Sam68 together with most splicing factors were retained in the nuclear matrix-attached insoluble fraction, suggesting the major role Sam68 plays in the nucleus is splicing-related (*254*). Importantly, it has been noticed that the Sam68-dependent alternative splicing was also regulated by post-translational modification. Activities of tyrosine kinases such as $p59^{fyn}$ (*154, 258*) and extracellular signal-regulated kinases (ERKs) (*238, 251*) have been found to interfere with Sam68-dependent RNA splicing. As aforementioned, PRMTs and CBP cooperatively regulate gene expression by exerting their activities towards their common substrates like histone H4 (*50*). Since PRMT1, PRMT2, and CBP can interact with and even modify Sam68, as well as affect its RNA-binding ability and sub-cellular localization, these modifying enzymes may potentially play a role in regulating Sam68-dependent alternative splicing.

Plausible roles of PRMT2 in programmed cell death. Programmed cell death or apoptosis is a way to maintain normal tissue homeostasis by removing malfunctioning or DNA-damaged cells (*259*). Resistance to apoptosis can result in the inappropriate survival of DNA-damaged cells, and thus an increased the susceptibility to cancer (*260*). The interplay between pro- and anti-apoptotic members of the B-cell lymphoma 2 (Bcl-2) related protein family is

important for balancing apoptotic activity in cells (*261*). Bcl-x is one of the best-characterized members of the Bcl-2-related protein family. At least two human isoforms for Bcl-x have been described; the larger isoform denoted Bcl-x_L contains the highly conserved BH1 and BH2 domains that are essential for the anti-apoptotic function, whereas the small isoform named Bcl-x_S devoid of these conserved domains is generated by utilizing a distinct splice site in *Bcl-x* exon 2 during alternative splicing to form a pro-apoptotic form of Bcl-x_L (*261, 262*).

Is has been discussed in the previous section that Sam68 regulates the production of the two Bcl-x isoforms (*154*). Similarly, the PRMT2 SH3 domain binder RBM25 have also been found to modulate alternative splicing of *Bcl-x*. Zhou *et al*. reported that RBM25 promoted the usage of a weak 5' splice site within exon 2 of the *Bcl-x* gene by recruiting U1 snRNP through an interaction with the U1 snRNP-associated protein Luc7L3, hence stimulating *Bcl-x_S* instead of *Bcl-x_L* formation (*196*). Notably, Luc7L3 is one of the two proteins identified in the PRMT2 SH3 domain pull down that does not contain a PXXP motif. Since it interacts with other PRMT2 SH3 domain-associated proteins, it may simply associate with its binders such as RBM25 and U1 snRNP in the pull down assay. This result suggests that the PRMT2 SH3 domain interacts with factors regulating alternative splicing of *Bcl-x*. Further studies are needed to investigate the role PRMT2 may play in the control of Bcl-x isoform expression.

4 PRMT1/2 Protein Complex[4]

4.1 Introduction

I have demonstrated in Chapter 2 that the formation of a PRMT1/2 complex may be regulated through interactions between the SH3 domain of PRMT2 and other interacting partners of the PRMT1/2 complex in a methylation-dependent fashion. This result suggests that the PRMT2 SH3 domain is able to respond to the overall methylation state in cells and modulate the sub-cellular localization of associated proteins like Sam68. However, whether Sam68 or other proteins identified in Chapter 3 can regulate PRMT1/2 complex formation through their interactions with PRMT2 remains unclear.

In order to gain a better understanding of PRMT1/2 complex formation, I pursued the identity of interacting partners common to both PRMT1 and -2. I immunoprecipitated HA-PRMT1 and HA-PRMT2 overexpressed in HeLa cells and then characterized the purified immuno-complex using mass spectrometry proteomics. Co-immunoprecipitation coupled with LC-MS/MS is a technique that is routinely used to look for protein binding partners (*263*). The co-immunoprecipitation step allows for the isolation of the protein complexes comprised of the protein of interest (bait) and associated proteins (prey) under the experimental condition. The isolated protein complexes can be either resolved on a SDS-PAGE gel in which specific protein bands can then be excised and subjected to in-gel proteolysis followed by LC-MS/MS sequencing, or these protein complexes can be precipitated out of solution, reconstituted for

[4] The LC-MS/MS proteomic study was preformed in the Proteomics Core Facility at UBC. The Core Facility manager, Suzanne C. Perry digested the protein samples and ran them on a LC-MS/MS followed by a MASCOT search.
The baculovirus lysates for 6×His-PML-I and 6×His-PML-IV were gifts from Dr. Graham Dellaire at Dalhousie University.

proteolytic digestion, and then sequenced by LC-MS/MS analysis. The first method enables one to visualize the banding pattern of the interacting partners of the bait protein, thus one can identify one or few specific interacting partners. For example, the first approach presented in Chapter 3 employed a GST-pull down experiment as another means to isolate protein complexes in order to determine associated proteins that prefer the PRMT2 SH3 domain to the Abl SH3 domain. In the absence of the SDS-PAGE gel resolution step no *a priori* knowledge about possible components of the isolated protein complexes is required, thus permitting one to screen for all protein-protein interaction that can be captured and detected within experimental limits. Therefore, no resolving step was used after co-IP to identify as many interacting partners for PRMT1 and -2 as possible.

I found that the majority of proteins found in the experimental samples associated with both PRMT1 and PRMT2 specifically. Two of the identified PRMT2-associated proteins, the promyelocytic leukemia protein (PML) and extra eleven nineteen (EEN) were confirmed as PRMT2 interacting partners in cells. Furthermore, the PRMT2 SH3 domain was required for the association between PML and PRMT2, which suggests that PML may serve as a plausible regulator of the PRMT1/2 complex. In addition, I found that the tumor suppressor and transcription factor p53, which is known to bind to PRMT1 and PML (*50, 264*), co-immunoprecipitated with PRMT2. These results suggest that PRMT1, PRMT2, PML and p53 may be involved in the same protein complex that regulates transcriptional activation.

4.2 Methods

DNA constructs. pcDNA3.1(+)/Neo-HA-PRMT1 and pcDNA3.1(+)/Neo-HA-PRMT2 were generated and purified as described in section 2.2.

Tissue culture. HeLa cells were cultured under the same condition as described in section 2.2, and were transiently transfected with pcDNA3.1(+)/Neo-HA-PRMT1 or pcDNA3.1(+)/Neo-HA-PRMT2 (24 μg) using Lipofectamine 2000 (Invitrogen) per the manufacturer's instructions. The Opti-MEM medium was replaced with regular growth medium (DMEM supplemented with 5% FBS, 50 units/mL penicillin, and 50 μg/mL streptomycin) 8 h post-transfection. The transfected cells were split 24-h post-transfection and allowed to grow to 80% confluency for an additional 48 h before they were harvested.

Sample preparation for proteomic study. Anti-HA antibody was crosslinked to the NHS-activated sepharose (GE Healthcare) per manufacturer's instructions. HA-PRMT1 and HA-PRMT2 were overexpressed in HeLa cells, and cells were harvested and lysed in hypotonic lysis buffer as described in section 2.2. Cell lysates containing 3 mg total protein from wild type HeLa cells or HeLa cells that overexpressed HA-PRMT1 or HA-PRMT2 were incubated with 50 µl of sepharose cross-linked with 4.5 μg of monoclonal anti-HA antibody (Sigma) in 3 mL of co-IP buffer [50 mM HEPES (pH 7.4), 150 mM NaCl, 1x proteases inhibitor cocktail (Roche)] at 4 °C for 2 h with rotation. Subsequently, the resin was washed thoroughly with 0.05% (v/v) Tween 20 in PBS five times before the bound proteins were eluted in 150 μl 6 M urea and 2 M thiourea followed by adding 3 times volume of absolute ethanol. The composition of this solution was adjusted to 50 mM $NaCH_3COO$, pH 5.0 by adding 2.5 M $NaCH_3COO$ (pH5.0). Glycogen (20 μg) was then added to the sample to facilitate protein precipitation. The sample was incubated at room temperature for 2 h before precipitants were pelleted by centrifuging at

20,000 x *g* for 10 minutes. Precipitated proteins were dried in a vacuum centrifuge prior to sample submission. These experiments were performed in duplicate.

Proteomic study. The immunoprecipitated proteins were submitted as dried pellets in duplicate to the Proteomics Core Facility within the Centre for High-Throughput Biology at UBC for *de novo* sequencing of PRMT-associated proteins using LC-MS/MS. The samples were digested with trypsin and desalted using ZipTip (Millipore) C-18 cartridges. Tryptic fragments were analyzed by an API QSTAR PULSARI Hybrid LC-MS/MS and identified by a human database search using the MASCOT (Matrix Science) search engine. Proteins were disregarded if their MASCOT score did not meet the $p \geq 0.05$ threshold, if they were identified in only one of the duplicates, or if they were identified in the negative controls. We identified 22 proteins unique to both HA-PRMT1 duplicates, 15 proteins unique to both HA-PRMT2 duplicates, and 79 proteins shared between HA-PRMT1 and HA-PRMT2 samples.

GST-pull down. For GST-pull down with PML-I or PML-IV, total proteins (200 μg) from lysate overexpressing 6xHis-PML-I or 6xHis-PML-IV were incubated with 100 μg of GST-SH3(PRMT2) in co-IP buffer [50 mM HEPES (pH 7.4), 150 mM NaCl, 1x proteases inhibitor cocktail (Roche)] at 4 °C for 2 hours with rotation. The pull down assay was performed as described in section 3.2. Protein eluents from GST-pull downs were resolved on a 10% SDS-PAGE gel before being transferred to a piece of PVDF membrane and blotted for PML using an anti-PML antibody (Santa Cruz) at 1:500 dilution. Goat anti-rabbit IgG-HRP (Santa Cruz) antibody and ECL Western blotting detection reagents (GE Healthcare) were used for protein visualization.

Immunoprecipitation and Western blotting. HA-PRMT2 and HA-ΔSH3PRMT2 were overexpressed in HeLa cells as previously described in section 2.2. Cells were harvested and

lysed 72 h after transfection using hypotonic lysis buffer. Cell lysate (500 μg protein) was aliquoted and the buffer was adjusted to 50 mM HEPES-KOH, 150 mM NaCl. Aliquoted cell lysate was then supplemented with 4.0 μg of polyclonal anti-Smac, anti-IKKγ, anti-PML, polyclonal anti-PP2A-B55α, anti-EEN, or 2.0 μg of monoclonal anti-HA antibody or mouse IgG, and the volume was adjusted to 0.5 mL with co-IP buffer [50 mM HEPES-KOH, pH 7.4, 150 mM NaCl, 1x protease inhibitor cocktail (Roche #04693132001)]. The protein/antibody mixtures were incubated at 4 °C for 16 h with rotation. The cell lysate/antibody mixture was added to 30 μL pre-washed protein G-sepharose (Invitrogen) and was rotated at 4 °C for 2 h. Subsequently, the resin was washed thoroughly with 0.05% (v/v) Tween 20 in PBS five times before the bound proteins were eluted in SDS-PAGE sample buffer.

To study the interaction between p53 and PRMT1, PRMT2, or PRMT6, the proteins Myc-p53 and HA-PRMT1, HA-PRMT2, HA-ΔSH3, or HA-PRMT6 were overexpressed in HeLa cells, and the co-IP experiments were performed as described above using 2.0 μg of monoclonal anti-HA or anti-Myc antibody.

For Western blots, proteins were separated on 10% SDS-PAGE gels, transferred to PVDF membranes and blotted with anti-HA, anti-Myc, anti-PML, or anti-EEN antibody. Goat anti-mouse light chain HRP conjugated secondary antibody (Millipore) or goat anti-rabbit IgG-HRP (Santa Cruz) and ECL Western blotting detection reagents (GE Healthcare) were used for protein visualization.

Immunofluorescence and Confocal Microscopy. Approximately 1.0×10^7 HeLa cells were co-transfected with either pcDNA3.1(+)/Neo-mCitrine-PRMT2 or pcDNA3.1(+)/Neo-mCitrine-ΔSH3PRMT2 and pcDNA3.1(+)/Neo-mCitrine-PRMT2 (12 μg each) using Lipofectamine 2000 (Invitrogen) as described in section 2.2.

The cells were permeabilized and blocked as aforementioned. The cells were co-blotted with anti-HA (Sigma) and anti-PML antibodies (Santa Cruz) at 1:500 and 1:50 dilution in 1% (w/v) PBST-BSA solution at room temperature for 1 h, respectively. The cells were then washed with PBST for three times before blotting with Alexa Fluor 546-conjugated goat anti-rabbit secondary and Alexa Fluor 647-conjugated goat anti-mouse secondary antibodies (Invitrogen) at 1:1000 dilution in 1% (w/v) PBST-BSA solution at room temperature for 1 h. DAPI stain and confocal microscopy were performed as previously mentioned in Chapter 3.

4.3 Results

Identification of interacting partners of PRMT1 and -2. HA-PRMT1 or HA-PRMT2 was expressed in HeLa cells individually to serve as bait proteins. All other proteins expressed endogenously in HeLa cells served as prey. HeLa cells were harvested and lysed; the bait proteins together with their associating partners were immunoprecipitated using an anti-HA antibody conjugated sepharose resin. A similar co-IP using non-transfected wild type HeLa cell lysate was done as a negative control for non-specific interactions that may occur between endogenous proteins and the anti-HA antibody-conjugated sepharose resin. The protein complexes were eluted from resin under denaturing conditions, and proteins in the eluents were precipitated out of solution, dried, reconstituted into a trypsin buffer system, and then trypsinized. The tryptic peptides were injected into the LC-MS/MS system and MS/MS raw spectra were generated as outputs, which were subsequently analyzed using the MASCOT algorithm (Matrix Science).

The software package MASCOT is developed by Matrix Science to convert mass spectral data into protein identities. MASCOT compares or queries (MASCOT terminology) each MS/MS spectrum against a database of known protein sequences, thereby determining the most likely match. However, false positives caused by random matching can also be produced by MASCOT. To address this problem, all MASCOT reports contain an "ion score significance threshold" representing a 5% confidence threshold. In a MASCOT report, the ion score is reported as -10Log(P), where P is the probability that the observed match between the experimental data and the database sequence is a random event. Because more than one MS/MS spectra (queries) can be matched to an identified protein, an ion score will be assigned to each of these queries. In general, a confident identification should have two or more matching queries;

and the individual ion score should be greater than the 5% confidence threshold, thus falling into the 95% confidence interval, which indicates that the query match chance of being a false positive is less than 1 in 20 ($p<0.05$). One more term, the protein score is introduced to represent the sum of the highest ion score for each distinct matched query sequence. Protein score is therefore used to rank the protein hits because it takes into consideration two different parameters, the number of distinct matched queries and the ion score for each matched query.

Besides using these thresholds given by MASCOT to rule out false positive protein hits, the present study also employed a negative control in which a mock co-immunoprecipitation was done using untransfected wild type HeLa cell lysate and the same anti-HA antibody conjugated resin. The protein hits generated by this negative control represented non-specific protein-protein and protein-resin interactions captured by the co-immunoprecipitation experiment. Moreover, all of the co-immunoprecipitation experiments including the negative controls were done in duplicate. Only those protein hits with ions scores above the 5% confidence threshold identified in both duplicates of the experimental groups but not found in any of the negative control replicates are considered as unique binders for PRMT1 or -2. Additionally, the protein hits with ions scores above the threshold identified in both duplicates of co-IPs for one PRMT and one or both duplicates for the other PRMT were considered as common associated proteins for the two PRMTs.

Applying the above selection criteria, a total of 101 PRMT1-associated proteins and 94 PRMT2-associated proteins were identified with 79 hits from these groups associated with both PRMTs (Figure 4.1). Out of the 79 PRMT1 and -2 common binders, 32 hits have been identified in both HA-PRMT1 samples and in only one HA-PRMT2 sample; 26 hits have been identified in both HA-PRMT2 samples and in only one HA-PRMT1 sample; and 21 hits have been identified

in all four co-IP samples (Figure 4.1). Moreover, 208 hits showed up once in only one HA-PRMT1 sample, and 304 hits showed up once in only one HA-PRMT2 sample, while another 91 hits were found once in the HA-PRMT1 and HA-PRMT2 samples (Figure 4.1). Although the proteins that were identified only once in the duplicates represent additional potential PRMT1 and/or PRMT2-associated proteins, I did not consider them as hits in this screen for the purpose of stringency.

The identified hits exhibit an array of biological functions, intriguingly, at least 55 out of the 116 identified PRMT1 and/or -2 interacting partners play roles in controlling gene expression through DNA replication, RNA processing, transcription, translation, post-translational modification, and cell cycle regulation (Table A.3). The functional diversity of the PRMT-associated proteins implicates the involvement of PRMTs in a variety of cellular processes, and hence underscores the significance of PRMTs. Further, the result of this proteomic study reveals that the majority of identified interacting partners are shared by both PRMT1 and -2. It is quite possible that more than one PRMT is needed for most of the PRMT-facilitated biological processes.

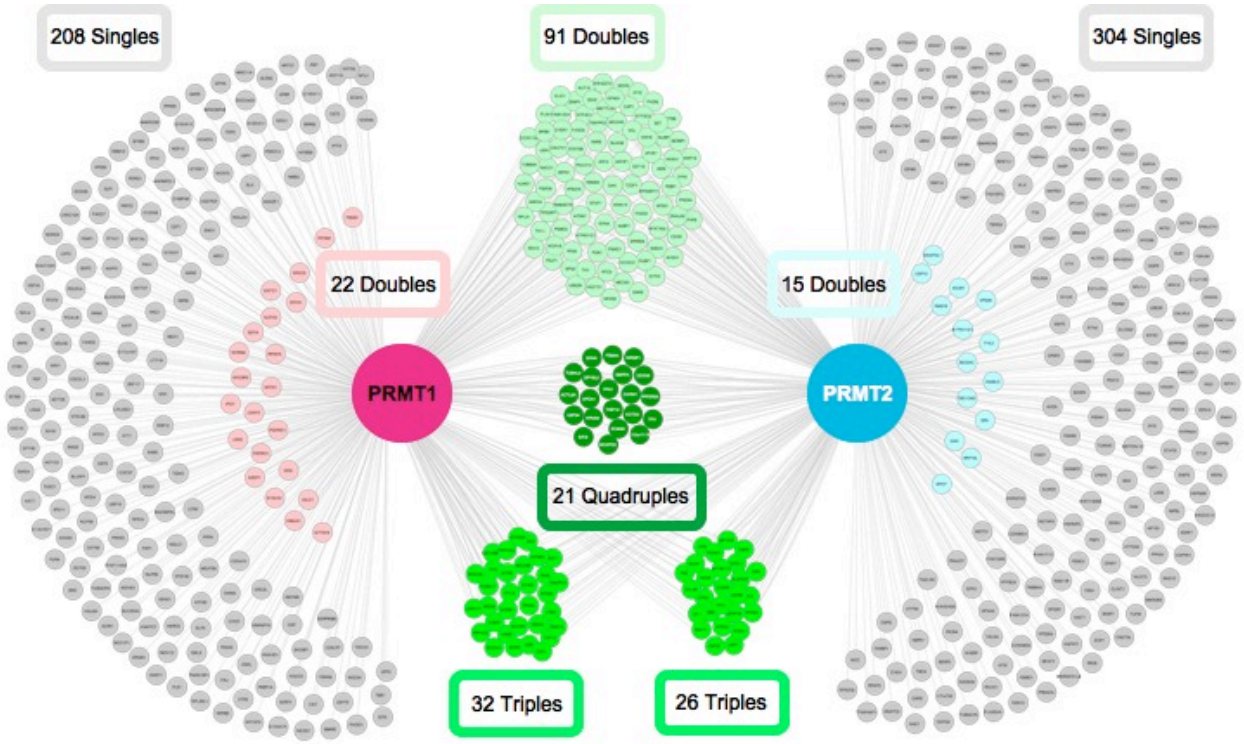

Figure 4.1. Identified PRMT1 and PRMT2 interacting partners. An illustration of associated proteins of PRMT1 and/or PRMT2 as determined by co-immunoprecipitation and LC-MS/MS. "Doubles" in *pink* and *blue* are hits identified in both duplicates of PRMT1 or -2, respectively. "Singles" are hits identified once in a sample of either PRMT1 or -2. "Doubles" in *light green* are hits identified in one sample of each PRMT. "Triples" are hits identified in both duplicates of one PRMT and in one sample of the other PRMT. "Quadruples" are hits identified in both duplicates of both PRMTs. This diagram is prepared using the Cytoscape Software.

Confirmation of PRMT-protein interactions. Five proteomic hits with previously known roles in regulating apoptosis or oncogenesis, second mitochondria-derived activator of caspase (Smac), NF-κB essential modulator (NEMO/IKKγ), PML, EEN, alpha isoform of the 55 kDa regulatory subunit for serine/threonine-protein phosphatase 2A (PP2A-B55α), were selected to confirm associations with PRMT2 in HeLa cells expressing HA-PRMT2 and either immunoprecipitating the five proteins of interest and blotting for HA-PRMT2, or immunoprecipitating HA-PRMT2 and blotting for proteins of interest with appropriate antibodies. With the exception of EEN and Smac, the other three hits used to confirm associations were isolated in both PRMT1 and -2 proteomic samples.

EEN. HeLa cells were transfected with DNA constructs encoding either HA tagged full-length PRMT1 (HA-PRMT1), PRMT2 (HA-PRMT2), or truncated PRMT2 lacking its SH3 domain (HA-ΔSH3). The immunoprecipitated protein complexes were resolved on a 10% SDS-PAGE gel, and then transferred to a piece of PVDF membrane. Consistent with an earlier observation reported by Cheung *et al.* showing that EEN co-immunoprecipitated with PRMT1, my co-IP result illustrates association of endogenous EEN and HA-PRMT1 (Figure 4.2) even though EEN has only been identified to associate with PRMT2 in the proteomic portion of this study. The existence of endogenous EEN in the immunoprecipitated HA-PRMT2 or HA-ΔSH3 protein complexes was confirmed by blotting with an anti-EEN antibody (Figure 4.2). Therefore, I have verified the association between EEN and PRMT2. Furthermore, the SH3 domain of PRMT2 is dispensable for the interaction these two proteins.

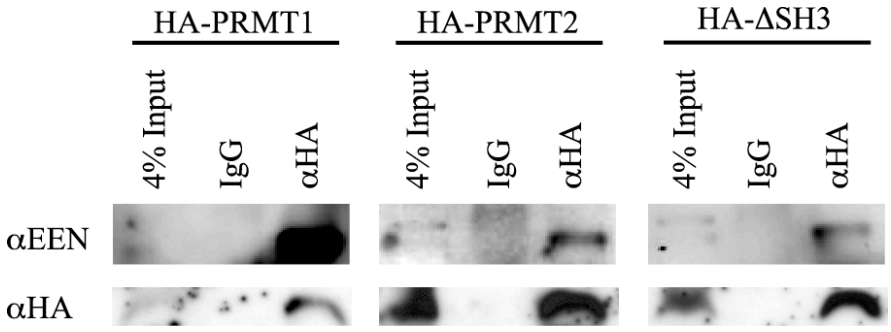

Figure 4.2. PRMT2 and EEN co-immunoprecipitate in cells. HA-PRMT1, HA-PRMT2, or HA-ΔSH3PRMT2 was expressed in HeLa cells and cell lysate was immunoprecipitated with anti-HA antibody, or with mouse IgG (negative control). Immunoprecipitates were immunoblotted with anti-EEN (*top)* or anti-HA (*bottom)* antibodies.

EEN is an SH3 domain-containing gene of endophilin family. It was discovered as a fusion to the mixed lineage leukemia (MLL) as a result of t(11; 19) chromosomal translocation in a case of infant acute myeloid leukemia (AML) (*265*). An earlier study showed that the EEN SH3 domain could interact with Sam68, thereby recruiting Sam68-associated PRMT1 to methylate histone H4 at its R3 position (*148*). The same study also demonstrated that histone H4 methylation and acetylation, as well as cell transformation of hematopoietic cells mediated by the oncogenic fusion MLL-EEN require the EEN SH3 domain (*148*). The present study demonstrates that PRMT2, in addition to PRMT1, can associate with EEN. Whether PRMT1, Sam68 and/or the SH3 domain of EEN are necessary for the association of EEN and PRMT2 remains to be tested.

Despite that endogenous EEN had been shown to co-immunoprecipitate with both HA-PRMT2 and HA-ΔSH3, these PRMT2 proteins were not detected in the co-IP with EEN (Figure 4.3). Moreover, no interaction between these PRMT2 proteins and endogenous Smac, IKKγ, or PP2A-B55α was observed (Figure 4.3). In fact, none of the other identified protein hits, namely Smac, IKKγ, and PP2A-B55α were pulled down by endogenous PRMT2 (data not shown). These discrepancies could be due to many variants such as the nature of the interactions between the proteins of interest and PRMT2, the relative expression levels of these proteins, or the sensitivity of detection method. Nevertheless, the associations of Smac, IKKγ, and PP2A-B55α to PRMT2 still need to be further investigated by other methods such as co-expressing the epitope tagged versions of these proteins and HA-PRMT2 in cells, or by *in vitro* techniques such as the GST-pull down.

PML. Endogenous PML was immunoprecipitated from HeLa cells expressing either HA tagged full-length PRMT2 (HA-PRMT2) or truncated PRMT2 lacking its SH3 domain (HA-

ΔSH3) using an anti-PML antibody. Western blots using an anti-HA antibody were used to test if any of the ectopically expressed proteins had co-immunoprecipitated with the endogenous PML. As shown in Figure 4.3, only the full-length but not the truncated PRMT2 was isolated with the endogenous PML. Consistent with the proteomic study, this co-IP result also verifies an association between PML and PRMT2, possibly mediated by the SH3 domain of PRMT2.

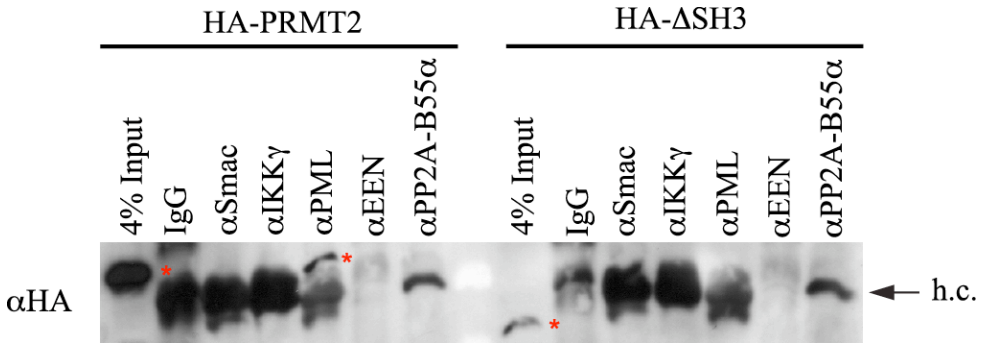

Figure 4.3. PRMT2 and PML co-immunoprecipitate in cells. HA-PRMT2 or HA-ΔSH3PRMT2 was expressed in HeLa cells and cell lysate was immunoprecipitated with anti-Smac, anti-IKKγ, anti-PML, anti-EEN, anti-PP2A-B55α, or with mouse IgG (negative control). Immunoprecipitates were immunoblotted with an anti-HA antibody. The HA-PRMT2 or HA-ΔSH3PRMT2 is indicated by *red asterisks*. The arrow indicates the antibody heavy chain contamination (h.c.).

In 1990, the *PML* gene was originally cloned from the frequent t(15; 17) chromosomal translocation that generates the *PML-RARα* and *RARα-PML* fusion genes in acute promyelocytic leukemia (APL) (*266, 267*). APL is a distinct subtype that comprises 10% to 15% of all cases of adult AML, while the *PML-RARα/ RARα-PML* fusions have been associated with more than 90% of APL (*268*). PML acts as a tumor suppressor *in vivo*, and the PML-RARα fusion protein may act as an anti-apoptotic oncogene by interacting with and antagonizing PML (*269*). It has been reported that PML is the major component of the sub-nuclear structure named PML-NBs that host various transcriptional regulators and play a role in transcriptional regulation [reviewed

in (*270*)]. It will be interesting to test if the interaction between PML and PRMT2 through the PRMT2 SH3 domain brings PRMT2 into PML-NBs.

PRMT2 SH3 domain binds PML isoforms I and IV. The *PML* gene contains nine exons, and at least seven groups of alternatively spliced PML transcripts denoted PML I-VII; the PML isoforms contain different sequences at their C-termini, but express at comparable levels in all cell lines tested to date (*271*). To investigate if the SH3 domain of PRMT2 is sufficient for PML binding, GST-pull down experiments were performed using GST-SH3(PRMT2) as a bait and baculovirus lysate expressing either 6×His-PML-I or 6×His-PML-IV as a prey. The baculovirus lysates for PML-I and PML-IV were kindly provided by Dr. Graham Dellaire at Dalhousie University. PML-I is the largest PML variant reported, and PML-IV is the most studied PML isoform by far due to its involvement in mediating p53-dependent apoptosis through directly interacting with p53 (*272*). The presence of PML isoforms in the final GST-pull down was examined by Western blotting with an anti-PML antibody (Figure 4.4). Both of the two PML isoforms tested were isolated by GST-SH3(PRMT2), indicating that the SH3 domain portion is sufficient for the association of PML and PRMT2. Since both PML isoforms were able to bind to the PRMT2 SH3 domain, the interaction between PML and PRMT2 is likely to occur through the conserved N-terminus of PML, which contains a proline-rich region.

To test whether PML is a substrate for PRMT1 and/or -2, an *in vitro* methylation assay as described in section 2.2 was performed using recombinantly expressed GST-PRMT2 or 6xHis-PRMT1 as a methylation source, and heat inactivated baculovirus lysate expressing either 6×His-PML-I or 6×His-PML-IV as a substrate. The heating step has been shown to inactivate endogenous methyltransferase activities in cell lysate (*43*). Proteins from the methylation reactions were separated on 15% tricine gels and exposed to storage phosphor screens. PRMT1

and PRMT2 did not methylate either of the two PML isoforms (data not shown). The biological consequence of the interaction between PRMT2 and PML requires further study.

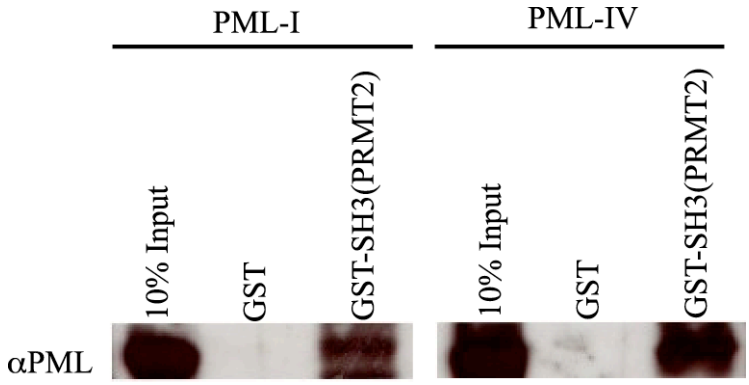

Figure 4.4. PRMT2 SH3 domain interacts with PML isoforms I and IV. GST-pull down experiments were performed using baculovirus lysate expressing either 6×His-PML-I or 6×His-PML-IV as prey. Eluents were resolved on a 10% SDS-PAGE gel and blotted with an anti-PML antibody.

PRMT2 interacts with the tumor suppressor p53. As discussed in an earlier section, several of proteomic hits are known to regulate apoptosis through the p53 pathway. Both PRMT1 and CARM1 are able to bind p53 and exert their transactivating functions in conjunction with the histone acetylase p300 (*50*). Although CARM1 associated with PRMT1 and -2, p53 was not identified in this proteomic study. However, it has been reported that p53 levels in HeLa cells are undetectable, which may be due to its high instability in this cell line (*273*). Therefore, it is not surprising that endogenous p53 has not been isolated in any of the co-IPs.

To examine the interaction between p53 and the two PRMTs, HeLa cells were co-transfected with DNA constructs encoding Myc-p53 along with HA-PRMT1, HA-PRMT2, or HA-ΔSH3. The HA tagged PRMT was immunoprecipitated by an anti-HA antibody and subsequently blotted for Myc-p53 using an anti-Myc antibody. Consistent with a previous observation (*50*), my co-IP result also showed an association between PRMT1 and p53 (Figure 4.5A). Additionally, p53 was pulled down by both full-length PRMT2 and PRMT2 devoid of its SH3 domain (Figure 4.5A). Strikingly, endogenous PRMT2 was detected in the same protein complex containing HA-PRMT1 and p53 (Figure 4.5B). Furthermore, endogenous PRMT2 was also isolated within the immunoprecipitated HA-p53 protein complex (Figure 4.5C). These results illustrate that both PRMT1 and -2 interact with p53 when it is stably expressed, and that the interaction between PRMT2 and p53 does not require the PRMT2 SH3 domain even though p53 contains many PXXP motifs that could serve as binding sites for SH3 domains (*274*).

In another one of my co-IP experiments I found that HA-PRMT6 also associated with Myc-p53 (Figure A.14), and an interaction between PRMT5 and p53 has been reported earlier by another group of researchers (*47*). Thus, five out of nine members of the PRMT family have been shown to associate with p53 so far, and in the proteomic experiment in this study several

proteins involved in the p53 pathway were pulled down by co-IP with PRMT1 and -2. All of these observations suggest a role for the family of PRMTs in p53-dependent pathways.

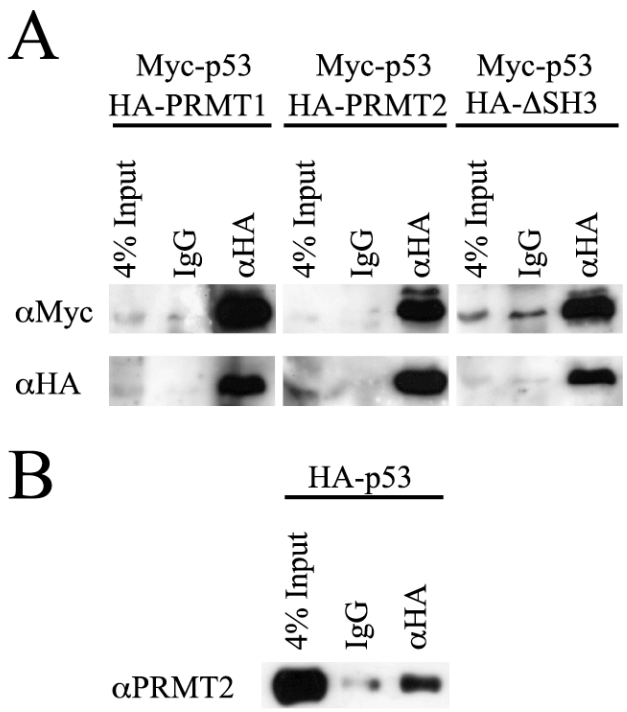

Figure 4.5. PRMT2 and p53 co-immunoprecipitate in cells. (A) Myc-p53 and HA-PRMT1, HA-PRMT2, or HA-ΔSH3PRMT2 were co-expressed in HeLa cells and cell lysate was immunoprecipitated with anti-HA antibody, or with mouse IgG (negative control). Immunoprecipitates were immunoblotted with anti-Myc (*top)* or anti-HA (*bottom)* antibodies. (B) HA-PRMT1 was expressed in HeLa cells and cell lysate was immunoprecipitated with anti-HA antibody, or with mouse IgG (negative control). Immunoprecipitates were immunoblotted with an anti-PRMT2 antibody.

4.4 Discussion

In this study, I used a proteomic approach to identify proteins that associate with PRMT1 and/or -2. Although some identified proteins are uniquely associated to either enzyme sample, most of the hits were identified in both. This proteomic analysis reveals several previously known PRMT binders, and more importantly, it captures a handful of mostly PRMT1/2-associated proteins involved in regulating gene expression, mRNA splicing, protein degradation, inflammatory response, and apoptosis. This result suggests the involvement of PRMT1 and -2 in various essential cellular pathways through a series of PRMT-protein interactions.

Identification of known PRMT1 binders.

TAF15. Identified as a hit for PRMT1 and -2 by co-IP, TAF15 has been reported as a PRMT1 substrate (*97*). Jobert *et al.* pointed out in 2009 that the PRMT1 methylation of TAF15 within its C-terminal GAR domain is important for its shuttling between the nucleus and the cytoplasm. These authors demonstrated that TAF15 accumulated in stress granules (SG) within the cytoplasm of HeLa cells upon AdOx treatment or PRMT1 knockdown, whereas it localized predominantly in the nucleus without treatment. Moreover, the authors found that the transactivation function of TAF15 required PRMT1 mediated-methylation. Since TAF15 was able to associate with both PRMT1 and -2, it is plausible that these two PRMTs could cooperate in the methylation of TAF15.

HMGA1. HMGA1 has been proposed as a potential *in vivo* substrate for PRMT1 based on the observation that PRMT1 and -3 preferentially methylate HMGA1 at residues R25 and R23 *in vitro*, respectively (*275*). An earlier study suggested that PRMT6 methylates HMGA1 at residues R57 and R59 *in vivo* (*276*). HMGA1 is an architectural nuclear factor that plays an important role in chromatin dynamics and serves as a central 'hub' of nuclear function by

interacting with a large number of other proteins such as various transcription factors including NF-κB (*277, 278*). The monomethylation of HMGA1 has been shown to increase in four leukemic cell lines when treated with drug or virus to induce of apoptosis (*279*). A different group of researchers later reported that the amount of monomethylated HMGA1 can reach up to 50% of total HMGA1 in some tumor cell lines; and the degree of monomethylation, specifically at amino acid residue R25, appears to increase during apoptosis (*280*). PRMT1 is the only known Type I PRMT that methylates HMGA1 at R25 *in vitro* (*275, 281*), though it is unclear if PRMT1 is responsible for the methylation at this residue *in vivo*. The present study reveals the association of PRMT1 but not PRMT2 with HMGA1, which supports the existing hypothesis that PRMT1 is responsible for HMGA1 methylation at R25.

CARM1. The association between PRMT1 and CARM1 has already been established via a co-IP experiment (*21*). In this study, CARM1 was detected in both duplicates of the PRMT1 and -2 immunoprecipitation samples but in neither of the negative controls by LC-MS/MS. This observation not only provides additional evidence for a CARM1-PRMT1 association, but also reveals a new association between CARM1 and PRMT2. Since PRMT1 is able to form a heteromeric complex with PRMT2 and PRMTs share highly similar ternary structures (*5*), heteromeric complexes containing CARM1 and PRMT1 or -2 may also exist, yet no common substrate shared by these three PRMTs has been discovered. It will be interesting to test whether CARM1 can directly interact with PRMT1 and/or 2 *in vitro*. It has been shown that PRMT1 and CARM1 regulate gene expression cooperatively (*50, 51*); therefore, it is reasonable to postulate that all three PRMTs can be coordinated in their roles as transcriptional regulators.

EEN. The known PRMT1-associated protein EEN was only found in the PRMT2 co-IP. EEN is a SH3 domain-containing protein first identified as the C-terminal component of the

oncogenic MLL-EEN fusion protein where the C-terminal truncation of the lysine methyltransferase MLL is fused to the N-terminus of EEN lacking its first 15 amino acid residues (*265*). MLL is the gene product of the *Mixed Lineage Leukemia (MLL)* gene located on chromosome 11q23, where chromosomal translocations have been frequently observed in patients with AML and acute lymphoid leukemia (ALL) (*282*). *MLL* rearrangements account for 5-10% of childhood and adult AML and ALL, and up to 80% of infant ALL and approximate 60% of infant AML (*283*). At least 51 partner genes of *MLL* have been discovered in patients with various leukemias so far (*284*).

EEN is the only member of the endophilin protein family expressed in hematopoietic cells. It has been reported that EEN may play a role in endocytosis and signal transduction (*265, 285*); however, more studies have been performed to explore the function of EEN's in hematopoietic cells and oncogenesis, especially as an MLL-EEN fusion protein. It has been reported that the knock-in of an *MLL-EEN* gene causes myeloid leukemia in chimeric mice (*286*), and only the MLL-EEN fusion protein but not the truncated form of MLL is oncogenic (*282*). It is noteworthy that the MLL portion of the MLL-EEN fusion protein contains a DNA-binding motif that contributes to the DNA-binding ability of the fusion protein. In a 2004 study, Liu *et al.* attempted to tackle the functional contribution of EEN to leukemogenic transformation by the MLL-EEN fusion protein (*282*). They noticed that MLL-EEN interacted with EEN through the coiled-coil domain of EEN, and directed the normally cytoplasmic EEN to the nucleus. Furthermore, they demonstrated that either the SH3 domain or the coiled-coil domain of EEN when expressed alone could activate transcription using a reporter gene assay. They then proposed that EEN might obtain transactivation activity through protein-protein interactions mediated by its coiled-coil and SH3 domains.

In support of this hypothesis, Cheung *et al.* determine that the EEN SH3 domain ias necessary and sufficient for leukemogenesis since the deletion of the coiled-coil domain does not abolish cell transformation (*148*). These authors conducted a GST-pull down experiment by using GST-SH3(EEN) as bait and total proteins in HeLa cell lysate as prey and identified Sam68, $p54^{nrb}$, and PSF as the major EEN SH3 domain-associated proteins. Additionally, they were able to detect the presence of PRMT1 in their purified GST-SH3(EEN) pull down. The presence of PRMT2, however, was not tested.

Although EEN has been shown to associate with PRMT1 (*148*), it was not detected as a PRMT1-associated protein, but rather a PRMT2 interacting partner by the present co-IP followed by proteomic analysis. However, the association of endogenous EEN and HA-PRMT1 was demonstrated using co-IP followed by Western blotting (Figure 4.2). Many factors such as the relative abundance of the proteins, the binding affinity of the interactions, or the sensitivity of the detection method can cause these inconsistencies.

p53. It has been reported that p53 interacts with PRMT1 and CARM1 (*50*). The present study demonstrated the association between p53 and PRMT2 via a co-IP experiment. p53 is a tumor suppressor that regulates the transcription of a range of genes in response to cellular stresses such as DNA damage and hyper-proliferation, directing cells to undergo cell cycle arrest and DNA damage repair, or apoptosis (*287*). For example, after exposure of normal cells to genotoxic agents, p53 activates transcription of a protein named p21, which is an inhibitor of multiple G1 phase cyclin-dependent kinase (Cdk) complexes that phosphorylate the retinoblastoma tumor suppressor protein (pRb) [reviewed in (*288*)]. Non-phosphorylated pRb binds and inactivates E2F transcription factors that control the expression of a number of genes essential for DNA synthesis, leading to cell cycle arrest [(*289*) and references therein].

Interestingly, PRMT2 can bind pRb directly through the AdoMet binding domain, forming a ternary PRMT2:E2F:pRb complex that represses E2F activity and G1-S transition in an pRb-dependent manner (*128*). p53 can actually play dual roles since it can induce expression of pro-apoptotic proteins such as the Bcl-2-associated X protein (BAX), as well as repress translation of the anti-apoptotic Bcl-2 to promote apoptosis [reviewed in (*288*)].

Arginine methylation can regulate p53 response and direct cells towards apoptosis or cell cycle arrest. It has been reported that tetramerization is important for p53 nuclear retention and DNA-binding ability (*290, 291*). In 2008, Jansson *et al.* demonstrated that PRMT5 promotes p53 oligomerization by methylating its oligomerization domain, resulting in p53-dependent G1 arrest in response to DNA damage (*47*). A year later, Scoumanne *et al.* confirmed the role of PRMT5 in controlling p53-dependent G1 arrest. Moreover, these authors, aware of the association of PRMT1 and CARM1 with p53, further pointed out that PRMT5 is the only reported p53-binding PRMT responsible for G1-S phase transition (*292*).

Results of my co-IP experiments uncovered the association of multiple Type I PRMTs with p53. Additionally, the PRMT1 hit S100A4 has been known to bind to p53, disrupt p53 tetramerization, and affect the sub-cellular localization and stability of p53 (*293*). Despite that PRMT1, -2, and -5 are all able to associate with p53, PRMT1 and -2 interact with proteins that destabilize p53 or promote protein synthesis and tumorigenesis, while PRMT5 stabilizes p53 tetramers and induces cell cycle arrest. In fact, PRMT5 was isolated in one of the two PRMT2 proteomic samples and not in the negative controls. I showed in Chapter 2 that both aDMA and sDMA levels increased when PRMT1 and -2 were overexpressed in HeLa cells (*150*). Taken together, a potential crosstalk between Type I and Type II PRMTs may exist; and these PRMTs

may be involved in fine-tuning the p53 pathway and regulating cell cycle progression by participating in different protein complexes.

Newly identified PRMT-associated proteins involved in gene expression.

DNA replication. In addition to the known PRMT1 binder HMGA1, which induces chromatin structural changes and promotes DNA replication by directly binding to DNA and their associated nucleosomes (*294*), five other identified protein hits are directly involved in regulating DNA replication. These hits include DNA replication licensing factor MCM7 (MCM7) for PRMT2, and four hits for both PRMT1 and -2. Interestingly, the PRMT2 hit MCM7 interacts with the hit for both PRMT1 and -2, DNA replication licensing factor MCM4, as part of the MCM complex that is essential for the initiation and elongation of DNA replication (*295, 296*). Another shared hit, the mini-chromosome maintenance complex-binding protein (MCM-BP) acts as a replacement of MCM2, another component of the MCM complex, and also regulates the dissociation of the MCM complex from chromatin (*297, 298*). The other two hits, replication factor C (RF-C) subunit 1 and ATPase WRNIP1 (WRNIP1) both work in conjunction with DNA polymerase δ (pol δ). While RF-C is required for proliferating cell nuclear antigen (PCNA)-dependent DNA elongation by pol δ (*299*), WRNIP1 modulates pol δ-mediated DNA synthesis initiation independent of PCNA (*300*).

Transcription. A total of 17 protein hits have been implicated in transcriptional regulation, including the known PRMT1 binders HMGA1, TAF15, and CARM1. The general transcription factor IIH subunit 5 (TFB5) and protein S100-A4 (S100A4) were identified in the HA-PRMT1 co-IP. Four and a half LIM domains protein 2 (FHL2) and PRMT2 itself were found exclusively in the HA-PRMT2 co-IP. The remaining 12 protein hits showed up in both co-IPs.

Some of these PRMT-associated proteins act as transcription factors, transcriptional regulators, or co-regulators. TFB5 is a subunit of transcription factor TFIIH that regulates the TFIIH expression level in cells (*301*). The leucine-rich repeat flightless-interacting protein 1 (GCF2), chromodomain Y-like protein (CDYL), and developmentally-regulated GTP-binding protein 1 (DRG1) all have been reported as transcriptional repressors (*302-304*), whereas thyroid receptor-interacting protein 6 (TRIP6), protein furry homolog-like (AF4P12), and 59 kDa 2'-5'-oligoadenylate synthase-like protein (OASL/TRIP14) have been known for their transcriptional activation abilities (*50, 97, 305-307*). In addition, although the detailed mechanism has yet to be studied, it has been reported that RF-C subunit 1 mentioned above as a hit associated with PRMT1 and -2 can stimulate the expression of the damage-inducible *RNR3* gene in response to DNA damage (*308*). Furthermore, it has been observed by different research groups that another protein that associated with both PRMT1 and -2, the cellular nucleic acid-binding protein (CNBP), can either negatively control the activity of a human *beta-myosin heavy chain* (*β-MHC*) reporter construct and the expression of the JC virus early promoter-enhancer [JCV(E)] (*309, 310*), or up-regulate the promoter activities of the mouse *macrophage colony-stimulating factor 1* (*Csf-1*) and the human c-*MYC* genes (*311, 312*).

Several of the hits affect transcription through regulating the activity of transcription factors. FHL2 identified in the HA-PRMT2 co-IP associates and inhibits the repressive capacity of the transcription factor E4F1, leading to transcriptional activation and cell proliferation (*313*). A second hit to fall into this category is the NF-κB essential modulator (NEMO/IKKγ), which is a regulatory subunit of the IκB kinase (IKK) complex. Additionally, PRMT1 pulled down an NF-κB activator, the protein S100-A4 (S100A4) (*314*).

Some of the hits in this study are known to regulate transcription through changes to chromatin structure. For example, the PRMT1 binder HMGA1 interacts with transcription factors and causes targeted unfolding of compact chromatin as a first step in transcriptional activation (*315*). A second example is the common PRMT binder, the actin-like protein 6A (BAF53), which is involved in transcriptional regulation by serving as an essential element necessary for the association of the mammalian chromatin remodeling BAF complex with chromatin (*316*).

Last but not least, the scaffolding protein PML has been recognized as a protein that associates with both PRMT1 and -2 in the present proteomic study. Further, the co-IP result suggests the PRMT2 SH3 domain is essential for the interaction between PRMT2 and PML (Figure 4.3 and Figure 4.4). The association of PML and PRMT1 and -2 may bring the two PRMTs into the PML-NBs, which host different transcriptional regulators [reviewed in (*270*)], so that PRMTs can work in concert with other transcriptional regulators in close proximity.

RNA processing. Similar to the GST-SH3(PRMT2) pull down results presented in Chapter 3, the results of the co-IP experiments also reveal the association between at least six splicing-related proteins and PRMTs. However, besides the two splicing-related proteins that associated with PRMT1, at least four other hits with previously known roles in pre-mRNA splicing were pulled down by both HA-PRMT1 and HA-PRMT2, suggesting that the two PRMTs may both involve in splicing regulation.

Selection of splicing sites-The U2 auxiliary factor (U2AF) is composed of two subunits, a 35 kDa subunit (U2AF1) and a 65 kDa subunit (U2AF2) (*199*), the latter was co-immunoprecipitated with PRMT1. As mentioned in Chapter 3, U2AF is important for the formation of pre-splicing complexes E and A by binding to the polyprimidine tract at the 3'

splice site and recruiting U2 snRNP to the BPS (*199, 200*). However, U2AF2 itself can bind to the polypyrimidine tract (*317*), and it is the only U2AF subunit required for *in vitro* splicing (*318*). On the other hand, the interaction of U1 snRNP to the 5' splice site is important for the selection of a 3' splice site mediated by U2AF (*319*); furthermore, the U1 snRNP at the 5' splice site facilitates U2AF2 binding to the 3' splice site by recruiting other factors (*320*). Therefore, protein-protein interactions spanning the RNA sequence between 5' and 3' splice sites are important for the regulation of alternative splicing. Most of essential elements for the formation of the pre-splicing complexes E and A have been found in the PRMT2 SH3 domain-associated protein complex as described in Chapter 3. It is exciting to see a subunit of U2AF, the missing piece of the puzzle, actually being introduced to the pre-splicing complexes by PRMT1.

Intriguingly, SC35 identified in co-IPs for PRMT1 and -2 and SF1 found to associate with the PRMT2 SH3 domain (Chapter 3) have been suggested to work in bridging the 5' and 3' splice sites. SC35 interacts with the U1-70K subunit in the U1 snRNP complex and also U2AF1, which sits at the BPS and interacts with the C-terminus of U2AF2; whereas SF1 is a *bona fide* U1-snRNP component, and non-phosphorylated SF1 interacts with U2AF2 through the U2AF2 N-terminus positioned proximal to the 3' splice site (*172, 321, 322*). Interestingly, SC35 is able to act as a functional substitute for U2AF2 (*323*). Additionally, the spliceosome RNA helicase DDX39B (UAP56) has been found to associate with both PRMT1 and -2. UAP56 has been discovered as a U2AF2-associated protein required for the recruitment of U2 snRNP to the BPS, leading to the formation of the pre-splicing complex A (*324*). The association of PRMT1 and -2 with these splicing factors implicates the participation of these PRMTs in splice site selection during the regulation of pre-mRNA splicing.

One of the few reported regulators of PRMT1-dependent arginine methylation, CCR4-associated factor 1 (hCAF1), interacts with PRMT1 and down-regulates PRMT1 activity towards Sam68 and histone H4, but not hnRNP A1 (*74*). Interestingly, PRMT1:hCAF1 complexes specifically localize to nuclear speckles, which are enriched in elements of the pre-mRNA splicing machinery and might function in the regulation of splicing and transcription by modulating the storage, assembly, modification, and localization of splicing factors (*74, 207*). Curiously, neither PRMT1 nor hCAF1 contain an SR domain, which helps to direct proteins to nuclear speckles (*74*). It has been proposed that SC35, a known speckle protein, may carry the PRMT1:hCAF1 complex into the nuclear speckle (*74*). However, no evidence in support of an interaction between SC35 and PRMT1 or hCAF1 has been reported. Other SR proteins such as ASF/SF2 and SFRS9/SRp30c were found to be *in vitro* substrates of PRMT1 (*73, 325*). Further, arginine methylation is important for the subnuclear localization of SFRS9/SRp30c in HEK293 cells (*325*). Results of the present study suggest an association of SC35 and PRMT1, though whether SC35 is a PRMT1 substrate has yet to be addressed.

Assembly of spliceosomal snRNPs-The core domain of all snRNPs is built by a group of Sm proteins [Sm-like proteins (LSms) for U6 and U6atac] (*175*). Interestingly, the U6 snRNA-associated Sm-like protein LSm5 (LSm5) that binds U6 snRNA and may facilitate the formation of the U4/U6 snRNP (*326*), was identified in the HA-PRMT1 co-IP. Additionally, one protein that associates with both PRMTs, the component of gems 4 (Gemin4) has been shown to interact with several of the Sm proteins including the identified PRMT2 SH3 domain-associated protein SmB (*327*). Gemin 4 associates tightly with SMN and forms the SMN complex that is essential for the assembly of spliceosomal snRNPs (*327*). On the other hand, it has been observed that the catalytic subunit of protein phosphatase 4 (Ppp4c) and its regulatory subunit R2 can interact with

Gemin4 and enhance the function of the SMN complex in maturing snRNPs (*328*). Interestingly, the present proteomic analysis revealed R1, another regulatory subunit of Ppp4c, associated with both PRMT1 and -2 like Gemin4, yet the interaction between R1 and Gemin4 still needs to be tested.

Mutations in the *SMN* gene account for a recessive neuromuscular disorder named proximal spinal muscular atrophy (SMA) (*329*). The exons of the *SMN* gene encoding a SMN homodimerization domain and a tudor domain contain extensive mutations in SMA patients (*330, 331*). While the homodimerization domain has been considered to be responsible for SMN oligomerization and its correct localization in the sub-nuclear structure termed Cajal bodies/Gems (*330, 331*), the SMN tudor domain resembles the ternary structure of Sm core proteins and facilitates the SMN-Sm protein interaction (*332*). Interestingly, it has been shown that the SMN-Sm interaction is sDMA-dependent but not aDMA-dependent (*333*). Furthermore, the tudor domain of SMN prefers to bind to methylated endogenous Sm proteins over non-methylated Sm proteins (*56*).

PRMT5 is the only known Sm protein methyltransferase reported to date [reviewed in (*55*)], although PRMT7 has been found to be required for Sm-class snRNPs biogenesis as well (*48*). It has been demonstrated that PRMT5 interacts with the SMN complex and potentiates the assisted assembly of spliceosomal snRNPs (*334*). As an integral component of the SMN complex, Gemin4 has also been identified in this SMN-PRMT5 complex (*334*).

The present data reveal that Gemin4 is able to associate with PRMT1 and -2. Indeed, the SMN protein has been identified in one of the PRMT1 samples and both of the PRMT2 samples. Unfortunately, one negative control also displayed a SMN hit, thus SMN was excluded from the list of hits according to a relatively stringent selection criterion that had been applied to reduce

false positives. However, showing up in the negative control does not necessarily mean that SMN does not interact with PRMT1 and -2. The current proteomic analysis was not done in a quantitative way, and the relative amount of protein hits in the experimental groups and the control groups was not reflected in the output. Therefore, whether a hit like SMN interacts with PRMT1 and -2 remains inconclusive. It is noteworthy that PRMT1 itself was identified in all of the samples including negative controls. Again, the stringency for hit selection prevented its inclusion in the final list of PRMT1- and/or PRMT2-associated proteins. Regardless of any technical shortcomings of this proteomic study, the existing data suggest that both Type II and Type I PRMTs could function in SMN complex formation and spliceosomal assembly.

Other PRMT-associated RNA processing proteins-The pre-mRNA-processing factor 40 homolog A (FNBP3) is an orthologue of the *S. cerevisiae* splicing factor PRP40, however, its role in human splicing remains unclear (*335*). Associating with both PRMTs, the probable ATP-dependent RNA helicase DDX56 (NOH61) has been postulated to be a factor involved in the assembly process of the large (60S) ribosomal subunit (*336*). Another protein hit in both co-IPs is the lysyl-tRNA synthetase (LysRS) that charges the $tRNA^{Lys}$ with the amino acid lysine (*337*). The exosome complex component RRP41 (Rrp41) that associated with PRMT1 is a part of the human 3'-5' exoribonuclease complex that degrades RNA (*338*). These results illustrate that PRMTs may play roles in various steps of RNA metabolism.

Translation. Both PRMT1 and -2 associate with eukaryotic translation initiation factors such as initiation factor 3 subunit I (eIF3I) and factor 4E type 2 (eIF4E2). Both of these two PRMT-associated initiation factors are involved in the early steps of translation initiation during which mRNAs are brought to the translational machinery. eIF3I is a component of the eIF3 complex, which stabilizes initiator Met-$tRNA_i$ binding on the 40 S ribosome and is also needed

for the ribosomal binding of a mRNA template (*339, 340*). eIF4E controls the rate-limiting step of eukaryotic translational initiation by recognizing the 7-methylguanine cap at the 5' end of mature mRNAs and recruits them to ribosomes (*341*). It has been used as a tumor marker since its overexpression is observed in numerous cancers (*342, 343*). One of many ways that p53 controls senescence and tumorigenesis is by modulating the activity of eIF4E. Evidence suggests that p53 can inhibit eIF4E-dependent translation initiation by increasing the stability of the eIF4E-binding protein 4E-BP1, which is an inhibitor of eIF4E (*344, 345*). The identified PRMT-associated protein eIF4E2 is a divergent eIF4E homologue that shares only 28% sequence identity to human eIF4E, but is still able to interact with the mRNA cap-structure and the eIF4E-binding proteins (4E-BPs) (*346*). In addition, a structural protein of the 40S ribosome (*347*), the 40S ribosomal protein S20 has been identified as a PRMT1-associated protein in this study.

p53-dependent cell cycle regulation. The present study pointed out at least six PRMT-associated proteins that participate in cell cycle control through the p53-mediated pathway. Additionally, the interaction between p53 and PRMT2 was demonstrated by co-IP (Figure 4.5). In the absence of a stress stimulus, p53 associates with its negative regulators such as the mouse double-minute 2 protein (MDM2), which is an E3 ligase, and many other cellular factors such as additional E3 ubiquitin ligases; these negative regulators cause ubiquitination, nuclear export and proteasomal degradation of p53 catalyzed by the 26S proteasome, thereby maintaining the cellular p53 concentration at a low level (*348, 349*). Stress results in the phosphorylation of MDM2 and p53, leading to MDM2 degradation and p53-dependent transcriptional activation (*350*).

It has been shown that the ubiquitinated cytoplasmic p53 could be recycled by a cytoplasmic enzyme that deubiquitinates p53, namely ubiquitin carboxyl-terminal hydrolase 10 (USP10) (*351*). Interestingly, USP10 has been identified as a PRMT2-associated protein in this proteomic study. Moreover, both nuclear and mitochondrial p53 trigger the expression of another PRMT2-associated protein, the human homolog of the mitochondrial protein Diablo from *D. melanogaster* termed the second mitochondria-derived activator of caspase (Smac), leading to the release of several downstream pro-apoptotic proteins (*352*).

The PRMT1-associatd proteins, the 40S ribosomal protein S27-like (RPS27L) and proteasome subunit beta type-1 (PSMB1) both take part in the p53 pathway. RPS27L is a p53-inducible target, and once expressed it competes for MDM2 binding with p53 and promotes apoptosis (*353, 354*), whereas PSMB1 is a proteolytic subunit of the 20S core of the 26S proteasome that is responsible for the degradation of ubiquitinated p53 (*355, 356*). Indeed, two other subunits of the 26S proteasome have also been identified in this proteomic study, associating with both PRMT1 and -2. One of them is the proteasome subunit alpha type-4 (PSMA4) and the other is the 26S proteasome non-ATPase regulatory subunit 11 (PSMD11). Furthermore, one additional hit is the proteasome-associated protein ECM29 homolog (ECM29) (*357*).

Other proteins involved in cell cycle regulation. Three proteins involved in cell cycle regulation not through the p53 pathway were also identified in this study. The PRMT1-associated protein kinetochore-associated protein 1 (hRod) is a component of the kinetochore, and is required for mitotic checkpoint arrest that enables faithful chromosome segregation during mitosis (*358*). Another PRMT1-associated protein nucleoporin NUP43 (NUP43) is also needed for normal kinetochore microtubule attachment and chromosome segregation (*359*). Condensin-

2 complex subunit D3 (NCAPD3), a hit in both co-IPs, is a component of the condensin II complex that plays a key role in chromosome condensation that is needed for accurate segregation of sister chromatids in anaphase of mitosis (*360*). Another hit in both co-IPs, the CD2-associated protein (CMS) contains three SH3 domains in it N-terminus and a proline-rich domain in its C-terminus that allows it to interact with many proline-rich domains and SH3 domain-containing signaling proteins (*361*). CMS has been found to be essential for the activation of a signal transduction pathway necessary for transforming growth factor-β (TGF-β)-induced apoptosis (*362*).

Post-translational modifying enzymes. Besides the methyltransferases PRMT2 and CARM1, the aforementioned protein phosphatase 4 regulatory subunit R1, and the hydrolase with deubiquitination activity USP10, eleven additional modifying enzymes associated with PRMT1 and -2. Two proteins isolated with PRMT1 and -2 in addition to USP10 have demonstrated deubiquitination activities. One of them is the ubiquitin carboxyl-terminal hydrolase 24 (USP24) (*363*); and another one is the probable ubiquitin carboxyl-terminal hydrolase FAF-X (USP9X) (*364, 365*). Plus, two more subunits of serine/threonine-protein phosphatases were pulled down with the two PRMTs. The catalytic subunit of the protein phosphatase 1 (Ppp1CC) interacts with over fifty regulatory subunits of the protein phosphatase 1 (PP1), contributing to the regulation of many cellular functions such as cell division and protein synthesis (*366*). PP2A-B55α, which associated with both PRMTs, is the alpha isoform of the 55 kDa regulatory subunit for serine/threonine-protein phosphatase 2A (PP2A). PP2A contains a catalytic subunit and various regulatory subunits similar to PP1 in addition to a scaffolding subunit. Through associating with different regulatory subunits, PP2A regulates the cell cycle either positively or negatively (*367*). Found in both co-IPs, the only kinase identified

in this proteomic study is the serine/threonine-protein kinase MRCK beta ($MRCK_{\beta}$), which phosphorylates a regulatory subunit of PP1 (Uniprot Database).

Cullin-4B (CUL4B), which was identified in both co-IPs, is a scaffold protein that brings together the substrate and the ubiquitin-conjugating enzyme within the cullin-RING E3 ubiquitin-protein ligase complexe to catalyze the ubiquitination reaction necessary for the subsequent proteasomal degradation of their targeted proteins (*368*). However, the cullins interact with neither the ubiquitin-conjugating enzyme nor the substrate directly, but through recruiting two conjugating enzyme binders and many substrate receptors (*369*). Interestingly, the PRMT1 co-IP experiments have pulled down the DDB1- and CUL4-associated factor 7 (WDR68) that could be a possible substrate receptor for a CUL4-RING complex (*370*). Additionally, two possible substrate receptors for other cullin-RING ligase complexes have also been identified. The F-box only protein 30 (FBXO30) isolated with PRMT1 and -2 has been proposed as a substrate-recognition component of SKP1-CUL1-F-box protein E3 ubiquitin ligase complex based on sequence similarity (Uniprot Database). Found to associate with PRMT2 in this study, gigaxonin (GAN1) is known to interact with CUL3 and recruit protein targets to the BTB-CUL3-Roc1 ubiquitin ligase complex together with other substrate adaptors (*371*).

Another E3 ubiquitin-protein ligase that was associated with both PRMT1 and -2 is the probable E3 ubiquitin-protein ligase TRIP12 (TRIP12). The yeast homolog of TRIP12, UFD4, interacts with particles within the 19S subunit of the 26S proteasome and facilitates the proteolysis process (*372*). In conjunction with the other enzymes involved in the ubiquitin fusion degradation pathway, TRIP12 acts as an E3 enzyme that covalently links ubiquitin moieties to the N-terminus of its targets, serving as a degradation signal recognized by the 26S

proteasome (*373*). TRIP12 also contributes to the ubiquitination and degradation of monomeric ubiquitin (*374*).

Other cellular processes. Other isolated proteins associated with PRMT1 and/or -2 participate in many different cellular processes such as protein folding and transport, actin binding, and a variety of metabolic pathways (Table A.3). It is unclear what the significance of these hits can be. Although a number of these PRMT-associated proteins may not directly impact gene expression, they may be able to do so indirectly.

For instance, importin-7 (Imp7), which associated with PRMT1, mediates the nuclear import of histone H1 (*375*); and *in vitro* evidence suggests that Imp7 can also mediate the nuclear import of histones H2A, H2B, H3, and H4 (*376*). The PRMT2-associated hit endophilin-A2 (EEN) contributes to the EEN portion of the oncogenic MLL-EEN fusion protein, which has been observed in a subgroup of acute leukemia patients (*265*). The MLL part of the MLL-EEN fusion protein is thought to provide DNA binding affinity, whereas the EEN part demonstrates transactivation property (*282*). Last but not least, identified in both co-IPs the nuclear fragile X mental retardation-interacting protein 2 (82-FIP) interacts with the PRMT1 substrate FMRP, and shows a cell cycle-dependent sub-cellular localization (*377*). It has been shown that PRMT1-catalyzes arginine methylation affects both the protein-protein and protein-RNA binding ability of FMRP (*378*). Although we cannot rule out the possibility that the 82-FIP associates with PRMT1 through FMRP, it may be more than a coincidence to see a binding partner of a PRMT1 substrate being isolated with PRMT1 while the substrate FMRP itself has not been identified in the same assay.

Interactions among PRMTs, protein phosphatases, and NF-κB protein complexes. Components of at least three serine/threonine-protein phosphatases that are responsible for

dephosphorylating phosphorylated serine and threonine residues in proteins (*379*), namely PP1, PP2A, and PP4, were isolated in co-IPs of PRMT1 and -2. All three protein phosphatases are comprised of one catalytic subunit and one or more regulatory subunits, while the PP2A also contains a scaffolding subunit (*379*).

Three highly similar (> 89% identical in amino acid sequence) PP1 isoforms, α, β/δ, and γ, encoded by different genes have been documented (*380*). These isoforms demonstrate various tissue distribution and distinct sub-cellular localization patterns (*380, 381*). The catalytic subunit of the PP1γ has been detected in the PRMT1 and -2 protein complexes in the present proteomic study. This finding is consistent with the result of an earlier study that suggests the presence of PRMT1 in both PP1α and PP1γ interactomes (*381*). In contrast to the other isoforms, PP1γ shows a higher expression level in brain. Within cells, PP1γ localizes to nucleoli and associates with chromatin during mitosis, suggesting its role in cellular events such as transcription, chromatin remodeling, chromosome condensation and segregation (*380, 381*). As mentioned above, PRMT1 and -2 also act in regulating these cellular processes. The association of PP1γ with the two PRMTs, and their overlapping functions give rise to the possibility that these proteins may work cooperatively in certain cellular pathways.

Another protein isolated by both PRMTs is PP2A-B55α, one of the many known regulatory subunits for PP2A (*379*). PP2A is able to dephosphorylate Bcl-2 antagonist of cell death (BAD) and enhance its pro-apoptotic activity, while PRMT1 is also able to specifically methylate BAD at its consensus phosphorylation motif and thereby prevent phosphorylation of BAD (*111*). Based on these observations, I postulate that PRMT1, possibly in complex with PRMT2, maintains BAD in its dephosphorylated state not only by methylating BAD to prevent its phosphorylation, but also via recruiting PP2A through associating with the PP2A-B55α.

Unlike PP2A that can be regulated through binding to various regulatory subunits, only two structurally distinct core regulatory subunits unique for the protein phosphatase 4 catalytic subunit (Ppp4c) have been uncovered so far. The regulatory subunit R1 was found to associate with PRMT1 and -2; and the second one is a smaller protein termed R2 (*382*), yet it is still unclear whether R1 and R2 differentially regulate Ppp4c activity. Emerging evidence indicates that Ppp4c-R1 complexes may positively regulate transcription by decreasing the activity of a histone deacetylase (HADC) that is believed to be a transcriptional repressor (*383*). On the other hand, PRMT1 works in conjunction with the histone acetyltransferase p300 during transactivation (*50, 79*). It has been shown that PRMT1 facilitates methylation of histone H4 preceding acetylation by p300, whereas prior acetylation of histone H4 preventes it from being a PRMT1 substrate (*79*). The present result implies that PRMT1 may mediate transactivation through a more comprehensive mechanism, such that PRMT1 and its associated Ppp4c-R1 complex recruit HDAC and deacetylate histone H4, then work in concert with p300, resulting in transcriptional activation. PRMT2 may exert its function in PRMT1-mediated transactivation by forming heteromeric PRMT1/2 complexes and potentiating PRMT1 activity, as well as through introducing other PRMT-associated modifying proteins to the PRMT complexes. Although not being identified in the present proteomic study, R2 in complex with Ppp4c is known to be involved in spliceosomal assembly through interacts with the SMN complex containing Gemin4, PRMT5, and SMN (*328*). However, the exact role of Ppp4c-R2 complexes and whether Ppp4c-R1 complexes also exist in the same SMN complex have yet to be investigated.

Moreover, both PP2A and PP4C have been implicated in regulating NF-κB-mediated transcription dependent on their dephosphorylation activity (*382*). NF-κB family of proteins can be further divided into two subfamilies: the NF-κB subfamily, which contains p50 and p52 that

do not display the C-terminal transactivation domains; and the Rel subfamily including c-Rel, RelB, and p65 that do contain the C-terminal transactivation domains [reviewed in (*384*)]. Therefore, the NF-κB subfamily members p50 and p52 generally lack transactivation abilities unless heterodimerizing with the Rel subfamily members (*384*). PP4C has been co-immunoprecipitated with NF-κB subunits c-Rel, p65, and p50, and overexpression of PP4C leads to activation of NF-κB-mediated transcription (*385*). In contrast, PP2A dephosphorylates p65, resulting in decreased NF-κB transactivation activity (*386*). PRMT1 and -2, in addition to interacting with these two phosphatases, also interact with NF-κB subunits. A previous study has revealed a direct interaction between PRMT1 and p65, which resultes in NF-κB-mediated transactivation (*52*). However, PRMT2 helps to maintain an association between NF-κB and its inhibitor IκB-α in the nucleus by binding to p50 and p65 through the PRMT2 SH3 domain, while binding to the NF-κB inhibitor IκB-α via other domains of PRMT2, resulting in the inhibition of NF-κB-dependent transcription and promotion of apoptosis (*32*).

Moreover, IKKγ that phosphorylate the inhibitors of κB (IκBs) and release NF-κB from inhibition (*387*), was also detected in the PRMT1 and -2 protein complexes according to this current proteomic analysis. It has been shown that IκBs attenuate NF-κB transcriptional activation activity by changing its DNA-binding affinity and retaining its localization to the cytoplasm [reviewed in (*388*)]. Upon stimulation with inducers such as pro-inflammatory cytokines, the IKK complex phosphorylates IκBs, which triggers IκB polyubiquitination and degradation, leading to NF-κB transactivation (*389*). IKKγ is a non-catalytic subunit of the IKK complex that recruits the other two catalytic subunits, IKKα and IKKβ, and assembles the IKKs into a high molecular weight signalosome complex (*390*). Additionally, IKKγ also facilitates the association of the IKK complex with its substrate IκBs (*391*).

An earlier study has demonstrated that the newly identified PRMT1-associated protein S100A4 can activate NF-κB by inducing phosphorylation of IKKα and IKKβ (*314*). The interaction between PRMT1 and S100A4 may provide an alternative mechanism for PRMT1-facilitated NF-κB activation in addition to interacting with the NF-κB subunit p65 (*52*). Taken together, although the mechanism by which PRMT1 and -2 coordinate NF-κB-mediated transactivation has not been fully elucidates, it is clear that both PRMT1 and -2 are able to either positively or negatively influence the NF-κB pathway via interacting with various signaling proteins such as phosphatases and kinases.

PRMT 1, -2, and 26S proteasome-mediated protein degradation. These proteomic screens for PRMT1 and/or -2 unveiled their associations with components of cullin-RING E3 ubiquitin-protein ligase complexes and the 26S proteasome. The cullin-RING E3 ubiquitin-protein ligase complexes (CRLs) comprise the largest known family of ubiquitin ligases, which attaches multiple ubiquitin proteins to its substrates (*392*). Although ubiquitination could alter protein function or localization, this post-translational modification is most well known as a mark for degradation by the 26S proteasome (*393*). The 26S proteasome is composed of a 20S core that carries out the catalytic activity of the proteasome, and a 19S regulatory subunit that recognizes polyubiquitin chains and directs the substrates into the 20S cavity (*356*). The 20S core consists of four stacked rings, with two proteolytic inner β-rings and two structural outer α-rings (*355*). The newly identified PRMT1-associated protein PSMB1 is a component of the inner β-rings (*394*), and PSMA4 that was pulled-down by both PRMT1 and -2 is a structural element of outer α-rings of the 20S core (*395*). Moreover, PSMD11, which is involved in the 19S regulatory subunit of the 26S proteasome (*396*), and a 26S proteasome-associated protein termed ECM29 were also found to associate with PRMT1 and -2. On the other hand, four CRL

components were isolated in the PRMT protein complexes, including CUL4B, WDR68, FBXO30, and GAN1. Additionally, TRIP12, an E3 ubiquitin ligase that does a similar job as CRLs but not in the CRL family was also co-purified with both PRMT1 and -2.

One possible explanation for this observation is that the 26S proteasome is responsible for the degradation of PRMTs or their associated proteins. However, it has been reported that not only the proteolytic activity of the proteasome is required for p53-mediated transactivation (*293*), the 19S regulatory subunit of the proteasome can also function as a transcriptional regulator (*397*), and can be recruited to genes following the mono-ubiquitination of histone H2B (*398*). Hence, it will be interesting to test if PRMT-catalyzed arginine methylation is a prerequisite or a consequence of 19S subunit recruitment. Altogether, these compelling results make one speculate as to the possible roles of PRMT1 and -2 in 26S proteasome-mediated protein degradation, particularly in transferring the ubiquitin mark to a target catalyzed by an E3 ubiquitin ligase, recognizing this mark facilitated by the 19S subunit of the 26S proteasome, and degrading the target in the 20S catalytic subunit.

Although the 26S is responsible for degrading a broad spectrum of substrates, several of its substrates are worth mentioning here due to their roles in regulating transcription and DNA repair. It has been observed that the expression of genes encoding components of the ubiquitin/proteasome pathway can be induced by DNA damage. Additionally, transcription mediated by RNA polymerase II can be paused at the site of DNA damage by ubiquitination of the RNA polymerase II followed by its degradation (*399*). In respect to this dissertation, important elements of NF-κB and p53 pathways such as IκBα, MDM2, and p53 are all subject to E3 ubiquitin ligase-catalyzed ubiquitination followed by 26S proteasome-mediated proteolysis (*400-403*). Once the NF-κB inhibitor IκBα gets phosphorylated upon extracellular stimulation,

the SKP1-CUL1-F-box protein E3 ubiquitin ligase complex will ubiquitinate it, leading to degradation of IκBα by the 26S proteasome and activation of the NF-κB pathway (*400*). Interestingly, FBXO30, identified in co-IPs with PRMT1 and -2, may recognize the phosphorylation signal on IκBα and thus recruit it to the E3 ubiquitin ligase complex [(*400*) and Uniprot Database]. On the other hand, MDM2 mediates p53 and its own ubiquitination and proteasomal degradation in cells (*402, 403*).

Furthermore, the list of PRMT1 and/or -2 hits contains three deubiquitinating enzymes (DUBs). DUBs antagonize the ubiquitination of proteins by cleaving the polyubiquitin chain from target proteins; and they are also responsible for activating, recycling, and regenerating monoubiquitin (*404*). All three identified DUBs belong to the largest class of deubiquitinase family known as the USP family. Expression of DUB genes can be induced by cytokines, and DNA damage has been found to serve as a signal to activate DUBs. It has been reported the transcription of a DUB gene is induced by activation of the NF-κB pathway, whereas the activities of certain DUBs result in a feedback inhibition of NF-κB signaling [reviewed in (*404*)]. Importantly, the PRMT2-associated protein USP10 is responsible for deubiquitination and nuclear translocation of cytoplasmic p53 after DNA damage, thereby reversing MDM2-induced p53 nuclear export and degradation (*351*).

Taken together, PRMT1 and -2 may act in NF-κB and p53-dependent transcription by controlling degradation of essential elements of these pathways through protein-protein interactions, leading to activation or suppression of transcription. As another consideration, the 26S proteasome catalyzes the proteolysis of numerous proteins. The association of PRMT1 and -2 to the 26S proteasome and E3 ubiquitin ligase could also suggest that PRMT1 and -2 are both substrates of the 26S proteasome.

PRMT 1 and -2 as residents of PML-NBs. Revealing the association of both PRMT1 and -2 with PML may help us to look into the PRMT-protein interactome and its function as a whole in regulating cell growth from a different angle. PML and PML-NBs have been suggested to play significant roles in controlling programmed cell death and are involved in several apoptotic pathways [reviewed in (*405*)]. For instance, Fogal *et al.* have shown that PML isoform IV directly interacts with p53 and acts as a p53 transcriptional coactivator (*264*). However, these authors also noted that the physical interaction of PML IV and p53 is not sufficient to activate p53-dependent transcription. They pointed out the PML-NB localization of p53 mediated by PML IV is actually a key factor for promoting p53 activity. Later, researchers realized the PML-NBs might be the hubs of the pro-apoptotic transcriptional network by virtue of hosting a wide variety of transcriptional regulators. Both the acetylase CBP/p300 and the homeodomain-interacting protein kinase-2 (HIPK2) are recruited to the PML-NBs where they modify p53 and thus trigger p53-dependent transcription (*406, 407*). Additionally, a DUB deubiquitinating p53 named HAUSP (herpesvirus-associated ubiquitin-specific protease) has also been found in PML-NBs where it induces p53 stabilization and activation (*408*). The present study demonstrates PRMT interactions with PML IV and p53, suggesting that PRMT1 and -2 as proteins residing in the PML-NBs may influence p53-dependent transcription.

In fact, it has been shown that PRMT1 and its substrate MRE11 co-localize in the PML-NBs (*113*). MRE11 is a subunit of the MRE11-RAD50-NBS1 complex that is important for DNA damage repair. PRMT1-mediated arginine methylation of MRE11 is required for its association with PML-NBs and sites of DNA damage (*115*). The observed interaction between PML and PRMT2 through the PRMT2 SH3 domain raises the possibility that PML, PRMT1, and

PRMT2 may work in DNA damage repair cooperatively. The present result raises the possibility that PML, PRMT1, and PRMT2 may work in DNA damage repair cooperatively.

PML also acts as a transcriptional repressor of the NF-κB pathway, inducing apoptosis upon TNFα stimulation (*409*). To do so, PML interacts with the NF-κB subunit p65 and traps p65 in PML-NBs. Moreover, PML sequesters pRb and E2F in the PML-NBs thereby down-regulating transcription and promoting cell cycle arrest (*410*). Another study has shown that PML regulates cell cycle arrest by bringing both phosphorylated pRb and the phosphatase PP1α to the PML-NBs, leading to dephosphorylation of pRb (*411*). The non-phosphorylated pRb can then bind to E2F and inhibit its transcriptional activity (*289*). Interestingly, PRMT2 represses E2F transcriptional activity by forming a ternary complex of PRMT2:E2F:pRb (*128*).

The present study uncovers the interaction of PRMT2 and PML in a SH3 domain-dependent manner. More specifically, the PRMT2 SH3 domain was able to bind PML I and -IV. All PML isoforms contain a proline-rich motif at its N-terminus, which could serve as a docking site for PRMT2 SH3 domain. It is unclear whether PML directly interacts with either pRb or E2F, though it has been demonstrated that PRMT2 physically interacts with pRb through its AdoMet binding domain (*128*). Therefore, PRMT2 may facilitate the formation of a PRMT2:E2F:pRb:PML quadruplex by interacting with PML via the N-terminal SH3 domain, while binding to pRb through the AdoMet binding domain, hence promoting cell cycle arrest.

Astonishingly, many of the newly identified and/or previously reported PRMT-associated proteins have also been shown to co-localize to PML-NBs. As aforementioned, p53 and p65 interact with both PRMT1 and -2 (*32, 50, 52*), pRb interacts with PRMT2 (*128*). Additionally, another translation initiation factor found in PML-NBs was the non-conserved subunit of the eIF3 complex termed eIF3E (*412*). Interestingly, the evolutionarily conserved subunit of the

eIF3 complex, eIF3I, was isolated as a component for both PRMT1 and -2 protein complexes. The PML-NB resident CBP/p300 has been shown as a CARM1 substrate (*245, 413*). It has been shown that PRMT1, p300, and CARM1 can cooperatively activate p53-dependent transcription (*50*). Similar to PRMT1 and -2, CARM1 is also able to bind p65 and activate NF-κB-mediated transcription in concert with CBP/p300 (*414*). Furthermore, it has been shown that a direct interaction between PML and eIF4E (a homologue of eIF4E2 that associates with both PRMT1 and -2) can disable eIF4E in transporting transcripts encoding proteins that are essential for cell transformation (*415*). Since the overall human eIF4E2 crystal structure is similar to that of eIF4E (*416*), their biological roles and interacting partners may be quite similar.

Altogether, PRMT1 and -2, and probably other PRMTs such as CARM1, may work in conjunction with PML for recruitment of translation initiation factors and transcriptional regulators such as p53, p65, CBP/p300, E2F, and pRb to PML-NBs in order to regulate cell growth and transformation.

5 Conclusions

In Chapter 2 of this dissertation I have presented evidence that PRMT1 and -2 interact *in vitro* and in cells, and that PRMT1 activity was increased as a result. A kinetic analysis of PRMT1 with catalytically inactive E153Q or E220Q mutants revealed that these subunits increased V_{max} and k_{cat} for PRMT1 while differentially affecting AdoMet and histone H4 K_M values. These data suggest that the PRMT1 binding partner, in this case PRMT2, can influence substrate specificity of the resulting complex. A sequence alignment of regions purported to be involved in dimer formation among human PRMT family members indicates that dimer-contacting residues are conserved (Figure 1.5). In fact, an interaction between PRMT1 and -6 has also been detected using BiFC (Figure A.16). Therefore, it is interesting to speculate that different heteromeric PRMT combinations could form, resulting in a host of distinct substrate preferences that enhance the diversity of PRMT functions on the cellular level.

Results generated by the GST-SH3(PRMT2) pull down assay presented in Chapter 3 unveil an array of potential PRMT2-protein interactions that is mediated by the PRMT2 SH3 domain. Strikingly, the results of the pull down assay indicate a consistent connection between PRMT2 and multiple splicing-related proteins, and raise the likelihood that PRMT2 may participate in different steps of splicing and other pre-mRNA processing events by recruiting splicing-related proteins through the PRMT2 SH3 domain. The interaction between PRMT2 and Sam68, requiring the SH3 domain of PRMT2, has been uncovered using co-IP and immunofluorescence, underscoring the potential role of PRMT2 in coupling alternative splicing and signal transduction.

The proteomic study described in Chapter 4 provide a panel of PRMT1- and PRMT2-interacting proteins from a board spectrum of biological processes, suggesting that the functions of these two PRMTs may be involved together in gene expression, post-translational modification, DNA damage and repair, inflammatory response, apoptosis, and other processes. Furthermore, p53, EEN, and PML have been verified as three more novel PRMT2-interacting proteins besides Sam68. The interaction between PML and PRMT2, similar to the inertaction between Sam68 and PRMT2, required the SH3 domain of PRMT2.

In summary, the scaffolding proteins Sam68 and PML could be two plausible mediators of the PRMT1/2 complex as mediated through SH3 domain binding. The results from this work also indicate that PRMT2 or the heteromeric PRMT1/2 complex could play a role in regulating alternative splicing by interacting with and/or modifying other splicing-related proteins. PRMT2, possibly in collaboration with other PRMTs, may facilitate the integration of signal transduction, alternative splicing and gene expression through the PRMT2-protein interaction network.

Significance. The present study sheds light on the diverse biological functions of the less studied PRMT2. My results indicate that the minor arginine methyltransferase PRMT2 indeed works cooperatively with the major arginine methyltransferase PRMT1 by forming a heteromeric PRMT1/2 complex with an increased enzymatic activity. The proteomic data from this study reveals that PRMT1 and -2 share lots of interacting partners in common, revealing potentially overlapping pathways in which these two PRMTs are involved. These results also uncover an interaction between PRMT2 and EEN, a protein which has been reported to recruit PRMT1 to the oncogenic MLL-EEN complex through a bridging interaction with Sam68 that results in aberrant histone methylation and gene expression (*148*). Therefore, the relatively less

active PRMT2 may tailor the activity of other PRMTs by forming heteromeric PRMT complexes and directing these complexes to different PRMT-mediated pathways.

Results from other groups have suggested that PRMT2 participates in cellular inflammation, though its precise role as a methyltransferase is unclear. The *PRMT2* gene was implicated in controlling lung inflammation and function in response to local intranasal lipopolysaccharide (LPS) administration (*417*); and PRMT2 acted downstream of TNF-α signaling by sequestering IκB-α in the nucleus, thus inhibiting NF-κB-dependent transcription and rendering cells susceptible to apoptosis by cytokines and cytotoxic drugs (*32*). The *PRMT2*$^{-/-}$ mice appeared devoid of any anatomical abnormalities or malignancies, but mouse embryonic fibroblasts exhibited an abbreviated G1-S cell cycle transition, furthermore, upon vascular injury *PRMT2*$^{-/-}$ mice exhibited striking cellular proliferation and blood vessel thickening compared to wild type fibroblasts (*128*).

Consistent with the previous observations, my Ph.D. work provides additional evidence that PRMT2 may play roles in pathogenesis of inflammation and cancer by coordinating inflammatory response and apoptosis via PRMT2-protein interactions facilitated by its unique SH3 domain. A handful of PRMT2-associated proteins including p53, Sam68, NEMO, Smac, various splicing-related proteins and phosphatases have demonstrated functions in controlling gene expression upon extracellular stimuli through directing transcription, signal transduction, and alternative splicing.

A link between inflammatory diseases and cancers has been suggested (*418*). It has been reported that chronic inflammation was associated with the pathogenesis of 15 to 20% of human tumors (*419*). Given that PRMT2 has been implicated in the inflammatory response, apoptosis, and tumorgenesis, I propose that PRMT2 may serve as a key factor in linking inflammation and

cancers, and therefore may represent a potential therapeutic target for the treatment of these diseases.

Strengths and limitations.

BiFC. BiFC allows us to visualize direct protein-protein interactions in a native cellular environment (*138, 140*). It is able to detect sub-stoichiometric and transient protein interactions (*420*). BiFC between fragments of fluorescent proteins senses bindings occurring at the sub-cellular level, which is the highest spatial resolution one can obtain using currently available complementation methods (*421*). The short linker (GGGGS) used for the present BiFC constructs is only approximately 19 Å when extended, which is an optimized linker length to ensure the mCitrine fragment-tagged proteins sit as close as possible to one another (*136*). Although this short and relatively inflexible linker improves the specificity of the BiFC method, it may reveal protein-protein interactions in an orientation dependent manner and result in false negatives. For example, only one of the two BiFC pairings of PRMT1 and -2 yielded positive fluorescent signal indicative of an interaction. Despite several pieces of evidence for PRMT2 homodimerization, the present BiFC results showed no interaction between PRMT2 fused to two mCitrine fragments (*9, 21*). Therefore, the absence of a reconstituted fluorescent signal in the present study does not indicate a lack of interaction between the two proteins under investigation. Moreover, the formation of a BiFC complex appears to be an irreversible process, at least *in vitro* (*422*), thereby BiFC does not demonstrate changes in dynamic protein-protein interactions in real time. Last but not least, PRMT1 localization is affected by AdOx treatment or when it is rendered inactive (*147*), and ectopically tagged PRMT1 demonstrates an altered substrate specificity *in vitro* (*423*). Hence BiFC may not accurately reflect the subcellular localization of the PRMT complex under current experimental conditions.

Co-immunoprecipitation coupled to LC-MS/MS. Protein complex purification coupled with mass spectrometry analysis allows us to efficiently identify components of the protein complex of interest. However, there are systematic and random errors associated with such an approach, which could lead to false positives and false negatives. In the protein complex isolating step, the HA-tagged PRMT1 or -2 protein complexes in HeLa cell lysate were immunoprecipitated using an antibody specific for the HA tag cross-linked to sepharose resin, although other protein complexes may also be pulled down due to non-specific interactions with the antibody or the sepharose resin. Proteins that are abundant in the HeLa cell lysate may also survive the affinity isolation and the subsequent washes, and be detected as a hit in the proteomic analysis. To reduce false positives, untransfected HeLa cell lysate was use as a negative control to reveal non-specific binders for the antibody and/or the resin. Isolated protein complexes were also washed with PBS buffer containing 0.05% Tween 20 several times in order to eliminate non-specific interactions in the experimental samples.

Despite a low false-positive rate that can be obtained using the current experimental design, the high false-negative rate of this process is difficult to avoid (*424*). Edwards *et al.* have estimated the false negative rate at about 50% by using two of the ten RNA polymerase II subunits as bait that resulted in the identification of half of their known direct binders (*425*). Many aspects of an experiment can cause of false negatives. First, not all of the tryptic peptides obtained from the purified immuno-complex can finally find their way to the mass spectrometer. These tryptic peptides were first separated in a reversed-phase capillary liquid chromatography (RPLC) column based such that hydrophobic peptides tend to be retained on the column. The bias with this method is that very hydrophilic and hydrophobic peptides will not be resolved through the RPLC column. The RPLC is built in-line with a mass spectrometer; and the tryptic

peptides are ionized before entering the MS, where the mass/charge (*m/z*) ratios of these peptides are measured in real time. The effective *m/z* scan range of the MS is usually between 200 and 2000 Da, peptides that are not efficiently ionized or have *m/z* ratios above or below the effective range of MS cannot be detected (*426*). Second, the relative concentration of prey proteins in the sample may be dramatically different. The MS may not be able to detect prey at low concentrations when the MS is flooded with high concentrations of other peptides. Also, the relative concentration of proteins in co-IP samples may not reflect their real proportions in the cellular environment. The membrane system of the cells encapsulates proteins within different sub-cellular compartments or organelles. As a result, some proteins may have high local concentrations in the cells but not in the cell lysate. The experimental condition may drive the thermodynamic equilibrium toward dissociation, thereby causing false negatives.

Lots of the previously reported interaction partners of PRMT1 or -2 have not been detected in the present proteomic study. Moreover, most hits from the GST-pull down identified to interact with the PRMT2 SH3 domain listed in Table 3.1 are not found as hits in the co-IP experiment using HA-tagged PRMTs. Due to the aforementioned systemic and random errors, a protein present in the list of hits in the experimental groups but not in the negative control samples may have been simply missed in the negative controls because of peptide undersampling (*426*). Similarly, the absence of a protein in the experimental groups is not a sufficient proof for its absence in the sample. For the same reasons, the proteins identified only in the PRMT1 duplicates may also interact with PRMT2, and *vice versa*. On the other hand, the presence of a protein in the lists for both the negative control and experimental sample hits does not indicate that the given protein is a false-positive hit, since the present proteomic analysis is not a quantitative method (*426*).

In fact, many splicing-related proteins such as U1-70K, Sm-E (*427*), the serine/arginine-rich splicing factor 1 (SFRS1), RBM25, several hnRNPs including the known PRMT1 substrate hnRNP A1, and even PRMT1 itself showed up as hits in the negative controls or have only been detected in one of the experimental duplicates. Other research groups have encountered the same problems, and have detected known PRMT1 targets and/or binders including hnRNPs, U5 snRNP components, Sam68, and fibrillarin in their negative controls (*428, 429*).

A dual purification strategy termed tandem affinity purification (TAP)-tagging is able to reduce the false negative rate to approximately 15% (*430*); and quantitative MS methods such as using isotope-coded samples generated by stable isotope-labelled amino acids in cell culture (SILAC) or via a chemical labeling technique named isotope-coded affinity tagging (ICAT) will help to reduce false-negatives (*426*). Recently, Selbach *et al.* have proposed a new protein interaction screening method in which quantitative immunoprecipitation and MS analysis are combined with gene knockdown in order to improve the quality of screening outcomes by lowering the numbers of false-negative and false-positive hits at the same time (*431*).

Notably, the present proteomic analysis is not an ideal approach to determine the methylation states of the identified hits. The MS spectra only provide information on the methylation states of the detected tyrptic peptides, but they do not reflect the overall methylation states of the hits. In order to capture as many methylated PRMT binders as possible, enrichment of arginine-methylated proteins in the samples using arginine methylation-specific antibodies should be performed as previously reported (*432*).

Additionally, whether a given hit directly interacted with PRMT1 or -2, or was solely isolated as a component in the PRMT interactome, requires additional experimentation. Since PRMT1 and -2 interact, any identified hit for PRMT1 and -2 may not physically interact with

both PRMTs at the same time. In other words, the present study here provides evidence for plausible PRMT-protein interactions, however, specific interactions between endogenous PRMT1 and -2 and their associated proteins still need to be tested by other techniques such as cross-linking experiments followed by size-exclusion chromatograph and co-IPs with endogenous PRMTs.

GST-Pull down coupled to LC-MS/MS. The GST-pull down study coupled with proteomic analysis suffers similar drawbacks as the co-immunoprecipitation in-line with LC-MS/MS does because these two studies use LC-MS/MS to detect the presence of tryptic peptides of proteins. However, the protein complex isolated by the GST-pull down assay has been resolved and visualized on a 10% SDS-PAGE gel, and the proteins of interest with similar apparent molecular weights have been isolated in gel slices. Furthermore, direct binding between bait and prey of the GST-pull down assay was replicated by Far Western blotting.

Future Studies. Data presented in this dissertation can serve as the basis for a number of future studies. Once the PRMT-protein interactions detected by LC-MS/MS are verified by other methods, the first question one may ask is which of these proteins are PRMT targets, and which are solely binding to PRMTs without being methylated. The impact of the PRMT-protein interactions on multiple biological pathways such as pre-mRNA processing, transcriptional activation, DNA damage repair, and programmed cell death can then be investigated. Additionally, the present result also suggests crosstalk among different PRMTs, as well as among the arginine methylation mark and other post-translational modification marks such as phosphorylation, acetylation, and ubiquitination. The detailed mechanism of this crosstalk is worth further exploration.

Particularly, solving the mechanisms and consequences of the interactions between PRMT2 and four of its novel binders identified in this study, namely Sam68, p53, EEN, and PML, will help one to decipher PRMT2's functions in integrating signal transduction, alternative splicing and gene expressions, as well as in pathogenesis of cancer such as AML and APL. For instance, it will be interesting to test if Sam68 is a substrate of PRMT2; and if so, what the consequences of the PRMT2-mediated Sam68 arginine methylation in Sam68 activity and sub-cellular localization are. Additionally, how does the binding with PRMT2 influence the associations between Sam68 and other SH3 domain-containing signaling proteins? Another question to be ask is whether Sam68 associates with the PRMT1/2 complex via the PRMT2 SH3 domain and regulates the formation of the heteromeric PRMT complex in different methylation states. More important future experiments to be done include tackling changes in alternative splicing of Sam68-targeting genes such as *Bcl-x* in PRMT2 knockdown cells or in PRMT2 knockout animal models, as well as examining the impact of Sam68 phosphorylation on its arginine methylation, and *vice versa*.

Furthermore, one may ask what the function of PRMT2 is in the protein arginine-methyltransferase-dependent oncogenesis model proposed by Cheung *et al.* in 2007 (*148*). Since the SH3 domain of EEN interacts with Sam68 and PRMT1, and it is necessary and sufficient for MLL-EEN mediated transformation, it will be interesting to explore how PRMT2 binding to Sam68 and EEN fits into their model. Additionally, Boisvert *et al*. have suggested that PRMT1 actes in DNA double-strand break repair by co-localizing with MRE11 in PML-NBs and catalyzing the arginine methylation of MRE11 that is required for its localization to DNA damage foci (*113*). Given that PRMT2 interacts with PRMT1 and potentiates PRMT1 activity, it

is interesting to see how PRMT2 affects PRMT1-mediated DNA damage repair as a consequence of binding to PML through its SH3 domain.

Last but not least, one could inquire about the role PRMT2 may play in DNA damage repair, apoptosis, and inflammatory response by unveiling variations in p53-dependent transactivation or transcription mediated by NF-κB and other nuclear receptors upon different extracellular stimuli in the absence of PRMT2 using *PRMT2*$^{-/-}$ cells or animals. PRMT2-targeted genes in response to various stimuli can then be revealed by microarray and real-time PCR. The work described herein provides a platform upon which these possibilities should be explored.

References

1. Seet, B. T., Dikic, I., Zhou, M. M., and Pawson, T. (2006) Reading protein modifications with interaction domains, *Nat Rev Mol Cell Biol 7*, 473-483.
2. Bedford, M. T., and Clarke, S. G. (2009) Protein arginine methylation in mammals: who, what, and why, *Mol Cell 33*, 1-13.
3. Paik, W. K., and Kim, S. (1967) Enzymatic methylation of protein fractions from calf thymus nuclei, *Biochemical and biophysical research communications 29*, 14-20.
4. Paik, W. K., and Kim, S. (1968) Protein methylase I. Purification and properties of the enzyme, *The Journal of biological chemistry 243*, 2108-2114.
5. Ghosh, S. K., Paik, W. K., and Kim, S. (1988) Purification and molecular identification of two protein methylases I from calf brain. Myelin basic protein- and histone-specific enzyme, *The Journal of biological chemistry 263*, 19024-19033.
6. Rajpurohit, R., Lee, S. O., Park, J. O., Paik, W. K., and Kim, S. (1994) Enzymatic methylation of recombinant heterogeneous nuclear RNP protein A1. Dual substrate specificity for S-adenosylmethionine:histone-arginine N-methyltransferase, *The Journal of biological chemistry 269*, 1075-1082.
7. Lin, W. J., Gary, J. D., Yang, M. C., Clarke, S., and Herschman, H. R. (1996) The mammalian immediate-early TIS21 protein and the leukemia-associated BTG1 protein interact with a protein-arginine N-methyltransferase, *The Journal of biological chemistry 271*, 15034-15044.
8. Bedford, M. T. (2007) Arginine methylation at a glance, *J Cell Sci 120*, 4243-4246.
9. Lakowski, T. M., and Frankel, A. (2009) Kinetic analysis of human protein arginine N-methyltransferase 2: formation of monomethyl- and asymmetric dimethyl-arginine residues on histone H4, *Biochem J 421*, 253-261.
10. Tang, J., Gary, J. D., Clarke, S., and Herschman, H. R. (1998) PRMT 3, a type I protein arginine N-methyltransferase that differs from PRMT1 in its oligomerization, subcellular localization, substrate specificity, and regulation, *The Journal of biological chemistry 273*, 16935-16945.
11. Chen, D., Ma, H., Hong, H., Koh, S. S., Huang, S. M., Schurter, B. T., Aswad, D. W., and Stallcup, M. R. (1999) Regulation of transcription by a protein methyltransferase, *Science (New York, N.Y 284*, 2174-2177.
12. Schurter, B. T., Koh, S. S., Chen, D., Bunick, G. J., Harp, J. M., Hanson, B. L., Henschen-Edman, A., Mackay, D. R., Stallcup, M. R., and Aswad, D. W. (2001) Methylation of histone H3 by coactivator-associated arginine methyltransferase 1, *Biochemistry 40*, 5747-5756.
13. Frankel, A., Yadav, N., Lee, J., Branscombe, T. L., Clarke, S., and Bedford, M. T. (2002) The novel human protein arginine N-methyltransferase PRMT6 is a nuclear enzyme displaying unique substrate specificity, *The Journal of biological chemistry 277*, 3537-3543.
14. Lee, J., Sayegh, J., Daniel, J., Clarke, S., and Bedford, M. T. (2005) PRMT8, a new membrane-bound tissue-specific member of the protein arginine methyltransferase family, *The Journal of biological chemistry 280*, 32890-32896.
15. Branscombe, T. L., Frankel, A., Lee, J. H., Cook, J. R., Yang, Z., Pestka, S., and Clarke, S. (2001) PRMT5 (Janus kinase-binding protein 1) catalyzes the formation of symmetric

dimethylarginine residues in proteins, *The Journal of biological chemistry 276*, 32971-32976.
16. Zurita-Lopez, C. I., Sandberg, T., Kelly, R., and Clarke, S. G. Human Protein Arginine Methyltransferase 7 (PRMT7) is a Type III Enzyme Forming omega-NG-Monomethylated Arginine Residues, *The Journal of biological chemistry*.
17. Krause, C. D., Yang, Z. H., Kim, Y. S., Lee, J. H., Cook, J. R., and Pestka, S. (2007) Protein arginine methyltransferases: evolution and assessment of their pharmacological and therapeutic potential, *Pharmacology & therapeutics 113*, 50-87.
18. Zhang, X., Zhou, L., and Cheng, X. (2000) Crystal structure of the conserved core of protein arginine methyltransferase PRMT3, *The EMBO journal 19*, 3509-3519.
19. Cheng, X., Collins, R. E., and Zhang, X. (2005) Structural and sequence motifs of protein (histone) methylation enzymes, *Annual review of biophysics and biomolecular structure 34*, 267-294.
20. Teyssier, C., Chen, D., and Stallcup, M. R. (2002) Requirement for multiple domains of the protein arginine methyltransferase CARM1 in its transcriptional coactivator function, *The Journal of biological chemistry 277*, 46066-46072.
21. Herrmann, F., Pably, P., Eckerich, C., Bedford, M. T., and Fackelmayer, F. O. (2009) Human protein arginine methyltransferases in vivo--distinct properties of eight canonical members of the PRMT family, *J Cell Sci 122*, 667-677.
22. Zhang, X., and Cheng, X. (2003) Structure of the predominant protein arginine methyltransferase PRMT1 and analysis of its binding to substrate peptides, *Structure 11*, 509-520.
23. Yue, W. W., Hassler, M., Roe, S. M., Thompson-Vale, V., and Pearl, L. H. (2007) Insights into histone code syntax from structural and biochemical studies of CARM1 methyltransferase, *The EMBO journal 26*, 4402-4412.
24. Troffer-Charlier, N., Cura, V., Hassenboehler, P., Moras, D., and Cavarelli, J. (2007) Functional insights from structures of coactivator-associated arginine methyltransferase 1 domains, *The EMBO journal 26*, 4391-4401.
25. Weiss, V. H., McBride, A. E., Soriano, M. A., Filman, D. J., Silver, P. A., and Hogle, J. M. (2000) The structure and oligomerization of the yeast arginine methyltransferase, Hmt1, *Nature structural biology 7*, 1165-1171.
26. Rho, J., Choi, S., Seong, Y. R., Cho, W. K., Kim, S. H., and Im, D. S. (2001) Prmt5, which forms distinct homo-oligomers, is a member of the protein-arginine methyltransferase family, *The Journal of biological chemistry 276*, 11393-11401.
27. Sun, L., Wang, M., Lv, Z., Yang, N., Liu, Y., Bao, S., Gong, W., and Xu, R. M. Structural insights into protein arginine symmetric dimethylation by PRMT5, *Proceedings of the National Academy of Sciences of the United States of America 108*, 20538-20543.
28. Yu, Z., Chen, T., Hebert, J., Li, E., and Richard, S. (2009) A mouse PRMT1 null allele defines an essential role for arginine methylation in genome maintenance and cell proliferation, *Molecular and cellular biology 29*, 2982-2996.
29. Pawlak, M. R., Scherer, C. A., Chen, J., Roshon, M. J., and Ruley, H. E. (2000) Arginine N-methyltransferase 1 is required for early postimplantation mouse development, but cells deficient in the enzyme are viable, *Molecular and cellular biology 20*, 4859-4869.
30. Yadav, N., Lee, J., Kim, J., Shen, J., Hu, M. C., Aldaz, C. M., and Bedford, M. T. (2003) Specific protein methylation defects and gene expression perturbations in coactivator-

associated arginine methyltransferase 1-deficient mice, *Proceedings of the National Academy of Sciences of the United States of America 100*, 6464-6468.

31. Iwasaki, H., Kovacic, J. C., Olive, M., Beers, J. K., Yoshimoto, T., Crook, M. F., Tonelli, L. H., and Nabel, E. G. (2010) Disruption of Protein Arginine N-Methyltransferase 2 Regulates Leptin Signaling and Produces Leanness In Vivo Through Loss of STAT3 Methylation, *Circulation research 107*, 992-1001.
32. Ganesh, L., Yoshimoto, T., Moorthy, N. C., Akahata, W., Boehm, M., Nabel, E. G., and Nabel, G. J. (2006) Protein methyltransferase 2 inhibits NF-kappaB function and promotes apoptosis, *Molecular and cellular biology 26*, 3864-3874.
33. Swiercz, R., Cheng, D., Kim, D., and Bedford, M. T. (2007) Ribosomal protein rpS2 is hypomethylated in PRMT3-deficient mice, *The Journal of biological chemistry 282*, 16917-16923.
34. Nicholson, T. B., Chen, T., and Richard, S. (2009) The physiological and pathophysiological role of PRMT1-mediated protein arginine methylation, *Pharmacol Res 60*, 466-474.
35. Tang, J., Kao, P. N., and Herschman, H. R. (2000) Protein-arginine methyltransferase I, the predominant protein-arginine methyltransferase in cells, interacts with and is regulated by interleukin enhancer-binding factor 3, *The Journal of biological chemistry 275*, 19866-19876.
36. El-Andaloussi, N., Valovka, T., Toueille, M., Steinacher, R., Focke, F., Gehrig, P., Covic, M., Hassa, P. O., Schar, P., Hubscher, U., and Hottiger, M. O. (2006) Arginine methylation regulates DNA polymerase beta, *Mol Cell 22*, 51-62.
37. Guccione, E., Bassi, C., Casadio, F., Martinato, F., Cesaroni, M., Schuchlautz, H., Luscher, B., and Amati, B. (2007) Methylation of histone H3R2 by PRMT6 and H3K4 by an MLL complex are mutually exclusive, *Nature 449*, 933-937.
38. Swiercz, R., Person, M. D., and Bedford, M. T. (2005) Ribosomal protein S2 is a substrate for mammalian PRMT3 (protein arginine methyltransferase 3), *Biochem J 386*, 85-91.
39. Choi, S., Jung, C. R., Kim, J. Y., and Im, D. S. (2008) PRMT3 inhibits ubiquitination of ribosomal protein S2 and together forms an active enzyme complex, *Biochimica et biophysica acta 1780*, 1062-1069.
40. Kim, J. D., Kako, K., Kakiuchi, M., Park, G. G., and Fukamizu, A. (2008) EWS is a substrate of type I protein arginine methyltransferase, PRMT8, *International journal of molecular medicine 22*, 309-315.
41. Pahlich, S., Bschir, K., Chiavi, C., Belyanskaya, L., and Gehring, H. (2005) Different methylation characteristics of protein arginine methyltransferase 1 and 3 toward the Ewing Sarcoma protein and a peptide, *Proteins 61*, 164-175.
42. Sayegh, J., Webb, K., Cheng, D., Bedford, M. T., and Clarke, S. G. (2007) Regulation of protein arginine methyltransferase 8 (PRMT8) activity by its N-terminal domain, *The Journal of biological chemistry 282*, 36444-36453.
43. Kzhyshkowska, J., Schutt, H., Liss, M., Kremmer, E., Stauber, R., Wolf, H., and Dobner, T. (2001) Heterogeneous nuclear ribonucleoprotein E1B-AP5 is methylated in its Arg-Gly-Gly (RGG) box and interacts with human arginine methyltransferase HRMT1L1, *Biochem J 358*, 305-314.

44. Regis, G., Pensa, S., Boselli, D., Novelli, F., and Poli, V. (2008) Ups and downs: the STAT1:STAT3 seesaw of Interferon and gp130 receptor signalling, *Seminars in cell & developmental biology 19*, 351-359.
45. Blythe, S. A., Cha, S. W., Tadjuidje, E., Heasman, J., and Klein, P. S. (2010) beta-Catenin primes organizer gene expression by recruiting a histone H3 arginine 8 methyltransferase, Prmt2, *Developmental cell 19*, 220-231.
46. Berger, S. L. (2008) Out of the jaws of death: PRMT5 steers p53, *Nature cell biology 10*, 1389-1390.
47. Jansson, M., Durant, S. T., Cho, E. C., Sheahan, S., Edelmann, M., Kessler, B., and La Thangue, N. B. (2008) Arginine methylation regulates the p53 response, *Nature cell biology 10*, 1431-1439.
48. Gonsalvez, G. B., Tian, L., Ospina, J. K., Boisvert, F. M., Lamond, A. I., and Matera, A. G. (2007) Two distinct arginine methyltransferases are required for biogenesis of Sm-class ribonucleoproteins, *The Journal of cell biology 178*, 733-740.
49. Koh, S. S., Chen, D., Lee, Y. H., and Stallcup, M. R. (2001) Synergistic enhancement of nuclear receptor function by p160 coactivators and two coactivators with protein methyltransferase activities, *The Journal of biological chemistry 276*, 1089-1098.
50. An, W., Kim, J., and Roeder, R. G. (2004) Ordered cooperative functions of PRMT1, p300, and CARM1 in transcriptional activation by p53, *Cell 117*, 735-748.
51. Kleinschmidt, M. A., Streubel, G., Samans, B., Krause, M., and Bauer, U. M. (2008) The protein arginine methyltransferases CARM1 and PRMT1 cooperate in gene regulation, *Nucleic acids research 36*, 3202-3213.
52. Hassa, P. O., Covic, M., Bedford, M. T., and Hottiger, M. O. (2008) Protein arginine methyltransferase 1 coactivates NF-kappaB-dependent gene expression synergistically with CARM1 and PARP1, *Journal of molecular biology 377*, 668-678.
53. El-Andaloussi, N., Valovka, T., Toueille, M., Hassa, P. O., Gehrig, P., Covic, M., Hubscher, U., and Hottiger, M. O. (2007) Methylation of DNA polymerase beta by protein arginine methyltransferase 1 regulates its binding to proliferating cell nuclear antigen, *Faseb J 21*, 26-34.
54. Bedford, M. T., Frankel, A., Yaffe, M. B., Clarke, S., Leder, P., and Richard, S. (2000) Arginine methylation inhibits the binding of proline-rich ligands to Src homology 3, but not WW, domains, *The Journal of biological chemistry 275*, 16030-16036.
55. Chen, C., Nott, T. J., Jin, J., and Pawson, T. Deciphering arginine methylation: Tudor tells the tale, *Nat Rev Mol Cell Biol 12*, 629-642.
56. Cote, J., and Richard, S. (2005) Tudor domains bind symmetrical dimethylated arginines, *The Journal of biological chemistry 280*, 28476-28483.
57. Higashimoto, K., Kuhn, P., Desai, D., Cheng, X., and Xu, W. (2007) Phosphorylation-mediated inactivation of coactivator-associated arginine methyltransferase 1, *Proceedings of the National Academy of Sciences of the United States of America 104*, 12318-12323.
58. Feng, Q., He, B., Jung, S. Y., Song, Y., Qin, J., Tsai, S. Y., Tsai, M. J., and O'Malley, B. W. (2009) Biochemical control of CARM1 enzymatic activity by phosphorylation, *The Journal of biological chemistry 284*, 36167-36174.
59. Chang, B., Chen, Y., Zhao, Y., and Bruick, R. K. (2007) JMJD6 is a histone arginine demethylase, *Science (New York, N.Y 318*, 444-447.
60. Webby, C. J., Wolf, A., Gromak, N., Dreger, M., Kramer, H., Kessler, B., Nielsen, M. L., Schmitz, C., Butler, D. S., Yates, J. R., 3rd, Delahunty, C. M., Hahn, P., Lengeling, A.,

Mann, M., Proudfoot, N. J., Schofield, C. J., and Bottger, A. (2009) Jmjd6 catalyses lysyl-hydroxylation of U2AF65, a protein associated with RNA splicing, *Science (New York, N.Y 325*, 90-93.

61. Thompson, P. R., and Fast, W. (2006) Histone citrullination by protein arginine deiminase: is arginine methylation a green light or a roadblock?, *ACS chemical biology 1*, 433-441.
62. Raijmakers, R., Zendman, A. J., Egberts, W. V., Vossenaar, E. R., Raats, J., Soede-Huijbregts, C., Rutjes, F. P., van Veelen, P. A., Drijfhout, J. W., and Pruijn, G. J. (2007) Methylation of arginine residues interferes with citrullination by peptidylarginine deiminases in vitro, *Journal of molecular biology 367*, 1118-1129.
63. Bartel, R. L., and Borchardt, R. T. (1984) Effects of adenosine dialdehyde on S-adenosylhomocysteine hydrolase and S-adenosylmethionine-dependent transmethylations in mouse L929 cells, *Molecular pharmacology 25*, 418-424.
64. Cheng, D., Yadav, N., King, R. W., Swanson, M. S., Weinstein, E. J., and Bedford, M. T. (2004) Small molecule regulators of protein arginine methyltransferases, *The Journal of biological chemistry 279*, 23892-23899.
65. Obianyo, O., Causey, C. P., Osborne, T. C., Jones, J. E., Lee, Y. H., Stallcup, M. R., and Thompson, P. R. A chloroacetamidine-based inactivator of protein arginine methyltransferase 1: design, synthesis, and in vitro and in vivo evaluation, *Chembiochem 11*, 1219-1223.
66. Osborne, T., Roska, R. L., Rajski, S. R., and Thompson, P. R. (2008) In situ generation of a bisubstrate analogue for protein arginine methyltransferase 1, *Journal of the American Chemical Society 130*, 4574-4575.
67. Lakowski, T. M., t Hart, P., Ahern, C. A., Martin, N. I., and Frankel, A. Neta-substituted arginyl peptide inhibitors of protein arginine N-methyltransferases, *ACS chemical biology 5*, 1053-1063.
68. Rimokh, R., Rouault, J. P., Wahbi, K., Gadoux, M., Lafage, M., Archimbaud, E., Charrin, C., Gentilhomme, O., Germain, D., Samarut, J., and et al. (1991) A chromosome 12 coding region is juxtaposed to the MYC protooncogene locus in a t(8;12)(q24;q22) translocation in a case of B-cell chronic lymphocytic leukemia, *Genes, chromosomes & cancer 3*, 24-36.
69. Rouault, J. P., Rimokh, R., Tessa, C., Paranhos, G., Ffrench, M., Duret, L., Garoccio, M., Germain, D., Samarut, J., and Magaud, J. P. (1992) BTG1, a member of a new family of antiproliferative genes, *The EMBO journal 11*, 1663-1670.
70. Mayeda, A., and Krainer, A. R. (1992) Regulation of alternative pre-mRNA splicing by hnRNP A1 and splicing factor SF2, *Cell 68*, 365-375.
71. Caceres, J. F., Stamm, S., Helfman, D. M., and Krainer, A. R. (1994) Regulation of alternative splicing in vivo by overexpression of antagonistic splicing factors, *Science (New York, N.Y 265*, 1706-1709.
72. Scorilas, A., Black, M. H., Talieri, M., and Diamandis, E. P. (2000) Genomic organization, physical mapping, and expression analysis of the human protein arginine methyltransferase 1 gene, *Biochemical and biophysical research communications 278*, 349-359.
73. Goulet, I., Gauvin, G., Boisvenue, S., and Cote, J. (2007) Alternative splicing yields protein arginine methyltransferase 1 isoforms with distinct activity, substrate specificity, and subcellular localization, *The Journal of biological chemistry 282*, 33009-33021.

74. Robin-Lespinasse, Y., Sentis, S., Kolytcheff, C., Rostan, M. C., Corbo, L., and Le Romancer, M. (2007) hCAF1, a new regulator of PRMT1-dependent arginine methylation, *J Cell Sci 120*, 638-647.
75. van Galen, J. C., Kuiper, R. P., van Emst, L., Levers, M., Tijchon, E., Scheijen, B., Waanders, E., van Reijmersdal, S. V., Gilissen, C., van Kessel, A. G., Hoogerbrugge, P. M., and van Leeuwen, F. N. BTG1 regulates glucocorticoid receptor autoinduction in acute lymphoblastic leukemia, *Blood 115*, 4810-4819.
76. Rouault, J. P., Falette, N., Guehenneux, F., Guillot, C., Rimokh, R., Wang, Q., Berthet, C., Moyret-Lalle, C., Savatier, P., Pain, B., Shaw, P., Berger, R., Samarut, J., Magaud, J. P., Ozturk, M., Samarut, C., and Puisieux, A. (1996) Identification of BTG2, an antiproliferative p53-dependent component of the DNA damage cellular response pathway, *Nature genetics 14*, 482-486.
77. Passeri, D., Marcucci, A., Rizzo, G., Billi, M., Panigada, M., Leonardi, L., Tirone, F., and Grignani, F. (2006) Btg2 enhances retinoic acid-induced differentiation by modulating histone H4 methylation and acetylation, *Molecular and cellular biology 26*, 5023-5032.
78. Strahl, B. D., Briggs, S. D., Brame, C. J., Caldwell, J. A., Koh, S. S., Ma, H., Cook, R. G., Shabanowitz, J., Hunt, D. F., Stallcup, M. R., and Allis, C. D. (2001) Methylation of histone H4 at arginine 3 occurs in vivo and is mediated by the nuclear receptor coactivator PRMT1, *Curr Biol 11*, 996-1000.
79. Wang, H., Huang, Z. Q., Xia, L., Feng, Q., Erdjument-Bromage, H., Strahl, B. D., Briggs, S. D., Allis, C. D., Wong, J., Tempst, P., and Zhang, Y. (2001) Methylation of histone H4 at arginine 3 facilitating transcriptional activation by nuclear hormone receptor, *Science (New York, N.Y 293*, 853-857.
80. Boffa, L. C., Karn, J., Vidali, G., and Allfrey, V. G. (1977) Distribution of NG, NG,-dimethylarginine in nuclear protein fractions, *Biochemical and biophysical research communications 74*, 969-976.
81. Beyer, A. L., Christensen, M. E., Walker, B. W., and LeStourgeon, W. M. (1977) Identification and characterization of the packaging proteins of core 40S hnRNP particles, *Cell 11*, 127-138.
82. Wilk, H. E., Werr, H., Friedrich, D., Kiltz, H. H., and Schafer, K. P. (1985) The core proteins of 35S hnRNP complexes. Characterization of nine different species, *European journal of biochemistry / FEBS 146*, 71-81.
83. Liu, Q., and Dreyfuss, G. (1995) In vivo and in vitro arginine methylation of RNA-binding proteins, *Molecular and cellular biology 15*, 2800-2808.
84. Nichols, R. C., Wang, X. W., Tang, J., Hamilton, B. J., High, F. A., Herschman, H. R., and Rigby, W. F. (2000) The RGG domain in hnRNP A2 affects subcellular localization, *Experimental cell research 256*, 522-532.
85. Chang, Y. I., Hsu, S. C., Chau, G. Y., Huang, C. Y., Sung, J. S., Hua, W. K., and Lin, W. J. Identification of the methylation preference region in heterogeneous nuclear ribonucleoprotein K by protein arginine methyltransferase 1 and its implication in regulating nuclear/cytoplasmic distribution, *Biochemical and biophysical research communications 404*, 865-869.
86. Passos, D. O., Quaresma, A. J., and Kobarg, J. (2006) The methylation of the C-terminal region of hnRNPQ (NSAP1) is important for its nuclear localization, *Biochemical and biophysical research communications 346*, 517-525.

87. Herrmann, F., Bossert, M., Schwander, A., Akgun, E., and Fackelmayer, F. O. (2004) Arginine methylation of scaffold attachment factor A by heterogeneous nuclear ribonucleoprotein particle-associated PRMT1, *The Journal of biological chemistry 279*, 48774-48779.
88. Rawal, N., Rajpurohit, R., Lischwe, M. A., Williams, K. R., Paik, W. K., and Kim, S. (1995) Structural specificity of substrate for S-adenosylmethionine:protein arginine N-methyltransferases, *Biochimica et biophysica acta 1248*, 11-18.
89. Kim, S., Merrill, B. M., Rajpurohit, R., Kumar, A., Stone, K. L., Papov, V. V., Schneiders, J. M., Szer, W., Wilson, S. H., Paik, W. K., and Williams, K. R. (1997) Identification of N(G)-methylarginine residues in human heterogeneous RNP protein A1: Phe/Gly-Gly-Gly-Arg-Gly-Gly-Gly/Phe is a preferred recognition motif, *Biochemistry 36*, 5185-5192.
90. Kiledjian, M., and Dreyfuss, G. (1992) Primary structure and binding activity of the hnRNP U protein: binding RNA through RGG box, *The EMBO journal 11*, 2655-2664.
91. Calnan, B. J., Tidor, B., Biancalana, S., Hudson, D., and Frankel, A. D. (1991) Arginine-mediated RNA recognition: the arginine fork, *Science (New York, N.Y 252*, 1167-1171.
92. Rajpurohit, R., Paik, W. K., and Kim, S. (1994) Effect of enzymic methylation of heterogeneous ribonucleoprotein particle A1 on its nucleic-acid binding and controlled proteolysis, *Biochem J 304 (Pt 3)*, 903-909.
93. Ostareck-Lederer, A., Ostareck, D. H., Rucknagel, K. P., Schierhorn, A., Moritz, B., Huttelmaier, S., Flach, N., Handoko, L., and Wahle, E. (2006) Asymmetric arginine dimethylation of heterogeneous nuclear ribonucleoprotein K by protein-arginine methyltransferase 1 inhibits its interaction with c-Src, *The Journal of biological chemistry 281*, 11115-11125.
94. Chiou, Y. Y., Lin, W. J., Fu, S. L., and Lin, C. H. (2007) Direct mass-spectrometric identification of Arg296 and Arg299 as the methylation sites of hnRNP K protein for methyltransferase PRMT1, *The protein journal 26*, 87-93.
95. Cote, J., Boisvert, F. M., Boulanger, M. C., Bedford, M. T., and Richard, S. (2003) Sam68 RNA binding protein is an in vivo substrate for protein arginine N-methyltransferase 1, *Molecular biology of the cell 14*, 274-287.
96. Stetler, A., Winograd, C., Sayegh, J., Cheever, A., Patton, E., Zhang, X., Clarke, S., and Ceman, S. (2006) Identification and characterization of the methyl arginines in the fragile X mental retardation protein Fmrp, *Human molecular genetics 15*, 87-96.
97. Jobert, L., Argentini, M., and Tora, L. (2009) PRMT1 mediated methylation of TAF15 is required for its positive gene regulatory function, *Experimental cell research 315*, 1273-1286.
98. Rezai-Zadeh, N., Zhang, X., Namour, F., Fejer, G., Wen, Y. D., Yao, Y. L., Gyory, I., Wright, K., and Seto, E. (2003) Targeted recruitment of a histone H4-specific methyltransferase by the transcription factor YY1, *Genes & development 17*, 1019-1029.
99. Mowen, K. A., Tang, J., Zhu, W., Schurter, B. T., Shuai, K., Herschman, H. R., and David, M. (2001) Arginine methylation of STAT1 modulates IFNalpha/beta-induced transcription, *Cell 104*, 731-741.
100. Xie, Y., Ke, S., Ouyang, N., He, J., Xie, W., Bedford, M. T., and Tian, Y. (2009) Epigenetic regulation of transcriptional activity of pregnane X receptor by protein arginine methyltransferase 1, *The Journal of biological chemistry 284*, 9199-9205.

101. Barrero, M. J., and Malik, S. (2006) Two functional modes of a nuclear receptor-recruited arginine methyltransferase in transcriptional activation, *Mol Cell 24*, 233-243.
102. Le Romancer, M., Treilleux, I., Leconte, N., Robin-Lespinasse, Y., Sentis, S., Bouchekioua-Bouzaghou, K., Goddard, S., Gobert-Gosse, S., and Corbo, L. (2008) Regulation of estrogen rapid signaling through arginine methylation by PRMT1, *Mol Cell 31*, 212-221.
103. Teyssier, C., Ma, H., Emter, R., Kralli, A., and Stallcup, M. R. (2005) Activation of nuclear receptor coactivator PGC-1alpha by arginine methylation, *Genes & development 19*, 1466-1473.
104. Mostaqul Huq, M. D., Gupta, P., Tsai, N. P., White, R., Parker, M. G., and Wei, L. N. (2006) Suppression of receptor interacting protein 140 repressive activity by protein arginine methylation, *The EMBO journal 25*, 5094-5104.
105. Rizzo, G., Renga, B., Antonelli, E., Passeri, D., Pellicciari, R., and Fiorucci, S. (2005) The methyl transferase PRMT1 functions as co-activator of farnesoid X receptor (FXR)/9-cis retinoid X receptor and regulates transcription of FXR responsive genes, *Molecular pharmacology 68*, 551-558.
106. Ohno, M., Komakine, J., Suzuki, E., Nishizuka, M., Osada, S., and Imagawa, M. Interleukin enhancer-binding factor 3 functions as a liver receptor homologue-1 co-activator in synergy with the nuclear receptor co-activators PRMT1 and PGC-1alpha, *Biochem J 437*, 531-540.
107. Matsuda, H., Paul, B. D., Choi, C. Y., Hasebe, T., and Shi, Y. B. (2009) Novel functions of protein arginine methyltransferase 1 in thyroid hormone receptor-mediated transcription and in the regulation of metamorphic rate in Xenopus laevis, *Molecular and cellular biology 29*, 745-757.
108. Strahl, B. D., and Allis, C. D. (2000) The language of covalent histone modifications, *Nature 403*, 41-45.
109. Huang, S., Litt, M., and Felsenfeld, G. (2005) Methylation of histone H4 by arginine methyltransferase PRMT1 is essential in vivo for many subsequent histone modifications, *Genes & development 19*, 1885-1893.
110. Yamagata, K., Daitoku, H., Takahashi, Y., Namiki, K., Hisatake, K., Kako, K., Mukai, H., Kasuya, Y., and Fukamizu, A. (2008) Arginine methylation of FOXO transcription factors inhibits their phosphorylation by Akt, *Mol Cell 32*, 221-231.
111. Sakamaki, J., Daitoku, H., Ueno, K., Hagiwara, A., Yamagata, K., and Fukamizu, A. Arginine methylation of BCL-2 antagonist of cell death (BAD) counteracts its phosphorylation and inactivation by Akt, *Proceedings of the National Academy of Sciences of the United States of America 108*, 6085-6090.
112. Cho, J. H., Lee, M. K., Yoon, K. W., Lee, J., Cho, S. G., and Choi, E. J. Arginine methylation-dependent regulation of ASK1 signaling by PRMT1, *Cell death and differentiation*.
113. Boisvert, F. M., Dery, U., Masson, J. Y., and Richard, S. (2005) Arginine methylation of MRE11 by PRMT1 is required for DNA damage checkpoint control, *Genes & development 19*, 671-676.
114. Boisvert, F. M., Rhie, A., Richard, S., and Doherty, A. J. (2005) The GAR motif of 53BP1 is arginine methylated by PRMT1 and is necessary for 53BP1 DNA binding activity, *Cell cycle (Georgetown, Tex 4*, 1834-1841.

115. Boisvert, F. M., Hendzel, M. J., Masson, J. Y., and Richard, S. (2005) Methylation of MRE11 regulates its nuclear compartmentalization, *Cell cycle (Georgetown, Tex 4*, 981-989.
116. Katsanis, N., Yaspo, M. L., and Fisher, E. M. (1997) Identification and mapping of a novel human gene, HRMT1L1, homologous to the rat protein arginine N-methyltransferase 1 (PRMT1) gene, *Mamm Genome 8*, 526-529.
117. Scott, H. S., Antonarakis, S. E., Lalioti, M. D., Rossier, C., Silver, P. A., and Henry, M. F. (1998) Identification and characterization of two putative human arginine methyltransferases (HRMT1L1 and HRMT1L2), *Genomics 48*, 330-340.
118. Zhong, J., Cao, R. X., Zu, X. Y., Hong, T., Yang, J., Liu, L., Xiao, X. H., Ding, W. J., Zhao, Q., Liu, J. H., and Wen, G. B. Identification and characterization of novel spliced variants of PRMT2 in breast carcinoma, *The FEBS journal*.
119. Zhong, J., Cao, R. X., Hong, T., Yang, J., Zu, X. Y., Xiao, X. H., Liu, J. H., and Wen, G. B. Identification and expression analysis of a novel transcript of the human PRMT2 gene resulted from alternative polyadenylation in breast cancer, *Gene 487*, 1-9.
120. Pawson, T., and Gish, G. D. (1992) SH2 and SH3 domains: from structure to function, *Cell 71*, 359-362.
121. Cohen, G. B., Ren, R., and Baltimore, D. (1995) Modular binding domains in signal transduction proteins, *Cell 80*, 237-248.
122. Mayer, B. J., Ren, R., Clark, K. L., and Baltimore, D. (1993) A putative modular domain present in diverse signaling proteins, *Cell 73*, 629-630.
123. Ren, R., Mayer, B. J., Cicchetti, P., and Baltimore, D. (1993) Identification of a ten-amino acid proline-rich SH3 binding site, *Science (New York, N.Y 259*, 1157-1161.
124. Feng, S., Chen, J. K., Yu, H., Simon, J. A., and Schreiber, S. L. (1994) Two binding orientations for peptides to the Src SH3 domain: development of a general model for SH3-ligand interactions, *Science (New York, N.Y 266*, 1241-1247.
125. Espejo, A., Cote, J., Bednarek, A., Richard, S., and Bedford, M. T. (2002) A protein-domain microarray identifies novel protein-protein interactions, *Biochem J 367*, 697-702.
126. Meyer, R., Wolf, S. S., and Obendorf, M. (2007) PRMT2, a member of the protein arginine methyltransferase family, is a coactivator of the androgen receptor, *J Steroid Biochem Mol Biol 107*, 1-14.
127. Qi, C., Chang, J., Zhu, Y., Yeldandi, A. V., Rao, S. M., and Zhu, Y. J. (2002) Identification of protein arginine methyltransferase 2 as a coactivator for estrogen receptor alpha, *The Journal of biological chemistry 277*, 28624-28630.
128. Yoshimoto, T., Boehm, M., Olive, M., Crook, M. F., San, H., Langenickel, T., and Nabel, E. G. (2006) The arginine methyltransferase PRMT2 binds RB and regulates E2F function, *Experimental cell research 312*, 2040-2053.
129. Yildirim, A. O., Bulau, P., Zakrzewicz, D., Kitowska, K. E., Weissmann, N., Grimminger, F., Morty, R. E., and Eickelberg, O. (2006) Increased protein arginine methylation in chronic hypoxia: role of protein arginine methyltransferases, *American journal of respiratory cell and molecular biology 35*, 436-443.
130. Pullamsetti, S., Kiss, L., Ghofrani, H. A., Voswinckel, R., Haredza, P., Klepetko, W., Aigner, C., Fink, L., Muyal, J. P., Weissmann, N., Grimminger, F., Seeger, W., and Schermuly, R. T. (2005) Increased levels and reduced catabolism of asymmetric and symmetric dimethylarginines in pulmonary hypertension, *Faseb J 19*, 1175-1177.

131. Vallance, P., Leone, A., Calver, A., Collier, J., and Moncada, S. (1992) Accumulation of an endogenous inhibitor of nitric oxide synthesis in chronic renal failure, *Lancet 339*, 572-575.
132. Jacobs, A. T., and Ignarro, L. J. (2001) Lipopolysaccharide-induced expression of interferon-beta mediates the timing of inducible nitric-oxide synthase induction in RAW 264.7 macrophages, *The Journal of biological chemistry 276*, 47950-47957.
133. Klein, E., Weigel, J., Buford, M. C., Holian, A., and Wells, S. M. Asymmetric dimethylarginine potentiates lung inflammation in a mouse model of allergic asthma, *American journal of physiology 299*, L816-825.
134. Dalloneau, E., Pereira, P. L., Brault, V., Nabel, E. G., and Herault, Y. Prmt2 regulates the lipopolysaccharide-induced responses in lungs and macrophages, *J Immunol 187*, 4826-4834.
135. Thomas, D., Lakowski, T. M., Pak, M. L., Kim, J. J., and Frankel, A. (2010) Forster resonance energy transfer measurements of cofactor-dependent effects on protein arginine N-methyltransferase homodimerization, *Protein Sci 19*, 2141-2151.
136. Tilsner, J., Linnik, O., Christensen, N. M., Bell, K., Roberts, I. M., Lacomme, C., and Oparka, K. J. (2009) Live-cell imaging of viral RNA genomes using a Pumilio-based reporter, *Plant J 57*, 758-770.
137. Luger, K., Rechsteiner, T. J., Flaus, A. J., Waye, M. M., and Richmond, T. J. (1997) Characterization of nucleosome core particles containing histone proteins made in bacteria, *Journal of molecular biology 272*, 301-311.
138. Ghosh, I., Hamilton, A. D., and Regan, L. . (2000)
Antiparallel Leucine Zipper-Directed Protein Reassembly: Application to the Green Fluorescent Protein, *Journal of the American Chemical Society 122*, 2.
139. Magliery, T. J., Wilson, C. G., Pan, W., Mishler, D., Ghosh, I., Hamilton, A. D., and Regan, L. (2005) Detecting protein-protein interactions with a green fluorescent protein fragment reassembly trap: scope and mechanism, *Journal of the American Chemical Society 127*, 146-157.
140. Hu, C. D., Chinenov, Y., and Kerppola, T. K. (2002) Visualization of interactions among bZIP and Rel family proteins in living cells using bimolecular fluorescence complementation, *Mol Cell 9*, 789-798.
141. Kerppola, T. K. (2006) Visualization of molecular interactions by fluorescence complementation, *Nat Rev Mol Cell Biol 7*, 449-456.
142. Kerppola, T. K. (2009) Visualization of molecular interactions using bimolecular fluorescence complementation analysis: characteristics of protein fragment complementation, *Chem Soc Rev 38*, 2876-2886.
143. Morell, M., Espargaro, A., Aviles, F. X., and Ventura, S. (2007) Detection of transient protein-protein interactions by bimolecular fluorescence complementation: the Abl-SH3 case, *Proteomics 7*, 1023-1036.
144. Vidi, P. A., and Watts, V. J. (2009) Fluorescent and bioluminescent protein-fragment complementation assays in the study of G protein-coupled receptor oligomerization and signaling, *Molecular pharmacology 75*, 733-739.
145. Griesbeck, O., Baird, G. S., Campbell, R. E., Zacharias, D. A., and Tsien, R. Y. (2001) Reducing the environmental sensitivity of yellow fluorescent protein. Mechanism and applications, *The Journal of biological chemistry 276*, 29188-29194.

146. Martin, G., Ostareck-Lederer, A., Chari, A., Neuenkirchen, N., Dettwiler, S., Blank, D., Ruegsegger, U., Fischer, U., and Keller, W. (2010) Arginine methylation in subunits of mammalian pre-mRNA cleavage factor I, *RNA (New York, N.Y 16*, 1646-1659.
147. Herrmann, F., Lee, J., Bedford, M. T., and Fackelmayer, F. O. (2005) Dynamics of human protein arginine methyltransferase 1(PRMT1) in vivo, *The Journal of biological chemistry 280*, 38005-38010.
148. Cheung, N., Chan, L. C., Thompson, A., Cleary, M. L., and So, C. W. (2007) Protein arginine-methyltransferase-dependent oncogenesis, *Nature cell biology 9*, 1208-1215.
149. Wu, Y., Li, Q., and Chen, X. Z. (2007) Detecting protein-protein interactions by Far western blotting, *Nature protocols 2*, 3278-3284.
150. Pak, M. L., Lakowski, T. M., Thomas, D., Vhuiyan, M. I., Husecken, K., and Frankel, A. A Protein Arginine N-Methyltransferase 1 (PRMT1) and 2 Heteromeric Interaction Increases PRMT1 Enzymatic Activity, *Biochemistry 50*, 8226-8240.
151. Ceballos-Cancino, G., Espinosa, M., Maldonado, V., and Melendez-Zajgla, J. (2007) Regulation of mitochondrial Smac/DIABLO-selective release by survivin, *Oncogene 26*, 7569-7575.
152. Cuatrecasas, P., Fuchs, S., and Anfinsen, C. B. (1967) Catalytic properties and specificity of the extracellular nuclease of Staphylococcus aureus, *The Journal of biological chemistry 242*, 1541-1547.
153. Reddy, T. R. (2000) A single point mutation in the nuclear localization domain of Sam68 blocks the Rev/RRE-mediated transactivation, *Oncogene 19*, 3110-3114.
154. Paronetto, M. P., Achsel, T., Massiello, A., Chalfant, C. E., and Sette, C. (2007) The RNA-binding protein Sam68 modulates the alternative splicing of Bcl-x, *The Journal of cell biology 176*, 929-939.
155. Pedrotti, S., Bielli, P., Paronetto, M. P., Ciccosanti, F., Fimia, G. M., Stamm, S., Manley, J. L., and Sette, C. The splicing regulator Sam68 binds to a novel exonic splicing silencer and functions in SMN2 alternative splicing in spinal muscular atrophy, *The EMBO journal 29*, 1235-1247.
156. Lukong, K. E., and Richard, S. (2003) Sam68, the KH domain-containing superSTAR, *Biochimica et biophysica acta 1653*, 73-86.
157. Licatalosi, D. D., and Darnell, R. B. RNA processing and its regulation: global insights into biological networks, *Nature reviews 11*, 75-87.
158. Saltzman, A. L., Pan, Q., and Blencowe, B. J. Regulation of alternative splicing by the core spliceosomal machinery, *Genes & development 25*, 373-384.
159. Lander, E. S., Linton, L. M., Birren, B., Nusbaum, C., Zody, M. C., Baldwin, J., Devon, K., Dewar, K., Doyle, M., FitzHugh, W., Funke, R., Gage, D., Harris, K., Heaford, A., Howland, J., Kann, L., Lehoczky, J., LeVine, R., McEwan, P., McKernan, K., Meldrim, J., Mesirov, J. P., Miranda, C., Morris, W., Naylor, J., Raymond, C., Rosetti, M., Santos, R., Sheridan, A., Sougnez, C., Stange-Thomann, N., Stojanovic, N., Subramanian, A., Wyman, D., Rogers, J., Sulston, J., Ainscough, R., Beck, S., Bentley, D., Burton, J., Clee, C., Carter, N., Coulson, A., Deadman, R., Deloukas, P., Dunham, A., Dunham, I., Durbin, R., French, L., Grafham, D., Gregory, S., Hubbard, T., Humphray, S., Hunt, A., Jones, M., Lloyd, C., McMurray, A., Matthews, L., Mercer, S., Milne, S., Mullikin, J. C., Mungall, A., Plumb, R., Ross, M., Shownkeen, R., Sims, S., Waterston, R. H., Wilson, R. K., Hillier, L. W., McPherson, J. D., Marra, M. A., Mardis, E. R., Fulton, L. A., Chinwalla, A. T., Pepin, K. H., Gish, W. R., Chissoe, S. L., Wendl, M. C., Delehaunty,

K. D., Miner, T. L., Delehaunty, A., Kramer, J. B., Cook, L. L., Fulton, R. S., Johnson, D. L., Minx, P. J., Clifton, S. W., Hawkins, T., Branscomb, E., Predki, P., Richardson, P., Wenning, S., Slezak, T., Doggett, N., Cheng, J. F., Olsen, A., Lucas, S., Elkin, C., Uberbacher, E., Frazier, M., Gibbs, R. A., Muzny, D. M., Scherer, S. E., Bouck, J. B., Sodergren, E. J., Worley, K. C., Rives, C. M., Gorrell, J. H., Metzker, M. L., Naylor, S. L., Kucherlapati, R. S., Nelson, D. L., Weinstock, G. M., Sakaki, Y., Fujiyama, A., Hattori, M., Yada, T., Toyoda, A., Itoh, T., Kawagoe, C., Watanabe, H., Totoki, Y., Taylor, T., Weissenbach, J., Heilig, R., Saurin, W., Artiguenave, F., Brottier, P., Bruls, T., Pelletier, E., Robert, C., Wincker, P., Smith, D. R., Doucette-Stamm, L., Rubenfield, M., Weinstock, K., Lee, H. M., Dubois, J., Rosenthal, A., Platzer, M., Nyakatura, G., Taudien, S., Rump, A., Yang, H., Yu, J., Wang, J., Huang, G., Gu, J., Hood, L., Rowen, L., Madan, A., Qin, S., Davis, R. W., Federspiel, N. A., Abola, A. P., Proctor, M. J., Myers, R. M., Schmutz, J., Dickson, M., Grimwood, J., Cox, D. R., Olson, M. V., Kaul, R., Raymond, C., Shimizu, N., Kawasaki, K., Minoshima, S., Evans, G. A., Athanasiou, M., Schultz, R., Roe, B. A., Chen, F., Pan, H., Ramser, J., Lehrach, H., Reinhardt, R., McCombie, W. R., de la Bastide, M., Dedhia, N., Blocker, H., Hornischer, K., Nordsiek, G., Agarwala, R., Aravind, L., Bailey, J. A., Bateman, A., Batzoglou, S., Birney, E., Bork, P., Brown, D. G., Burge, C. B., Cerutti, L., Chen, H. C., Church, D., Clamp, M., Copley, R. R., Doerks, T., Eddy, S. R., Eichler, E. E., Furey, T. S., Galagan, J., Gilbert, J. G., Harmon, C., Hayashizaki, Y., Haussler, D., Hermjakob, H., Hokamp, K., Jang, W., Johnson, L. S., Jones, T. A., Kasif, S., Kaspryzk, A., Kennedy, S., Kent, W. J., Kitts, P., Koonin, E. V., Korf, I., Kulp, D., Lancet, D., Lowe, T. M., McLysaght, A., Mikkelsen, T., Moran, J. V., Mulder, N., Pollara, V. J., Ponting, C. P., Schuler, G., Schultz, J., Slater, G., Smit, A. F., Stupka, E., Szustakowski, J., Thierry-Mieg, D., Thierry-Mieg, J., Wagner, L., Wallis, J., Wheeler, R., Williams, A., Wolf, Y. I., Wolfe, K. H., Yang, S. P., Yeh, R. F., Collins, F., Guyer, M. S., Peterson, J., Felsenfeld, A., Wetterstrand, K. A., Patrinos, A., Morgan, M. J., de Jong, P., Catanese, J. J., Osoegawa, K., Shizuya, H., Choi, S., and Chen, Y. J. (2001) Initial sequencing and analysis of the human genome, *Nature 409*, 860-921.

160. (2004) Finishing the euchromatic sequence of the human genome, *Nature 431*, 931-945.
161. Brett, D., Pospisil, H., Valcarcel, J., Reich, J., and Bork, P. (2002) Alternative splicing and genome complexity, *Nature genetics 30*, 29-30.
162. Matlin, A. J., Clark, F., and Smith, C. W. (2005) Understanding alternative splicing: towards a cellular code, *Nat Rev Mol Cell Biol 6*, 386-398.
163. Konig, H., Matter, N., Bader, R., Thiele, W., and Muller, F. (2007) Splicing segregation: the minor spliceosome acts outside the nucleus and controls cell proliferation, *Cell 131*, 718-729.
164. Jurica, M. S., and Moore, M. J. (2003) Pre-mRNA splicing: awash in a sea of proteins, *Mol Cell 12*, 5-14.
165. Will, C. L., and Luhrmann, R. Spliceosome structure and function, *Cold Spring Harbor perspectives in biology 3*.
166. Query, C. C., Moore, M. J., and Sharp, P. A. (1994) Branch nucleophile selection in pre-mRNA splicing: evidence for the bulged duplex model, *Genes & development 8*, 587-597.
167. Lund, M., and Kjems, J. (2002) Defining a 5' splice site by functional selection in the presence and absence of U1 snRNA 5' end, *RNA (New York, N.Y 8*, 166-179.

168. Arning, S., Gruter, P., Bilbe, G., and Kramer, A. (1996) Mammalian splicing factor SF1 is encoded by variant cDNAs and binds to RNA, *RNA (New York, N.Y 2*, 794-810.
169. Siomi, H., Choi, M., Siomi, M. C., Nussbaum, R. L., and Dreyfuss, G. (1994) Essential role for KH domains in RNA binding: impaired RNA binding by a mutation in the KH domain of FMR1 that causes fragile X syndrome, *Cell 77*, 33-39.
170. Peled-Zehavi, H., Berglund, J. A., Rosbash, M., and Frankel, A. D. (2001) Recognition of RNA branch point sequences by the KH domain of splicing factor 1 (mammalian branch point binding protein) in a splicing factor complex, *Molecular and cellular biology 21*, 5232-5241.
171. Graveley, B. R. (2000) Sorting out the complexity of SR protein functions, *RNA (New York, N.Y 6*, 1197-1211.
172. Wu, J. Y., and Maniatis, T. (1993) Specific interactions between proteins implicated in splice site selection and regulated alternative splicing, *Cell 75*, 1061-1070.
173. Kohtz, J. D., Jamison, S. F., Will, C. L., Zuo, P., Luhrmann, R., Garcia-Blanco, M. A., and Manley, J. L. (1994) Protein-protein interactions and 5'-splice-site recognition in mammalian mRNA precursors, *Nature 368*, 119-124.
174. Eperon, I. C., Makarova, O. V., Mayeda, A., Munroe, S. H., Caceres, J. F., Hayward, D. G., and Krainer, A. R. (2000) Selection of alternative 5' splice sites: role of U1 snRNP and models for the antagonistic effects of SF2/ASF and hnRNP A1, *Molecular and cellular biology 20*, 8303-8318.
175. Neuenkirchen, N., Chari, A., and Fischer, U. (2008) Deciphering the assembly pathway of Sm-class U snRNPs, *FEBS letters 582*, 1997-2003.
176. van Dam, A., Winkel, I., Zijlstra-Baalbergen, J., Smeenk, R., and Cuypers, H. T. (1989) Cloned human snRNP proteins B and B' differ only in their carboxy-terminal part, *The EMBO journal 8*, 3853-3860.
177. Query, C. C., Bentley, R. C., and Keene, J. D. (1989) A common RNA recognition motif identified within a defined U1 RNA binding domain of the 70K U1 snRNP protein, *Cell 57*, 89-101.
178. Scherly, D., Boelens, W., Dathan, N. A., van Venrooij, W. J., and Mattaj, I. W. (1990) Major determinants of the specificity of interaction between small nuclear ribonucleoproteins U1A and U2B" and their cognate RNAs, *Nature 345*, 502-506.
179. Wahl, M. C., Will, C. L., and Luhrmann, R. (2009) The spliceosome: design principles of a dynamic RNP machine, *Cell 136*, 701-718.
180. Will, C. L., Urlaub, H., Achsel, T., Gentzel, M., Wilm, M., and Luhrmann, R. (2002) Characterization of novel SF3b and 17S U2 snRNP proteins, including a human Prp5p homologue and an SF3b DEAD-box protein, *The EMBO journal 21*, 4978-4988.
181. Gozani, O., Feld, R., and Reed, R. (1996) Evidence that sequence-independent binding of highly conserved U2 snRNP proteins upstream of the branch site is required for assembly of spliceosomal complex A, *Genes & development 10*, 233-243.
182. Makarova, O. V., Makarov, E. M., and Luhrmann, R. (2001) The 65 and 110 kDa SR-related proteins of the U4/U6.U5 tri-snRNP are essential for the assembly of mature spliceosomes, *The EMBO journal 20*, 2553-2563.
183. Frilander, M. J., and Steitz, J. A. (1999) Initial recognition of U12-dependent introns requires both U11/5' splice-site and U12/branchpoint interactions, *Genes & development 13*, 851-863.

184. Benecke, H., Luhrmann, R., and Will, C. L. (2005) The U11/U12 snRNP 65K protein acts as a molecular bridge, binding the U12 snRNA and U11-59K protein, *The EMBO journal 24*, 3057-3069.
185. Smith, C. W., and Valcarcel, J. (2000) Alternative pre-mRNA splicing: the logic of combinatorial control, *Trends in biochemical sciences 25*, 381-388.
186. Del Gatto-Konczak, F., Olive, M., Gesnel, M. C., and Breathnach, R. (1999) hnRNP A1 recruited to an exon in vivo can function as an exon splicing silencer, *Molecular and cellular biology 19*, 251-260.
187. Zhu, J., Mayeda, A., and Krainer, A. R. (2001) Exon identity established through differential antagonism between exonic splicing silencer-bound hnRNP A1 and enhancer-bound SR proteins, *Mol Cell 8*, 1351-1361.
188. Guil, S., Gattoni, R., Carrascal, M., Abian, J., Stevenin, J., and Bach-Elias, M. (2003) Roles of hnRNP A1, SR proteins, and p68 helicase in c-H-ras alternative splicing regulation, *Molecular and cellular biology 23*, 2927-2941.
189. Martinez-Contreras, R., Cloutier, P., Shkreta, L., Fisette, J. F., Revil, T., and Chabot, B. (2007) hnRNP proteins and splicing control, *Advances in experimental medicine and biology 623*, 123-147.
190. Expert-Bezancon, A., Le Caer, J. P., and Marie, J. (2002) Heterogeneous nuclear ribonucleoprotein (hnRNP) K is a component of an intronic splicing enhancer complex that activates the splicing of the alternative exon 6A from chicken beta-tropomyosin pre-mRNA, *The Journal of biological chemistry 277*, 16614-16623.
191. Rothrock, C. R., House, A. E., and Lynch, K. W. (2005) HnRNP L represses exon splicing via a regulated exonic splicing silencer, *The EMBO journal 24*, 2792-2802.
192. Hui, J., Stangl, K., Lane, W. S., and Bindereif, A. (2003) HnRNP L stimulates splicing of the eNOS gene by binding to variable-length CA repeats, *Nature structural biology 10*, 33-37.
193. Gabler, S., Schutt, H., Groitl, P., Wolf, H., Shenk, T., and Dobner, T. (1998) E1B 55-kilodalton-associated protein: a cellular protein with RNA-binding activity implicated in nucleocytoplasmic transport of adenovirus and cellular mRNAs, *Journal of virology 72*, 7960-7971.
194. Dong, B., Horowitz, D. S., Kobayashi, R., and Krainer, A. R. (1993) Purification and cDNA cloning of HeLa cell p54nrb, a nuclear protein with two RNA recognition motifs and extensive homology to human splicing factor PSF and Drosophila NONA/BJ6, *Nucleic acids research 21*, 4085-4092.
195. Peng, R., Dye, B. T., Perez, I., Barnard, D. C., Thompson, A. B., and Patton, J. G. (2002) PSF and p54nrb bind a conserved stem in U5 snRNA, *RNA (New York, N.Y 8*, 1334-1347.
196. Zhou, A., Ou, A. C., Cho, A., Benz, E. J., Jr., and Huang, S. C. (2008) Novel splicing factor RBM25 modulates Bcl-x pre-mRNA 5' splice site selection, *Molecular and cellular biology 28*, 5924-5936.
197. Shen, H., and Green, M. R. (2004) A pathway of sequential arginine-serine-rich domain-splicing signal interactions during mammalian spliceosome assembly, *Mol Cell 16*, 363-373.
198. Cazalla, D., Newton, K., and Caceres, J. F. (2005) A novel SR-related protein is required for the second step of Pre-mRNA splicing, *Molecular and cellular biology 25*, 2969-2980.

199. Zamore, P. D., and Green, M. R. (1989) Identification, purification, and biochemical characterization of U2 small nuclear ribonucleoprotein auxiliary factor, *Proceedings of the National Academy of Sciences of the United States of America 86*, 9243-9247.
200. Ruskin, B., Zamore, P. D., and Green, M. R. (1988) A factor, U2AF, is required for U2 snRNP binding and splicing complex assembly, *Cell 52*, 207-219.
201. Llorian, M., Beullens, M., Andres, I., Ortiz, J. M., and Bollen, M. (2004) SIPP1, a novel pre-mRNA splicing factor and interactor of protein phosphatase-1, *Biochem J 378*, 229-238.
202. Craggs, G., Finan, P. M., Lawson, D., Wingfield, J., Perera, T., Gadher, S., Totty, N. F., and Kellie, S. (2001) A nuclear SH3 domain-binding protein that colocalizes with mRNA splicing factors and intermediate filament-containing perinuclear networks, *The Journal of biological chemistry 276*, 30552-30560.
203. Page-McCaw, P. S., Amonlirdviman, K., and Sharp, P. A. (1999) PUF60: a novel U2AF65-related splicing activity, *RNA (New York, N.Y 5*, 1548-1560.
204. Fox, A. H., Lam, Y. W., Leung, A. K., Lyon, C. E., Andersen, J., Mann, M., and Lamond, A. I. (2002) Paraspeckles: a novel nuclear domain, *Curr Biol 12*, 13-25.
205. Fox, A. H., Bond, C. S., and Lamond, A. I. (2005) P54nrb forms a heterodimer with PSP1 that localizes to paraspeckles in an RNA-dependent manner, *Molecular biology of the cell 16*, 5304-5315.
206. Dettwiler, S., Aringhieri, C., Cardinale, S., Keller, W., and Barabino, S. M. (2004) Distinct sequence motifs within the 68-kDa subunit of cleavage factor Im mediate RNA binding, protein-protein interactions, and subcellular localization, *The Journal of biological chemistry 279*, 35788-35797.
207. Lamond, A. I., and Spector, D. L. (2003) Nuclear speckles: a model for nuclear organelles, *Nat Rev Mol Cell Biol 4*, 605-612.
208. Myojin, R., Kuwahara, S., Yasaki, T., Matsunaga, T., Sakurai, T., Kimura, M., Uesugi, S., and Kurihara, Y. (2004) Expression and functional significance of mouse paraspeckle protein 1 on spermatogenesis, *Biology of reproduction 71*, 926-932.
209. Xie, S. Q., Martin, S., Guillot, P. V., Bentley, D. L., and Pombo, A. (2006) Splicing speckles are not reservoirs of RNA polymerase II, but contain an inactive form, phosphorylated on serine2 residues of the C-terminal domain, *Molecular biology of the cell 17*, 1723-1733.
210. Clemson, C. M., Hutchinson, J. N., Sara, S. A., Ensminger, A. W., Fox, A. H., Chess, A., and Lawrence, J. B. (2009) An architectural role for a nuclear noncoding RNA: NEAT1 RNA is essential for the structure of paraspeckles, *Mol Cell 33*, 717-726.
211. Chen, L. L., and Carmichael, G. G. (2009) Altered nuclear retention of mRNAs containing inverted repeats in human embryonic stem cells: functional role of a nuclear noncoding RNA, *Mol Cell 35*, 467-478.
212. Bryantsev, A. L., Chechenova, M. B., and Shelden, E. A. (2007) Recruitment of phosphorylated small heat shock protein Hsp27 to nuclear speckles without stress, *Experimental cell research 313*, 195-209.
213. Landry, J., and Huot, J. (1995) Modulation of actin dynamics during stress and physiological stimulation by a signaling pathway involving p38 MAP kinase and heat-shock protein 27, *Biochemistry and cell biology = Biochimie et biologie cellulaire 73*, 703-707.

214. Wahle, E., and Ruegsegger, U. (1999) 3'-End processing of pre-mRNA in eukaryotes, *FEMS microbiology reviews 23*, 277-295.
215. Ruegsegger, U., Beyer, K., and Keller, W. (1996) Purification and characterization of human cleavage factor Im involved in the 3' end processing of messenger RNA precursors, *The Journal of biological chemistry 271*, 6107-6113.
216. Maniatis, T., and Reed, R. (2002) An extensive network of coupling among gene expression machines, *Nature 416*, 499-506.
217. Awasthi, S., and Alwine, J. C. (2003) Association of polyadenylation cleavage factor I with U1 snRNP, *RNA (New York, N.Y 9*, 1400-1409.
218. Albers, M., Diment, A., Muraru, M., Russell, C. S., and Beggs, J. D. (2003) Identification and characterization of Prp45p and Prp46p, essential pre-mRNA splicing factors, *RNA (New York, N.Y 9*, 138-150.
219. Siegers, K., Bolter, B., Schwarz, J. P., Bottcher, U. M., Guha, S., and Hartl, F. U. (2003) TRiC/CCT cooperates with different upstream chaperones in the folding of distinct protein classes, *The EMBO journal 22*, 5230-5240.
220. Spiess, C., Meyer, A. S., Reissmann, S., and Frydman, J. (2004) Mechanism of the eukaryotic chaperonin: protein folding in the chamber of secrets, *Trends in cell biology 14*, 598-604.
221. Moreau, V., Frischknecht, F., Reckmann, I., Vincentelli, R., Rabut, G., Stewart, D., and Way, M. (2000) A complex of N-WASP and WIP integrates signalling cascades that lead to actin polymerization, *Nature cell biology 2*, 441-448.
222. Stewart, D. M., Tian, L., and Nelson, D. L. (1999) Mutations that cause the Wiskott-Aldrich syndrome impair the interaction of Wiskott-Aldrich syndrome protein (WASP) with WASP interacting protein, *J Immunol 162*, 5019-5024.
223. Hamm, J., Kazmaier, M., and Mattaj, I. W. (1987) In vitro assembly of U1 snRNPs, *The EMBO journal 6*, 3479-3485.
224. Puig, O., Gottschalk, A., Fabrizio, P., and Seraphin, B. (1999) Interaction of the U1 snRNP with nonconserved intronic sequences affects 5' splice site selection, *Genes & development 13*, 569-580.
225. Lee, Y. H., and Stallcup, M. R. (2009) Minireview: protein arginine methylation of nonhistone proteins in transcriptional regulation, *Molecular endocrinology (Baltimore, Md 23*, 425-433.
226. Shav-Tal, Y., and Zipori, D. (2002) PSF and p54(nrb)/NonO--multi-functional nuclear proteins, *FEBS letters 531*, 109-114.
227. Lee, M. S., and Silver, P. A. (1997) RNA movement between the nucleus and the cytoplasm, *Current opinion in genetics & development 7*, 212-219.
228. Shen, E. C., Henry, M. F., Weiss, V. H., Valentini, S. R., Silver, P. A., and Lee, M. S. (1998) Arginine methylation facilitates the nuclear export of hnRNP proteins, *Genes & development 12*, 679-691.
229. Reddy, T. R., Xu, W., Mau, J. K., Goodwin, C. D., Suhasini, M., Tang, H., Frimpong, K., Rose, D. W., and Wong-Staal, F. (1999) Inhibition of HIV replication by dominant negative mutants of Sam68, a functional homolog of HIV-1 Rev, *Nature medicine 5*, 635-642.
230. Du, K., Arai, S., Kawamura, T., Matsushita, A., and Kurokawa, R. TLS and PRMT1 synergistically coactivate transcription at the survivin promoter through TLS arginine methylation, *Biochemical and biophysical research communications 404*, 991-996.

231. Tradewell, M. L., Yu, Z., Tibshirani, M., Boulanger, M. C., Durham, H. D., and Richard, S. Arginine methylation by PRMT1 regulates nuclear-cytoplasmic localization and toxicity of FUS/TLS harbouring ALS-linked mutations, *Human molecular genetics*.
232. Haile, S., Lal, A., Myung, J. K., and Sadar, M. D. FUS/TLS is a co-activator of androgen receptor in prostate cancer cells, *PloS one 6*, e24197.
233. Uranishi, H., Tetsuka, T., Yamashita, M., Asamitsu, K., Shimizu, M., Itoh, M., and Okamoto, T. (2001) Involvement of the pro-oncoprotein TLS (translocated in liposarcoma) in nuclear factor-kappa B p65-mediated transcription as a coactivator, *The Journal of biological chemistry 276*, 13395-13401.
234. Mathur, M., Tucker, P. W., and Samuels, H. H. (2001) PSF is a novel corepressor that mediates its effect through Sin3A and the DNA binding domain of nuclear hormone receptors, *Molecular and cellular biology 21*, 2298-2311.
235. McKenna, N. J., Lanz, R. B., and O'Malley, B. W. (1999) Nuclear receptor coregulators: cellular and molecular biology, *Endocrine reviews 20*, 321-344.
236. Sewer, M. B., and Waterman, M. R. (2002) Adrenocorticotropin/cyclic adenosine 3',5'-monophosphate-mediated transcription of the human CYP17 gene in the adrenal cortex is dependent on phosphatase activity, *Endocrinology 143*, 1769-1777.
237. Najib, S., Martin-Romero, C., Gonzalez-Yanes, C., and Sanchez-Margalet, V. (2005) Role of Sam68 as an adaptor protein in signal transduction, *Cell Mol Life Sci 62*, 36-43.
238. Huot, M. E., Vogel, G., and Richard, S. (2009) Identification of a Sam68 ribonucleoprotein complex regulated by epidermal growth factor, *The Journal of biological chemistry 284*, 31903-31913.
239. Hong, W., Resnick, R. J., Rakowski, C., Shalloway, D., Taylor, S. J., and Blobel, G. A. (2002) Physical and functional interaction between the transcriptional cofactor CBP and the KH domain protein Sam68, *Mol Cancer Res 1*, 48-55.
240. Yang, J. P., Reddy, T. R., Truong, K. T., Suhasini, M., and Wong-Staal, F. (2002) Functional interaction of Sam68 and heterogeneous nuclear ribonucleoprotein K, *Oncogene 21*, 7187-7194.
241. Michelotti, E. F., Michelotti, G. A., Aronsohn, A. I., and Levens, D. (1996) Heterogeneous nuclear ribonucleoprotein K is a transcription factor, *Molecular and cellular biology 16*, 2350-2360.
242. Rajan, P., Gaughan, L., Dalgliesh, C., El-Sherif, A., Robson, C. N., Leung, H. Y., and Elliott, D. J. (2008) The RNA-binding and adaptor protein Sam68 modulates signal-dependent splicing and transcriptional activity of the androgen receptor, *The Journal of pathology 215*, 67-77.
243. Richard, S., Vogel, G., Huot, M. E., Guo, T., Muller, W. J., and Lukong, K. E. (2008) Sam68 haploinsufficiency delays onset of mammary tumorigenesis and metastasis, *Oncogene 27*, 548-556.
244. Rajan, P., Gaughan, L., Dalgliesh, C., El-Sherif, A., Robson, C. N., Leung, H. Y., and Elliott, D. J. (2008) Regulation of gene expression by the RNA-binding protein Sam68 in cancer, *Biochemical Society transactions 36*, 505-507.
245. Xu, W., Chen, H., Du, K., Asahara, H., Tini, M., Emerson, B. M., Montminy, M., and Evans, R. M. (2001) A transcriptional switch mediated by cofactor methylation, *Science (New York, N.Y 294*, 2507-2511.

246. Weng, Z., Rickles, R. J., Feng, S., Richard, S., Shaw, A. S., Schreiber, S. L., and Brugge, J. S. (1995) Structure-function analysis of SH3 domains: SH3 binding specificity altered by single amino acid substitutions, *Molecular and cellular biology 15*, 5627-5634.
247. Lettau, M., Pieper, J., Gerneth, A., Lengl-Janssen, B., Voss, M., Linkermann, A., Schmidt, H., Gelhaus, C., Leippe, M., Kabelitz, D., and Janssen, O. The adapter protein Nck: role of individual SH3 and SH2 binding modules for protein interactions in T lymphocytes, *Protein Sci 19*, 658-669.
248. Lin, Q., Taylor, S. J., and Shalloway, D. (1997) Specificity and determinants of Sam68 RNA binding. Implications for the biological function of K homology domains, *The Journal of biological chemistry 272*, 27274-27280.
249. Paronetto, M. P., Cappellari, M., Busa, R., Pedrotti, S., Vitali, R., Comstock, C., Hyslop, T., Knudsen, K. E., and Sette, C. Alternative splicing of the cyclin D1 proto-oncogene is regulated by the RNA-binding protein Sam68, *Cancer research 70*, 229-239.
250. Cheng, C., and Sharp, P. A. (2006) Regulation of CD44 alternative splicing by SRm160 and its potential role in tumor cell invasion, *Molecular and cellular biology 26*, 362-370.
251. Matter, N., Herrlich, P., and Konig, H. (2002) Signal-dependent regulation of splicing via phosphorylation of Sam68, *Nature 420*, 691-695.
252. Valacca, C., Bonomi, S., Buratti, E., Pedrotti, S., Baralle, F. E., Sette, C., Ghigna, C., and Biamonti, G. Sam68 regulates EMT through alternative splicing-activated nonsense-mediated mRNA decay of the SF2/ASF proto-oncogene, *The Journal of cell biology 191*, 87-99.
253. Chawla, G., Lin, C. H., Han, A., Shiue, L., Ares, M., Jr., and Black, D. L. (2009) Sam68 regulates a set of alternatively spliced exons during neurogenesis, *Molecular and cellular biology 29*, 201-213.
254. Paronetto, M. P., Messina, V., Barchi, M., Geremia, R., Richard, S., and Sette, C. Sam68 marks the transcriptionally active stages of spermatogenesis and modulates alternative splicing in male germ cells, *Nucleic acids research 39*, 4961-4974.
255. Phatnani, H. P., and Greenleaf, A. L. (2006) Phosphorylation and functions of the RNA polymerase II CTD, *Genes & development 20*, 2922-2936.
256. Chen, T., Damaj, B. B., Herrera, C., Lasko, P., and Richard, S. (1997) Self-association of the single-KH-domain family members Sam68, GRP33, GLD-1, and Qk1: role of the KH domain, *Molecular and cellular biology 17*, 5707-5718.
257. Babic, I., Jakymiw, A., and Fujita, D. J. (2004) The RNA binding protein Sam68 is acetylated in tumor cell lines, and its acetylation correlates with enhanced RNA binding activity, *Oncogene 23*, 3781-3789.
258. Hartmann, A. M., Nayler, O., Schwaiger, F. W., Obermeier, A., and Stamm, S. (1999) The interaction and colocalization of Sam68 with the splicing-associated factor YT521-B in nuclear dots is regulated by the Src family kinase p59(fyn), *Molecular biology of the cell 10*, 3909-3926.
259. Jacobson, M. D., Weil, M., and Raff, M. C. (1997) Programmed cell death in animal development, *Cell 88*, 347-354.
260. Williams, G. T., and Smith, C. A. (1993) Molecular regulation of apoptosis: genetic controls on cell death, *Cell 74*, 777-779.
261. Ban, J., Eckhart, L., Weninger, W., Mildner, M., and Tschachler, E. (1998) Identification of a human cDNA encoding a novel Bcl-x isoform, *Biochemical and biophysical research communications 248*, 147-152.

262. Grillot, D. A., Gonzalez-Garcia, M., Ekhterae, D., Duan, L., Inohara, N., Ohta, S., Seldin, M. F., and Nunez, G. (1997) Genomic organization, promoter region analysis, and chromosome localization of the mouse bcl-x gene, *J Immunol 158*, 4750-4757.
263. Falsone, S. F., Gesslbauer, B., and Kungl, A. J. (2008) Coimmunoprecipitation and proteomic analyses, *Methods in molecular biology (Clifton, N.J 439*, 291-308.
264. Fogal, V., Gostissa, M., Sandy, P., Zacchi, P., Sternsdorf, T., Jensen, K., Pandolfi, P. P., Will, H., Schneider, C., and Del Sal, G. (2000) Regulation of p53 activity in nuclear bodies by a specific PML isoform, *The EMBO journal 19*, 6185-6195.
265. So, C. W., Caldas, C., Liu, M. M., Chen, S. J., Huang, Q. H., Gu, L. J., Sham, M. H., Wiedemann, L. M., and Chan, L. C. (1997) EEN encodes for a member of a new family of proteins containing an Src homology 3 domain and is the third gene located on chromosome 19p13 that fuses to MLL in human leukemia, *Proceedings of the National Academy of Sciences of the United States of America 94*, 2563-2568.
266. Rowley, J. D., Golomb, H. M., and Dougherty, C. (1977) 15/17 translocation, a consistent chromosomal change in acute promyelocytic leukaemia, *Lancet 1*, 549-550.
267. de The, H., Chomienne, C., Lanotte, M., Degos, L., and Dejean, A. (1990) The t(15;17) translocation of acute promyelocytic leukaemia fuses the retinoic acid receptor alpha gene to a novel transcribed locus, *Nature 347*, 558-561.
268. Chan, I. T., Kutok, J. L., Williams, I. R., Cohen, S., Moore, S., Shigematsu, H., Ley, T. J., Akashi, K., Le Beau, M. M., and Gilliland, D. G. (2006) Oncogenic K-ras cooperates with PML-RAR alpha to induce an acute promyelocytic leukemia-like disease, *Blood 108*, 1708-1715.
269. Rego, E. M., Wang, Z. G., Peruzzi, D., He, L. Z., Cordon-Cardo, C., and Pandolfi, P. P. (2001) Role of promyelocytic leukemia (PML) protein in tumor suppression, *The Journal of experimental medicine 193*, 521-529.
270. Carracedo, A., Ito, K., and Pandolfi, P. P. The nuclear bodies inside out: PML conquers the cytoplasm, *Current opinion in cell biology 23*, 360-366.
271. Jensen, K., Shiels, C., and Freemont, P. S. (2001) PML protein isoforms and the RBCC/TRIM motif, *Oncogene 20*, 7223-7233.
272. Bernardi, R., Papa, A., and Pandolfi, P. P. (2008) Regulation of apoptosis by PML and the PML-NBs, *Oncogene 27*, 6299-6312.
273. May, E., Jenkins, J. R., and May, P. (1991) Endogenous HeLa p53 proteins are easily detected in HeLa cells transfected with mouse deletion mutant p53 gene, *Oncogene 6*, 1363-1365.
274. Dornan, D., Shimizu, H., Burch, L., Smith, A. J., and Hupp, T. R. (2003) The proline repeat domain of p53 binds directly to the transcriptional coactivator p300 and allosterically controls DNA-dependent acetylation of p53, *Molecular and cellular biology 23*, 8846-8861.
275. Zou, Y., Webb, K., Perna, A. D., Zhang, Q., Clarke, S., and Wang, Y. (2007) A mass spectrometric study on the in vitro methylation of HMGA1a and HMGA1b proteins by PRMTs: methylation specificity, the effect of binding to AT-rich duplex DNA, and the effect of C-terminal phosphorylation, *Biochemistry 46*, 7896-7906.
276. Sgarra, R., Lee, J., Tessari, M. A., Altamura, S., Spolaore, B., Giancotti, V., Bedford, M. T., and Manfioletti, G. (2006) The AT-hook of the chromatin architectural transcription factor high mobility group A1a is arginine-methylated by protein arginine methyltransferase 6, *The Journal of biological chemistry 281*, 3764-3772.

277. Grosschedl, R., Giese, K., and Pagel, J. (1994) HMG domain proteins: architectural elements in the assembly of nucleoprotein structures, *Trends Genet 10*, 94-100.
278. Reeves, R. (2001) Molecular biology of HMGA proteins: hubs of nuclear function, *Gene 277*, 63-81.
279. Diana, F., Sgarra, R., Manfioletti, G., Rustighi, A., Poletto, D., Sciortino, M. T., Mastino, A., and Giancotti, V. (2001) A link between apoptosis and degree of phosphorylation of high mobility group A1a protein in leukemic cells, *The Journal of biological chemistry 276*, 11354-11361.
280. Sgarra, R., Diana, F., Bellarosa, C., Dekleva, V., Rustighi, A., Toller, M., Manfioletti, G., and Giancotti, V. (2003) During apoptosis of tumor cells HMGA1a protein undergoes methylation: identification of the modification site by mass spectrometry, *Biochemistry 42*, 3575-3585.
281. Miranda, T. B., Webb, K. J., Edberg, D. D., Reeves, R., and Clarke, S. (2005) Protein arginine methyltransferase 6 specifically methylates the nonhistone chromatin protein HMGA1a, *Biochemical and biophysical research communications 336*, 831-835.
282. Liu, H., Chen, B., Xiong, H., Huang, Q. H., Zhang, Q. H., Wang, Z. G., Li, B. L., Chen, Z., and Chen, S. J. (2004) Functional contribution of EEN to leukemogenic transformation by MLL-EEN fusion protein, *Oncogene 23*, 3385-3394.
283. Nguyen, A. T., Taranova, O., He, J., and Zhang, Y. DOT1L, the H3K79 methyltransferase, is required for MLL-AF9-mediated leukemogenesis, *Blood 117*, 6912-6922.
284. Meyer, C., Schneider, B., Jakob, S., Strehl, S., Attarbaschi, A., Schnittger, S., Schoch, C., Jansen, M. W., van Dongen, J. J., den Boer, M. L., Pieters, R., Ennas, M. G., Angelucci, E., Koehl, U., Greil, J., Griesinger, F., Zur Stadt, U., Eckert, C., Szczepanski, T., Niggli, F. K., Schafer, B. W., Kempski, H., Brady, H. J., Zuna, J., Trka, J., Nigro, L. L., Biondi, A., Delabesse, E., Macintyre, E., Stanulla, M., Schrappe, M., Haas, O. A., Burmeister, T., Dingermann, T., Klingebiel, T., and Marschalek, R. (2006) The MLL recombinome of acute leukemias, *Leukemia 20*, 777-784.
285. Lua, B. L., and Low, B. C. (2005) Activation of EGF receptor endocytosis and ERK1/2 signaling by BPGAP1 requires direct interaction with EEN/endophilin II and a functional RhoGAP domain, *J Cell Sci 118*, 2707-2721.
286. Kong, C. T., Sham, M. H., So, C. W., Cheah, K. S., Chen, S. J., and Chan, L. C. (2006) The Mll-Een knockin fusion gene enhances proliferation of myeloid progenitors derived from mouse embryonic stem cells and causes myeloid leukaemia in chimeric mice, *Leukemia 20*, 1829-1839.
287. Meek, D. W. (2009) Tumour suppression by p53: a role for the DNA damage response?, *Nat Rev Cancer 9*, 714-723.
288. Stewart, Z. A., and Pietenpol, J. A. (2001) p53 Signaling and cell cycle checkpoints, *Chemical research in toxicology 14*, 243-263.
289. Dimri, G. P., Nakanishi, M., Desprez, P. Y., Smith, J. R., and Campisi, J. (1996) Inhibition of E2F activity by the cyclin-dependent protein kinase inhibitor p21 in cells expressing or lacking a functional retinoblastoma protein, *Molecular and cellular biology 16*, 2987-2997.
290. McLure, K. G., and Lee, P. W. (1998) How p53 binds DNA as a tetramer, *The EMBO journal 17*, 3342-3350.

291. Stommel, J. M., Marchenko, N. D., Jimenez, G. S., Moll, U. M., Hope, T. J., and Wahl, G. M. (1999) A leucine-rich nuclear export signal in the p53 tetramerization domain: regulation of subcellular localization and p53 activity by NES masking, *The EMBO journal 18*, 1660-1672.
292. Scoumanne, A., Zhang, J., and Chen, X. (2009) PRMT5 is required for cell-cycle progression and p53 tumor suppressor function, *Nucleic acids research 37*, 4965-4976.
293. Fernandez-Fernandez, M. R., Veprintsev, D. B., and Fersht, A. R. (2005) Proteins of the S100 family regulate the oligomerization of p53 tumor suppressor, *Proceedings of the National Academy of Sciences of the United States of America 102*, 4735-4740.
294. Reeves, R., and Beckerbauer, L. (2001) HMGI/Y proteins: flexible regulators of transcription and chromatin structure, *Biochimica et biophysica acta 1519*, 13-29.
295. Labib, K., Kearsey, S. E., and Diffley, J. F. (2001) MCM2-7 proteins are essential components of prereplicative complexes that accumulate cooperatively in the nucleus during G1-phase and are required to establish, but not maintain, the S-phase checkpoint, *Molecular biology of the cell 12*, 3658-3667.
296. Labib, K., Tercero, J. A., and Diffley, J. F. (2000) Uninterrupted MCM2-7 function required for DNA replication fork progression, *Science (New York, N.Y 288*, 1643-1647.
297. Sakwe, A. M., Nguyen, T., Athanasopoulos, V., Shire, K., and Frappier, L. (2007) Identification and characterization of a novel component of the human minichromosome maintenance complex, *Molecular and cellular biology 27*, 3044-3055.
298. Nishiyama, A., Frappier, L., and Mechali, M. MCM-BP regulates unloading of the MCM2-7 helicase in late S phase, *Genes & development 25*, 165-175.
299. Mossi, R., Jonsson, Z. O., Allen, B. L., Hardin, S. H., and Hubscher, U. (1997) Replication factor C interacts with the C-terminal side of proliferating cell nuclear antigen, *The Journal of biological chemistry 272*, 1769-1776.
300. Tsurimoto, T., Shinozaki, A., Yano, M., Seki, M., and Enomoto, T. (2005) Human Werner helicase interacting protein 1 (WRNIP1) functions as a novel modulator for DNA polymerase delta, *Genes Cells 10*, 13-22.
301. Giglia-Mari, G., Coin, F., Ranish, J. A., Hoogstraten, D., Theil, A., Wijgers, N., Jaspers, N. G., Raams, A., Argentini, M., van der Spek, P. J., Botta, E., Stefanini, M., Egly, J. M., Aebersold, R., Hoeijmakers, J. H., and Vermeulen, W. (2004) A new, tenth subunit of TFIIH is responsible for the DNA repair syndrome trichothiodystrophy group A, *Nature genetics 36*, 714-719.
302. Reed, A. L., Yamazaki, H., Kaufman, J. D., Rubinstein, Y., Murphy, B., and Johnson, A. C. (1998) Molecular cloning and characterization of a transcription regulator with homology to GC-binding factor, *The Journal of biological chemistry 273*, 21594-21602.
303. Caron, C., Pivot-Pajot, C., van Grunsven, L. A., Col, E., Lestrat, C., Rousseaux, S., and Khochbin, S. (2003) Cdyl: a new transcriptional co-repressor, *EMBO reports 4*, 877-882.
304. Bandyopadhyay, S., Wang, Y., Zhan, R., Pai, S. K., Watabe, M., Iiizumi, M., Furuta, E., Mohinta, S., Liu, W., Hirota, S., Hosobe, S., Tsukada, T., Miura, K., Takano, Y., Saito, K., Commes, T., Piquemal, D., Hai, T., and Watabe, K. (2006) The tumor metastasis suppressor gene Drg-1 down-regulates the expression of activating transcription factor 3 in prostate cancer, *Cancer research 66*, 11983-11990.
305. Kassel, O., Schneider, S., Heilbock, C., Litfin, M., Gottlicher, M., and Herrlich, P. (2004) A nuclear isoform of the focal adhesion LIM-domain protein Trip6 integrates activating

and repressing signals at AP-1- and NF-kappaB-regulated promoters, *Genes & development 18*, 2518-2528.
306. Hayette, S., Cornillet-Lefebvre, P., Tigaud, I., Struski, S., Forissier, S., Berchet, A., Doll, D., Gillot, L., Brahim, W., Delabesse, E., Magaud, J. P., and Rimokh, R. (2005) AF4p12, a human homologue to the furry gene of Drosophila, as a novel MLL fusion partner, *Cancer research 65*, 6521-6525.
307. Andersen, J. B., Strandbygard, D. J., Hartmann, R., and Justesen, J. (2004) Interaction between the 2'-5' oligoadenylate synthetase-like protein p59 OASL and the transcriptional repressor methyl CpG-binding protein 1, *European journal of biochemistry / FEBS 271*, 628-636.
308. Sugimoto, K., Ando, S., Shimomura, T., and Matsumoto, K. (1997) Rfc5, a replication factor C component, is required for regulation of Rad53 protein kinase in the yeast checkpoint pathway, *Molecular and cellular biology 17*, 5905-5914.
309. Flink, I. L., and Morkin, E. (1995) Alternatively processed isoforms of cellular nucleic acid-binding protein interact with a suppressor region of the human beta-myosin heavy chain gene, *The Journal of biological chemistry 270*, 6959-6965.
310. Liu, M., Kumar, K. U., Pater, M. M., and Pater, A. (1998) Identification and characterization of a JC virus pentanucleotide repeat element binding protein: cellular nucleic acid binding protein, *Virus research 58*, 73-82.
311. Konicek, B. W., Xia, X., Rajavashisth, T., and Harrington, M. A. (1998) Regulation of mouse colony-stimulating factor-1 gene promoter activity by AP1 and cellular nucleic acid-binding protein, *DNA and cell biology 17*, 799-809.
312. Michelotti, E. F., Tomonaga, T., Krutzsch, H., and Levens, D. (1995) Cellular nucleic acid binding protein regulates the CT element of the human c-myc protooncogene, *The Journal of biological chemistry 270*, 9494-9499.
313. Paul, C., Lacroix, M., Iankova, I., Julien, E., Schafer, B. W., Labalette, C., Wei, Y., Le Cam, A., Le Cam, L., and Sardet, C. (2006) The LIM-only protein FHL2 is a negative regulator of E4F1, *Oncogene 25*, 5475-5484.
314. Grotterod, I., Maelandsmo, G. M., and Boye, K. Signal transduction mechanisms involved in S100A4-induced activation of the transcription factor NF-kappaB, *BMC cancer 10*, 241.
315. Nagpal, S., Ghosn, C., DiSepio, D., Molina, Y., Sutter, M., Klein, E. S., and Chandraratna, R. A. (1999) Retinoid-dependent recruitment of a histone H1 displacement activity by retinoic acid receptor, *The Journal of biological chemistry 274*, 22563-22568.
316. Zhao, K., Wang, W., Rando, O. J., Xue, Y., Swiderek, K., Kuo, A., and Crabtree, G. R. (1998) Rapid and phosphoinositol-dependent binding of the SWI/SNF-like BAF complex to chromatin after T lymphocyte receptor signaling, *Cell 95*, 625-636.
317. Zamore, P. D., Patton, J. G., and Green, M. R. (1992) Cloning and domain structure of the mammalian splicing factor U2AF, *Nature 355*, 609-614.
318. Zamore, P. D., and Green, M. R. (1991) Biochemical characterization of U2 snRNP auxiliary factor: an essential pre-mRNA splicing factor with a novel intranuclear distribution, *The EMBO journal 10*, 207-214.
319. Michaud, S., and Reed, R. (1993) A functional association between the 5' and 3' splice site is established in the earliest prespliceosome complex (E) in mammals, *Genes & development 7*, 1008-1020.

320. Hoffman, B. E., and Grabowski, P. J. (1992) U1 snRNP targets an essential splicing factor, U2AF65, to the 3' splice site by a network of interactions spanning the exon, *Genes & development 6*, 2554-2568.
321. Abovich, N., and Rosbash, M. (1997) Cross-intron bridging interactions in the yeast commitment complex are conserved in mammals, *Cell 89*, 403-412.
322. Wang, X., Bruderer, S., Rafi, Z., Xue, J., Milburn, P. J., Kramer, A., and Robinson, P. J. (1999) Phosphorylation of splicing factor SF1 on Ser20 by cGMP-dependent protein kinase regulates spliceosome assembly, *The EMBO journal 18*, 4549-4559.
323. MacMillan, A. M., McCaw, P. S., Crispino, J. D., and Sharp, P. A. (1997) SC35-mediated reconstitution of splicing in U2AF-depleted nuclear extract, *Proceedings of the National Academy of Sciences of the United States of America 94*, 133-136.
324. Fleckner, J., Zhang, M., Valcarcel, J., and Green, M. R. (1997) U2AF65 recruits a novel human DEAD box protein required for the U2 snRNP-branchpoint interaction, *Genes & development 11*, 1864-1872.
325. Bressan, G. C., Moraes, E. C., Manfiolli, A. O., Kuniyoshi, T. M., Passos, D. O., Gomes, M. D., and Kobarg, J. (2009) Arginine methylation analysis of the splicing-associated SR protein SFRS9/SRP30C, *Cellular & molecular biology letters 14*, 657-669.
326. Achsel, T., Brahms, H., Kastner, B., Bachi, A., Wilm, M., and Luhrmann, R. (1999) A doughnut-shaped heteromer of human Sm-like proteins binds to the 3'-end of U6 snRNA, thereby facilitating U4/U6 duplex formation in vitro, *The EMBO journal 18*, 5789-5802.
327. Charroux, B., Pellizzoni, L., Perkinson, R. A., Yong, J., Shevchenko, A., Mann, M., and Dreyfuss, G. (2000) Gemin4. A novel component of the SMN complex that is found in both gems and nucleoli, *The Journal of cell biology 148*, 1177-1186.
328. Carnegie, G. K., Sleeman, J. E., Morrice, N., Hastie, C. J., Peggie, M. W., Philp, A., Lamond, A. I., and Cohen, P. T. (2003) Protein phosphatase 4 interacts with the Survival of Motor Neurons complex and enhances the temporal localisation of snRNPs, *J Cell Sci 116*, 1905-1913.
329. Sendtner, M. (2001) Molecular mechanisms in spinal muscular atrophy: models and perspectives, *Current opinion in neurology 14*, 629-634.
330. Lorson, C. L., Strasswimmer, J., Yao, J. M., Baleja, J. D., Hahnen, E., Wirth, B., Le, T., Burghes, A. H., and Androphy, E. J. (1998) SMN oligomerization defect correlates with spinal muscular atrophy severity, *Nature genetics 19*, 63-66.
331. Mohaghegh, P., Rodrigues, N. R., Owen, N., Ponting, C. P., Le, T. T., Burghes, A. H., and Davies, K. E. (1999) Analysis of mutations in the tudor domain of the survival motor neuron protein SMN, *Eur J Hum Genet 7*, 519-525.
332. Selenko, P., Sprangers, R., Stier, G., Buhler, D., Fischer, U., and Sattler, M. (2001) SMN tudor domain structure and its interaction with the Sm proteins, *Nature structural biology 8*, 27-31.
333. Brahms, H., Meheus, L., de Brabandere, V., Fischer, U., and Luhrmann, R. (2001) Symmetrical dimethylation of arginine residues in spliceosomal Sm protein B/B' and the Sm-like protein LSm4, and their interaction with the SMN protein, *RNA (New York, N.Y 7*, 1531-1542.
334. Meister, G., and Fischer, U. (2002) Assisted RNP assembly: SMN and PRMT5 complexes cooperate in the formation of spliceosomal UsnRNPs, *The EMBO journal 21*, 5853-5863.

335. Bai, S. W., Herrera-Abreu, M. T., Rohn, J. L., Racine, V., Tajadura, V., Suryavanshi, N., Bechtel, S., Wiemann, S., Baum, B., and Ridley, A. J. Identification and characterization of a set of conserved and new regulators of cytoskeletal organization, cell morphology and migration, *BMC biology 9*, 54.
336. Zirwes, R. F., Eilbracht, J., Kneissel, S., and Schmidt-Zachmann, M. S. (2000) A novel helicase-type protein in the nucleolus: protein NOH61, *Molecular biology of the cell 11*, 1153-1167.
337. Zamecnik, P. C., Stephenson, M. L., Janeway, C. M., and Randerath, K. (1966) Enzymatic synthesis of diadenosine tetraphosphate and diadenosine triphosphate with a purified lysyl-sRNA synthetase, *Biochemical and biophysical research communications 24*, 91-97.
338. van Dijk, E. L., Schilders, G., and Pruijn, G. J. (2007) Human cell growth requires a functional cytoplasmic exosome, which is involved in various mRNA decay pathways, *RNA (New York, N.Y 13*, 1027-1035.
339. Benne, R., and Hershey, J. W. (1976) Purification and characterization of initiation factor IF-E3 from rabbit reticulocytes, *Proceedings of the National Academy of Sciences of the United States of America 73*, 3005-3009.
340. Trachsel, H., Erni, B., Schreier, M. H., and Staehelin, T. (1977) Initiation of mammalian protein synthesis. II. The assembly of the initiation complex with purified initiation factors, *Journal of molecular biology 116*, 755-767.
341. Niedzwiecka, A., Marcotrigiano, J., Stepinski, J., Jankowska-Anyszka, M., Wyslouch-Cieszynska, A., Dadlez, M., Gingras, A. C., Mak, P., Darzynkiewicz, E., Sonenberg, N., Burley, S. K., and Stolarski, R. (2002) Biophysical studies of eIF4E cap-binding protein: recognition of mRNA 5' cap structure and synthetic fragments of eIF4G and 4E-BP1 proteins, *Journal of molecular biology 319*, 615-635.
342. Nathan, C. O., Sanders, K., Abreo, F. W., Nassar, R., and Glass, J. (2000) Correlation of p53 and the proto-oncogene eIF4E in larynx cancers: prognostic implications, *Cancer research 60*, 3599-3604.
343. Petroulakis, E., Parsyan, A., Dowling, R. J., LeBacquer, O., Martineau, Y., Bidinosti, M., Larsson, O., Alain, T., Rong, L., Mamane, Y., Paquet, M., Furic, L., Topisirovic, I., Shahbazian, D., Livingstone, M., Costa-Mattioli, M., Teodoro, J. G., and Sonenberg, N. (2009) p53-dependent translational control of senescence and transformation via 4E-BPs, *Cancer cell 16*, 439-446.
344. Horton, L. E., Bushell, M., Barth-Baus, D., Tilleray, V. J., Clemens, M. J., and Hensold, J. O. (2002) p53 activation results in rapid dephosphorylation of the eIF4E-binding protein 4E-BP1, inhibition of ribosomal protein S6 kinase and inhibition of translation initiation, *Oncogene 21*, 5325-5334.
345. Constantinou, C., Elia, A., and Clemens, M. J. (2008) Activation of p53 stimulates proteasome-dependent truncation of eIF4E-binding protein 1 (4E-BP1), *Biology of the cell / under the auspices of the European Cell Biology Organization 100*, 279-289.
346. Joshi, B., Cameron, A., and Jagus, R. (2004) Characterization of mammalian eIF4E-family members, *European journal of biochemistry / FEBS 271*, 2189-2203.
347. Vladimirov, S. N., Ivanov, A. V., Karpova, G. G., Musolyamov, A. K., Egorov, T. A., Thiede, B., Wittmann-Liebold, B., and Otto, A. (1996) Characterization of the human small-ribosomal-subunit proteins by N-terminal and internal sequencing, and mass spectrometry, *European journal of biochemistry / FEBS 239*, 144-149.

348. Brooks, C. L., and Gu, W. (2006) p53 ubiquitination: Mdm2 and beyond, *Mol Cell 21*, 307-315.
349. Tsvetkov, P., Reuven, N., and Shaul, Y. Ubiquitin-independent p53 proteasomal degradation, *Cell death and differentiation 17*, 103-108.
350. Meulmeester, E., Pereg, Y., Shiloh, Y., and Jochemsen, A. G. (2005) ATM-mediated phosphorylations inhibit Mdmx/Mdm2 stabilization by HAUSP in favor of p53 activation, *Cell cycle (Georgetown, Tex 4*, 1166-1170.
351. Yuan, J., Luo, K., Zhang, L., Cheville, J. C., and Lou, Z. USP10 regulates p53 localization and stability by deubiquitinating p53, *Cell 140*, 384-396.
352. Yang, X., Fraser, M., Moll, U. M., Basak, A., and Tsang, B. K. (2006) Akt-mediated cisplatin resistance in ovarian cancer: modulation of p53 action on caspase-dependent mitochondrial death pathway, *Cancer research 66*, 3126-3136.
353. He, H., and Sun, Y. (2007) Ribosomal protein S27L is a direct p53 target that regulates apoptosis, *Oncogene 26*, 2707-2716.
354. Xiong, X., Zhao, Y., He, H., and Sun, Y. Ribosomal protein S27-like and S27 interplay with p53-MDM2 axis as a target, a substrate and a regulator, *Oncogene 30*, 1798-1811.
355. Goldberg, A. L. (2003) Protein degradation and protection against misfolded or damaged proteins, *Nature 426*, 895-899.
356. Kulikov, R., Letienne, J., Kaur, M., Grossman, S. R., Arts, J., and Blattner, C. Mdm2 facilitates the association of p53 with the proteasome, *Proceedings of the National Academy of Sciences of the United States of America 107*, 10038-10043.
357. Gorbea, C., Goellner, G. M., Teter, K., Holmes, R. K., and Rechsteiner, M. (2004) Characterization of mammalian Ecm29, a 26 S proteasome-associated protein that localizes to the nucleus and membrane vesicles, *The Journal of biological chemistry 279*, 54849-54861.
358. Chan, G. K., Jablonski, S. A., Starr, D. A., Goldberg, M. L., and Yen, T. J. (2000) Human Zw10 and ROD are mitotic checkpoint proteins that bind to kinetochores, *Nature cell biology 2*, 944-947.
359. Zuccolo, M., Alves, A., Galy, V., Bolhy, S., Formstecher, E., Racine, V., Sibarita, J. B., Fukagawa, T., Shiekhattar, R., Yen, T., and Doye, V. (2007) The human Nup107-160 nuclear pore subcomplex contributes to proper kinetochore functions, *The EMBO journal 26*, 1853-1864.
360. Ono, T., Losada, A., Hirano, M., Myers, M. P., Neuwald, A. F., and Hirano, T. (2003) Differential contributions of condensin I and condensin II to mitotic chromosome architecture in vertebrate cells, *Cell 115*, 109-121.
361. Moncalian, G., Cardenes, N., Deribe, Y. L., Spinola-Amilibia, M., Dikic, I., and Bravo, J. (2006) Atypical polyproline recognition by the CMS N-terminal Src homology 3 domain, *The Journal of biological chemistry 281*, 38845-38853.
362. Schiffer, M., Mundel, P., Shaw, A. S., and Bottinger, E. P. (2004) A novel role for the adaptor molecule CD2-associated protein in transforming growth factor-beta-induced apoptosis, *The Journal of biological chemistry 279*, 37004-37012.
363. Quesada, V., Diaz-Perales, A., Gutierrez-Fernandez, A., Garabaya, C., Cal, S., and Lopez-Otin, C. (2004) Cloning and enzymatic analysis of 22 novel human ubiquitin-specific proteases, *Biochemical and biophysical research communications 314*, 54-62.
364. Dupont, S., Mamidi, A., Cordenonsi, M., Montagner, M., Zacchigna, L., Adorno, M., Martello, G., Stinchfield, M. J., Soligo, S., Morsut, L., Inui, M., Moro, S., Modena, N.,

Argenton, F., Newfeld, S. J., and Piccolo, S. (2009) FAM/USP9x, a deubiquitinating enzyme essential for TGFbeta signaling, controls Smad4 monoubiquitination, *Cell 136*, 123-135.
365. Al-Hakim, A. K., Zagorska, A., Chapman, L., Deak, M., Peggie, M., and Alessi, D. R. (2008) Control of AMPK-related kinases by USP9X and atypical Lys(29)/Lys(33)-linked polyubiquitin chains, *Biochem J 411*, 249-260.
366. Cohen, P. T. (2002) Protein phosphatase 1--targeted in many directions, *J Cell Sci 115*, 241-256.
367. Li, H. H., Cai, X., Shouse, G. P., Piluso, L. G., and Liu, X. (2007) A specific PP2A regulatory subunit, B56gamma, mediates DNA damage-induced dephosphorylation of p53 at Thr55, *The EMBO journal 26*, 402-411.
368. Nakagawa, T., and Xiong, Y. X-linked mental retardation gene CUL4B targets ubiquitylation of H3K4 methyltransferase component WDR5 and regulates neuronal gene expression, *Mol Cell 43*, 381-391.
369. Petroski, M. D., and Deshaies, R. J. (2005) Function and regulation of cullin-RING ubiquitin ligases, *Nat Rev Mol Cell Biol 6*, 9-20.
370. Jin, J., Arias, E. E., Chen, J., Harper, J. W., and Walter, J. C. (2006) A family of diverse Cul4-Ddb1-interacting proteins includes Cdt2, which is required for S phase destruction of the replication factor Cdt1, *Mol Cell 23*, 709-721.
371. Furukawa, M., He, Y. J., Borchers, C., and Xiong, Y. (2003) Targeting of protein ubiquitination by BTB-Cullin 3-Roc1 ubiquitin ligases, *Nature cell biology 5*, 1001-1007.
372. Xie, Y., and Varshavsky, A. (2002) UFD4 lacking the proteasome-binding region catalyses ubiquitination but is impaired in proteolysis, *Nature cell biology 4*, 1003-1007.
373. Park, Y., Yoon, S. K., and Yoon, J. B. (2008) TRIP12 functions as an E3 ubiquitin ligase of APP-BP1, *Biochemical and biophysical research communications 374*, 294-298.
374. Park, Y., Yoon, S. K., and Yoon, J. B. (2009) The HECT domain of TRIP12 ubiquitinates substrates of the ubiquitin fusion degradation pathway, *The Journal of biological chemistry 284*, 1540-1549.
375. Jakel, S., Albig, W., Kutay, U., Bischoff, F. R., Schwamborn, K., Doenecke, D., and Gorlich, D. (1999) The importin beta/importin 7 heterodimer is a functional nuclear import receptor for histone H1, *The EMBO journal 18*, 2411-2423.
376. Muhlhausser, P., Muller, E. C., Otto, A., and Kutay, U. (2001) Multiple pathways contribute to nuclear import of core histones, *EMBO reports 2*, 690-696.
377. Bardoni, B., Castets, M., Huot, M. E., Schenck, A., Adinolfi, S., Corbin, F., Pastore, A., Khandjian, E. W., and Mandel, J. L. (2003) 82-FIP, a novel FMRP (fragile X mental retardation protein) interacting protein, shows a cell cycle-dependent intracellular localization, *Human molecular genetics 12*, 1689-1698.
378. Dolzhanskaya, N., Merz, G., Aletta, J. M., and Denman, R. B. (2006) Methylation regulates the intracellular protein-protein and protein-RNA interactions of FMRP, *J Cell Sci 119*, 1933-1946.
379. Shi, Y. (2009) Serine/threonine phosphatases: mechanism through structure, *Cell 139*, 468-484.
380. Takizawa, N., Mizuno, Y., Ito, Y., and Kikuchi, K. (1994) Tissue distribution of isoforms of type-1 protein phosphatase PP1 in mouse tissues and its diabetic alterations, *Journal of biochemistry 116*, 411-415.

381. Trinkle-Mulcahy, L., Andersen, J., Lam, Y. W., Moorhead, G., Mann, M., and Lamond, A. I. (2006) Repo-Man recruits PP1 gamma to chromatin and is essential for cell viability, *The Journal of cell biology 172*, 679-692.
382. Cohen, P. T., Philp, A., and Vazquez-Martin, C. (2005) Protein phosphatase 4--from obscurity to vital functions, *FEBS letters 579*, 3278-3286.
383. Zhang, X., Ozawa, Y., Lee, H., Wen, Y. D., Tan, T. H., Wadzinski, B. E., and Seto, E. (2005) Histone deacetylase 3 (HDAC3) activity is regulated by interaction with protein serine/threonine phosphatase 4, *Genes & development 19*, 827-839.
384. Gilmore, T. D. (2006) Introduction to NF-kappaB: players, pathways, perspectives, *Oncogene 25*, 6680-6684.
385. Hu, M. C., Tang-Oxley, Q., Qiu, W. R., Wang, Y. P., Mihindukulasuriya, K. A., Afshar, R., and Tan, T. H. (1998) Protein phosphatase X interacts with c-Rel and stimulates c-Rel/nuclear factor kappaB activity, *The Journal of biological chemistry 273*, 33561-33565.
386. Yang, J., Fan, G. H., Wadzinski, B. E., Sakurai, H., and Richmond, A. (2001) Protein phosphatase 2A interacts with and directly dephosphorylates RelA, *The Journal of biological chemistry 276*, 47828-47833.
387. Miyamoto, S. Nuclear initiated NF-kappaB signaling: NEMO and ATM take center stage, *Cell research 21*, 116-130.
388. Ruland, J. Return to homeostasis: downregulation of NF-kappaB responses, *Nature immunology 12*, 709-714.
389. Karin, M. (1999) How NF-kappaB is activated: the role of the IkappaB kinase (IKK) complex, *Oncogene 18*, 6867-6874.
390. May, M. J., D'Acquisto, F., Madge, L. A., Glockner, J., Pober, J. S., and Ghosh, S. (2000) Selective inhibition of NF-kappaB activation by a peptide that blocks the interaction of NEMO with the IkappaB kinase complex, *Science (New York, N.Y 289*, 1550-1554.
391. Yamamoto, Y., Kim, D. W., Kwak, Y. T., Prajapati, S., Verma, U., and Gaynor, R. B. (2001) IKKgamma /NEMO facilitates the recruitment of the IkappaB proteins into the IkappaB kinase complex, *The Journal of biological chemistry 276*, 36327-36336.
392. Bosu, D. R., and Kipreos, E. T. (2008) Cullin-RING ubiquitin ligases: global regulation and activation cycles, *Cell division 3*, 7.
393. Pickart, C. M., and Fushman, D. (2004) Polyubiquitin chains: polymeric protein signals, *Current opinion in chemical biology 8*, 610-616.
394. Trachtulec, Z., Hamvas, R. M., Forejt, J., Lehrach, H. R., Vincek, V., and Klein, J. (1997) Linkage of TATA-binding protein and proteasome subunit C5 genes in mice and humans reveals synteny conserved between mammals and invertebrates, *Genomics 44*, 1-7.
395. Tamura, T., Lee, D. H., Osaka, F., Fujiwara, T., Shin, S., Chung, C. H., Tanaka, K., and Ichihara, A. (1991) Molecular cloning and sequence analysis of cDNAs for five major subunits of human proteasomes (multi-catalytic proteinase complexes), *Biochimica et biophysica acta 1089*, 95-102.
396. Hoffman, L., and Rechsteiner, M. (1997) Molecular cloning and expression of subunit 9 of the 26S proteasome, *FEBS letters 404*, 179-184.
397. Collins, G. A., and Tansey, W. P. (2006) The proteasome: a utility tool for transcription?, *Current opinion in genetics & development 16*, 197-202.
398. Laribee, R. N., Fuchs, S. M., and Strahl, B. D. (2007) H2B ubiquitylation in transcriptional control: a FACT-finding mission, *Genes & development 21*, 737-743.

399. Ratner, J. N., Balasubramanian, B., Corden, J., Warren, S. L., and Bregman, D. B. (1998) Ultraviolet radiation-induced ubiquitination and proteasomal degradation of the large subunit of RNA polymerase II. Implications for transcription-coupled DNA repair, *The Journal of biological chemistry 273*, 5184-5189.
400. Maniatis, T. (1999) A ubiquitin ligase complex essential for the NF-kappaB, Wnt/Wingless, and Hedgehog signaling pathways, *Genes & development 13*, 505-510.
401. Stommel, J. M., and Wahl, G. M. (2004) Accelerated MDM2 auto-degradation induced by DNA-damage kinases is required for p53 activation, *The EMBO journal 23*, 1547-1556.
402. Fang, S., Jensen, J. P., Ludwig, R. L., Vousden, K. H., and Weissman, A. M. (2000) Mdm2 is a RING finger-dependent ubiquitin protein ligase for itself and p53, *The Journal of biological chemistry 275*, 8945-8951.
403. Fuchs, S. Y., Adler, V., Buschmann, T., Wu, X., and Ronai, Z. (1998) Mdm2 association with p53 targets its ubiquitination, *Oncogene 17*, 2543-2547.
404. Reyes-Turcu, F. E., Ventii, K. H., and Wilkinson, K. D. (2009) Regulation and cellular roles of ubiquitin-specific deubiquitinating enzymes, *Annual review of biochemistry 78*, 363-397.
405. Bernardi, R., and Pandolfi, P. P. (2003) Role of PML and the PML-nuclear body in the control of programmed cell death, *Oncogene 22*, 9048-9057.
406. Guo, A., Salomoni, P., Luo, J., Shih, A., Zhong, S., Gu, W., and Pandolfi, P. P. (2000) The function of PML in p53-dependent apoptosis, *Nature cell biology 2*, 730-736.
407. Hofmann, T. G., Moller, A., Sirma, H., Zentgraf, H., Taya, Y., Droge, W., Will, H., and Schmitz, M. L. (2002) Regulation of p53 activity by its interaction with homeodomain-interacting protein kinase-2, *Nature cell biology 4*, 1-10.
408. Li, M., Chen, D., Shiloh, A., Luo, J., Nikolaev, A. Y., Qin, J., and Gu, W. (2002) Deubiquitination of p53 by HAUSP is an important pathway for p53 stabilization, *Nature 416*, 648-653.
409. Wu, W. S., Xu, Z. X., Hittelman, W. N., Salomoni, P., Pandolfi, P. P., and Chang, K. S. (2003) Promyelocytic leukemia protein sensitizes tumor necrosis factor alpha-induced apoptosis by inhibiting the NF-kappaB survival pathway, *The Journal of biological chemistry 278*, 12294-12304.
410. Vernier, M., Bourdeau, V., Gaumont-Leclerc, M. F., Moiseeva, O., Begin, V., Saad, F., Mes-Masson, A. M., and Ferbeyre, G. Regulation of E2Fs and senescence by PML nuclear bodies, *Genes & development 25*, 41-50.
411. Regad, T., Bellodi, C., Nicotera, P., and Salomoni, P. (2009) The tumor suppressor Pml regulates cell fate in the developing neocortex, *Nature neuroscience 12*, 132-140.
412. Asano, K., Merrick, W. C., and Hershey, J. W. (1997) The translation initiation factor eIF3-p48 subunit is encoded by int-6, a site of frequent integration by the mouse mammary tumor virus genome, *The Journal of biological chemistry 272*, 23477-23480.
413. Chevillard-Briet, M., Trouche, D., and Vandel, L. (2002) Control of CBP co-activating activity by arginine methylation, *The EMBO journal 21*, 5457-5466.
414. Covic, M., Hassa, P. O., Saccani, S., Buerki, C., Meier, N. I., Lombardi, C., Imhof, R., Bedford, M. T., Natoli, G., and Hottiger, M. O. (2005) Arginine methyltransferase CARM1 is a promoter-specific regulator of NF-kappaB-dependent gene expression, *The EMBO journal 24*, 85-96.

415. Cohen, N., Sharma, M., Kentsis, A., Perez, J. M., Strudwick, S., and Borden, K. L. (2001) PML RING suppresses oncogenic transformation by reducing the affinity of eIF4E for mRNA, *The EMBO journal 20*, 4547-4559.
416. Rosettani, P., Knapp, S., Vismara, M. G., Rusconi, L., and Cameron, A. D. (2007) Structures of the human eIF4E homologous protein, h4EHP, in its m7GTP-bound and unliganded forms, *Journal of molecular biology 368*, 691-705.
417. Besson, V., Brault, V., Duchon, A., Togbe, D., Bizot, J. C., Quesniaux, V. F., Ryffel, B., and Herault, Y. (2007) Modeling the monosomy for the telomeric part of human chromosome 21 reveals haploinsufficient genes modulating the inflammatory and airway responses, *Human molecular genetics 16*, 2040-2052.
418. Janes, K. A., Gaudet, S., Albeck, J. G., Nielsen, U. B., Lauffenburger, D. A., and Sorger, P. K. (2006) The response of human epithelial cells to TNF involves an inducible autocrine cascade, *Cell 124*, 1225-1239.
419. Tili, E., Michaille, J. J., Wernicke, D., Alder, H., Costinean, S., Volinia, S., and Croce, C. M. Mutator activity induced by microRNA-155 (miR-155) links inflammation and cancer, *Proceedings of the National Academy of Sciences of the United States of America 108*, 4908-4913.
420. Kerppola, T. K. (2008) Bimolecular fluorescence complementation (BiFC) analysis as a probe of protein interactions in living cells, *Annual review of biophysics 37*, 465-487.
421. Kerppola, T. K. (2006) Complementary methods for studies of protein interactions in living cells, *Nature methods 3*, 969-971.
422. Kerppola, T. K. (2006) Design and implementation of bimolecular fluorescence complementation (BiFC) assays for the visualization of protein interactions in living cells, *Nature protocols 1*, 1278-1286.
423. Pawlak, M. R., Banik-Maiti, S., Pietenpol, J. A., and Ruley, H. E. (2002) Protein arginine methyltransferase I: substrate specificity and role in hnRNP assembly, *Journal of cellular biochemistry 87*, 394-407.
424. Sharp, J. L., Anderson, K. K., Hurst, G. B., Daly, D. S., Pelletier, D. A., Cannon, W. R., Auberry, D. L., Schmoyer, D. D., McDonald, W. H., White, A. M., Hooker, B. S., Victry, K. D., Buchanan, M. V., Kery, V., and Wiley, H. S. (2007) Statistically inferring protein-protein associations with affinity isolation LC-MS/MS assays, *Journal of proteome research 6*, 3788-3795.
425. Edwards, A. M., Kus, B., Jansen, R., Greenbaum, D., Greenblatt, J., and Gerstein, M. (2002) Bridging structural biology and genomics: assessing protein interaction data with known complexes, *Trends Genet 18*, 529-536.
426. Gingras, A. C., Aebersold, R., and Raught, B. (2005) Advances in protein complex analysis using mass spectrometry, *The Journal of physiology 563*, 11-21.
427. Pillai, R. S., Will, C. L., Luhrmann, R., Schumperli, D., and Muller, B. (2001) Purified U7 snRNPs lack the Sm proteins D1 and D2 but contain Lsm10, a new 14 kDa Sm D1-like protein, *The EMBO journal 20*, 5470-5479.
428. de Boer, E., Rodriguez, P., Bonte, E., Krijgsveld, J., Katsantoni, E., Heck, A., Grosveld, F., and Strouboulis, J. (2003) Efficient biotinylation and single-step purification of tagged transcription factors in mammalian cells and transgenic mice, *Proceedings of the National Academy of Sciences of the United States of America 100*, 7480-7485.
429. van Dijk, T. B., Gillemans, N., Stein, C., Fanis, P., Demmers, J., van de Corput, M., Essers, J., Grosveld, F., Bauer, U. M., and Philipsen, S. Friend of Prmt1, a novel

chromatin target of protein arginine methyltransferases, *Molecular and cellular biology 30*, 260-272.
430. Dziembowski, A., and Seraphin, B. (2004) Recent developments in the analysis of protein complexes, *FEBS letters 556*, 1-6.
431. Selbach, M., and Mann, M. (2006) Protein interaction screening by quantitative immunoprecipitation combined with knockdown (QUICK), *Nature methods 3*, 981-983.
432. Boisvert, F. M., Cote, J., Boulanger, M. C., and Richard, S. (2003) A proteomic analysis of arginine-methylated protein complexes, *Mol Cell Proteomics 2*, 1319-1330.
433. Rickles, R. J., Botfield, M. C., Weng, Z., Taylor, J. A., Green, O. M., Brugge, J. S., and Zoller, M. J. (1994) Identification of Src, Fyn, Lyn, PI3K and Abl SH3 domain ligands using phage display libraries, *The EMBO journal 13*, 5598-5604.

Appendix

Experimental Details

Construction of mCitrineN- or mCitrineC-tagged PRMTs in pET28a. The mCitrineN and mCitrineC were PCR-amplified from a plasmid contained mCitrine gene (*135*). *NdeI* and *BamHI* sites were constructed at the ends of mCitrineN, and *XhoI* site was constructed at both ends of mCitrineC. Both amplicons were digested with the proper restriction enzymes and inserted in pET28a vectors. The *XhoI* site downstream to the mCitrineC gene in the pET28a vector was deleted by site directed mutagenesis. PRMT1, PRMT2, and ΔSH3PRMT2 were PCR-amplified from vectors contained the PRMT1 and -2 genes (*9*) with primers containing *BamHI* and *XhoI* sites at the 5' ends. The amplified PRMT genes were digested and inserted into the *BamHI* and *XhoI* sites of the previously described constructs pET28a-mCitrineN or pET28a-mCitrineC (*135*).

Construction of full length mCitrine-tagged PRMTs in pcDNA3.1(+)/Hygro. The mCitrine gene was PCR-amplified from a plasmid containing the mCitrine gene (*135*) using primers flanked with *NdeI* and *BamHI* sites. The amplicon was digested with *NdeI* and *BamHI* and inserted into a pET28a vector. PRMT1, PRMT2, and ΔSH3PRMT2 were PCR-amplified from vectors containing the PRMT1 and -2 genes (*9*) with primers containing *BamHI* and *XhoI* sites at the 5' ends. The amplified PRMT genes were digested and inserted into the *BamHI* and *XhoI* sites of pET28a-mCitrine. The full-length mCitrine-tagged PRMT genes were then amplified with primers flanked with *HindIII* and *XhoI*. The amplicons were digested with *HindIII* and *XhoI* and ligated into pcDNA3.1(+)/Hygro.

BiFC assays for visualization of interactions among PRMT1 splice variants. The mCitrineN- or mCitrineC-tagged PRMT1 splice variants were constructed as described in section 2.2. BiFC assays for visualization of interactions among PRMT1 splice variants and for capturing PRMT1 and -6 interaction were performed in HeLa cells as described in section 2.2.

Western blotting. For western blotting, samples were separated on 10% SDS-PAGE gels and transferred to nitrocellulose membranes. The membranes were blocked with 5% TBS-milk solution at 37°C for 2 h, and blotted with the proper antibodies in 3% TBS-milk solution per the manufacturer's suggested dilution at 4°C for 16 h. In order to blot for β-actin, anti-actin antibody (Santa Cruz Biotechnology; 1-19) was used. For detection, goat anti-mouse horseradish peroxidase-conjugated antibody (Santa Cruz Biotechnology) and ECL Western blotting detection reagents (GE Healthcare) were used. We noticed that the anti-PRMT1 antibody we used cannot readily detect mCitrineN-tagged PRMT1, and the anti-PRMT2 antibody we used cannot detect ΔSH3PRMT2 because it was raised against a sequence within the SH3 domain. The anti-PRMT1 and anti-PRMT2 antibodies may recognize the tagged wild type and mutant PRMTs to a different extend than they do for untagged PRMTs. Therefore, the Western blots presented here only illustrate the successful expression, but not the level of expression, of mCitrineC-tagged PRMT1 and its mutants, as well as mCitrineN-PRMT2, mCitrineN-PRMT2E220Q, and mCitrineN-PRMT2Δ256-294.

In order to detect arginine methylation via Western blotting, 20 μg cell lysate protein from each sample (HeLa cells transfected as described in section 2.2) was separated on a 15% SDS-PAGE gel by electrophoresis and transferred to nitrocellulose membranes. The membranes were blocked with 5% TBS-milk solution at 37°C for 2 h, and blotted separately with anti-aDMA antibody (39231, Active Motif), anti-H4R3me2a antibody (39705, Active Motif), anti-

histone H4 antibody (sc-8658-R, Santa Cruz Biotechnology), anti-c-Myc antibody (9E10, Sigma), and anti-HA antibody (HA-7, Sigma) in 3% TBST-milk solution per the manufacturer's suggested dilution at 4 °C for 16 h. Goat anti-mouse IgG HRP secondary antibody (sc-2005, Santa Cruz Biotechnology), goat anti-rabbit IgG HRP secondary antibody (sc-2030, Santa Cruz Biotechnology), and ECL Western blotting detection reagents (GE Healthcare) were used for protein visualization.

Immunofluorescence and confocal microscopy. HeLa cells were transiently co-transfected with 12 μg of pcDNA3.1(+)/Neo-mCitrine-PRMT2 or pcDNA3.1(+)/Neo-mCitrine-ΔSH3PRMT2 and 12 μg of pcDNA3.1(+)/Neo-HA-PRMT1 or pcDNA3.1(+)/Neo-E153Q using Lipofectamine 2000 (Invitrogen) per the manufacturer's instructions. The immunofluorescence experiment was performed as described in section 3.2 using an anti-Sam68 antibody (Santa Cruz) and an anti-HA antibody, then with an Alexa Fluor 546-conjugated goat anti-rabbit secondary antibody (Invitrogen) and an Alexa Fluor 647-conjugated goat anti-mouse secondary antibody (Invitrogen). Subsequently, the cells were stained with 50 nM DAPI. Cell images were captured using a FluoView FV10i confocal microscope (Olympus) with an oil lens at 60x magnification, and were processed with ImageJ software (NIH image).

Appendix Tables

Table A.1. PCR primers. DNA primer sequences with corresponding restriction sites (underlined sequences) are listed.

Construct	Primers (5' – 3')	Restriction Site
PRMT1	Forward: CGGGATCCATGGCGGCAGCCGAGGCCGCGAACTGC	*BamHI*
	Reverse with stop codon: CCGCTCGAGTCAGCGCATCCGGTAGTCGGTGGAAC	*XhoI*
	Reverse without stop codon: CCGCTCGAGGCGCATCCGGTAGTCGGTGGAAC	*XhoI*
PRMT2	Forward: CGGGATCCATGGCAACATCAGGTGACTGTCCC	*BamHI*
	Reverse with stop codon: CCGCTCGAGTCATCTCCAGATGGGGAAGACTTTTTCTCC	*XhoI*
	Reverse without stop codon: CCGCTCGAGTCTCCAGATGGGGAAGACTTTTTCTCC	*XhoI*
ΔSH3PRMT2	Forward: CCGGGATCCCATGTGGGGAAGCACGTGGATGAG	*BamHI*
	Reverse with stop codon: CCGCTCGAGTCATCTCCAGATGGGGAAGACTTTTTCTCC	*XhoI*
	Reverse without stop codon: CCGCTCGAGTCTCCAGATGGGGAAGACTTTTTCTCC	*XhoI*
mCitrineN	Forward: GGGAATTCCATATGATGGTGAGCAAGGGCGAGGAGCTGTTCACCGGGG	*NdeI*
	Forward: CCCAAGCTTATGGTGAGCAAGGGCGAGGAGCTGTTCACCGGGG	*HindIII*
	Reverse: CGCGGATCCGCTGCCGCCGCCGCCCTCGATGTTGTGGCGGATCTTGAAGTTCACC	*BamHI*
mCitrineC	Forward: CCGCTCGAGGGCGGCGGCGGCAGCGACGGCAGCGTGCAGCTCGCCGACCACTACC	*XhoI*
	Reverse: CCGCTCGAGTCACTTGTACAGCTCGTCCATGCCGAGAGTGATCCC	*XhoI*
HA	Forward: pCTAGCACCATGTACCCATACGATGTTCCAGATTACGCTACG	*NheI*
	Reverse: pCTAGCGTAGCGTAATCTGGAACATCGTATGGGTACATGGTG	*NheI*
c-Myc	Forward: pCTAGCACCATGGAACAAAAGCTGATTAGCGAAGAGGACCTGACG	*NheI*
	Reverse: pCTAGCGTCAGGTCCTCTTCGCTAATCAGCTTTTGTTCCATGGTG	*NheI*

Table A.2. Site-directed mutagenesis primers. Primers for generating PRMT mutants are listed (only one primer is shown for primer pairs used in QuikChange). Bolded nucleotides indicate mutated sites.

Construct	Primers (5' – 3')
PRMT1E153Q	GGTTATTGCCTCTTCTAT**C**AGTCCATGCTCAACACTGTGC
PRMT2E220Q	GCTGTTT**C**AGTTCATGATCGAGTCCATCCTGTATGC
PRMT1Δ188-222	CCTGTATGTGACAGCCATTGAGGACGACCCAAAGCAGCTGGTCACCAACG
PRMT2Δ256-294	GCACCTTGTGCCCTGCAGTGCTGATAAACCAGAAGACTGTCTCTCTGAAC
Histone H4 R3K	GGAGATATACATATGTCTGGTA**A**GGGTAAAGGTGGTAAAGGTCTGG
pET-41a (+)	GTGGTGGCGACCATCCTCCA**TTA**AAATCGGATGGTTCAACTAG

Table A.3. Summary of biological functions of identified PRMT binders. The PRMT-associated proteins identified in the proteomic study have been listed (general annotation from UniProt database). The identified PRMT1-associated proteins are highlighted in *yellow*. The identified PRMT2-associated proteins are highlighted in *green*. Proteins interact with both PRMTs are highlighted in *blue*. The protein scores for each identified hit in the sample duplicates are listed in the order of scores for the PRMT1 duplicate(s) followed by scores for the PRMT2 duplicate(s). The scores for the proteins that were not identified in a particular sample are indicated as (-). The scores for the insignificant hits are shown in *red*.

Gene Name	Protein Name	Protein Scores
DNA replication		
*HMGA1**	High mobility group protein HMG-I/HMG-Y	38;38;-;-
MCM7	DNA replication licensing factor MCM7	-;-;43;47
C10orf119	Mini-chromosome maintenance complex-binding protein	157;154;41;64
RFC5	Replication factor C subunit 1	179;-;50;45
MCM4	DNA replication licensing factor MCM4	87;-;75;47
WRNIP1	ATPase WRNIP1	77;28;44;45
Transcription		
GTF2H5	General transcription factor IIH subunit 5	87;62;-;-
S100A4	Protein S100-A4	38;39;-;-
*HMGA1**	High mobility group protein HMG-I/HMG-Y	38;38;-;-
PRMT2	Protein arginine N-methyltransferase 2	-;-;79;236
FHL2	Four and a half LIM domains protein 2	-;-;46;62
RFC5	Replication factor C subunit 1	179;-;75;45
LRRFIP1	Leucine-rich repeat flightless-interacting protein 1	79;115;74;29
ACTL6A	Actin-like protein 6A	98;102;88;58
IKBKG	NF-kappa-B essential modulator	71;49;-;94
TAF15	TATA-binding protein-associated factor 2N	109;73;-;39
CDYL	Chromodomain Y-like protein	104;61;-;80
CARM1	Protein arginine N-methyltransferase 4	71;43;42;73
DRG1	Developmentally-regulated GTP-binding protein 1	82;-;74;42
PML	Promyelocytic leukemia protein	40;-;39;56
CNBP	Cellular nucleic acid-binding protein	38;-;71;47
TRIP6	Thyroid receptor-interacting protein 6	72;40;57;48
FRYL	Protein furry homolog-like	-;-;46;43
OASL	59 kDa 2'-5'-oligoadenylate synthase-like protein	231;62;103;26
p53-mediated Transcriptional Regulation		
RPS27L	40S ribosomal protein S27-like	43;39;-;-
PSMB1	Proteasome subunit beta type-1	67;60;-;-
USP10	Ubiquitin carboxyl-terminal hydrolase 10	-;-;41;55
DIABLO	Diablo homolog, mitochondrial	-;-;49;43
PSMA4	Proteasome subunit alpha type-4	61;62;59;81
PSMD11	26S proteasome non-ATPase regulatory subunit 11	51;47;60;-
Other proteins involving in cell cycle, cell division, and mitosis		
KNTC1	Kinetochore-associated protein 1	39;35;-;-
NUP43	Nucleoporin Nup43	49;49;-;-
NCAPD3	Condensin-2 complex subunit D3	128;47;105;89
CD2AP	CD2-associated protein	-;55;49;41
RNA processing		
mRNA processing		
U2AF2	Splicing factor U2AF 65 kDa subunit	42;46;-;-
LSM5	U6 snRNA-associated Sm-like protein LSm5	53;31;-;-
SFRS2	Serine/arginine-rich splicing factor 2	137;67;-;-
GEMIN4	Component of gems 4	111;-;58;77
PPP4R1	Serine/threonine-protein phosphatase 4 regulatory subunit 1	60;38;75;48
BAT1	Spliceosome RNA helicase DDX39B	61;29;52;29
PRPF40A	Pre-mRNA-processing factor 40	42;32;60;-
rRNA processing		
DDX56	Probable ATP-dependent RNA helicase DDX56	83;70;80;85
tRNA processing		
KARS	Lysyl-tRNA synthetase	55;38;53;-
RNA degradation		
EXOSC4	Exosome complex component RRP41	40;68;-;-

Table A.3 continue

Translation		
Initiation		
EIF3I	Eukaryotic translation initiation factor 3 subunit I	45;67;69;68
EIF4E2	Eukaryotic translation initiation factor 4E type 2	50;41;-;43
Elongation and termination		
RPS20	40S ribosomal protein S20	71;36;-;-
Post-translational modification		
Arginine methylation		
PRMT2	Protein arginine N-methyltransferase 2	-;-;79;236
CARM1	Protein arginine N-methyltransferase 4	71;43;42;73
Phosphorlation		
CDC42BPB	Serine/threonine-protein kinase MRCK beta	52;47;47;-
Dephosphorylation		
PPP1CC	Serine/threonine-protein phosphatase PP1-gamma catalytic subunit	89;100;115;155
PPP2R2A	Serine/threonine-protein phosphatase 2A 55 kDa regulatory subunit B alpha isoform	135;53;103;59
PPP4R1	Serine/threonine-protein phosphatase 4 regulatory subunit 1	60;38;75;29
Ubiquitination		
WDR68	DDB1- and CUL4-associated factor 7	41;61;-;-
GAN	Gigaxonin	-;-;53;36
TRIP12	Probable E3 ubiquitin-protein ligase TRIP12	170;160;40;197
FBXO30	F-box only protein 30	102;134;70;-
CUL4B	Cullin-4B	93;-;65;67
Deubiquitination		
USP10	Ubiquitin carboxyl-terminal hydrolase 10	-;-;41;55
USP24	Ubiquitin carboxyl-terminal hydrolase 24	254;119;126;266
USP9X	Probable ubiquitin carboxyl-terminal hydrolase FAF-X	47;-;109;48
Non-ubiquitin-dependent protein catabolic process		
ECM29	Proteasome-associated protein ECM29 homolog	211;-;378;157
Protein folding		
PFDN2	Prefoldin subunit 2	43;50;-;-
SGTA	Small glutamine-rich tetratricopeptide repeat-containing protein alpha	45;30;-;-
PFDN1	Prefoldin subunit 1	-;86;46;106
MDN1	Midasin	96;-;35;66
PRKCSH	Glucosidase 2 subunit beta	68;55;56;-
Protein transport		
Nucleus-cytoplasm transport		
NUP43	Nucleoporin Nup43	49;49;-;-
IPO7	Importin-7	36;35;-;-
XPO7	Exportin-7	-;-;81;65
KPNA6	Importin subunit alpha-7	114;56;232;127
NUP205	Nuclear pore complex protein Nup205	37;-;84;78
ER-Golgi transport		
RAB1B	Ras-related protein Rab-1B	-;-;65;68
SEC24C	Protein transport protein Sec24C	-;-;57;38
SEC23B	Protein transport protein Sec23B	41;36;-;169
TRAPPC1	Trafficking protein particle complex subunit 1	64;32;-;97
SEC24A	Protein transport protein Sec24A	47;49;-;57
Endocytosis		
SH3GL1	Endophilin-A2	-;-;36;93
RUFY1	RUN and FYVE domain-containing protein 1	67;-;133;54
Endosome transport		
VPS28	Vacuolar protein sorting-associated protein 28 homolog	-;-;63;40
Polarized transport		
RAB13	Ras-related protein Rab-13	39;39;35;-
Actin binding		
BAIAP2L1	Brain-specific angiogenesis inhibitor 1-associated protein 2-like protein 1	-;-;88;69
TPM3L	Putative tropomyosin alpha-3 chain-like protein	78;74;-;89
SPTAN1	Spectrin alpha chain, brain	46;-;58;73
CFL1	Cofilin-1	55;-;76;44

Table A.3 continue

Metabolic pathways		
Glycolysis		
TPI1	Triosephosphate isomerase	83;71;229;76
PGAM1	Phosphoglycerate mutase 1	39;-;85;41
Tricarboxylic acid cycle		
SDHA	Succinate dehydrogenase [ubiquinone] flavoprotein subunit, mitochondrial	63;31;98;87
Creatine metabolic process		
CKB	Creatine kinase B-type	47;-;127;57
Diphosphate metabolia process		
PPA1	Inorganic pyrophosphatase	122;102;41;137
Lipid Transport		
APOL2	Apolipoprotein L2	94;-;92;98
APOA1	Apolipoprotein A-I	46;61;52;69
Lipid catabolic process		
AZGP1	Zinc-alpha-2-glycoprotein	82;77;-;-
ATPase		
ATP6V1G1	V-type proton ATPase subunit G 1	-;-;54;64
ATP6V1D	V-type proton ATPase subunit D	62;-;72;110
Nucleotide catabolic process		
GDA	Guanine deaminase	117;56;-;-
UPP1	Uridine phosphorylase 1	43;-;60;58
Nucleotide metabolic process		
ITPA	Inosine triphosphate pyrophosphatase	71;-;56;48
Nucleotide biosynthesis		
UCKL1	Uridine-cytidine kinase-like 1	54;-;62;40
Nucleotide-sugar biosynthesis		
GMDS	GDP-mannose 4,6 dehydratase	80;-;72;52
GMPPA	Mannose-1-phosphate guanyltransferase alpha	57;26;66;48
Fructose biosynthesis		
SORD	Sorbitol dehydrogenase	38;25;-;37
Molybdenum cofactor biosynthesis		
MOCS2	Molybdopterin synthase sulfur carrier subunit	68;66;-;57
Other proteins		
GTPase binding		
TBC1D9B	TBC1 domain family member 9B	-;-;49;46
TUBAL3	Tubulin alpha chain-like 3	85;54;54;84
RNA binding		
NUFIP2	Nuclear fragile X mental retardation-interacting protein 2	73;91;-;82
Protein binding		
BRP16L	Protein FAM203B	-;-;48;35
WDR61	WD repeat-containing protein 61	78;74;43;107
S100P	Protein S100-P	90;56;-;107
Immune response		
IGLC1	Ig lambda-1 chain C regions	101;138;-;-
DEFA1	Neutrophil defensin 1	37;35;-;-
LRBA	Lipopolysaccharide-responsive and beige-like anchor protein	59;34;54;-
Miscellaneous		
KRT81	Keratin, type II cuticular Hb1	46;77;-;-
GSR	Glutathione reductase, mitochondrial	81;39;-;-
ISOC1	Isochorismatase domain-containing protein 1	41;65;62;-
DPYSL2	Dihydropyrimidinase-related protein 2	112;105;48;60
MYL6	Myosin light polypeptide 6	72;63;53;71
KCTD3	BTB/POZ domain-containing protein KCTD3	81;61;-;58
FLG	Filaggrin-2	54;58;35;45
KTU	Protein kintoun	45;58;34;49
* Proteins identified as arginine methylated		

Appendix Figures

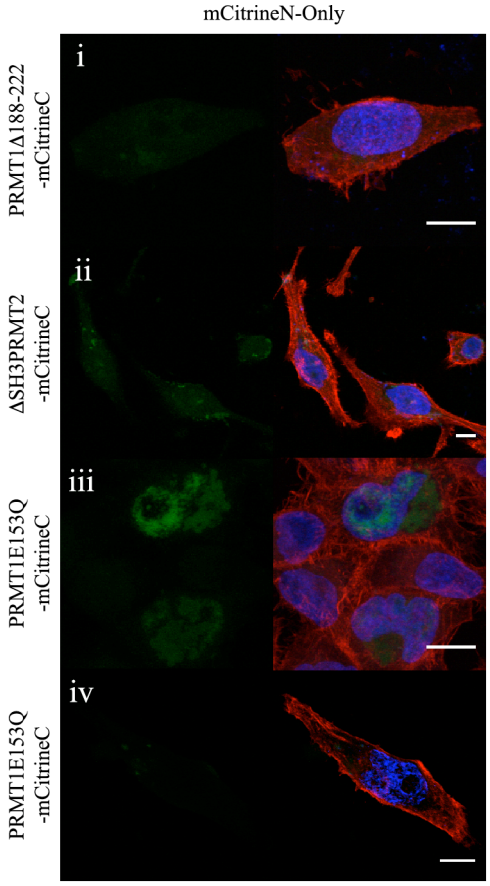

Figure A.1. Negative controls for BiFC. HeLa cells were co-transfected with the two constructs indicated in the column and rows (representative images are shown). The laser input used for (i), (ii), and (iii) was 14.1%. The PRMT1E153Q-mCitrineC construct yield a high background signal at 14.1% laser input (iii). Therefore, the laser input used for generating images of cells co-transfected with PRMT1E153Q-mCitrineC construct was reduced by half to 7.2%. The left image of each group shows the formation of a BiFC complex as *green* fluorescence. The right image of each group shows an overlay of BiFC (*green*), DAPI (*blue*), and fluorescence-labeled phalloidin (*red*). The bar indicates 10 μm.

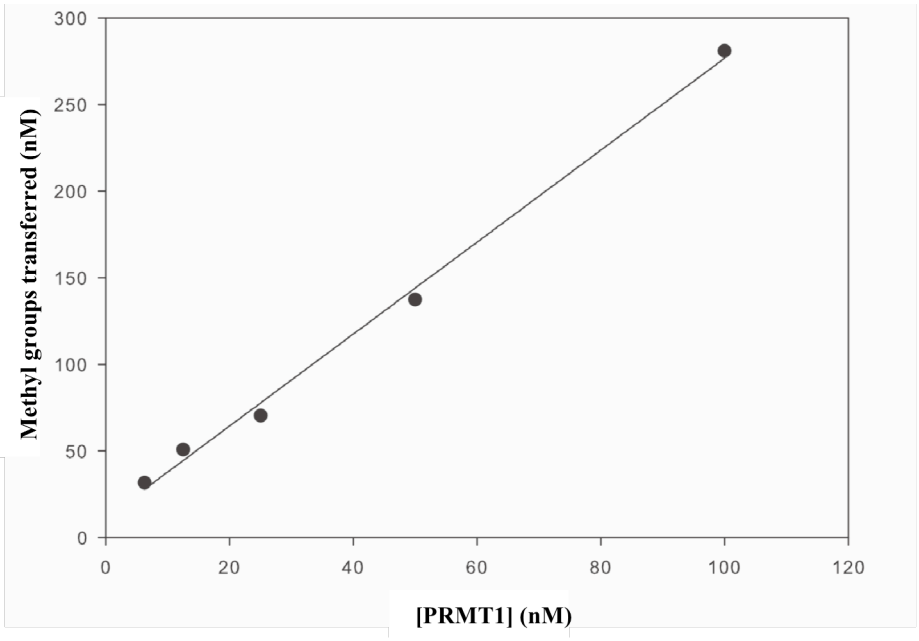

Figure A.2. The concentration of total methyl groups produced with increasing enzyme. Shown is a linear increase in methylarginine formation with increasing PRMT1 concentrations. PRMT1 at 6.25, 12.5, 25, 50, and 100 nM with constant 250 nM histone H4 and 120 µM AdoMet concentrations were incubated at 37 °C in methylation buffer for 1 h. Reactions were terminated at 90 °C for 10-min. Values are determined using UPLC MS/MS as described in section 2.2. Total methylation was summed using the equation (2aDMA+MMA).

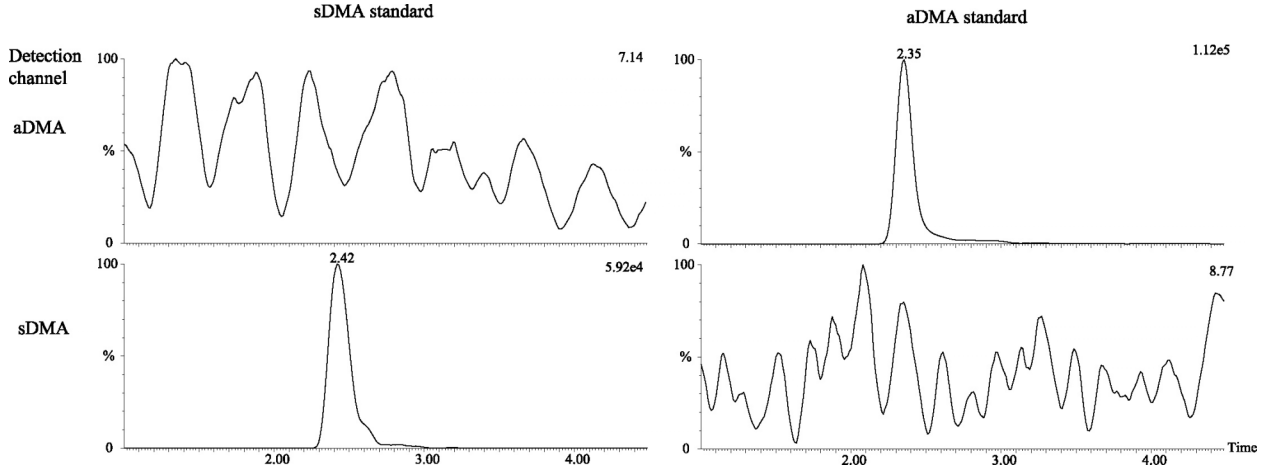

Figure A.3. Measurements of aDMA and sDMA via tandem mass spectrometry. Detection of 5.0 μM sDMA (*left*) and 5.0 μM aDMA (*right*) standards using parent ion 203 m/z and fragment ions 172 m/z and 46 m/z, respectively, are displayed in the chromatograms for the aDMA channel (*top*) and sDMA channel (*bottom*). Using this method aDMA and sDMA can be simultaneously and unambiguously detected without the need for derivatization or extended chromatographic run times. For relative intensities are listed in the upper right corner of each chromatogram in arbitrary units.

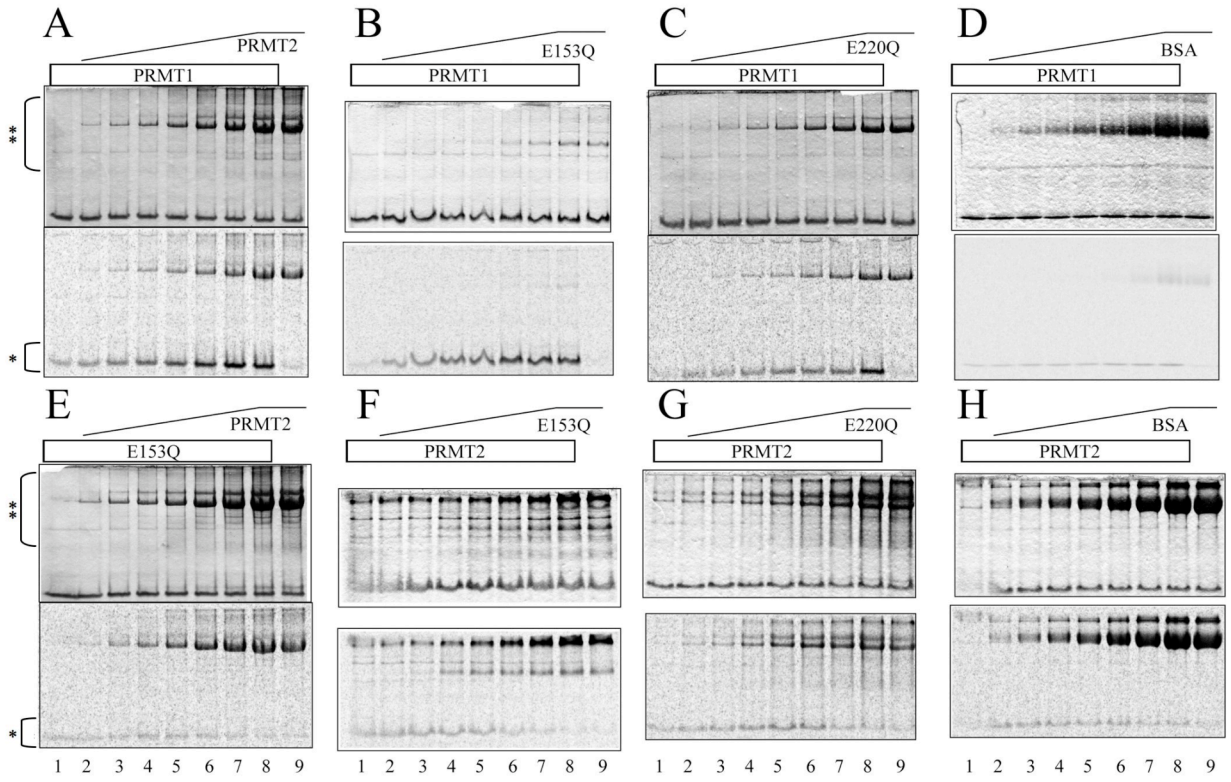

Figure A.4. Synergystic methylation of histone H4 by PRMT1 and -2. (A) Pre-incubations at 37 ˚C for 1 h in methylation buffer with 100 nM PRMT1 alone (*lane 1*), 100 nM PRMT1 with 210 to 5000 nM PRMT2 (*lanes 2-8*), and 5000 nM PRMT2 alone (*lane 9*) were performed prior to initiating 1-h methylation reactions. Similar reactions were prepared with PRMT1 and (B) PRMT1 E153Q, (C) 100 to 2500 nM PRMT2 E220Q, and (D) BSA. (E) Samples were prepared as in (A) except 100 nM PRMT1 E153Q was used in place of PRMT1. (F) Pre-incubations were performed as in (A) with 400 nM PRMT2 alone (*lane 1*), 400 nM PRMT2 with 800 to 20000 nM PRMT1 E153Q (*lanes 1-8*), and 20000 nM PRMT1 E153Q alone (*lane 9*) prior to initiating 16-h methylation reactions. Similar reactions were prepared with PRMT2 and (G) PRMT2 E220Q, and (H) BSA. Coomassie-stained gels are shown on top (only histone H4 and higher concentrations of PRMTs are visible), and storage phosphor images are shown on the bottom. The position of histone H4 is indicated with an asterisk, and the position of enzyme or BSA is indicated with two asterisks.

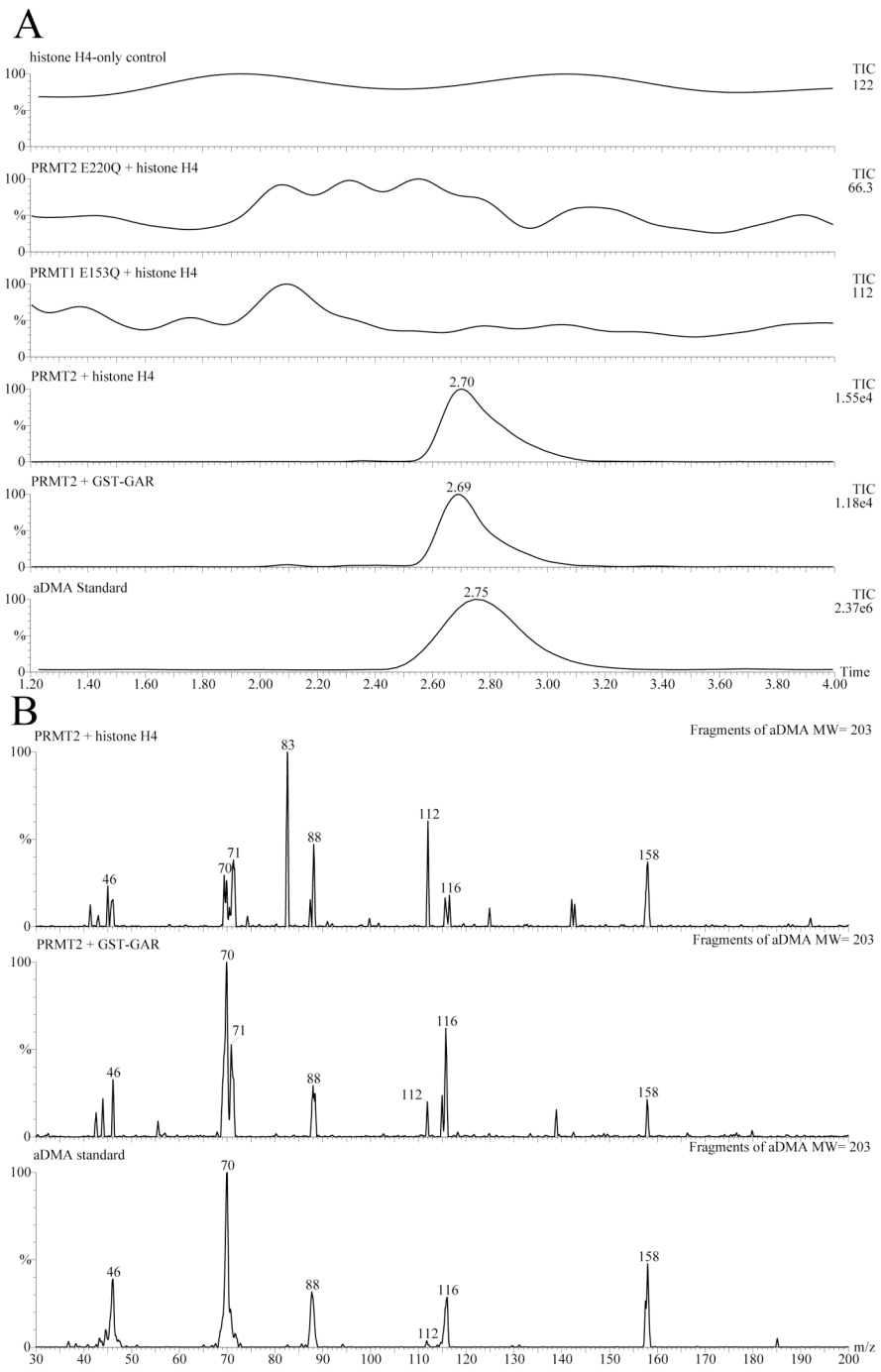

Figure A.5. Activities of wild type and mutant enzymes. (A) Detection of aDMA using a previously described UPLC tandem mass spectrometry assay (*9*). The chromatograms for the detection of aDMA show no activity towards histone H4 in the no-enzyme control, as well as for reactions with PRMT2 E220Q and PRMT1 E153Q mutants. Chromatograms showing a peak for aDMA include reactions in which PRMT2 methylated histone H4 and GST-GAR. The total ion count (TIC) records the signal intensity in arbitrary units. (B) The fragmentation patterns of aDMA detected in PRMT2 reactions with histone H4 and GST-GAR. Fragmentation of an aDMA standard is shown at the bottom.

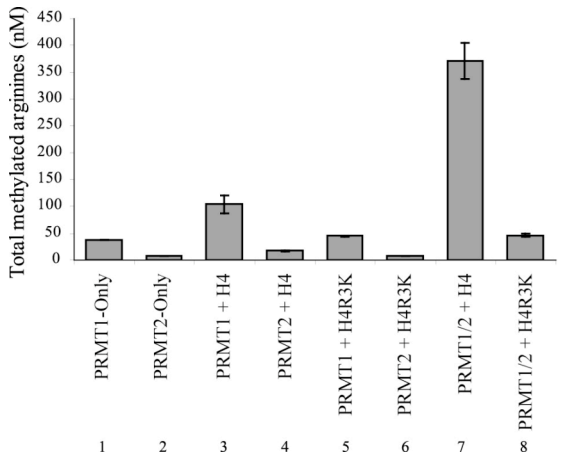

Figure A.6. Methylation of histone H4 at R3. The production of total methylated arginines was measured by tandem mass spectrometry for methylation reaction samples (enzyme and substrate combinations are indicated). The mean and standard deviation are shown for two replicates of each reaction. Experiments are preformed as in Figure 2.1 with 100 nM PRMT1 and a 1:50 ratio PRMT1:PRMT2 with 10 μM histone H4 and 100 μM AdoMet in methylation buffer.

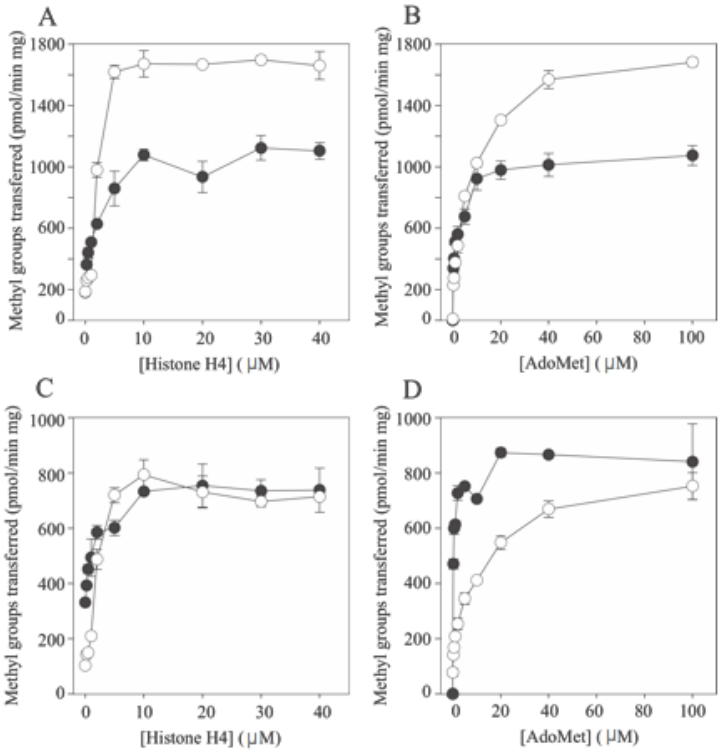

Figure A.7. Substrate concentration-dependent increases in methylarginine species. The rates of formation of MMA (black circles) and aDMA (open circles) are shown for PRMT1 with E153Q at a 25:750 nM ratio and increasing histone H4 (A) or AdoMet (B) as the variable substrate. Similar rates of MMA and aDMA formation are shown for PRMT1 with E220Q at a 25:750 nM ratio and increasing histone H4 (C) or AdoMet (D) as the variable substrate. Data are plotted as means and standard deviations of two samples determined using UPLC MS/MS described in section 2.

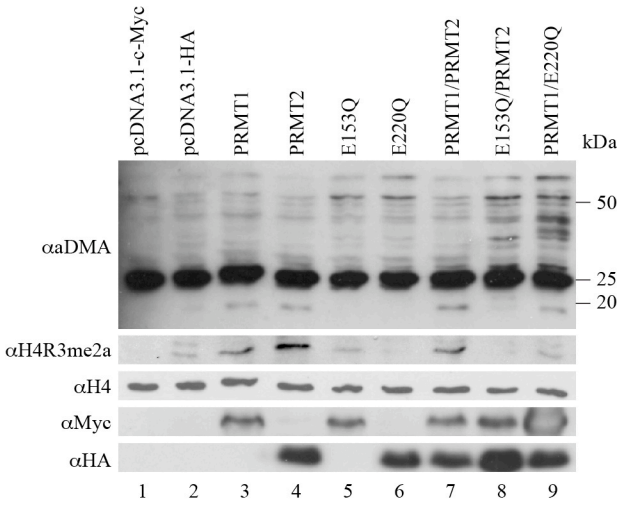

Figure A.8. PRMT1- and PRMT2-dependent changes in arginine methylation. Cell lysate from HeLa cells transfected with the same amount of plasmid DNA as denoted were immunoblotted.

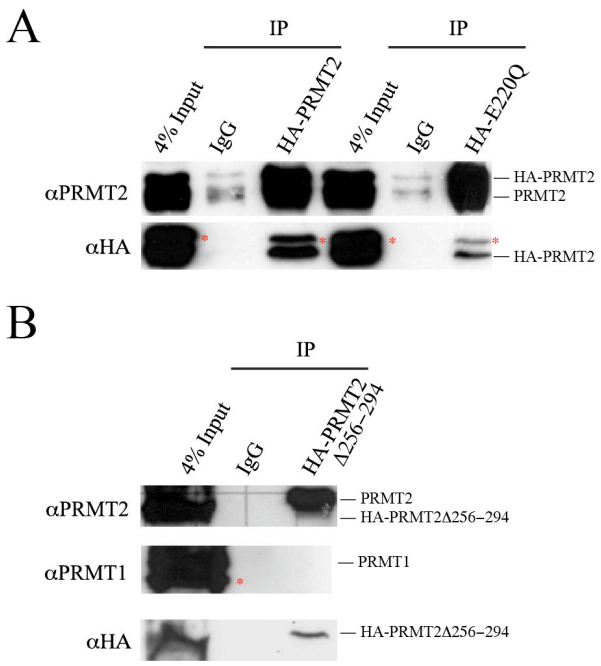

Figure A.9. Co-immunoprecipitation of endogenous and ectopically-expressed PRMT2 in cells. (A) HA-PRMT2 or HA-E220Q was expressed in HeLa cells, and cell lysate was immunoprecipitated with anti-HA antibody, or with mouse IgG (negative control). Immunoprecipitates were immunoblotted with anti-PRMT2 (*top)* or anti-HA (*bottom)* antibodies. (B) HA-PRMT2DArm was expressed in HeLa cells, and cell lysate was immunoprecipitated with anti-HA antibody or with mouse IgG. Immunoprecipitates were immunoblotted with anti-PRMT2 (*top)*, anti-PRMT1 (*middle*), or anti-HA (*bottom)* antibodies. Non-specific bands are labeled with *red asterisks*.

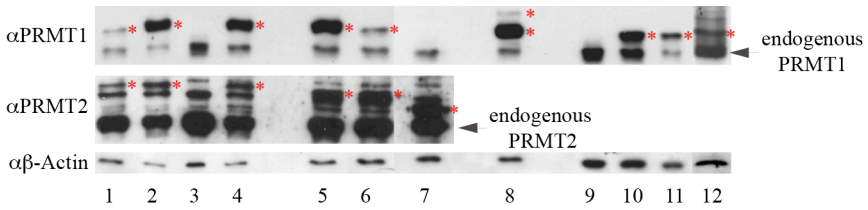

Figure A.10. Expression of the BiFC constructs in cells with negative BiFC signals. HeLa cells co-transfected with BiFC constructs that showed no BiFC signal were lysed, and proteins from the resulting cell lysates were separated on 10% SDS-PAGE gels. The expression of BiFC constructs was detected by Western blotting. Western blots of the following samples are shown: mCitrineN-PRMT2E220Q/ PRMT1Δ188-222-mCitrineC (*lane 1*), mCitrineN-PRMT2E220Q/ PRMT1E153Q-mCitrineC (*lane 2*), mCitrineN-PRMT2/ PRMT1E153Q-mCitrineC (*lane 4*), mCitrineN-PRMT2Δ256-294/ PRMT1E153Q-mCitrineC (*lane 5*), mCitrineN-PRMT2Δ256-294/ PRMT1Δ188-222-mCitrineC (*lane 6*), mCitrineN-PRMT1/ PRMT2-mCitrineC (*lane 7*), mCitrineN-PRMT1Δ188-222/ PRMT1Δ188-222-mCitrineC (*lane 8*), mCitrineN-ΔSH3PRMT2E220Q/ PRMT1Δ188-222-mCitrineC (*lane 10*), and mCitrineN-ΔSH3PRMT2/ PRMT1Δ188-222-mCitrineC (*lane 11*). HeLa cells that were not transfected serve as negative controls (*lanes 3* and *9*), and HeLa cells that expressed the mCitrineN-PRMT1/ PRMT1-mCitrineC pair (showing a positive BiFC signal) were included as a positive control (*lane 12*). *Red asterisks* indicate locations of BiFC constructs.

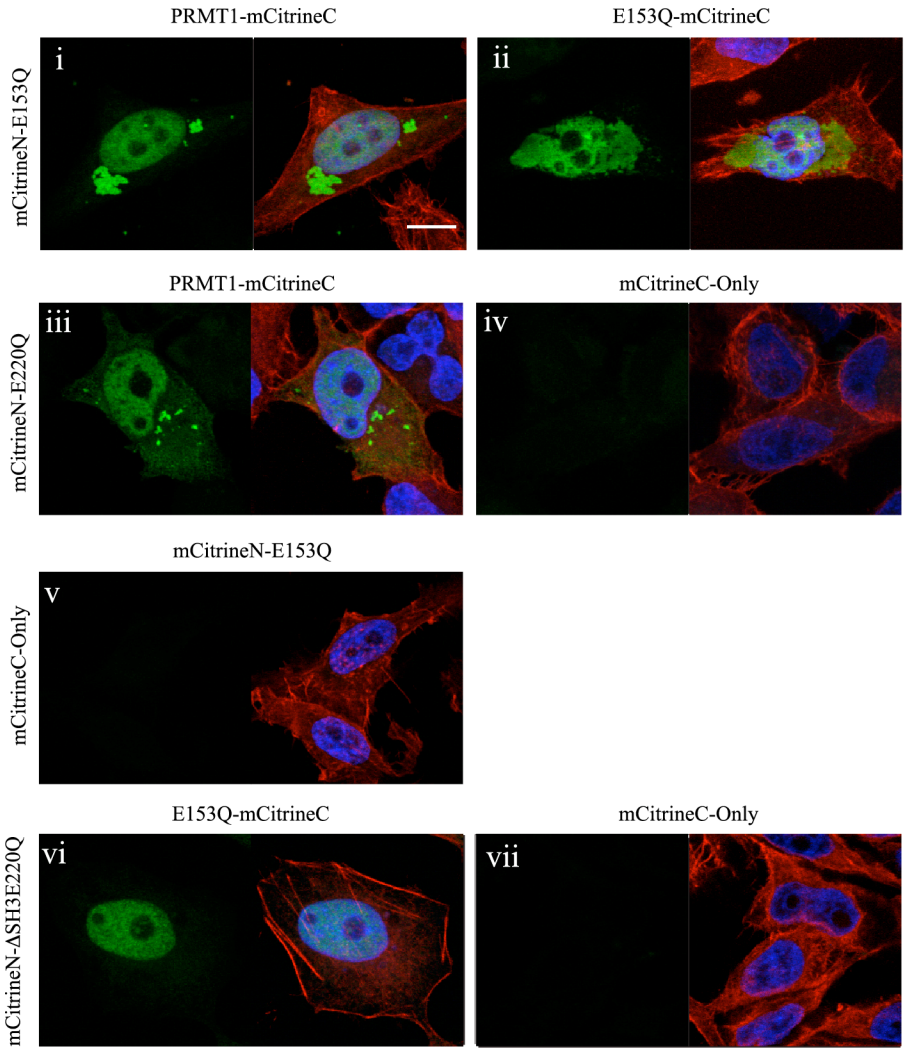

Figure A.11. Effects of catalytically inactive PRMT1 and -2 on BiFC complex formation. HeLa cells were co-transfected with the two constructs indicated in the columns and rows (representative images are shown). The left image of each panel shows the formation of a BiFC complex. The right image of each panel shows an overlay of BiFC (*green*), DAPI (*blue*), and fluorescence-labeled phalloidin (*red*). The scale bar indicates 10 μm.

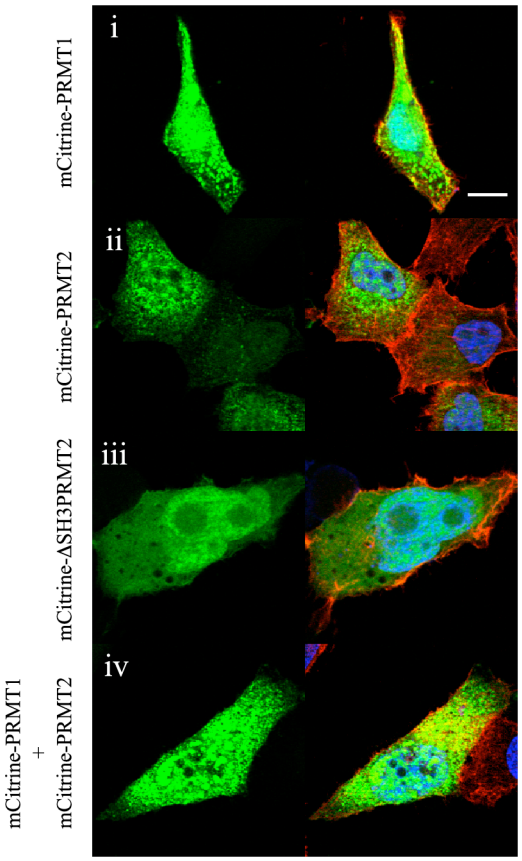

Figure A.12. Visualization of PRMT1, PRMT2, and ΔSH3PRMT2 in HeLa cells. HeLa cells were co-transfected with constructs indicated (representative images are shown). The left image of each group shows the formation of a BiFC complex as *green* fluorescence. The right image of each group shows an overlay of BiFC (*433*), DAPI (*blue*), and fluorescence-labeled phalloidin (*red*). The bar indicates 10 μm.

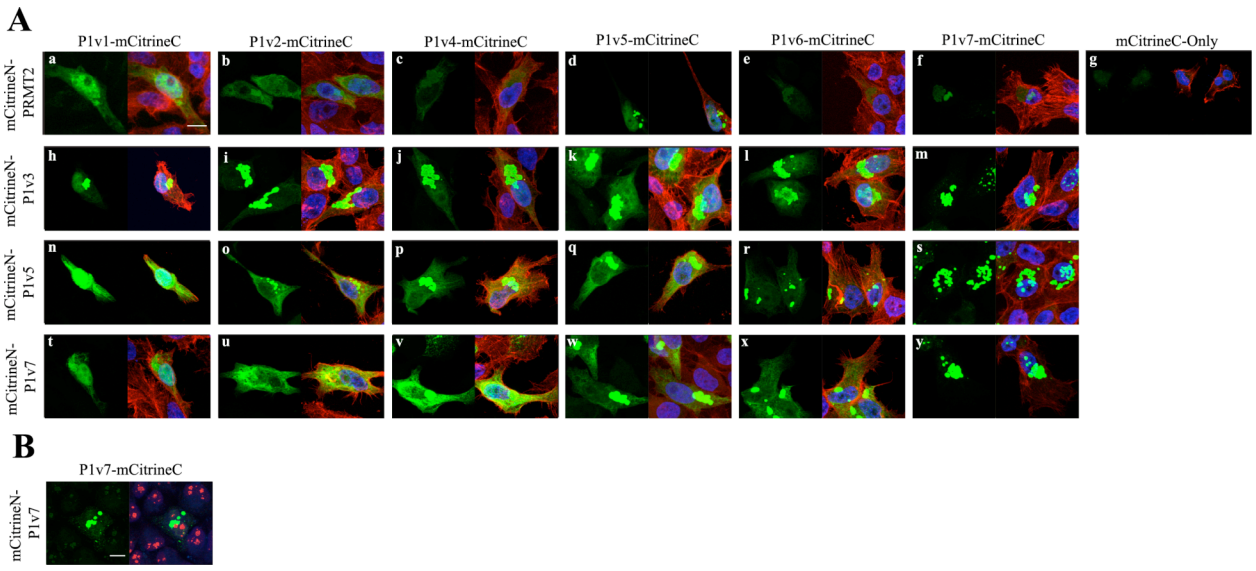

Figure A.13. Visualization of PRMT1 isoforms and PRMT2 interactions via BiFC. (A) HeLa cells were co-transfected with the two constructs indicated in columns and rows (representative images are shown). The left image of each panel shows the formation of a BiFC complex. The right image of each panel shows an overlay of BiFC *(green),* DAPI (*blue*), and fluorescence-labeled phalloidin (*red*). The scale bar indicates 10 μm. (B) HeLa cells were co-transfected with mCitrineN-P1v7 and P1v7-mCitrineC. The left image shows the formation of a BiFC complex. The right image shows an overlay of BiFC *(green),* DAPI (*blue*), and Nop1 (*red*). The scale bar indicates 10 μm.

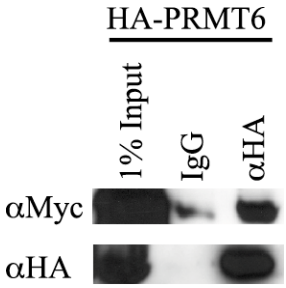

Figure A.2. Co-immunoprecipitation of HA-PRMT6 and Myc-p53. Myc-p53 and HA-PRMT6 were co-expressed in HeLa cells and cell lysate was immunoprecipitated with anti-HA antibody, or with mouse IgG (negative control). Immunoprecipitates were immunoblotted with anti-Myc (*top)* or anti-HA (*bottom)* antibodies.

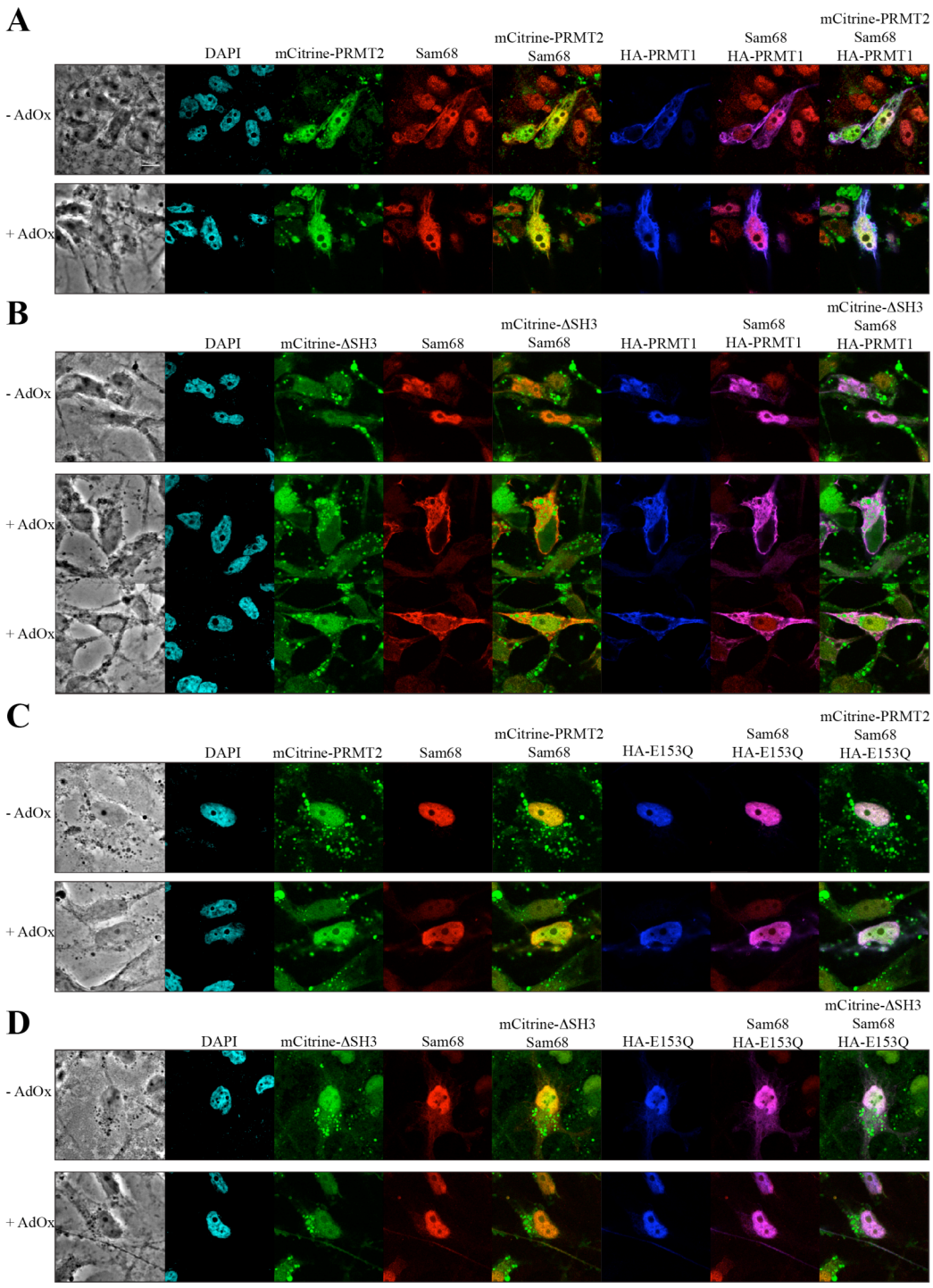

Figure A.15. The change of Sam68 sub-cellular localization in hypomethylated HeLa cells co-expressing wild type or inactive mutant form of PRMT1 and full length or truncated version of PRMT2. HeLa cells co-transfected with HA-PRMT1 (A and B, *blue*) or HA-E153Q (C and D, *blue*) and mCitrine-PRMT2 (A and C, *green*) or mCitrine-ΔSH3 (B and D, *green*) were treated with or without 20 μM AdOx as indicated. The cells were fixed and co-immunostained with an anti-Sam68 antibody and an anti-HA antibody, followed by secondary antibodies conjugated to Alexa Fluor 546 (*red*) and Alexa Fluor 647 (*blue*). Nuclei were visualized by the DAPI stain (*cyan*). The phase contrast images (*left*) and the merged images were also shown as indicated. The scale bar indicates 10 μm.

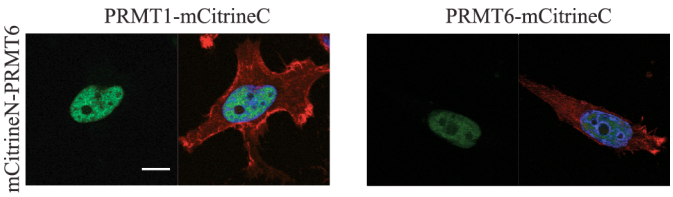

Figure A.16. Visualization of PRMT1 and -6 interaction via BiFC. HeLa cells were co-transfected with the two constructs indicated in columns and rows (representative images are shown). The left image of each panel shows the formation of a BiFC complex. The right image of each panel shows an overlay of BiFC *(green)*, DAPI (*blue*), and fluorescence-labeled phalloidin (*red*). The scale bar indicates 10 μm.